

Bangor University

DOCTOR OF PHILOSOPHY

Regional cerebral conduit artery blood flow regulation in hypoxia

Friend, Alex

Award date:
2024

Awarding institution:
Bangor University

[Link to publication](#)

General rights

Copyright and moral rights for the publications made accessible in the public portal are retained by the authors and/or other copyright owners and it is a condition of accessing publications that users recognise and abide by the legal requirements associated with these rights.

- Users may download and print one copy of any publication from the public portal for the purpose of private study or research.
- You may not further distribute the material or use it for any profit-making activity or commercial gain
- You may freely distribute the URL identifying the publication in the public portal ?

Take down policy

If you believe that this document breaches copyright please contact us providing details, and we will remove access to the work immediately and investigate your claim.

Download date: 25. Jun. 2024



PRIFYSGOL
BANGOR
UNIVERSITY

School of Psychology and Sport Science
College of Medicine and Health

Regional cerebral conduit artery blood flow
regulation in hypoxia

Alexander Thomas Friend

A thesis submitted to
Bangor University
in fulfilment of the requirements of the degree of
Doctor of Philosophy

Supervisors: Prof. Samuel J. Oliver *and* Prof. Jamie H. Macdonald
and Dr. Aamer Sandoo *and* Dr. Gabriella Rossetti

2023

Acknowledgements

I am privileged to have had an incredible team of colleagues, collaborators, friends, and family who have supported me throughout this PhD.

First, words cannot express my gratitude to the guidance and mentorship from all my supervisory team. To Prof. Sam Oliver, the unwavering confidence that you have in me as a scientist (less so in surfing and skiing) and your calm, enthusiastic, and encouraging approach to science is something I hope to emulate in my career. You are an incredible mentor and I have enjoyed every moment working together – I hope to have many more. To Prof. Jamie Macdonald, Dr. Aamer Sandoo, and Dr. Gabriella Rossetti, thank you for continually pushing my capabilities as a researcher, for pulling me (and Sam) out of rabbit holes of thought, and being a solid foundation of support through my many ups and downs. There are few who are lucky enough to get to learn from four incredible people who genuinely cared for me in my scientific and personal development. I am so fortunate to have been one of them.

To the collaborators outside of my supervisory team, Prof. Paul Mullins, Prof. Justin Lawley, and Prof. Masa Horiuchi, thank you for your insight into our work and welcoming me with open arms to each of your worlds of science. I also wish to extend my gratitude to Dr. Julian Owen who provided a warmth and kindness in his supporting role as my thesis chair.

Science isn't without hiccups along the way. To Kevin Williams and Shaun McKiernan, thank you for your technical support, but more importantly for the friendly corridor catch-ups. Thank you also to Dr Shieak Tzeng and the Ensemble team for transfer function analysis support.

A big thank you must go to all the participants who got involved (sometimes multiple!), this thesis wouldn't exist without you all volunteering your time and effort. Big thanks must also go to PhD candidates Michiel Ewalts, Guto Hughes, and Ferrida Ponce, and students Poppy

Barsby, Liam Joyce, Harry Nicholson, Jonathan O'Duffy, Flynn Owen, and Sophia Wakefield for their contribution to data collection. It was a pleasure to work with you all.

I would like to thank a few friends who were integral to my PhD journey. To Liam Colley, through the fun times and tough times of a PhD, you always had my back. We started this adventure together (you said I should apply) and, whilst we will be finishing it in different countries, I cannot wait to celebrate our achievements. To Dr. Matthew Rogan, you are a gentle and thoughtful soul; it was an absolute delight to work together throughout the years. To Dr. Lydia Simpson, thank you for your friendship throughout the years, (and for being the only one to regularly Hoover the house), you are a talented scientist who never hesitates to help others. To Daniel Hill, from my first experiences as a pillion passenger and paddleboarding to lazy hangouts on the Xbox (smashing you at FIFA and being smashed in any racing game), you always knew how to break away from PhD and bring some well needed down time. To the numerous colleagues that have come and gone or recently joined the department, thank you for keeping me sane with the daily chats, vents, and laughs. You are all wonderful, talented people. To my friends outside of academia, notably those back home in Leicester and the Brum Crew, who likely haven't the foggiest what I do, your ignorance is exactly what got me through this. Thank you for the continuous laughter and joy that you all bring to my life that reminds me that there is another world outside of academia.

To Sophie (it's Dr. Harrison, actually), your love and support got me over the line. Thank you for the continual need to keep life busy and entertaining, these times are the most precious. Your passion for science is infectious; I am excited to see your career blossom. We've got this.

To Mum, Dad, and Dom, you are all my rock. Thank you for your unconditional love, guidance, and support. Weekly chin-wags. Roast dinners. Feedback on drafts. To being able come home and have all of my troubles disappear. You are always there. I love you all.

Declaration and Consent

I hereby declare that this thesis is the results of my own investigations, except where otherwise stated. All other sources are acknowledged by bibliographic references. This work has not previously been accepted in substance for any degree and is not being concurrently submitted in candidature for any degree unless, as agreed by the University, for approved dual awards.

I confirm that I am submitting this work with the agreement of my Supervisor(s).

Yr wyf drwy hyn yn datgan mai canlyniad fy ymchwil fy hun yw'r thesis hwn, ac eithrio lle nodir yn wahanol. Caiff ffynonellau eraill eu cydnabod gan droednodiadau yn rhoi cyfeiriadau eglur. Nid yw sylwedd y gwaith hwn wedi cael ei dderbyn o'r blaen ar gyfer unrhyw radd, ac nid yw'n cael ei gyflwyno ar yr un pryd mewn ymgeisiaeth am unrhyw radd oni bai ei fod, fel y cytunwyd gan y Brifysgol, am gymwysterau deuol cymeradwy.

Rwy'n cadarnhau fy mod yn cyflwyno'r gwaith hwn gyda chytundeb fy Ngoruchwyliwr (Goruchwylwyr)

Thesis Format

This thesis contains a general introduction (Chapter 1), which provides a brief background on the importance of cerebral blood flow regulation for brain health and outlines the general aim of the thesis. The literature review (Chapter 2) then outlines, in more depth, the background literature, the current gaps in knowledge, and the main research aims presented in the thesis. This thesis contains a study conducted to establish the operator reliability of duplex and transcranial Doppler ultrasound that are used in the subsequent empirical chapters (Chapter 3). The thesis consists of three empirical chapters. The first empirical chapter investigates the bilateral regional blood flow response in the extracranial cerebral conduit arteries to acute poikilocapnic hypoxia and unilateral duplex ultrasound measurement error (Chapter 4). The second empirical chapter investigates regional dynamic cerebral autoregulation in the intracranial and extracranial cerebral conduit arteries in hypoxia (Chapter 5). The third empirical chapter investigates, in normoxia and hypoxia, the effect of the metabolic state of the visual cortices on regional extracranial vascular tone and dynamic cerebral autoregulation in the intracranial cerebral conduit arteries (Chapter 6). The empirical chapters in this thesis are presented in a paper format. Chapter 4 is a peer-reviewed article accepted by the journal *Experimental Physiology* and has been included as published. Chapter 5 is under review to the *Journal of Cerebral Blood Flow and Metabolism* and has been included according to the journal's formatting requirements, except for conversion of the reference format to be consistent with the rest of the thesis. A general discussion (Chapter 7) provides a summary and critical analysis of the main findings in relation to the broader literature, with a consideration of the limitations, and potential areas for future research.

List of Publications

Publications arising from work presented within this thesis:

Friend AT, Ewalts M, Horiuchi M, Rossetti GMK, Sandoo A, Macdonald JH & Oliver SJ (under review). Regional dynamic cerebral autoregulation in acute poikilocapnic hypoxia. *Journal of Cerebral Blood Flow & Metabolism*

Friend AT, Rogan M, Rossetti GMK, Lawley JS, Mullins PG, Sandoo A, Macdonald JH & Oliver SJ (2021). Bilateral regional extracranial blood flow regulation to hypoxia and unilateral duplex ultrasound measurement error. *Experimental Physiology* **106**, 1535–1548.

Conference Proceedings

Friend, A. T., Rossetti, G. M. K., Sandoo, A., Macdonald, J., & Oliver, S. (2022). *Regional dynamic cerebral autoregulation of the intracranial and extracranial arteries during acute poikilocapnic hypoxia*. **‘Best Student’ Oral Presentation – CARNet Annual Meeting 2022, Leicester, UK.**

Friend, A. T., Rogan, M., Rossetti, G. M. K., Lawley, J., Mullins, P., Sandoo, A., Macdonald, J., & Oliver, S. (2020). *Extracranial regional cerebral blood flow regulation in hypoxia: A left and right-side assessment by Doppler ultrasound*. **Oral Presentation - Cerebral Blood Flow Virtual Seminar Series.**

Friend, A. T., Rogan, M., Rossetti, G. M. K., Lawley, J., Mullins, P., Sandoo, A., Macdonald, J., & Oliver, S. (2020). *Measurement bias in the unilateral assessment of cerebral blood flow responses to hypoxia*. **Oral Presentation [Cancelled Conference] - Okanagan Cardiovascular and Respiratory Symposium, Canada.**

Friend, A. T., Rogan, M., Rossetti, G. M. K., Mullins, P., Sandoo, A., Macdonald, J., & Oliver, S. (2019). *Duplex Ultrasound Assessment of Cerebral Blood Flow in Hypoxia: A Potential Source of Methodological Bias*. **Poster Presentation - British Mountain Medicine Society, Bamford, Derbyshire, UK.**

Summary of Findings

The aim of this thesis was to investigate regional blood flow regulation between the cerebral conduit arteries that source the anterior and posterior regions of the brain in acute poikilocapnic hypoxia.

The aims of the first study (Chapter 3) were to determine if bilateral extracranial blood flow response to acute poikilocapnic hypoxia is different between the internal carotid arteries (ICA) and vertebral arteries (VA), and to determine the measurement error in unilateral extracranial artery assessments compared to bilateral. Hypoxia caused the same vasodilation and similar relative increases in blood flow in the ICA and VA. These responses were not influenced by vessel side, i.e., if measured unilaterally on the left- or right- side only. Compared to bilateral assessment, unilateral measurements of extracranial arteries with smaller resting normoxic blood flow caused the greatest and most varied error. Methodologically, assessing the vessel with the larger resting blood flow, rather than selecting a vessel based on location (left or right), is most effective at reducing unilateral measurement error.

The second study (Chapter 4) aimed to determine whether the extra- and intra-cranial posterior cerebral conduit arteries [VA and posterior cerebral artery (PCA)] have an exacerbated reduction in dynamic cerebral autoregulation (dCA) compared to the anterior cerebral conduit arteries [ICA and middle cerebral artery (MCA)] in acute poikilocapnic hypoxia. Here, in a mixed-sex cohort, we report that volumetric dCA to abrupt reductions in blood pressure is comparable between the ICA and VA in normoxia and hypoxia. With sex as an additional fixed effect, hypoxia reduced the rate of regulation of the VA in men only, indicating a reduced dCA (i.e., pressure-passive) of the posterior circulation. In contrast, hypoxia did not reduce dCA in the ICA in men. Hypoxia induced vasodilation of the ICA, but not the VA in men. dCA of the

MCA and PCA were comparable by region, condition, and sex. These findings suggest that volumetric dCA of the cerebral conduit arteries to hypoxia is regionally different in men and may not be influenced by changes in vascular tone.

In the final empirical chapter (Chapter 5), we investigated whether the metabolic activation of the visual cortices from ambient light modulates a lower basal vascular tone of the posterior cerebral circulation and contributes to the reduced dCA of the posterior compared to the anterior circulation. In normoxia and hypoxia, high ambient visual input (lights on – eyes open), compared to low ambient visual input (lights off – eyes closed), evoked a greater response in blood velocity and blood flow in the posterior (VA and PCA) than anterior circulation (ICA and MCA). In contrast, extracranial vascular tone was unchanged with visual stimulation in normoxia and hypoxia. Visual stimulation reduced very low-frequency phase of the PCA, but not the MCA, to spontaneous oscillations in blood pressure at rest in normoxia, indicating a reduced posterior compared to anterior intracranial dCA. In contrast, there was no regional difference in dCA with visual stimulation in hypoxia. This study concluded visual stimulation elicited a regional intracranial and extracranial blood velocity increase in normoxia and hypoxia but did not reduce extracranial vessel tone, suggesting other mechanisms are responsible for the regional differences in intracranial dCA to visual stimulation.

In conclusion, the findings of this thesis suggest regional differences between the anterior and posterior cerebral conduit arteries exists in dCA in hypoxia and with visual stimulation in normoxia, but not the blood flow response to hypoxia. This thesis also emphasises the importance of capturing vascular tone and volumetric blood flow measurements to fully understand the regional regulation of the cerebral circulation.

Contents

1. General introduction	1
2. Literature review	3
2.1 Cerebral conduit artery anatomy	3
2.2 Doppler ultrasound assessment of cerebral blood flow	7
2.2.1 Transcranial Doppler ultrasound	8
2.2.2 Duplex ultrasound.....	10
2.3 Cerebral conduit artery anatomical variability.....	12
2.4 Mechanisms of cerebral blood flow regulation.....	17
2.4.1 Metabolic	19
2.4.2 Neurogenic.....	21
2.4.3 Myogenic	22
2.4.4 Endothelial.....	22
2.4.5 Neurovascular coupling.....	23
2.4.6 Cerebral autoregulation	24
2.5 Cerebral blood flow response to hypoxia.....	31
2.5.1 Cerebral autoregulation during hypoxia	35
2.6 Regional regulation of blood flow at the cerebral conduit arteries	43
2.6.1 Regional cerebral autoregulation during normoxia	43
2.6.2 Regional cerebral blood flow response to hypoxia	47
2.6.3 Regional cerebral autoregulation during hypoxia	49
2.6.4 Mechanisms of regional cerebral blood flow regulation	50
2.7 Thesis aims.....	52
3. Between-trial reliability of duplex and transcranial Doppler ultrasound measurements in the cerebral conduit arteries	56
3.1 Abstract	56
3.2 Introduction	57
3.3 Methods.....	59
3.4 Results	64
3.5 Discussion	68
4. Bilateral regional extracranial blood flow regulation to hypoxia and unilateral duplex ultrasound measurement error.....	73
4.1 Abstract	73
4.2 Introduction	74

4.3 Methods	77
4.4 Results	83
4.5 Discussion	98
5. Regional dynamic cerebral autoregulation in acute poikilocapnic hypoxia.....	106
5.1 Abstract	106
5.2 Introduction	107
5.3 Methods	109
5.4 Results	117
5.5 Discussion	124
6. Effect of the metabolic state of the visual cortices on regional vascular tone and dynamic cerebral autoregulation in normoxia and acute hypoxia.....	131
6.1 Abstract	131
6.2 Introduction	132
6.3 Methods	135
6.4 Results	141
6.5 Discussion	156
7. General discussion	164
7.1 Summary of main findings.....	164
7.2 Regional regulation of the cerebral conduit arteries	165
7.2.1 Regional dynamic cerebral autoregulation of the cerebral conduit arteries to acute poikilocapnic hypoxia and with visual stimulation	165
7.2.2 Visual stimulation elicits regional blood velocity and blood flow responses in the cerebral conduit arteries.....	167
7.2.3 Comparable regional cerebral conduit artery haemodynamics to acute hypoxia..	168
7.3 Importance of volumetric flow measures of cerebrovascular regulation.....	169
7.3.1 Cerebral conduit extracranial arteries do vasodilate to acute poikilocapnic hypoxia	170
7.3.2 Reduced posterior dCA in hypoxia was only identified with volumetric flow measurements of the extracranial arteries	170
7.3.3 The regional haemodynamic response to visual stimulation is detected with volumetric blood flow measurements of the extracranial arteries.....	171
7.4 Unilateral volumetric assessments of cerebral conduit arteries	172
7.5 Thesis methodological considerations	174
7.5.1 End-tidal CO ₂ control	174
7.5.2 Complexities of measuring dynamic cerebral autoregulation	175
7.6 Future directions.....	176

7.6.1 Implementation of volumetric regional assessment to mechanisms of cerebrovascular regulation.....	176
7.6.2 Identifying possible cellular mechanisms that underpin the regional difference in cerebral conduit artery regulation.....	177
7.6.3 Regional regulation of the cerebral conduit arteries in the development of pathophysiology.....	178
7.6.4 Regional cerebral blood flow regulation and sex	180
7.7 Conclusions	182

List of Figures

Figure 2.1. The anatomical structure of the cerebral conduit artery network. Image was acquired using magnetic resonance angiography. The purple, light blue, dark blue, and green pathway reflects the anterior circulation through the common carotid artery (CCA), internal carotid artery (ICA), middle cerebral artery (MCA), and anterior cerebral artery (ACA), respectively. The purple and brown pathway reflects the CCA and the external carotid artery (ECA) that perfuses structures of the neck, head, and face. The pink, yellow, and orange pathway reflects the posterior circulation through the vertebral artery (VA), basilar artery (BA), and posterior cerebral artery (PCA), respectively.

Figure 2.2. Cerebral conduit arteries supply blood flow to different regions of the brain. The cerebral conduit arteries can be categorised into those that supply the anterior regions and those that supply the posterior regions of the brain. The middle cerebral artery (MCA, blue) and anterior cerebral artery (ACA, green) supply the anterior motor and somatosensory cortices within the frontolateral and parietal lobes. The posterior cerebral artery (PCA, orange) supplies the thalamus above the midbrain and visual cortices within the occipital lobes. The upper portion of the vertebral artery (VA) and basilar artery (BA, yellow) supply the cerebellum and cardiorespiratory control brain regions, such as the pons, midbrain, and medulla that form the brainstem. Created with BioRender.com.

Figure 2.3. Transcranial Doppler ultrasound of the intracranial cerebral conduit arteries. Transcranial Doppler ultrasound is a non-invasive device with high temporal resolution that captures beat-to-beat measurements of intracranial artery haemodynamics. Four acoustic windows are used in transcranial Doppler ultrasound. The transtemporal window is used for insonation of the anterior cerebral artery (ACA), middle cerebral artery (MCA), and posterior cerebral artery (PCA) before (PCA-1) or after (PCA-2) the posterior communicating artery. The suboccipital window is used for insonation of the basilar artery (BA) and upper portions of the vertebral artery (VA). The transorbital window is used for the insonation of the carotid siphon segment of the internal carotid artery (ICA) and ophthalmic artery. The submandibular window (not shown) is located under the chin for insonation of the distal portion of the ICA. A representative example of the Doppler spectra waveform, vessel depth, and mean cerebral blood velocity (CBV_{mean}) accompany each intracranial artery. Created with BioRender.com.

Figure 2.4. Duplex ultrasound of the extracranial cerebral conduit arteries. Concurrent measurements of vessel diameter from B-mode imaging (left, top) and blood velocity spectra from pulse wave Doppler imaging (left, bottom) are captured from the extracranial artery using Duplex ultrasound. Post-capture calculations of volumetric blood flow are captured using automated-edge detection software (right). The high spatial and temporal resolution of duplex ultrasound enables the automated wall-edge detection software to track frame-by-frame diameter changes of a specific region of interest within the vessel across each cardiac cycle (right, A). The Doppler spectral signal of one complete cardiac cycle is analysed for its peak

velocity, velocity integral, and the time-averaged maximum velocity (right, B). The time-averaged maximum velocity calculates the mean from the average peak envelope velocity across the cardiac cycle. Half the time-averaged maximum velocity is estimated to be the mean blood velocity. Estimations of volumetric blood flow can be calculated from the formula: blood flow ($\text{ml}\cdot\text{min}^{-1}$) = [time-averaged maximum velocity ($\text{cm}\cdot\text{s}^{-1}$)/2] * [π * (mean artery diameter (cm)/2²)] * 60. Created with BioRender.com.

Figure 2.5. Representative example of vertebral artery imbalance. Top: Magnetic resonance angiography image of the vessel imbalances in vertebral artery (VA) calibre (red circle) before forming the basilar artery (BA), whereas the internal carotid arteries (ICA) are similar in size. Bottom: Duplex ultrasound-derived cross-section of the vertebral arteries between the vertebrae. Red line (of same length) reflects the vessel size imbalance comparison between the vertebral arteries.

Figure 2.6. Segmental cerebrovascular regulation. An illustration of how segmental changes in vascular tone (cerebrovascular resistance) between the upstream and downstream arteries organized in-series influence flow and microvascular pressure. Upstream-downstream segmental regulation may occur between the extracranial and intracranial arteries, or between the intracranial arteries and smaller arterioles or pial arteries, or along different sections of an intracranial artery. Changes in vasoactive tone (dilation or constriction) are labelled on each artery. Directional arrows reflect the changes in blood flow and microvascular pressure for each scenario, with more arrows representing a larger magnitude of effect and a sideways arrow representing no change. All blood flow and microvascular pressure changes are relative to the top row (upstream and downstream artery both at rest). Adapted from Hoiland et al., 2019.

Figure 2.7. The relationship between cerebral blood flow and changing tensions of oxygen and carbon dioxide. Representative schematic between cerebral blood flow (CBF, $\Delta\%$) and partial pressure of oxygen (PO_2 , mmHg) at differing partial pressures of carbon dioxide (PCO_2 , mmHg). Adapted from Mardimae et al., 2012.

Figure 2.8. The contemporary view of the cerebral autoregulation curve. Relationship between change in mean arterial pressure (MAP, $\Delta\%$) and concomitant change in cerebral blood flow (CBF, $\Delta\%$) using nonpharmacological methodologies. The grey section represents the autoregulatory plateau where the assessment of spontaneous dynamic cerebral autoregulation (dCA) occurs. The yellow section represents the area of induced hypotension for assessments of dynamic cerebral autoregulation using forced manoeuvres i.e., rapid thigh cuff deflation, sit-to-stand. Adapted from Brassard et al., 2021.

Figure 2.9. Summary of the evidence of anterior-posterior regional differences in the cerebral conduit arteries and the aims addressed in this thesis. *Chapter 4*) Anatomical variabilities, which are more prevalent in the posterior cerebral conduit arteries such as vessel flow imbalances and artery hypoplasia, are related to a reduced cerebrovascular function and may impact on regulation of posterior circulation to vasoactive stimuli, such as hypoxia, in comparison to the anterior circulation (Q1). It is proposed that cerebral blood flow regulation is different in the posterior cerebral conduit arteries compared to the anterior cerebral conduit arteries to hypoxia to preferentially maintain circulation of the posterior regions of the brain involved in homeostatic and cardiorespiratory control. However, due to small sample sizes, unilateral measurements of cerebral conduit arteries, and a limited number of studies which have directly measured vascular tone changes, evidence of regional differences in vascular tone and cerebral blood flow regulation between the anterior and posterior cerebral conduit arteries during hypoxia remains equivocal (Q2 & 3). Unilateral measurements of the posterior cerebral conduit arteries may not be reflective of the true bilateral cerebral blood flow regulation if lateral arteries are asymmetrical in size and blood flow (Q4). *Chapter 5*) Due to differences in vascular tone, the posterior circulation is proposed to have a greater capability to dampen fluctuations in blood pressure than the anterior circulation during normoxia at rest. To date, there is only one study that has explored regional intracranial artery regional dynamic cerebral autoregulation during hypoxia. Therefore, concurrent intracranial and extracranial artery regional dynamic cerebral autoregulation differences to capture volumetric and vasoactive regulation during hypoxia is yet to be explored (Q5). *Chapter 6*) The differences in dynamic cerebral autoregulation between the anterior and posterior cerebral conduit arteries may be a consequence of a lower resting vascular tone in the posterior circulation in response to an increased neuronal metabolic demand of the visual cortices caused by individuals eyes being open during cerebrovascular assessments (Q6). Abbreviations; AMS, acute mountain sickness; CBF, cerebral blood flow; CBv, cerebral blood velocity; dCA, dynamic cerebral autoregulation; HUT, head-up tilt; MAP, mean arterial pressure; MCA, middle cerebral artery; NO, nitric oxide; PCA, posterior cerebral artery; VA, vertebral artery; VAH, vertebral artery hypoplasia. Created with BioRender.com.

Figure 3.1. Coefficient of variation of the extracranial arteries measured using Siemens duplex ultrasound by logged hours of practice. Coefficient of variation of vessel diameter (a), blood velocity (b), and blood flow (c) in the left (circle) and right (triangle) common carotid artery (CCA, red), internal carotid artery (ICA, blue), and vertebral artery (VA, green) from repeat between-trial reliability studies with increasing hours of logged practice. Reliability was assessed at 50 h (left N = 6, right N = 4) and at 100 h (left and right N = 10) using the Siemens duplex ultrasound. A dotted line marked at 10% represents the recommended guidelines for proficiency in duplex ultrasound of the extracranial arteries (Thomas et al., 2015). Values are mean \pm standard deviation.

Figure 4.1. Extracranial artery blood flow regulation in normoxia and acute poikilocapnic hypoxia. Left and right internal carotid artery (ICA) and vertebral artery (VA) blood flow regulation was measured from normoxia (fraction of inspired oxygen [FiO_2] = 20.9%) to acute poikilocapnic hypoxia (FiO_2 = 12.0%). Linear mixed model analysis revealed no ‘Condition’ (normoxia or hypoxia) \times ‘Vessel Type’ (ICA or VA) \times ‘Vessel Side’ (left or right) interaction for blood flow (a, $\text{mL}\cdot\text{min}^{-1}$; $P = 0.62$), vessel diameter (b, mm; $P = 0.70$), and flow velocity (c, $\text{cm}\cdot\text{s}^{-1}$; $P = 0.64$), adding ‘Participant ID’ as a random effect. Data points are estimated marginal means (estimated SD) from LMM analysis. Raw mean (SD) data are presented in Table 2.

Figure 4.2. Extracranial artery blood flow response and reactivity to acute poikilocapnic hypoxia. Left and right internal carotid artery (ICA; grey circle or bars) and vertebral artery (VA; white triangle or bars) blood flow response to acute poikilocapnic hypoxia (fraction of inspired oxygen [FiO_2] = 12.0%). Linear mixed model (LMM) analysis revealed no ‘Vessel Type’ (ICA or VA) \times ‘Vessel Side’ (left or right) interaction for the absolute change in blood flow to hypoxia (a, $\Delta\text{mL}\cdot\text{min}^{-1}$; $P = 0.32$), absolute hypoxic reactivity (c, $\Delta\text{mL}\cdot\text{min}^{-1}\cdot\Delta\text{SpO}_2^{-1}$; $P = 0.37$), the relative change in blood flow to hypoxia (e, $\Delta\%$; $P = 0.15$), or relative hypoxic reactivity (g, $\Delta\%\cdot\Delta\text{SpO}_2^{-1}$; $P = 0.13$). There were no main effects of ‘Vessel Side’ for these blood flow variables (all $P > 0.05$). Main effects of ‘Vessel Type’ were revealed for the absolute change in bilateral blood flow to hypoxia (b; $P < 0.001$), absolute bilateral hypoxic reactivity (d; $P < 0.001$), but not for the relative change in bilateral blood flow to hypoxia (f; $P = 0.053$), or relative bilateral hypoxic reactivity (h; $P = 0.12$). * $P < 0.001$ between ICA and VA. Data points represent individuals' ICA and VA blood flow responses to acute hypoxia. Bars are estimated marginal means (estimated SD) from LMM analysis.

Figure 4.3. Relationships between resting normoxic blood flow and the absolute or relative blood flow response to acute poikilocapnic hypoxia in the extracranial arteries. Internal carotid arteries (ICA) and vertebral arteries (VA) blood flow response were assessed from normoxia (fraction of inspired oxygen [FiO_2] = 20.9%) to acute poikilocapnic hypoxia (FiO_2 = 12.0%). The blood flow response to hypoxia is presented as the absolute change ($\Delta\text{mL}\cdot\text{min}^{-1}$; a and b) and the relative change ($\Delta\%$; c and d) from resting normoxic blood flow ($\text{mL}\cdot\text{min}^{-1}$). Data plots include the left and right vessels of the ICA and the VA.

Figure 4.4. Bland-Altman plots of the measurement bias between a unilateral assessment of the vessel with the smaller or larger resting normoxic blood flow and the bilateral calculation of the relative change in blood flow from normoxia to acute poikilocapnic hypoxia of the extracranial arteries. Internal carotid arteries (ICA) and vertebral arteries (VA) relative blood flow response from normoxia (fraction of inspired oxygen [FiO_2] = 20.9%) to acute poikilocapnic hypoxia (FiO_2 = 12.0%) were calculated from doubling unilateral measurements of the vessel with the smaller (a and c) or larger (b and d) resting normoxic blood flow and compared to the bilateral calculation of the relative blood flow response to hypoxia. Average bias (solid black line) is reported with respective 95% confidence intervals (dashed black lines), and $\pm 1.96\text{SD}$ limits of agreement (dotted black lines).

Figure 4.5. Bland-Altman plots of the measurement bias between a unilateral assessment of the left or right vessel and the bilateral calculation of the relative change in blood flow from normoxia to acute poikilocapnic hypoxia of the extracranial arteries. Internal carotid arteries (ICA) and vertebral arteries (VA) relative blood flow response from normoxia (fraction of inspired oxygen [FiO_2] = 20.9%) to acute poikilocapnic hypoxia (FiO_2 = 12.0%) were calculated from doubling unilateral measurements of the left (a and c) or right (b and d) side and compared to the bilateral calculation of the relative blood flow response to hypoxia. Average bias (solid black line) is reported with respective 95% confidence intervals (dashed black lines), and $\pm 1.96\text{SD}$ limits of agreement (dotted black lines).

Figure 5.1. Representative illustration of the dynamic cerebral autoregulation metrics after rapid thigh cuff deflation induced hypotension. Mean arterial pressure (MAP, circle), cerebral blood flow (CBF) or velocity (CBv, square), and cerebrovascular conductance (CVC) or index (CVCi, triangle) after rapid thigh cuff method assessment of dynamic cerebral autoregulation. Data were normalised relative to their respective means during the four seconds immediately before the thigh cuff release. In accordance with previous methods (Labrecque et al., 2021), dCA after rapid thigh cuff deflation was characterised as the following metrics: 1) maximal reduction, 2) time to counter-regulation, and 3) rate of regulation (RoR).

Figure 5.2. Rate of regulation following rapid thigh cuff deflation induced hypotension in normoxia and hypoxia. Rate of regulation (RoR) of the extracranial internal carotid (ICA) and vertebral (VA) arteries (a) and of the intracranial middle cerebral (MCA) and posterior cerebral (PCA) arteries (b) in normoxia (white bars, fraction of inspired oxygen [FiO_2] = 20.9%) and acute poikilocapnic hypoxia (grey bars, FiO_2 = 12.5%). Data are raw means (standard deviation) and are presented with individual responses of a mixed cohort of men and women. Data were analysed by linear mixed model analysis.

Figure 5.3. Rate of regulation following rapid thigh cuff deflation induced hypotension and pre-thigh cuff deflation vessel diameter in normoxia and hypoxia in men. Rate of regulation (RoR) and vessel diameter of the ICA (a and b) and VA (c and d) in normoxia (white bars, fraction of inspired oxygen [FiO_2] = 20.9%) and acute poikilocapnic hypoxia (grey bars, FiO_2 = 12.5%) in men (N = 13). Data are raw means (standard deviation) and are presented with individual responses. Data were analysed by linear mixed model analysis.

Figure 5.4. Cerebrovascular responses after thigh cuff deflation induced hypotension in normoxia and hypoxia. Maximal relative reduction in cerebrovascular conductance (CVC) or index (CVCi) and time to CVC or CVCi counter-regulation in the extracranial (a and c) internal carotid (ICA) and vertebral (VA) arteries and the intracranial (b and d) middle cerebral (MCA) and posterior cerebral (PCA) arteries in normoxia (white bars, fraction of inspired oxygen [FiO_2] = 20.9%) and acute poikilocapnic hypoxia (grey bars, FiO_2 = 12.5%). Data are raw

means (standard deviation) and are presented with individual responses of a mixed cohort of men and women. Data were analysed by linear mixed model analysis.

Figure 6.1. Cerebrovascular response from low to high visual input in the intracranial and extracranial arteries in normoxia. Relative change from low (lights off – eyes closed) to high (lights on – eyes open) visual input in blood velocity (a, $P = 0.02$) of the middle cerebral artery (MCA) and posterior cerebral artery (PCA), and blood velocity (b, $P = 0.08$), vessel diameter (c, $P = 0.23$), and blood flow (d, $P = 0.31$) of the internal carotid artery (ICA) and vertebral artery (VA) in normoxia (fraction of inspired oxygen = 20.9%). Variables were analysed by a linear mixed model analysis with the primary outcome of interest was the effect of region, adding participant as random effect. Additional fixed effects of interest (e.g., sex or P_{ETCO_2}) did not change the statistical outcome for any other variable. Data are raw data means (standard deviation) with individual data points. * $P < 0.05$ between regions. † $P < 0.08$ between regions.

Figure 6.2. Visual stimulation in normoxia reduced dynamic cerebral autoregulation in the posterior but not anterior circulation. Very low frequency (VLF) phase of blood velocity in the middle cerebral artery (MCA) and posterior cerebral artery (PCA) during spontaneous oscillations in blood pressure at rest in low (lights off – eyes closed) to high (lights on – eyes open) visual input in normoxia (fraction of inspired oxygen = 20.9%). Variables were analysed by a linear mixed model analysis with the primary outcome of interest the interaction effect of visual input (low and high) and region (MCA and PCA), adding participant as random effect and partial pressure of end-tidal carbon dioxide (P_{ETCO_2}) at rest since it that improved the model fit using the Chi-square likelihood ratio test. Data are presented as estimated marginal mean (estimated standard deviation). * $P < 0.05$ between low and high visual input for PCA. † $P < 0.05$ between region.

Figure 6.3. Cerebrovascular response from low to high visual input in the intracranial and extracranial arteries in acute hypoxia. Relative change from low (lights off – eyes closed) to high (lights on – eyes open) visual input in blood velocity (a, $P < 0.05$) of the middle cerebral artery (MCA) and posterior cerebral artery (PCA), and blood velocity (b, $P < 0.05$), vessel diameter (c, $P = 0.98$), and blood flow (d, $P = 0.08$) of the internal carotid artery (ICA) and vertebral artery (VA) in normoxia (fraction of inspired oxygen = 20.9%). Variables were analysed by a linear mixed model analysis with the primary outcome of interest was the effect of region, adding participant as random effect. The addition of sex as a fixed factor to the change in blood velocity of the extracranial arteries improved the model fit and revealed that this regional difference was present in men only [Men; ICA, -1.7 (11.3) % and VA, 13.5 (14.8) %, $P < 0.05$, Women; ICA, 4.7 (7.4) % and VA, -1.1 (10.2) %, $P = 0.39$]. Data are raw data means (standard deviation) with individual data points. * $P < 0.05$ between regions. † $P < 0.08$ between region.

List of Tables

Table 2.1. Cerebral autoregulation during hypoxia. Abbreviations; AMS, acute mountain sickness; ARI, autoregulatory index; BBB, blood-brain barrier; CA, cerebral autoregulation; CCAbf, common carotid artery blood flow; CCAdia, common carotid artery diameter; D, day; dCA, dynamic cerebral autoregulation; EX, exercise; F, female; FiO₂, fraction of inspired oxygen; HA, high altitude; HH, hypobaric hypoxia; HLs, highlanders; ICAbf, internal carotid artery blood flow; IH, isocapnic hypoxia; LBNP, lower body negative pressure; LLs, lowlanders; MAP, mean arterial pressure; MCA_v, middle cerebral artery velocity; NH, normobaric hypoxia; PCA_v, posterior cerebral artery velocity; P_{ET}CO₂, partial pressure of end-tidal carbon dioxide; P_{ET}O₂, partial pressure of end-tidal oxygen; PH, poikilocapnic hypoxia; RoR, rate of regulation; TCD, transcranial Doppler ultrasound; TFA, transfer function analysis; Wk, Week.

Table 3.1. Between-trial variation of cerebrovascular haemodynamics of the extracranial arteries at rest using Siemens duplex ultrasound with 100 h of logged practice. Extracranial arteries were measured on two trials separated by at least 24 h. The left and right common carotid, internal carotid, and vertebral arteries were assessed by the left- and right-hand, respectively. The coefficient of variation (CV) and intra-class correlation (ICC) were calculated as an index of inter-rater reliability. Values are means ± standard deviation.

Table 3.2. Between-trial variation of cerebrovascular haemodynamics of the extracranial arteries at rest using Terason duplex ultrasound with 200 h of logged practice. The extracranial arteries were measured on two trials separated by at least 24 h. The left and right common carotid, internal carotid, and vertebral arteries were assessed by the left- and right-hand, respectively. The coefficient of variation (CV) and intra-class correlation (ICC) were calculated as an index of inter-rater reliability. Values are means ± standard deviation.

Table 3.3. Between-trial variation of blood velocity of the intracranial arteries at rest using Spencer Technologies transcranial Doppler ultrasound. The intracranial arteries were measured on two trials separated by at least 24 h. The coefficient of variation (CV) and intra-class correlation (ICC) were calculated as an index of inter-rater reliability. Values are means ± standard deviation.

Table 4.1. Cardiorespiratory responses to normoxia and acute poikilocapnic hypoxia. Data were collected during a seated baseline and during supine rest between 30–90 min in a temperature [26 (2) °C] and humidity [30 (4) %] controlled environmental chamber during normoxia (fraction of inspired oxygen [FiO₂] = 20.9%) and acute poikilocapnic hypoxia (FiO₂ = 12.0%). Linear mixed model analysis was completed for the period of supine rest. Values are

mean (SD). Abbreviations: SpO₂, peripheral arterial oxygen saturation; MAP, mean arterial pressure; PETCO₂, partial pressure of end-tidal carbon dioxide; $\dot{V}E$, minute ventilation.

Table 4.2. Extracranial artery blood flow, vessel diameter, and flow velocity in normoxia and acute poikilocapnic hypoxia. Blood flow (mL·min⁻¹), vessel diameter (mm), and flow velocity (time-averaged maximum velocity; cm·s⁻¹) were assessed in the left and right internal carotid arteries (ICA) and vertebral arteries (VA) during normoxia (fraction of inspired oxygen [FiO₂] = 20.9%) and acute poikilocapnic hypoxia (FiO₂ = 12.0%). Left and right vessel blood flows were calculated by doubling unilateral measurements, whereas bilateral blood flow was calculated as the sum of left and right unilateral measurements. Data are mean (SD) of the raw values, with the absolute (Δ) and relative change ($\Delta\%$) from normoxia. Linear mixed model analysis revealed no ‘Condition’ (normoxia or hypoxia) \times ‘Vessel Type’ (ICA or VA) \times ‘Vessel Side’ (left or right) interaction for blood flow (a, mL·min⁻¹; $P = 0.62$), vessel diameter (b, mm; $P = 0.70$), and flow velocity (c, cm·s⁻¹; $P = 0.64$), with ‘Participant ID’ as a random effect. LMM revealed no ‘Condition’ \times ‘Vessel Side’ interactions. * Interaction effect of ‘Condition’ \times ‘Vessel Type’ ($P < 0.001$).

Table 5.1. Cardiorespiratory and cerebrovascular responses before the rapid thigh cuff method in normoxia and hypoxia. Data were analysed by linear mixed model analysis. The primary outcome of interest for these cardiorespiratory and cerebrovascular variables was the effect of condition (normoxia and acute poikilocapnic hypoxia). Abbreviations: PETCO₂, partial pressure of end-tidal carbon dioxide; PETO₂, partial pressure of end-tidal oxygen; SpO₂, peripheral arterial oxygen saturation. Data are raw means (standard deviation).

Table 5.2. Haemodynamic responses to the rapid thigh cuff deflation induced hypotension in normoxia and hypoxia. Data were analysed by linear mixed model analysis. The primary outcome of interest for mean arterial pressure and cerebrovascular variables was the effect of condition (normoxia and acute poikilocapnic hypoxia). Data are raw means (standard deviation).

Table 6.1. Cardiorespiratory and cerebrovascular responses to low (lights off – eyes closed) and high (lights on – eyes open) visual input in normoxia (fraction of inspired oxygen = 20.9%). Data were analysed by a linear mixed model analysis. The primary outcome of interest for cardiorespiratory variables was the effect of visual input (low and high). The primary outcome of interest for cerebrovascular variables was the effect of interaction of visual input and region (anterior and posterior) with the intracranial (middle cerebral artery and posterior cerebral artery) or extracranial arteries (internal carotid artery and vertebral artery). There was no interaction effect between condition and region for any intracranial or extracranial cerebrovascular variable (all $P > 0.05$). * Main effect of condition ($P < 0.05$) † Main effect of region ($P < 0.05$). Additional fixed effects of interest (e.g., sex or PETCO₂) did

not change the statistical outcome for any other variable. Abbreviations: P_{ETCO_2} , partial pressure of end tidal carbon dioxide; P_{ETO_2} , partial pressure of end tidal oxygen; S_pO_2 , peripheral oxygen saturation. Values are raw data means (standard deviation).

Table 6.2. Transfer function analysis of the intracranial arteries during spontaneous oscillations in blood pressure in low (lights off – eyes closed) and high (lights on – eyes open) visual input in normoxia. Transfer function metrics of the middle cerebral artery and posterior cerebral artery at very low (0.02–0.07 Hz), low (0.07–0.2 Hz), and high (0.2–0.5 Hz) frequencies were collected during a period of seated rest with low and high visual input in normoxia (fraction of inspired oxygen = 20.9%). To accommodate for uneven group sizes, data were analysed by a linear mixed model analysis. The primary outcome of interest was the interaction effect of visual input (low and high) and region (middle cerebral artery and posterior cerebral artery), adding participant as random effect. Partial pressure of end-tidal carbon dioxide (P_{ETCO_2}) at rest was also added into the model as a covariate for each variable and model fits were compared using the Chi-square likelihood ratio test. The model which had the best fit is reported for each variable. * Main effect of visual input ($P < 0.05$). † Main effect of region ($P < 0.05$). ^a Interaction effect when modelled with P_{ETCO_2} ($P < 0.05$). ^b Main effect of visual input when modelled with P_{ETCO_2} ($P < 0.05$). ^c Main effect of region when modelled with P_{ETCO_2} ($P < 0.05$). Additional fixed effects of interest (e.g., sex or P_{ETCO_2}) did not change the statistical outcome for any other variable. Abbreviations: CBV, cerebral blood velocity; MAP, mean arterial pressure; nGain, normalised gain. Values are raw data means (standard deviation).

Table 6.3. Cardiorespiratory and cerebrovascular responses to low (lights off – eyes closed) and high (lights on – eyes open) visual input in acute poikilcapnic hypoxia (fraction of inspired oxygen = 12.5%). Data were analysed by a linear mixed model analysis. The primary outcome of interest for cardiorespiratory variables was the effect of visual input (low and high). The primary outcome of interest for cerebrovascular variables was the effect of interaction of visual input and region (anterior and posterior) with the intracranial (middle cerebral artery and posterior cerebral artery) or extracranial arteries (internal carotid artery and vertebral artery). There was no interaction effect between condition and region for any intracranial or extracranial cerebrovascular variable (all $P > 0.05$). * Main effect of condition ($P < 0.05$) † Main effect of region ($P < 0.05$). Additional fixed effects of interest (e.g., sex or P_{ETCO_2}) did not change the statistical outcome for any other variable. Abbreviations: P_{ETCO_2} , partial pressure of end tidal carbon dioxide; P_{ETO_2} , partial pressure of end tidal oxygen; S_pO_2 , peripheral oxygen saturation. Values are raw data means (standard deviation).

Table 6.4. Transfer function analysis of the intracranial arteries during spontaneous oscillations in blood pressure in low (lights off – eyes closed) and high (lights on – eyes open) visual input in acute poikilocapnic hypoxia. Transfer function metrics of the middle cerebral artery and posterior cerebral artery at very low (0.02–0.07 Hz), low (0.07–0.2 Hz), and high (0.2–0.5 Hz) frequencies were collected during a period of seated rest with low and high visual input in acute poikilocapnic hypoxia (fraction of inspired oxygen = 12.5%). To accommodate for uneven group sizes, data were analysed by a linear mixed model analysis with the primary outcome of interest the interaction effect of visual input (low and high) and region (middle cerebral artery and posterior cerebral artery), adding participant as random effect. Partial pressure of end-tidal carbon dioxide (P_{ETCO_2}) at rest was also added into the model as a covariate for each variable and model fits were compared using the Chi-square likelihood ratio test. The model which had the best fit is reported for each variable. * Main effect of visual input ($P < 0.05$). † Main effect of region ($P < 0.05$). ^a Interaction effect when modelled with P_{ETCO_2} ($P < 0.05$). ^b Main effect of visual input when modelled with P_{ETCO_2} ($P < 0.05$). ^c Main effect of region when modelled with P_{ETCO_2} ($P < 0.05$). Additional fixed effects of interest (e.g., sex or P_{ETCO_2}) did not change the statistical outcome for any other variable. Abbreviations: CBV, cerebral blood velocity; MAP, mean arterial pressure; nGain, normalised gain. Values are raw data means (standard deviation).

List of Abbreviations

Δ	absolute change
$\Delta\%$	relative change
°	degrees
°C	degrees Celsius
ACA	anterior cerebral artery
ANCOVA	analysis of covariance
BA	basilar artery
BOLD	blood oxygen level dependent
bpm	beats per minute
Ca ²⁺	calcium ion
CCA	common carotid artery
CI	confidence interval
cm	centimetre
CV	coefficient of variation
CVC	cerebrovascular conductance
CVCi	cerebrovascular conductance index
dCA	dynamic cerebral autoregulation
dL	decilitre
ECA	external carotid artery
FiO ₂	fraction of inspired oxygen
FMD	flow-mediated dilation
h	hour
H ⁺	hydrogen ion
HF	high frequency
Hz	hertz
ICA	internal carotid artery
ICC	intra-class correlation
K ⁺	potassium ion
kg	kilogram

L	litre
LF	low frequency
LMM	linear mixed model
MAP	mean arterial pressure
MCA	middle cerebral artery
MHz	megahertz
min	minute
mL	millilitre
mm	millimetre
mmHg	millimetres of mercury
MRI	magnetic resonance imaging
N	number
nGain	normalised gain
PCA	posterior cerebral artery
PCO ₂	partial pressure of carbon dioxide
PET	positron emission tomography
PETCO ₂	partial pressure of end-tidal carbon dioxide
PETO ₂	partial pressure of end-tidal oxygen
PO ₂	partial pressure of oxygen
RoR	rate of regulation
s	second
SD	standard deviation
SEM	standard error of the mean
S _p O ₂	peripheral oxygen saturation
TAM _x	time-averaged maximum velocity
TCD	transcranial Doppler ultrasound
VA	vertebral artery
VE	minute ventilation
VLF	very low frequency
yr	years

Chapter One

General introduction

The brain is a highly metabolically active organ that constitutes only 2% of body mass yet receives a disproportionate portion (up to 20%) of cardiac output to compensate for its limited capacity to store metabolites (Raichle & Gusnard, 2002). Accordingly, nutrient- and oxygen-rich cerebral blood flow is tightly coupled with cerebral oxygen delivery in the face of dynamic changes to oxygen supply and demand (Ainslie et al., 2016). Several overlapping mechanisms, such as chemoregulation, cerebral autoregulation, and neurovascular coupling work integratively to regulate cerebral blood flow (Ainslie & Duffin, 2009; Claassen et al., 2021). Too little or too much cerebral blood flow can cause neurocognitive symptoms and disorders such as headaches and slowed mental processing or, if left untreated, severe life-threatening complications like ischaemic injury, stroke, and death (Ainslie & Brassard, 2014; Claassen et al., 2021). The maintenance of cerebral blood flow is also important for optimal brain function and health throughout life. Indeed, progressive decline of cerebral blood flow with ageing is related to cognitive decline (Tarumi & Zhang, 2018), and an exaggeration of this age-related decline is one of the earliest biomarkers of Alzheimer's disease (Korte et al., 2020).

Recent evidence suggests that neurodegenerative disease-related reductions in cerebral blood flow are not uniform at the brain capillary beds (i.e., microvasculature) (Swinford et al., 2023; Weijs et al., 2023; H. Zhang et al., 2021). Furthermore, regional differences in blood flow regulation of the posterior compared to anterior cerebral conduit arteries may explain the stronger association of the posterior arteries with cerebrovascular and cardiovascular diseases (Hart, 2016; Liu et al., 2016; Ryan et al., 2015), age-related declines (Olesen et al., 2019), and pathophysiological conditions, such as acute mountain sickness (Barclay et al., 2021; Bian et al., 2014), orthostatic (in)tolerance (Kay & Rickards, 2016) and migraine (Chuang et al., 2012).

Regional differences in cerebral blood flow regulation may exist upstream of the capillary beds at the extra- and intra-cranial cerebral conduit arteries (i.e., large vasculature) given that the cerebral conduit arteries are known to modulate vessel tone to regulate cerebral blood flow (Coverdale et al., 2014; Liu et al., 2013; Verbree et al., 2014, 2017). Structural and functional differences between the cerebral conduit arteries that feed the anterior and posterior regions of the brain (Koep et al., 2022) may exist to preferentially preserve cerebral blood flow to the posterior regions involved in homeostatic, autonomic, and cardiorespiratory control (Sato, Sadamoto, et al., 2012; Willie et al., 2012), particularly during physiological stress such as orthostasis (Sato, Fisher, et al., 2012), and hypoxia (Kellawan et al., 2017; Lewis et al., 2014; Ogoh et al., 2013; Willie et al., 2012). This regional difference highlights that exposure to physiological stressors can be useful to elucidate the regulatory mechanisms of the cerebral circulation because the additional stress requires compensatory homeostatic responses. A reduction in oxygen availability in hypoxia is a particularly relevant manipulation to aid understanding of pathology as clinical populations are often afflicted with hypoxia.

Additional investigation of the cerebral conduit arteries during physiological stress, such as hypoxia, is warranted due to its importance in understanding regional differences in blood flow regulation. Indeed, evidence of regional differences in the mechanisms that regulate cerebral blood flow, such as chemoregulation, cerebral autoregulation, and neurovascular coupling remains conflicting or largely unexplored. Several ultrasound techniques are available to assess the cerebral conduit arteries non-invasively, with a high temporal resolution. Such high temporal resolution is essential to capture the dynamic nature of cerebrovascular regulation, that may be missed if other techniques, such as magnetic resonance imaging, are relied upon.

Therefore, the aim of this thesis was to investigate regional blood flow regulation between the cerebral conduit arteries that source the anterior and posterior regions of the brain in acute poikilocapnic hypoxia.

Chapter Two

Literature review

2.1 Cerebral conduit artery anatomy

The network of cerebral conduit arteries that deliver blood to the brain can be segmented into the extracranial arteries located outside of the cranium and the intracranial arteries located inside the cranium (Figure 2.1). Oxygenated blood ejected from the left ventricle through the aortic arch ascends towards the cerebrum via one of three major arteries located below the clavicle: the left common carotid artery, the left subclavian artery, and the brachiocephalic trunk, which in turn subdivides into the right subclavian artery and right common carotid artery. The common carotid arteries (Figure 2.1, purple) are the largest extracranial arteries in the neck and carry the greatest quantity of cerebral blood flow. At the distal end of each common carotid artery is the carotid bifurcation where each common carotid artery subdivides into the external carotid artery (Figure 2.1, brown) and the internal carotid artery (Figure 2.1, light blue). The external carotid artery supplies blood to areas outside of the cranium, including the neck, head, and face, whilst the internal carotid artery supplies blood to the cerebrum and the anterior regions of the brain. Located posteriorly in the neck, the vertebral arteries (Figure 2.1, pink) originate from the subclavian arteries and ascend parallel to the vertebrae from C6. The vertebral arteries provide circulation to the posterior and infratentorial regions of the brain before merging to form the basilar artery (Figure 2.1, yellow) within the cranium at the base of the pons. Total cerebral blood flow delivery can be calculated as the sum of the internal carotid arteries and vertebral arteries, with the relative internal carotid artery to vertebral artery contributions estimated to be 75% and 25%, respectively (Schöning et al., 1994; Zarrinkoob et al., 2015).

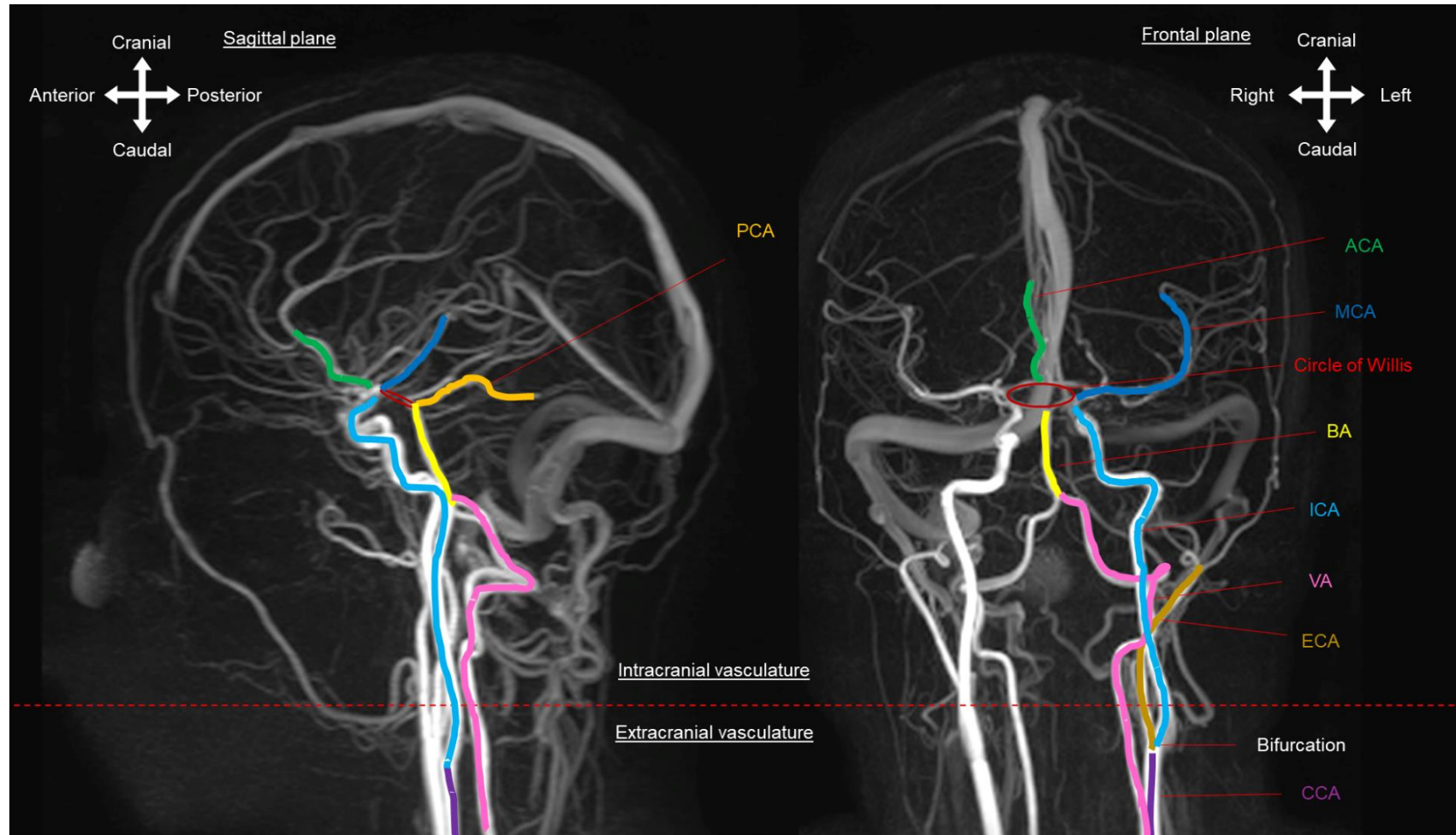


Figure 2.1. The anatomical structure of the cerebral conduit artery network. Image was acquired using magnetic resonance angiography. The purple, light blue, dark blue, and green pathway reflects the anterior circulation through the common carotid artery (CCA), internal carotid artery (ICA), middle cerebral artery (MCA), and anterior cerebral artery (ACA), respectively. The purple and brown pathway reflects the CCA and the external carotid artery (ECA) that perfuses structures of the neck, head, and face. The pink, yellow, and orange pathway reflects the posterior circulation through the vertebral artery (VA), basilar artery (BA), and posterior cerebral artery (PCA), respectively.

As they ascend into the cranial cavity, the internal carotid arteries give rise to the middle cerebral arteries (Figure 2.1, dark blue), which extend laterally, and the anterior cerebral arteries (Figure 2.1, green), which extend anteriorly to form the anterolateral portion of the circle of Willis. Blood from the internal carotid and middle cerebral arteries perfuse the cerebrum, including the motor and somatosensory cortices in the frontal and parietal lobes. The basilar artery gives rise to the posterior cerebral artery (Figure 2.1, orange) that forms the posterolateral portion of the circle of Willis. Blood from the basilar artery and posterior cerebral arteries feed the homeostatic, autonomic, and cardiorespiratory control brain regions, including the pons, medulla oblongata, thalamus, brainstem, and cerebellum. The posterior communicating artery connects the internal carotid/middle cerebral/anterior cerebral artery complex to the posterior cerebral arteries and the anterior communicating artery connects the two anterior cerebral arteries. These communicating arteries complete the ring-like structure of the circle of Willis and provide an avenue for collateral and compensatory circulation. From here, smaller branching arterioles extend from the intracranial arteries and vascularize the brain surface before pial arteries penetrate the cortex. Cerebral blood flow delivery from the cerebral conduit arteries can be categorised regionally by those that supply the anterior regions of the brain (Figure 2.2, blue and green, i.e., internal carotid and middle cerebral arteries) and those that supply the posterior regions of the brain (Figure 2.2, yellow and orange, i.e., the vertebral and posterior cerebral arteries) (Sato, Sadamoto, et al., 2012; Willie et al., 2012).

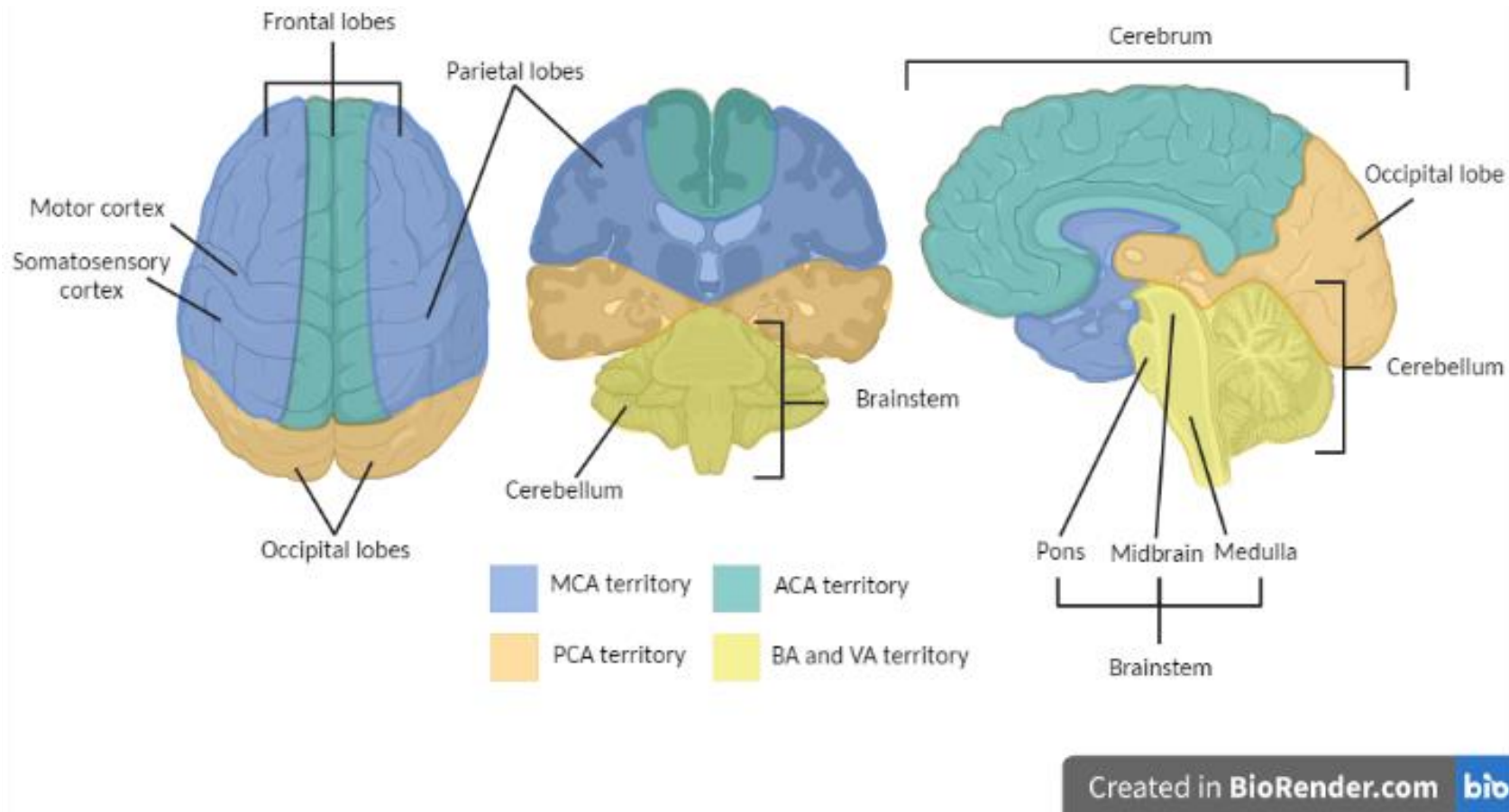


Figure 2.2. Cerebral conduit arteries supply blood flow to different regions of the brain. The cerebral conduit arteries can be categorised into those that supply the anterior regions and those that supply the posterior regions of the brain. The middle cerebral artery (MCA, blue) and anterior cerebral artery (ACA, green) supply the anterior motor and somatosensory cortices within the frontolateral and parietal lobes. The posterior cerebral artery (PCA, orange) supplies the thalamus above the midbrain and visual cortices within the occipital lobes. The upper portion of the vertebral artery (VA) and basilar artery (BA, yellow) supply the cerebellum and cardiorespiratory control brain regions, such as the pons, midbrain, and medulla that form the brainstem. Created with BioRender.com.

2.2 Doppler ultrasound assessment of cerebral blood flow

Cerebral blood flow can be assessed by several techniques. Invasive quantification of volumetric cerebral blood flow and cerebral metabolism was revolutionised with the Kety-Schmidt technique using the arterio-venous difference of inhaled nitrous oxide over a ten-minute period (Kety & Schmidt, 1945). Positron emission tomography is considered the reference standard for cerebral blood flow measurements, which requires injection of the radiotracer [^{15}O]-water that is absorbed by the cerebral tissues and the emitted radioactivity is detected by the scanner as a measure of brain perfusion (Fan et al., 2016). High spatial resolution whole-brain imaging with magnetic resonance imaging is also available, with several modalities including blood oxygen level dependent (BOLD) imaging for the assessment of neuronal activation, arterial spin labelling for tissue perfusion mapping, and four-dimensional blood flow quantification angiography within the cerebral arteries (Arngrim et al., 2016; Buck et al., 1998; Harris et al., 2013; Kellawan et al., 2017). The invasive nature, lower temporal resolution for beat-to-beat integration with other cardiorespiratory variables, high cost of assessment, additional requirements for specialist persons, and limitations to patient positioning and movement may preclude the use of these techniques as an appropriate measurement to capture the dynamic nature of cerebrovascular regulation.

Doppler ultrasound is a non-invasive, portable technique with high temporal resolution that can be used to produce real-time measurements of cerebral haemodynamics (Ng & Swanevelder, 2011; Oglat et al., 2018). High-frequency sound waves are emitted from the transducer and propagate through soft tissue to be either absorbed by the tissue or reflected to the transducer. Within an insonated blood vessel, the velocities of all moving blood cells are presented as a spectral display forming the Doppler signal and are calculated from the difference between the received and transmitted pulses using the Doppler frequency shift formula, also known as the

Doppler Principle (Ng & Swanevelder, 2011; Oglat et al., 2018). Transcranial Doppler ultrasound (TCD) and duplex ultrasound use the Doppler Principle and are commonly used to assess cerebral haemodynamics of the cerebral conduit arteries.

2.2.1 Transcranial Doppler ultrasound

The blood velocity of the intracranial arteries can be assessed using TCD (Aaslid et al., 1982). Small transducers emit low frequency ultrasound signals (2.0–3.5 MHz) that can travel through specific thin portions of the skull, known as acoustic windows, to enable the insonation of the major intracranial arteries, such as the middle cerebral artery (Figure 2.3). These probes are secured to the skull with the addition of a headband to maintain a fixed position for continuous measurements of blood velocity. The sonographer is required to insonate the strongest possible signal of a vessel by the audible and visual Doppler shift only. Whilst a variety of acoustic windows help achieve the advised lowest possible Doppler angle to minimise error of blood velocity measurements, the angle of insonation and subsequent measurement error is unknown. Therefore, TCD ultrasound only estimates the blood velocity measurement of a vessel from the spectral Doppler signal and can only be used as an index of cerebral blood flow since it does not provide an image of the vessel calibre. TCD is regularly used as an index of cerebral blood flow under the assumption that the intracranial arteries do not change in diameter, however emerging evidence of vasoactive responses in the intracranial arteries has led to an increased awareness of its utility and validity in investigations of cerebrovascular regulation (Ainslie & Hoiland, 2014). The high temporal resolution of TCD, coupled with time aligned beat-to-beat and breath-by-breath cardiorespiratory measurements, stability of signal, and low operator dependency once a signal is achieved makes TCD a widely accepted method to capture cerebral haemodynamics during dynamic movements where it may otherwise be difficult with other methods (e.g., squat-to-stand, exercise).

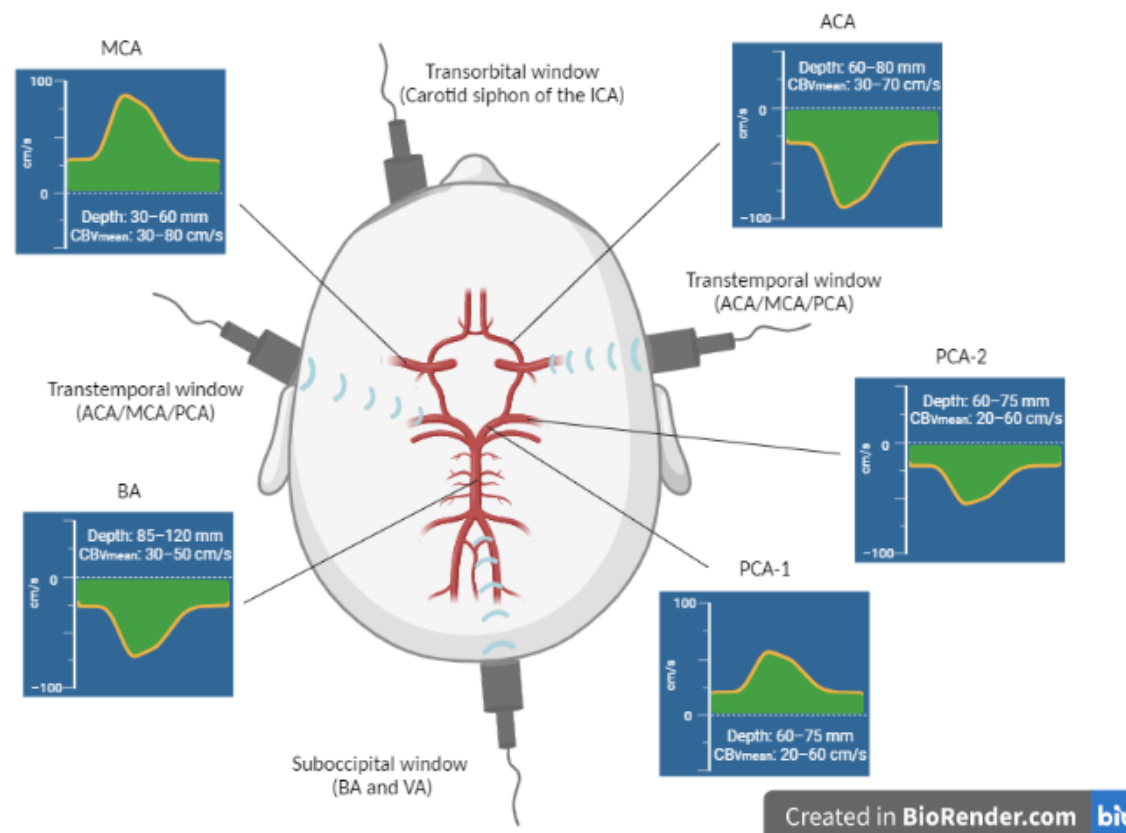


Figure 2.3. Transcranial Doppler ultrasound of the intracranial cerebral conduit arteries. Transcranial Doppler ultrasound is a non-invasive device with high temporal resolution that captures beat-to-beat measurements of intracranial artery haemodynamics. Four acoustic windows are used in transcranial Doppler ultrasound. The transtemporal window is used for insonation of the anterior cerebral artery (ACA), middle cerebral artery (MCA), and posterior cerebral artery (PCA) before (PCA-1) or after (PCA-2) the posterior communicating artery. The suboccipital window is used for insonation of the basilar artery (BA) and upper portions of the vertebral artery (VA). The transorbital window is used for the insonation of the carotid siphon segment of the internal carotid artery (ICA) and ophthalmic artery. The submandibular window (not shown) is located under the chin for insonation of the distal portion of the ICA. A representative example of the Doppler spectra waveform, vessel depth, and mean cerebral blood velocity (CBV_{mean}) accompany each intracranial artery. Created with BioRender.com.

2.2.2 Duplex ultrasound

Duplex ultrasound concurrently measures blood velocity and vessel diameter of a vessel to estimate volumetric blood flow (Figure 2.4). Handheld transducers emit high frequency ultrasound signals (10–15 MHz) through soft tissue structures at the neck to enable the insonation of the extracranial arteries, including the internal carotid and vertebral arteries. These high frequency probes provide blood velocity measurements from the spectral Doppler signal (Pulse-wave Doppler imaging) and high-spatial resolution measurements of vessel diameter from a greyscale 2-dimensional image where the brightness of the image is based on the intensity of each reflected sound wave and its depth (B-Mode Imaging). Most ultrasound systems can only record a brief period (< 30 s) of images and have a small storage capacity, so real-time images are screen-grabbed using an external screen capture system (e.g., Camtasia), stored, and processed offline later. Modern duplex ultrasound methodologies use automated edge-detection software to minimise investigator bias in blood vessel diameter measurements. Several commercial (Medical Imaging Applications' Vascular Research Tools, Quipu, Maui Hedgehog Medical), laboratory own brand (Woodman et al., 2001), and open source (FloWave.US) automated edge-detection software are available. A particular strength of Duplex ultrasound is it can be used to measure cerebral blood flow and the vasoactive responses of an extracranial artery at a high temporal resolution in a range of non-supine experimental procedures such as sitting, standing, and during exercise.

Doppler ultrasound techniques (TCD and duplex ultrasound) require highly skilled operators to acquire accurate high-quality images of the cerebral conduit arteries. In an untrained sonographer, tiny alterations in a spectral Doppler signal and/or a loss of resolution on the B-Mode image cause inaccuracies in diameter that cause gross deviations to cerebral blood flow volume estimations (Schoning et al., 1994, Thomas et al 2015). Before completing any

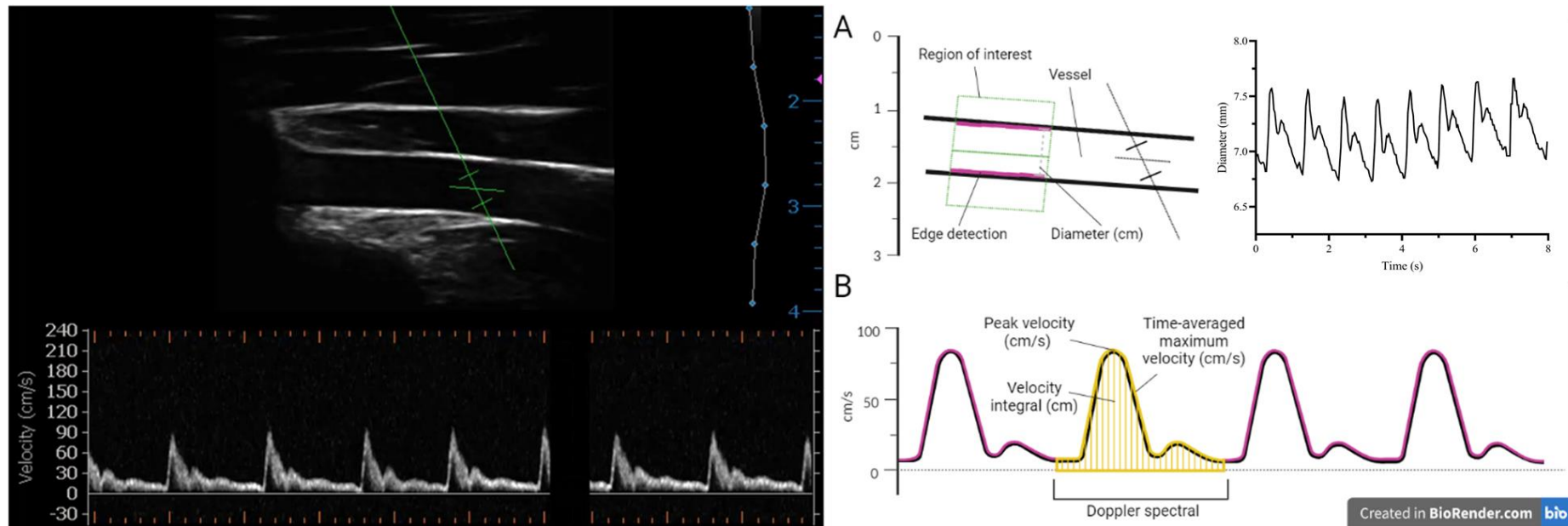


Figure 2.4. Duplex ultrasound of the extracranial cerebral conduit arteries. Concurrent measurements of vessel diameter from B-mode imaging (left, top) and blood velocity spectra from pulse wave Doppler imaging (left, bottom) are captured from the extracranial artery using Duplex ultrasound. Post-capture calculations of volumetric blood flow are captured using automated-edge detection software (right). The high spatial and temporal resolution of duplex ultrasound enables the automated wall-edge detection software to track frame-by-frame diameter changes of a specific region of interest within the vessel across each cardiac cycle (right, A). The Doppler spectral signal of one complete cardiac cycle is analysed for its peak velocity, velocity integral, and the time-averaged maximum velocity (right, B). The time-averaged maximum velocity calculates the mean from the average peak envelope velocity across the cardiac cycle. Half the time-averaged maximum velocity is estimated to be the mean blood velocity. Estimations of volumetric blood flow can be calculated from the formula: blood flow ($\text{ml}\cdot\text{min}^{-1}$) = $[\text{time-averaged maximum velocity (cm}\cdot\text{s}^{-1})/2] * [\pi * (\text{mean artery diameter (cm)}^2)] * 60$. Created with BioRender.com.

investigative research, sonographers should be thoroughly trained in the ultrasound technique and show evidence of proficiency by completing a measure of intra-rater reliability, such as the intra-class correlation coefficient (ICC) or coefficient of variation (CV) (Bahner et al., 2016; Ihnatsenka & Boezaart, 2010; Thomas et al., 2015).

To understand the regulation of the cerebral conduit arteries it is integral to measure vessel diameter and changes in vascular tone. Duplex ultrasound provides concurrent vessel diameter and blood velocity (and blood flow) measurements of the extracranial arteries that supply the intracranial arteries and can be used complimentary to TCD in partially modified dynamic procedures e.g., rapid thigh cuff deflation method for dynamic cerebral autoregulation and semi-recumbent cycling for exercise testing. Utilizing complimentary Doppler ultrasound methodologies (TCD and duplex ultrasound) to enable an integrative view of upstream (i.e., extracranial arteries) and downstream (i.e., intracranial arteries) cerebral conduit artery function is frequently employed (Lewis et al., 2015; Sato, Sadamoto, et al., 2012; Washio et al., 2022; Willie et al., 2012).

2.3 Cerebral conduit artery anatomical variability

The influence of anthropometrics on the cerebrovasculature have been explored previously (Hwaung et al., 2019; Krejza et al., 2006), whereas the influence of within-individual variability between lateral pairs of a cerebral conduit artery has been less researched. The classic circle of Willis structure is reported to be present in 20–51% of the population with the remaining population exhibiting either a missing vessel(s) forming an incomplete circle of Willis or exhibiting a hypoplastic vessel(s) forming a complete yet abnormal circle of Willis (Krabbe-Hartkamp et al., 1998; Riggs & Rupp, 1963; Ryan et al., 2015; Zarrinkoob et al., 2015). An incomplete or abnormal circle of Willis is associated with the development of white matter disease (Ryan et al., 2015), increased risk of stroke (Chuang et al., 2008), and increased

risk of infarcts (Zhou et al., 2016). Blood velocity of the intracranial arteries tend to be reported as similar between lateral pairs, but the accuracy of these values is unclear as the measurements are essentially captured ‘blind’ because there is no visualisation of the Doppler angle, therefore the angle is likely to be inconsistent both between and within individuals. Whilst speculative, there may be an unconscious bias against finding any within-individual differences because historically there has been an arbitrary set value for identification of an intracranial artery (i.e., guidance suggests basal middle cerebral artery velocity is 50cm/s).

In the extracranial arteries, whilst the common carotid and internal carotid arteries tend to have comparable vessel diameters and blood flow between lateral pairs, 68–97% of individuals exhibit asymmetrically sized vertebral arteries (Figure 2.5) (Gaigalaite et al., 2016; Jeng & Yip, 2004; Katsanos et al., 2013). Asymmetrical vessel diameters between lateral vertebral arteries are reported to cause the right vertebral artery to have approximately 20–30% less blood flow than the left (Jeng & Yip, 2004; Khan et al., 2017; Schöning et al., 1994; Seidel et al., 1999). This imbalance is speculated to be the result of architectural differences at the aortic arch, which alter shear stress and vascular resistance, therefore impacting flow profiles between lateral arteries (Hu et al., 2013; van Campen et al., 2018).

Vertebral artery hypoplasia is a common type of vertebral artery imbalance whereby one vertebral artery is substantially smaller than the contralateral vertebral artery. Vertebral artery hypoplasia reduces net vertebral artery and global blood flow since there is no compensatory increase in blood flow by the non-hypoplastic contralateral artery (Chen et al., 2010) nor by the internal carotid arteries (Acar et al., 2005). This contrasts with the compensatory increase in vertebral artery blood flow observed with internal carotid artery occlusion (Nicolau et al., 2001). Incidence rates of vertebral artery hypoplasia vary greatly and are a consequence of the many definitions that may include an arbitrary threshold of the vessel diameter, or the absolute

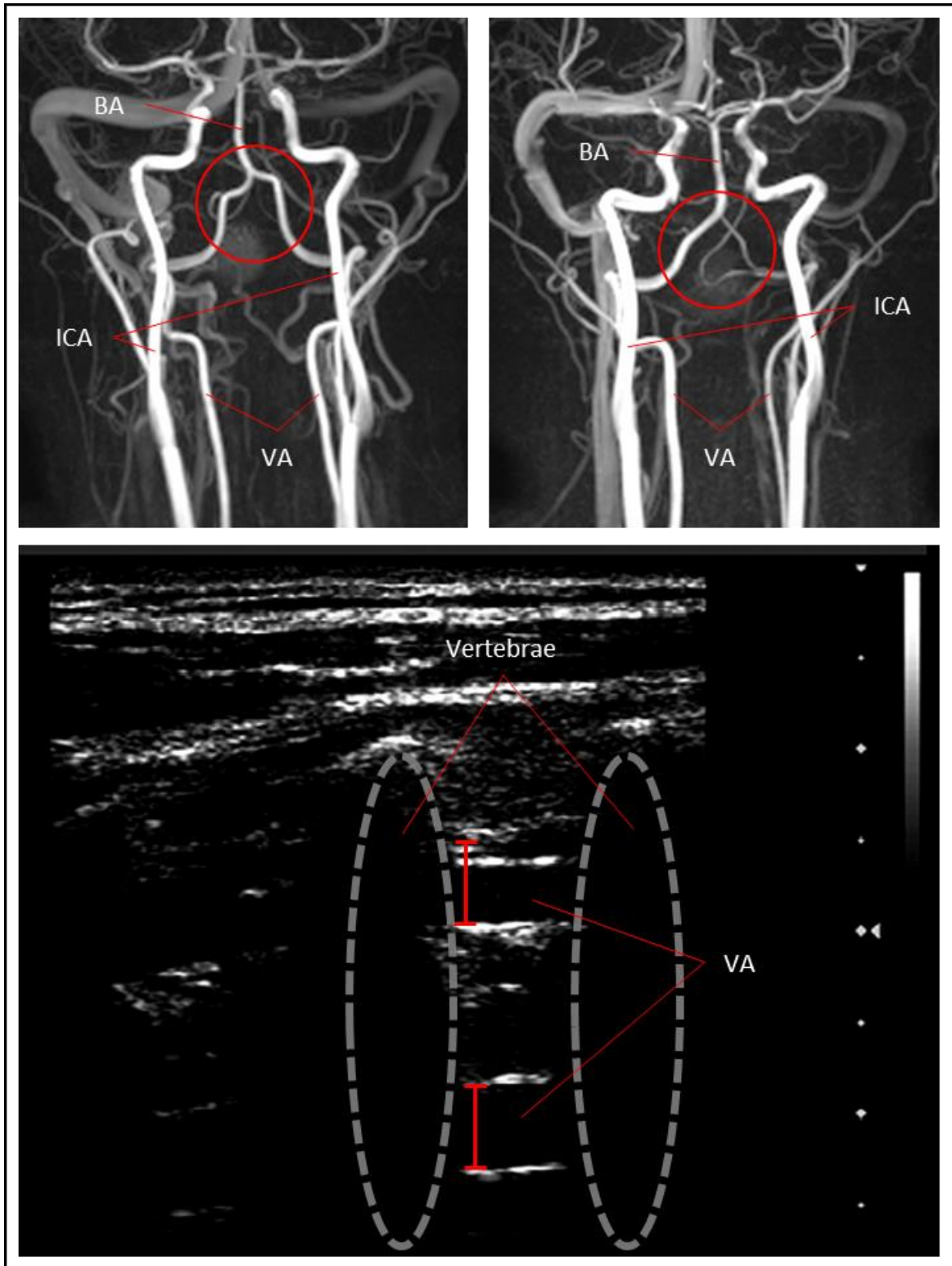


Figure 2.5. Representative example of vertebral artery imbalance. Top: Magnetic resonance angiography image of the vessel imbalances in vertebral artery (VA) calibre (red circle) before forming the basilar artery (BA), whereas the internal carotid arteries (ICA) are similar in size. Bottom: Duplex ultrasound-derived cross-section of the vertebral arteries between the vertebrae. Red line (of same length) reflects the vessel size imbalance comparison between the vertebral arteries.

differences, or ratios between lateral artery diameters (Acar et al., 2005; Chen et al., 2010; Gaigalaite et al., 2016; Jeng & Yip, 2004; Mazioti et al., 2013; Min & Lee, 2007; J. H. Park et al., 2007; Thierfelder et al., 2014).

The influence of vertebral artery hypoplasia on cerebrovascular pathophysiology is mixed. Some reports suggest of direct associations between vertebral artery hypoplasia with posterior ischaemic stroke and ischaemic posterior circulation symptoms of headache, migraine, vertigo, and syncope (Chuang et al., 2012; Gaigalaite et al., 2016; Katsanos et al., 2013; J. H. Park et al., 2007; Y. Wang et al., 2009). In contrast, some report that vertebral artery hypoplasia is frequently reported in healthy individuals suggesting that it is harmless anatomical variant, and that only in incidents of severe reductions in net vertebral artery blood flow can the vertebrobasilar pathophysiology and symptomology manifest (Jeng & Yip, 2004; Min & Lee, 2007; Touboul et al., 1986). Indeed, severe reductions in net vertebral artery blood flow (< 100ml/min), with or without hypoplasia, is defined as vertebrobasilar insufficiency (Chen et al., 2010). Incidence of vertebrobasilar insufficiency is higher in individuals with vertebral artery hypoplasia than those without (Chen et al., 2010) and is associated with symptoms of dizziness or vertigo, headaches, vomiting and nausea, imbalance, weakness, ataxia (Neto et al., 2017; Savitz & Caplan, 2005) and ischaemic attacks and infarcts in the vertebrobasilar territories (Chuang et al., 2012; Katsanos et al., 2013; Seidel et al., 1999). Furthermore, these congenital anatomical abnormalities in the posterior circulation that cause regional cerebral hypoperfusion and increased cerebrovasculature resistance are thought to instigate an elevated sympathetic nerve activity and essential hypertension to maintain cerebral perfusion in what is described as the ‘selfish brain hypothesis’ (Hart, 2016; Warnert, Hart, et al., 2016; Warnert, Rodrigues, et al., 2016).

Since there is a high incidence and a wide range of anatomical variations with the posterior cerebral conduit arteries, caution is advised with the interpretation of cerebral haemodynamic measurements of the posterior circulation (Min & Lee, 2007). Indeed, vertebral artery hypoplasia and net vertebral artery flow insufficiency are found to have lower absolute and relative carbon dioxide reactivities compared to healthy controls (Sato et al., 2015) and impact the neural-vascular coupling complex with delayed latencies during a vestibular evoked myogenic potential test (Chuang et al., 2012). Whilst associations between within-individual variability of lateral pairs of cerebral conduit arteries and symptomology is promising, the knowledge of its impact on the regulation of cerebral blood flow remains in its infancy.

It is common for investigators to complete unilateral assessment of the cerebral conduit arteries due to the technical interference that occurs between multiple probes in close vicinity to each other, the requirement of two trained sonographers, and the logistical difficulties which may come with certain experimental procedures, e.g., a short data collection window to capture the haemodynamic response. Calculations of regional and global cerebral blood flow are then doubled from a single-sided (unilateral) measurement, and cerebral conduit arteries are assumed to regulate similarly between lateral pairs. Despite the acknowledgment of side-to-side differences in basal cerebral blood flow within a vertebral artery pair (Lewis et al., 2014; Subudhi et al., 2014; Willie et al., 2012), the right vertebral artery is regularly chosen in unilateral assessments under the assumption that it is the smaller artery and that any cerebrovascular haemodynamic responses would underestimate the true value (Lewis et al., 2014). Whilst this is true for absolute values of cerebral blood flow, it is yet to be fully investigated whether the haemodynamics response (cerebral blood flow reactivity/sensitivity) between left-right cerebral conduit arteries are comparable (see Thesis Chapter 3). Whilst screening for abnormal anatomical architecture is more common (Hoiland et al., 2017), the range of vessel sizes, non-universal vessel side dominance, and hypoplasia presence is less

commonly screened, and we currently have a poor understanding of the impact these factors may have on the regulation of cerebral blood flow. This could contribute to why the posterior regions, where vessel flow imbalances are most prevalent, are reported to regulate differently from the anterior regions. Indeed, unilateral estimations may not be reflective of the true total posterior blood flow regulation of both lateral arteries.

2.4 Mechanisms of cerebral blood flow regulation

The brain requires tightly regulated mechanisms that modulate cerebral blood flow to maintain adequate perfusion for a constant nutrient and oxygen delivery, acid-base balance, and metabolic homeostasis (Hoiland et al., 2019). Mechanisms that modulate cerebral blood flow are unique within the body and require an independent understanding, such that observations from the peripheral vasculature act as a poor predictor for the cerebral vasculature (Claassen et al., 2021). The principal mechanisms of cerebral blood flow control are metabolic, neurogenic, myogenic, and endothelial and these mechanisms work as an integrative system for fundamental cerebrovascular regulatory responses such as cerebral autoregulation and neurovascular coupling (Ainslie & Duffin, 2009). The smaller microvascular pial arteries and capillaries beds within the parenchyma are regularly construed as the only site to modulate cerebrovascular resistance for maintenance of perfusion pressure and blood flow (Hoiland et al., 2019). In support of early animal model evidence (Faraci et al., 1987; Heistad et al., 1978), recent evidence in humans has confirmed that vascular tone regulation does occur outside the parenchyma within the cerebral conduit arteries (Coverdale et al., 2014; Verbree et al., 2014, 2017). Differences in the vascular tone regulation between the upstream cerebral conduit arteries relative to the downstream arteries dictate microvasculature driving pressure and blood flow (Figure 2.6). Moreover, the positive relationship between the prevalence of small and large artery diseases (Brisset et al., 2013) supports the proposal of crosstalk processes between the development of pathological dysfunction of the cerebral conduit arteries, such as

atherosclerosis and increased arterial stiffness, and the development of cerebral small vessel disease, such as white matter lesions, and its associated cognitive decline (Xu, 2014). Understanding the fundamental mechanisms underpinning the regulation of cerebral blood flow is integral when investigating for possible regional differences between conduit cerebral arteries as these mechanisms may reveal the targets to optimise resilience to, and to develop preventative therapies for, cerebrovascular diseases.





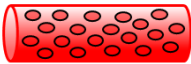









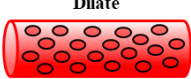









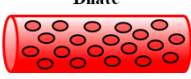





Upstream arteries e.g., extracranial arteries	Downstream arteries e.g., intracranial arteries	Blood flow	Microvascular pressure
Rest 	Rest 		
	Dilate 		
	Constrict 		
Dilate 	Rest 		
	Dilate 		
	Constrict 		
Constrict 	Rest 		
	Dilate 		
	Constrict 		

Figure 2.6. Segmental cerebrovascular regulation. An illustration of how segmental changes in vascular tone (cerebrovascular resistance) between the upstream and downstream arteries organized in-series influence flow and microvascular pressure. Upstream-downstream segmental regulation may occur between the extracranial and intracranial arteries, or between the intracranial arteries and smaller arterioles or pial arteries, or along different sections of an intracranial artery. Changes in vasoactive tone (dilation or constriction) are labelled on each artery. Directional arrows reflect the changes in blood flow and microvascular pressure for each scenario, with more arrows representing a larger magnitude of effect and a sideways arrow representing no change. All blood flow and microvascular pressure changes are relative to the top row (upstream and downstream artery both at rest). Adapted from Hoiland et al., 2019.

2.4.1 Metabolic

Maintaining an oxygen supply to the brain is dependent on arterial oxygen content and cerebral blood flow. Local increases in cerebral metabolism by neural activation are tightly coupled to local increases in cerebral blood flow using various feedforward and feedback mechanisms and is termed neurovascular coupling (see 2.5.5 *Neurovascular Coupling*) (Hoiland et al., 2019; Paulson et al., 1990; Peterson et al., 2011; Phillips et al., 2016; Willie, Tzeng, et al., 2014). Proposed mediators of neurovascular coupling include K^+ , H^+ , adenosine, and nitric oxide, which are all involved in increasing Ca^{2+} mobilization and synaptic transmission of the vascular smooth muscle to modulate arterial vascular tone (Paulson et al., 1990; Peterson et al., 2011). For example, cyclooxygenase, a prostaglandin, is involved in the regulation of basal cerebrovascular tone of the anterior and posterior intracranial and extracranial arteries (Kellawan et al., 2020), and blockade of nitric oxide synthase by L-NMMA to reduce nitric oxide bioavailability is shown to reduce global cerebral blood flow and reduce intracranial and extracranial cross-sectional area (K. J. Carter et al., 2021).

A potent metabolic regulator of cerebral blood flow is chemoregulation and refers to the response to changes in systemic carbon dioxide (and subsequent pH) and oxygen. Whilst moderate to severe hypoxia routinely evokes a cerebral blood flow response, the brain is much more sensitive to hypocapnia and hypercapnia, as such manipulations of carbon dioxide are commonly used to assess vascular reactivity (Poulin et al., 1996; Sato, Sadamoto, et al., 2012; Willie et al., 2012). The relationship between oxygen and carbon dioxide modulates the sensitivity and overall change of cerebral blood flow, such that hypercapnia increases and hypocapnia decreases the cerebral blood flow response to hypoxia (Figure 2.7). Emerging evidence suggests that the cerebral conduit arteries are sensitive to altered blood gases, which act as an upstream modulator of cerebral blood flow to maintain brain perfusion, in addition to

the well-established role of the downstream pial arteries (Willie et al., 2012; Willie, Tzeng, et al., 2014). Mechanisms that elicit the cerebrovascular response to blood gases may include the movement of carbon dioxide molecules across the blood-brain barrier and subsequent alteration to pH of the extracellular space, and hypoxia-induced increases in extracellular acidosis at the neurovascular unit or adenosine and/or nitric oxide release, each in turn activating K⁺ channels and Ca²⁺ mobilization of the vascular smooth muscle to modulate arterial vascular tone (Ainslie & Duffin, 2009; Willie, Tzeng, et al., 2014). Indeed, adenosine-triphosphate-sensitive K⁺ channels have been shown to play a key role in mediating hypoxia-induced cerebral vasodilation of the anterior circulation in humans (Rocha et al., 2020).

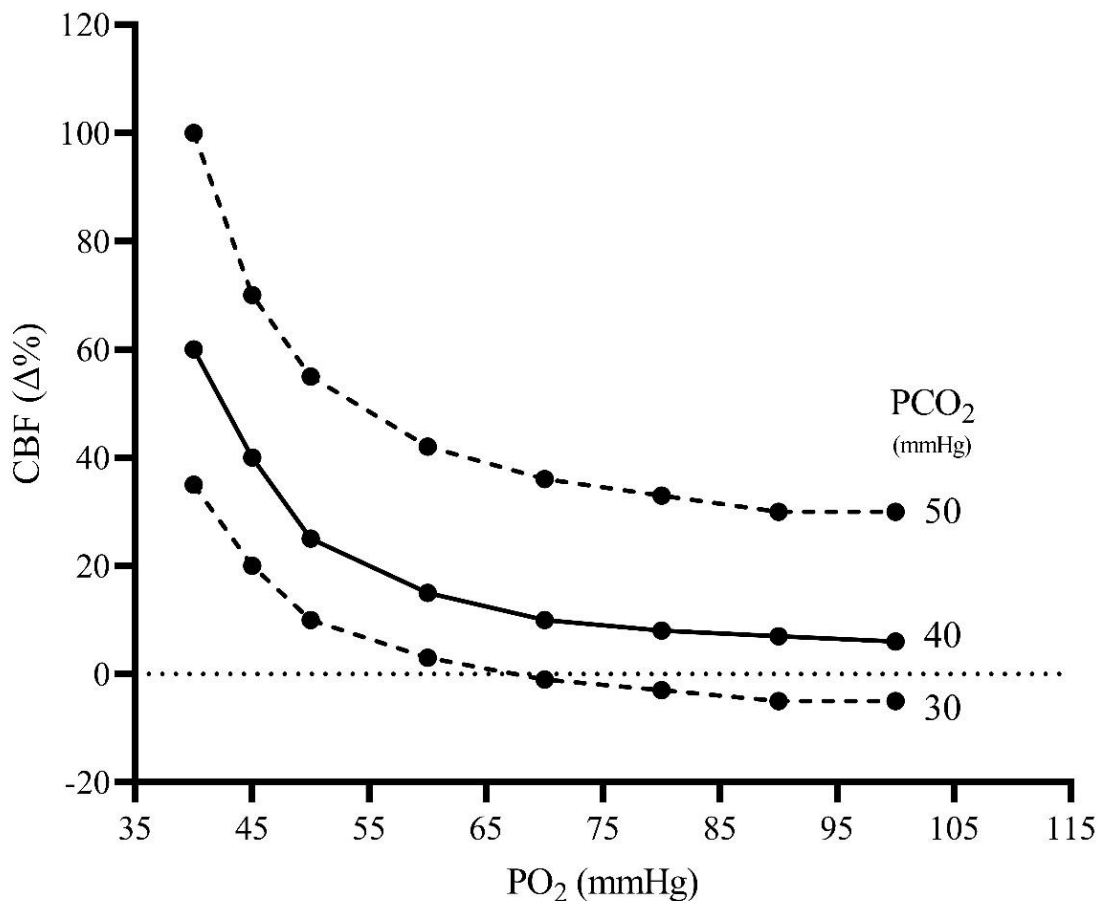


Figure 2.7. The relationship between cerebral blood flow and changing tensions of oxygen and carbon dioxide. Representative schematic between cerebral blood flow (CBF, Δ%) and partial pressure of oxygen (PO₂, mmHg) at differing partial pressures of carbon dioxide (PCO₂, mmHg). Adapted from Mardinae et al., 2012.

2.4.2 Neurogenic

It is fundamentally agreed that the cerebral vasculature is innervated by a variety of adrenergic and cholinergic nerves (Brassard et al., 2017). Intrinsic nerves deep within the parenchyma originating from the nucleus basalis, locus coeruleus, and raphe nucleus interact with astrocytes and local GABAergic interneurons to innervate microvasculature (Brassard et al., 2017; Cipolla, 2009; Paulson et al., 1990; Silverman & Petersen, 2023). The cerebral conduit arteries are provided with sympathetic, parasympathetic, and sensory input by the extra-parenchyma extrinsic perivascular nerves that originate from the trigeminal ganglion, superior cervical ganglion, and sphenopalatine ganglion (Claassen et al., 2021; Paulson et al., 1990; Peterson et al., 2011). Despite the plethora of innervation in the cerebrovasculature, the role of sympathetic and parasympathetic activity in the regulation of cerebral blood flow has provided an historic area of contention (Brassard et al., 2017; Strandgaard & Sigurdsson, 2008; van Lieshout & Secher, 2008). Under normal resting conditions the impact of increased sympathetic activity on cerebral blood flow regulation may be marginal and clouded by other more potent regulatory mechanisms, whereas under more severe circumstances sympathetic control may play a more integral role (Ainslie & Duffin, 2009; ter Laan et al., 2013). Neuronal control of the cerebrovasculature may directly be related to the regulation of changes in perfusion pressure, impact on cerebral blood volume, and intracranial pressure (Koep et al., 2022; Paulson et al., 1990). Notwithstanding, alpha-adrenergic receptor blockade during static handgrip exercise has shown to attenuate the contralateral-ipsilateral differences in internal carotid artery blood flow, suggesting a role of sympathetic nerve activity regulation in the internal carotid arteries (Fernandes et al., 2016). Differences in anatomical and receptor complexities compared to the peripheral vasculature are reported within the cerebrovasculature and cause cerebral sympathetic nerve activity to act opposingly to the peripheral vasculature (Koep et al., 2022). Consequently, using the peripheral vascular regulation as an index of cerebrovascular

regulation should be done with caution and further highlights the need to complete research examining regulation of both extra- and intra-cranial cerebral conduit arteries.

2.4.3 Myogenic

Myogenic control of cerebral blood flow refers to the intrinsic property of the vascular smooth muscle to alter vascular resistance in response to alterations in transmural pressure. The cerebral conduit arteries are encircled by multiple layers of vascular smooth muscle cells (Koep et al., 2022). In the face of changes to perfusion pressure, reflex alterations in vascular resistance normalize wall tension, where tension = pressure x radius, to maintain normal haemodynamic function (Cipolla, 2009). Known as the Bayliss Effect, the cerebral conduit arteries constrict in response to an increase in pressure to protect smaller downstream capillaries from damage and dilate in response to a decrease in blood pressure to maintain perfusion (Cipolla, 2009; Voets & Nilius, 2009). Vascular tone to changes in transmural pressure are primarily mediated by mechanotransduction of the artery, depolarization of the vascular smooth muscle, the release of Ca^{2+} , and the activation of myosin by phosphorylation (Claassen et al., 2021; Silverman & Petersen, 2023; Voets & Nilius, 2009).

2.4.4 Endothelial

The endothelium is a layer of specialised cells that line the lumen of the cerebral conduit arteries and have been shown to be a key regulator of vasoactive tone (Paulson et al., 1990; Peterson et al., 2011). The endothelium releases several vasoactive mediators that regulate vasoactive tone including nitric oxide, endothelium-derived hyperpolarizing factor, eicosanoids, and endothelin-1 (Ashby & Mack, 2021; Peterson et al., 2011). Increases in shear stress release signalling molecules, such as Ca^{2+} , to elicit the synthesis and release of endothelium vasoactive mediators to cause vasodilation and vasoconstriction (Ashby & Mack,

2021; Peterson et al., 2011). The endothelium plays an important role in neurovascular coupling propagated vasodilation, integrity of the blood-brain barrier, and prevention of circulating toxins and pathogens for maintenance of brain homeostasis (Ashby & Mack, 2021; Claassen et al., 2021). Dysfunction of the endothelial dependent vasodilation mechanism, as occurs in patients with hypertension, is shown to impair the cerebral vasodilation response to l-arginine, an important pre-cursor molecule for nitric oxide production, as well as to isocapnic hypoxia (Fernandes et al., 2018; Vianna et al., 2018).

2.4.5 Neurovascular coupling

The intricate relationship between local neural activity and local vascular blood flow to meet demand is termed neurovascular coupling. The three-component neurovascular unit comprises of the neuron, the astrocyte, and the blood vessel, whereby the astrocyte is thought to mediate the coupling between neuronal activity and cerebral blood flow (Hoiland et al., 2019; Paulson et al., 1990; Peterson et al., 2011; Phillips et al., 2016; Willie, Tzeng, et al., 2014). Functional hyperaemia, a region-specific gross influx in cerebral blood flow, occurs in response to an increased regional neuronal activity. Imaging the functional hyperaemia response at the microvasculature can be measured using BOLD imaging, whereby the displacement of the neuronal activity-induced increase in deoxyhaemoglobin by the large influx of oxygenated blood a few seconds later is captured (Glover, 2011). Functional hyperaemia can also be captured in the large vasculature using TCD of the intracranial arteries using visual stimulation. Visual stimulation can involve a single light stimulus (reading, eyes-open eyes-closed, or flashing checkerboard), and is a reproducible response for the assessment of neurovascular coupling in the intracranial arteries (Phillips et al., 2016). Visual stimulation-induced increases in blood velocity of the posterior cerebral artery between 10–20% are thought to reflect reductions in vascular tone of the capillary beds and recruitment of blood towards activated

neurovascular units in the occipital cortices as the posterior cerebral artery sources the posterior lobe. In comparison, the increase in blood velocity to the same visual stimulation in the middle cerebral artery (approx. 5%) is significantly lower (Aaslid, 1987; Phillips et al., 2016). Eliciting a visual stimulation evoked neurovascular coupling response in the posterior circulation that is different to the anterior circulation is a key example of localised regional regulation that occurs at the level of the cerebral conduit arteries (Phillips et al., 2016). Nitric oxide is thought to be a key mechanism involved in the localised neurovascular coupling response at the pial arteries and capillary beds, since inhibition of nitric oxide synthase with L-NMMA has shown to reduce the peak neurovascular coupling response in the posterior cerebral artery (Hoiland et al., 2020). Whether regional regulation extends to extracranial vertebral arteries during visually-evoked neurovascular coupling protocols remains relatively unexplored, with only one study investigating extracranial regulation to neurovascular coupling during lower body negative pressure (Samora et al., 2020). Capturing the vascular tone changes of extracranial arteries with duplex ultrasound may provide an insight into the vasoactive regulation of the intracranial cerebral conduit arteries.

2.4.6 Cerebral autoregulation

Blood pressure is known to fluctuate cyclically over time at rest and is challenged during postural movements, exercise, and exposure to environmental stress. If left unregulated, hypoperfusion or hyperperfusion of the brain from low or high systemic blood pressure can lead to complications, such as loss of consciousness and ischaemic injury or headaches and stroke, respectively (Ainslie & Brassard, 2014; Claassen et al., 2021; van Mook et al., 2005). Cerebral autoregulation is the ability for the cerebrovasculature to maintain a relatively constant blood flow, through changes in vascular tone, in the face of changes in perfusion pressure (Paulson et al., 1990; Strandgaard & Paulson, 1984). A maintained cerebral blood

flow despite fluctuations in blood pressure reflects an intact cerebral autoregulation, whereas if cerebral blood flow becomes pressure-passive to fluctuations in blood pressure this indicates a poorer cerebral autoregulation. Historically, the fundamental relationship between blood pressure and cerebral blood flow suggested that the cerebrovasculature can buffer a wide range of blood pressures and is only compromised with extreme changes in blood pressure (Lassen, 1959). The modern-day relationship (Figure 2.8) describes a smaller plateau region in the relationship between blood pressure and cerebral blood flow (± 10 mmHg) and a more curvilinear relationship across both hypotension and hypertension (Brassard et al., 2021; Lucas et al., 2010). Two types of cerebral autoregulation are referred to in the literature: static cerebral autoregulation and dynamic cerebral autoregulation. Both refer to the relationship between a change in blood pressure and concomitant change in cerebral blood flow but at different temporal resolutions.

Static cerebral autoregulation

Static cerebral autoregulation refers to the response of cerebral blood flow to slow and progressive changes in blood pressure. Using a step-change style methodology, cerebral blood flow is measured over a period of > 30 s pre- and post- a manipulation to arterial blood pressure during a range of blood pressures (60–150 mmHg) (Panerai, 2008). Invasive phenylephrine infusions have been used to assess static cerebral autoregulation by eliciting an increase in blood pressure and are quantified using linear regression analysis as an autoregulatory index (Jansen et al., 2000, 2007). Static cerebral autoregulation determines the cerebral pressure-flow relationship *after* the autoregulatory response has occurred and subsequently can make interpretation of the vasoactivity of the cerebral conduit arteries difficult.

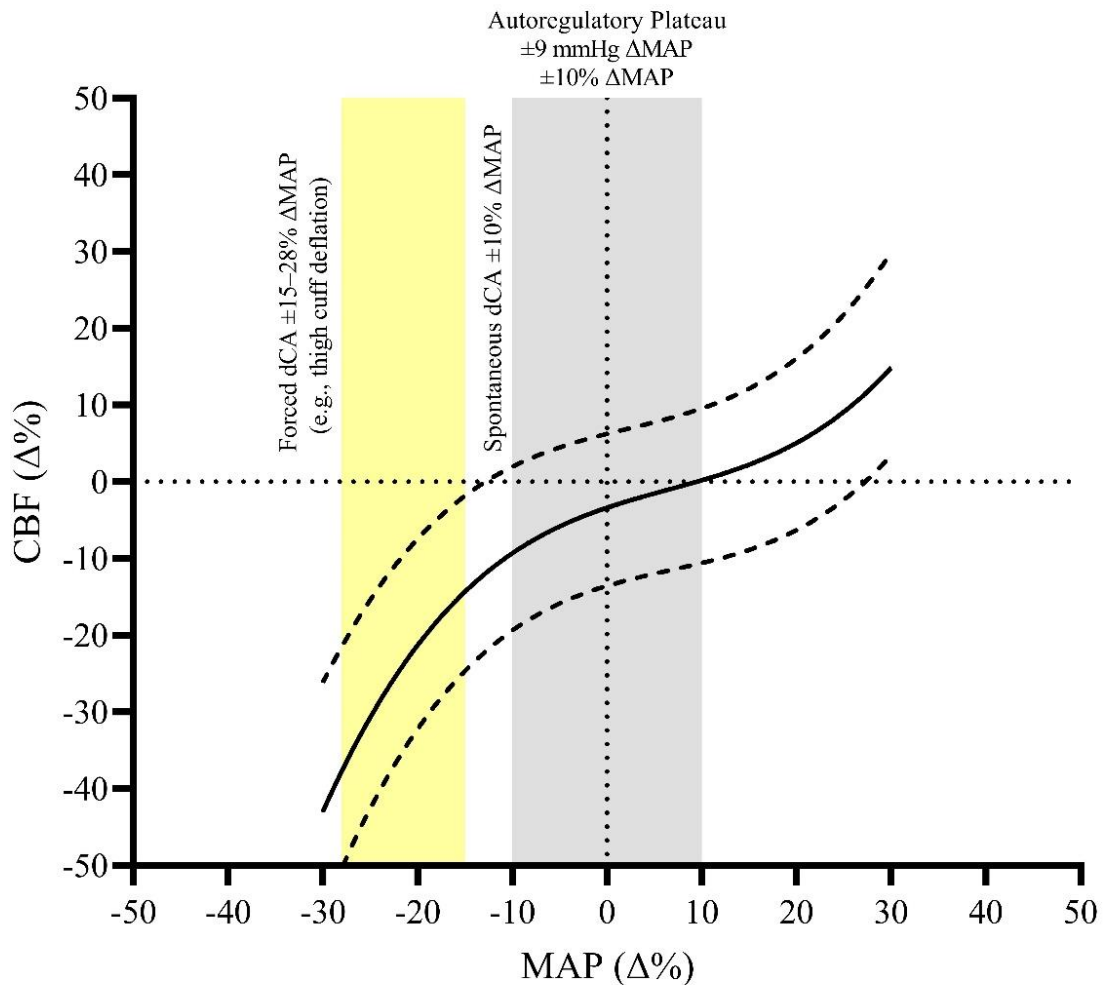


Figure 2.8. The contemporary view of the cerebral autoregulation curve. Relationship between change in mean arterial pressure (MAP, $\Delta\%$) and concomitant change in cerebral blood flow (CBF, $\Delta\%$) using nonpharmacological methodologies. The grey section represents the autoregulatory plateau where the assessment of spontaneous dynamic cerebral autoregulation (dCA) occurs. The yellow section represents the area of induced hypotension for assessments of dynamic cerebral autoregulation using forced manoeuvres i.e., rapid thigh cuff deflation, sit-to-stand. Adapted from Brassard et al., 2021.

Dynamic cerebral autoregulation

Dynamic cerebral autoregulation refers to the rapid response of cerebral blood flow to spontaneous oscillations or a sudden change in blood pressure back to its original value within a few seconds (Panerai, 2008). Dynamic cerebral autoregulation assesses the beat-to-beat relationship of cerebral blood flow and blood pressure at a high temporal resolution that can be

time-aligned with concomitant cardiorespiratory measurements. Dynamic cerebral autoregulation can be assessed during the steady-state spontaneous oscillations in blood pressure when an individual is at rest and that occur within the plateau region of the autoregulatory curve (R. Zhang et al., 1998). Alternatively, dynamic cerebral autoregulation can be assessed during forced oscillations in blood pressure during specific manoeuvres (e.g., sit-to-stand, tilt table, rapid thigh cuff deflation) that occur towards the extremities of the autoregulatory curve (Aaslid et al., 1989; Tzeng & Ainslie, 2014). Assessments of dynamic cerebral autoregulation have been described as a sensitive and reliable indicator for compromised cerebrovascular circulations in clinical applications (Panerai, 2008).

Dynamic cerebral autoregulation during spontaneous oscillations in blood pressure

To quantify the cerebral blood flow-blood pressure relationship during spontaneous oscillations in blood pressure, dynamic cerebral autoregulation is treated as a frequency-dependent phenomenon and assessed using transfer function analysis (Panerai et al., 2023; R. Zhang et al., 1998). Transfer function analysis assumes a simple linear control system model of cerebral autoregulation and, whilst it is recognised by investigators that the cerebral blood flow-blood pressure relationship is not linear in nature, this modelling provides an insight into the relationship (Claassen et al., 2016). Transfer function analysis outputs individual metrics of coherence function, transfer function gain, and transfer function phase in the very low- (0.02–0.07 Hz), low- (0.07–0.20 Hz), and high- (0.20–0.50 Hz) frequency ranges to reflect different patterns of the steady state blood pressure-cerebral blood flow relationship. Research suggests that focus should be in low and very low frequencies where cerebral autoregulation is most active and is least influenced by respiratory cycle and reflect autoregulatory mechanisms (Diehl et al., 1995; Subudhi et al., 2009; R. Zhang et al., 1998).

Coherence describes the linear relation between blood pressure and cerebral blood flow, where low coherence (< 0.5) reflects a tight autoregulation and higher coherence (towards 1.0) reflects a poor autoregulation and a dependence of cerebral blood flow on blood pressure (Iwasaki et al., 2007; Nishimura et al., 2010; R. Zhang et al., 1998). A high (> 0.5) coherence also indicates that the transfer function gain and transfer function phase metrics are valid (Ainslie, Ogoh, et al., 2008; Iwasaki et al., 2007). Transfer function gain describes the relative amplitude (signal transmission) of the blood pressure-cerebral blood flow relationship and reflects the ability of the cerebrovascular bed to buffer changes in cerebral blood flow induced by transient changes in blood pressure (Iwasaki et al., 2007, 2011; Ogoh et al., 2018; R. Zhang et al., 1998). Transfer function phase determines the temporal (time) relationship between blood pressure and cerebral blood flow and describes the tendency of cerebral blood flow to follow fluctuations in blood pressure (R. Zhang et al., 1998). Transfer function phase has been suggested as the primary criterion for evaluating cerebral autoregulation (Ogoh et al., 2018; R. Zhang et al., 1998). In short, increases in gain and decreases in phase reflect an increased effect of transmission of blood pressure on cerebral blood flow and are interpreted as a reduced cerebral autoregulation (i.e., a pressure-passive relationship) implying that any given change in blood pressure leads to greater change in cerebral blood flow (Nishimura et al., 2010; Ogoh et al., 2018). Conversely, decreases in gain and increases in phase reflects a decreased transmission effect of blood pressure on cerebral blood flow and are interpreted as an intact or improved cerebral autoregulation, implying that changes in blood pressure lead to little to no change in cerebral blood flow (Ainslie, Ogoh, et al., 2008).

Historically, the approach to transfer function analysis of dynamic cerebral autoregulation varied within the literature and made comparison between studies difficult. In recent years, the emergence of a frequently updated White Paper for transfer function analysis of dynamic cerebral autoregulation that incorporates global expert opinion and common practice guidelines

(Claassen et al., 2016; Panerai et al., 2023). In addition, readily available software from repositories (CARNet.org) and other commercial systems (Ensemble, Elucimed), have begun to improve the standardisation of transfer function analysis investigations and aid the translation of this method for clinical application.

Dynamic cerebral autoregulation during forced oscillations in blood pressure

The rapid thigh cuff release technique is one of the earliest and highest cited techniques for assessing dynamic cerebral autoregulation during forced oscillations in blood pressure (Aaslid et al., 1989). Bilateral thigh cuffs are inflated to a supra-systolic pressure for approximately 3 min following a period of baseline rest, and then rapidly deflated (< 1 s) causing a large transient fall in blood pressure (>15 mmHg). Repeated deflations (approx. 2–3 repeats) are conducted and the average response is reported. Another common non-invasive method of assessing forced oscillations in blood pressure involves a single manoeuvre or repeated manoeuvres at a defined depth and rate (i.e., a specified oscillatory frequency) from squat- or sit- to-stand (Querido et al., 2013; Smirl et al., 2014). Incremental lower-body negative pressure (van Helmond et al., 2018), tilt table manoeuvres (Blaber et al., 2003), and a transient carotid compression test (Ter Minassian et al., 2001) have also been used to assess response to a forced change in blood pressure. For a single forced oscillation in blood pressure, the calculation of the autoregulatory index (Tiecks et al., 1995) or rate of regulation (Aaslid et al., 1989; Labrecque et al., 2021; Sorond et al., 2005) can be used to describe dynamic cerebral autoregulation. For repeated squat- or sit- to-stand manoeuvres at the specified induced oscillation frequency, transfer function analysis can be used much like that for spontaneous oscillations in blood pressure (Smirl et al., 2014; van Helmond et al., 2018). Additional metrics such as a linear regression from the nadir to the peak response for each induced oscillation in blood pressure, the maximum reduction in cerebral blood flow, and time to recovery to change

in blood pressure have also been adopted for single and repeat oscillations in blood pressure (Labrecque et al., 2021; Querido et al., 2013).

Comparisons between metrics of cerebral autoregulation

The abundance of metrics available to assess dynamic cerebral autoregulation report a low level of agreement and poor convergence validity with each other, which consequently has made it difficult to compare results across studies (Tzeng et al., 2012). Only metrics that share mathematical parameters (LF gain vs LF n-gain) or that overlap frequency bands (0.10 Hz gain vs LF [0.07–0.20 Hz] gain) were strongly correlated, whereas there was poor agreement between transfer function analysis metrics and rate of regulation or autoregulatory index (Tzeng et al., 2012). This suggests that mechanisms of dynamic cerebral autoregulation during spontaneous and forced oscillations in blood pressure may not be reflective of one another and should be investigated individually. Without an agreed gold standard technique, it remains inconclusive which is the best method to assess dynamic cerebral autoregulation and therefore the method selected for any study should be governed by the research question. For example, whether a researcher wishes to use what is most appropriate for the population investigated (i.e., those with a lack of mobility), to reflect day-to-day functioning (i.e., postural changes), or to determine mechanistic insight to cerebral blood flow control (i.e., foot strike induced blood pressure oscillations during running) (Smirl et al., 2014; Subudhi et al., 2009; van Beek et al., 2008). To overcome some of these difficulties, researchers have adopted a holistic approach to assess dynamic cerebral autoregulation by incorporating multiple methodologies within the same cohort (Labrecque et al., 2021).

2.5 Cerebral blood flow response to hypoxia

Herein the focus of this thesis will be on the global and regional cerebral blood flow regulation of cerebral conduit arteries to acute hypoxia. Since the brain regulates cerebral blood flow to maintain oxygen delivery, altering the oxygen availability of the environment can help unravel and better understand the regulatory mechanisms involved in maintaining optimal functioning, and avoiding ischaemic brain damage and life-threatening complications. Environmental hypoxia reduces the partial pressure of oxygen throughout the oxygen transport cascade and causes arterial hypoxaemia (Kane et al., 2020). Reduced partial pressure of oxygen during environmental hypoxia causes a diffusion-limitation between the alveolar and pulmonary capillary since the transit time of a red blood cell to transverse the pulmonary capillary is insufficient to equalize the partial pressure of oxygen between the lung and capillary. Further, arterial hypoxaemia reduces tissue oxygenation delivery and compromises the metabolic needs of the cells. Hypobaric hypoxia arises through a reduction in barometric pressure with maintained inspired fraction of oxygen, which occurs in the natural high-altitude environment, whereas normobaric hypoxia arises through a maintenance of barometric pressure with a reduction in the inspired fraction of oxygen and is commonly used in simulated hypoxia environments e.g., altitude chambers.

Exposure to acute hypoxia is a commonly used stimulus to investigate the regulation of cerebral blood flow where oxygen availability and oxygen delivery is compromised. It is well documented that acute hypoxia elicits a reliable and repeatable increase in global cerebral blood flow via cerebral vasodilation of the vascular beds (Kellawan et al., 2017; Lawley et al., 2017; Lewis et al., 2014). However, the global and regional vascular regulation of the cerebral conduit arteries to acute hypoxia remains complex and contentious.

Cardiorespiratory response to acute hypoxia

Exposure to systemic hypoxia elicits a pronounced and highly-individualised cardiorespiratory response that impacts the mechanisms that regulate cerebral blood flow to maintain global cerebral oxygen delivery. Therefore, it is necessary to monitor and account for the magnitude of cardiorespiratory responses when investigating the regulation of cerebral blood flow. In response to acute hypoxia, alterations in ventilation and cardiac output occur to attenuate arterial hypoxaemia (West, 1982). Peripheral chemoreceptor stimulation in response to reduced partial pressure of oxygen initiates the triphasic hypoxic ventilatory response (Pamenter & Powell, 2016), which involves a rapid initial rise in ventilation within minutes of hypoxia, before the subsequent hypoxic ventilatory response associated hypocapnia returns ventilation towards baseline values over the following hours. With prolonged exposure, ventilation steadily increases alongside prolonged hypocapnia and a resetting of chemoreceptor sensitivities to carbon dioxide (Pamenter & Powell, 2016; Powell et al., 1998). Hypoxia is also a potent stimulant of the sympathetic nervous system. Hypoxia-induced elevations in sympathetic nerve activity increase myocardial contractility, heart rate, and cardiac output, whilst stroke volume remains unchanged, to attenuate tissue hypoxaemia (Hainsworth et al., 2007; West, 1982). Elevated sympathetic excitation also induces hypoxic pulmonary vasoconstriction and pulmonary hypertension that increases systemic total peripheral resistance and raises blood pressure (Hainsworth et al., 2007).

Cerebral blood flow response to acute hypoxia

Cerebral blood flow increases in response to reduced arterial oxygen content to preserve cerebral oxygen delivery (Ainslie et al., 2014; Hoiland et al., 2016; Subudhi et al., 2014), but is also dependent on the magnitude of the hypocapnia induced by the hypoxic ventilatory response (Poulin et al., 1996, 2002). Doppler ultrasound measurements of cerebral

haemodynamics at the intracranial and extracranial arteries report rapid increases in cerebral blood flow to acute poikilocapnic normobaric hypoxia (Poulin et al., 1996, 2002), reaching its peak within a couple hours before steadily falling at approximately 6% per hour towards baseline values (Lewis et al., 2014). This response is mirrored with exposure to hypobaric hypoxia, with cerebral blood flow peaking between the first and second day at high-altitude before decreasing thereafter and returning to near sea level values at a fortnight (Hoiland et al., 2018; Huang et al., 1987; Subudhi et al., 2014; Willie, Smith, et al., 2014). Reductions in cerebrovascular resistance mediate the increase in cerebral blood flow, reflecting the dilation of arteriolar pial vessels (Cohen et al., 1967). Historically, the cerebral conduit arteries were thought not to dilate in response to acute hypoxia (Poulin et al., 1996). Recent evidence using Doppler ultrasound and magnetic resonance imaging suggests that vasodilation of the cerebral conduit arteries is involved in mediating the increase in cerebral blood flow during hypoxia (Arngrim et al., 2016; Kellawan et al., 2020; Lewis et al., 2014), however this has not always been replicated (Lafave et al., 2019; Ogoh et al., 2013) and may be limited by small sample sizes (< 14 participants).

Influence of carbon dioxide on cerebral blood flow response to acute hypoxia

The relationship between the partial pressure of arterial oxygen and partial pressure of arterial carbon dioxide plays a defining role in the overall change in cerebral blood flow during exposure to hypoxia (Bruce et al., 2016; Lucas et al., 2010). The strength of the increase in cerebral blood flow to acute poikilocapnic hypoxia is greatly dependent on the balance between the contrasting cerebrovascular activity of the hypoxia-induced vasodilation and the hypoxic ventilatory response associated hypocapnic vasoconstriction (Mardimae et al., 2012; Poulin et al., 1996, 2002). Cerebrovascular reactivity challenges have shown that cerebral conduit artery blood flow sensitivities to carbon dioxide and oxygen are altered when the opposing arterial

blood gas is changed (i.e., carbon dioxide reactivity is attenuated during hypoxia and hypoxic reactivity is augmented during hypocapnia) (Ainslie & Poulin, 2004; Ogoh et al., 2014; Poulin et al., 2002). Gas clamping systems, such as the dynamic end-tidal forcing (Poulin et al., 1996) and Respiract (Fisher, 2016), are available to investigate the interaction of changing tensions of carbon dioxide and oxygen during acute poikilocapnic hypoxia. For example, tightly controlling against the prevailing hypocapnia during hypoxia (i.e., isocapnic hypoxia) and alleviation of the hypocapnia-induced vasoconstriction has shown to increase cerebral haemodynamics and improve cognitive function (Friend et al., 2019; van Dorp et al., 2007).

Mechanisms of cerebral blood flow response to acute hypoxia

The inter-individual variability of the cerebral blood flow response to acute hypoxia is as high as 640% on the first night at high altitude (Willie, Smith, et al., 2014), therefore elucidating the mechanisms involved in regulating the cerebral blood flow response to hypoxia is a complex, multifactorial phenomenon that remains unclear. An attenuated increase in cerebral blood flow to haemodilution-induced hypoxia compared to hypoxemia-induced hypoxia suggests that deoxyhaemoglobin is a key signalling mechanism for the release of vasoactive factors during hypoxia (Hoiland et al., 2016). Specifically, erythrocytes are thought to be a key regulator of hypoxic cerebral vasodilation through the release of the vasodilator S-nitrosothiols (Hoiland et al., 2023). Of the vasoactive factors, it is thought that cerebral hypoxic vasodilation is nitric oxide dependent, with reductions in vasodilation following nitric oxide synthase inhibition (Hoiland et al., 2023). In contrast, adenosine, another vasoactive factor, does not mediate the cerebral vasodilation and increased cerebral blood flow response during normobaric and hypobaric hypoxia (Hoiland et al., 2017). In contrast to cyclooxygenase's role in regulating basal cerebrovascular tone and hypercapnic vasodilation (Kellawan et al., 2020; Peltonen et al., 2015), cyclooxygenase may only play a role in hypoxic vasodilation when in combination

with reactive oxygen species (Harrell et al., 2019). The sympathetic nervous system is thought to have minimal contribution in the regulation of cerebral blood flow during hypoxia. Indeed, alpha-1 blockade does not alter the acute hypoxia-induced increase in cerebral blood flow at the internal carotid and vertebral arteries (Lewis et al., 2014) and no relationship was found between a heightened sympathetic nervous activity, as occurs in hypertensive men, and an attenuated hypoxia-induced increase in cerebral blood flow (Fernandes et al., 2018). A recent review has summarised the current mechanisms that mediate hypoxic cerebral vasodilation in humans, including nitric oxide synthase, oxygenation-coupled S-nitrosothiols, potassium channel-related vascular smooth muscle hyperpolarization, and prostaglandin and reactive oxygen species (Carr et al., 2023).

2.5.1 Cerebral autoregulation during hypoxia

Evidence overwhelmingly suggests that normobaric hypoxia [fraction of inspired oxygen (FiO_2) = 12–15%; peripheral arterial oxygen saturation (SpO_2) = 92–80%] and hypobaric hypoxia [elevation = 3,424–5,400m; SpO_2 = 90–75%] reduces cerebral autoregulation (Table 2.1) (Ainslie et al., 2007, 2012; Ainslie, Hamlin, et al., 2008; Ainslie, Ogoh, et al., 2008; Bailey et al., 2009; Blaber et al., 2003; Horiuchi et al., 2016, 2022; Iwasaki et al., 2007, 2011; Jansen et al., 2000, 2007; Levine et al., 1999; Nishimura et al., 2010; Ogoh et al., 2010, 2018; Querido et al., 2013; Smirl et al., 2014; Subudhi et al., 2009, 2010, 2014, 2015; Ter Minassian et al., 2001; Tymko et al., 2020; van Helmond et al., 2018) with only a few studies concluding no change (Ainslie et al., 2007; Ogoh et al., 2014; Van Osta et al., 2005), or improved cerebral autoregulation to hypoxia at rest (Ainslie, Ogoh, et al., 2008). Much of the literature has assessed dynamic cerebral autoregulation during hypoxia using TCD and transfer function analysis of the middle cerebral artery. However, few studies have assessed dynamic cerebral autoregulation using forced oscillations, such as rapid thigh cuff technique and lower body

negative pressure, or measured volumetric blood flow with duplex ultrasound (Hoiland et al., 2019; Horiuchi et al., 2016, 2022; Tymko et al., 2020; van Helmond et al., 2018). Stepwise-models of hypoxic dosage have shown that reductions in dynamic cerebral autoregulation occur during exposure to low to moderate hypoxia ($FiO_2 = 15\%$; $SpO_2 = 93\text{--}90\%$), with no further reductions experienced during severe hypoxia ($FiO_2 = 12\%$; $SpO_2 = 79\%$) (Horiuchi et al., 2016; Iwasaki et al., 2007). Reductions in dynamic cerebral autoregulation occur within minutes of hypoxic exposure (Iwasaki et al., 2007; Ogoh et al., 2018; Querido et al., 2013; Subudhi et al., 2009; van Helmond et al., 2018) and are shown to be sustained at 5 (Nishimura et al., 2010) and 9 h of exposure (Subudhi et al., 2010). Acclimatization to moderate or high-altitude hypoxia does not reverse reductions in dynamic cerebral autoregulation, with evidence of sustained reductions at 13 days (Subudhi et al., 2015), 16 days (Subudhi et al., 2014), one month (Iwasaki et al., 2011), and over 31 days (Levine et al., 1999), and upon re-exposure (Subudhi et al., 2014). Sherpa and Himalayan high-altitude natives also present reduced static cerebral autoregulation (Jansen et al., 2000, 2007), whereas they are reported to have intact dynamic cerebral autoregulation by squat-stand manoeuvre (Smirl et al., 2014) and rapid thigh cuff technique (Tymko et al., 2020).

The magnitude of reduction in dynamic cerebral autoregulation is related to an increased severity of acute mountain sickness during moderate to severe levels of normobaric hypoxia (Horiuchi et al., 2016). This relationship is thought to occur selectively in individuals with the greatest arterial hypoxaemia (Bailey et al., 2009; Van Osta et al., 2005). Poorer sea level dynamic cerebral autoregulation has been shown to account for 60% of the observed variance in acute mountain sickness and was suggested to be a useful indicator to identify acute mountain sickness-susceptible individuals for targeted pharmacological prophylaxis (Cochand et al., 2011). Whilst this evidence is promising, there are several studies that have not found a

relationship between dynamic cerebral autoregulation and acute mountain sickness (Smirl et al., 2014; Subudhi et al., 2010, 2014, 2015; Ter Minassian et al., 2001; Tymko et al., 2020).

Although evidence overwhelmingly suggests that cerebral autoregulation is reduced during hypoxia, of the studies that have compared spontaneous and forced dynamic cerebral autoregulation methodologies during hypoxia, some only report forced dynamic cerebral autoregulation to be reduced (Subudhi et al., 2009, 2015), whereas others only report a reduction to spontaneous dynamic cerebral autoregulation (Smirl et al., 2014). The conflicting results between comparisons of spontaneous and forced dynamic cerebral autoregulation (Smirl et al., 2014; Subudhi et al., 2009, 2015) has questioned the interpretation, reliability, and significance of reduced dynamic cerebral autoregulation during hypoxia. Forced dynamic cerebral autoregulation assessments, such as sit-to-stand, rapid thigh cuff deflation, are thought to have more relevance to daily activities at altitude, such as posture changes and exercise (Smirl et al., 2014). Whether reductions in spontaneous dynamic cerebral autoregulation reflect physiologically important alterations in capacity of the brain to regulate blood pressure and pose a threat to healthy individuals in hypoxia is thought to be unlikely (Smirl et al., 2014; Subudhi et al., 2015). However, assessment of spontaneous dynamic cerebral autoregulation may be more advantageous for individuals with limited capacity to complete repeated, uncomfortable thigh cuff or sit-to-stand challenges (Subudhi et al., 2009). Nevertheless, the underlying mechanisms of dynamic cerebral autoregulation during spontaneous and forced oscillations are likely to be different and could be attributed to the contrasting results. Therefore, future studies should incorporate assessments of both spontaneous and forced assessments to maximise understanding of dynamic cerebral autoregulation across a range of blood pressure perturbations during hypoxia.

Author (Year)	N (F)	Age (Years [Mean ± SD or Mean + Range])	Artery	Measure	Hypoxia (FiO ₂ [%], P _{ET} O ₂ [mmHg], or Altitude [m])	S _p O ₂ (%)	Duration	Aim	Assessment of CA	Calculation of CA	Hypoxic effect?
Levine et al., (1999)	11 (4)	N/A	N/A	TCD	5,200 m	84–91	> 1 month	Acclimatization HA with LLs vs HLs	Spontaneous dCA - Rest	TFA	Yes
Jansen et al., (2000)	10 LLs 9 HLs	27±10 26±10	MCAv	TCD	4,243 m	88–89	D5–D7	Acclimatization HA with LLs vs HLs	Static CA - Phenylephrine infusion	Regression Slope	Yes
Ter Minassian et al., (2001)	8 (0)	27 (23–37)	MCAv	TCD	5,000 m 6,000 m 7,000 m 8,000 m	90 90 80 74	31 days	Hypobaric chamber hypoxia, stepwise to Everest (8,848m)	Transient response of CCA compression	%Change in MCAv	Yes
Blaber et al., (2003)	14 (8)	24±1	MCAv	TCD	3,660 m	N/A	1 h	Orthostatic tolerance during hypobaric chamber hypoxia	Static CA – Head-up tilt	Coarse-gaining spectral analysis	Yes
Van Osta et al., (2005)	35 (6)	40 (26–58)	MCAv	TCD	4,559 m	79	20 h (D2)	dCA and AMS with preventive drugs	Forced dCA - Rapid thigh cuff deflation	ARI	No
Ainslie et al., (2007)	14 (8)	25±4	MCAv	TCD	12 %	80	20 min	Acute hypoxia dCA at rest and exercise	Spontaneous dCA - Rest	TFA	No (rest) Yes (EX)
Iwasaki et al., (2007)	15 (0)	22±2	MCAv	TCD	21 % 19 % 17 % 15 %	98 97 96 93	10 min	dCA effect of stepwise NH	Spontaneous dCA - Rest	TFA	Yes
Jansen et al., (2007)	40 [4 groups of 10 HLs]	24±6 – 32±10	MCAv	TCD	1,330 m 2,650 m 3,440 m 4,243 m	97 96 93 88	Resided >3.5yrs at each altitude	HLs at different HA	Static CA - Phenylephrine infusion	ARI	Yes
Ainslie et al., (2008a)	28 (12)	26±5	MCAv	TCD	14 %	80	10 min	Hypoxic exercise following intermittent hypercapnia, hypoxia, or continuous hypoxia	Spontaneous dCA - Rest	TFA	Yes
Ainslie et al., (2008b)	10 (1) 7 (3)	28±5 34±11	MCAv	TCD	10 % 5,400 m	80 75	5 min D1–2	dCA during acute NH dCA during acclimatization to HA	Spontaneous dCA - Rest	TFA	No (NH) Yes (HH)

Author (Year)	N (F)	Age (Years [Mean ± SD or Mean + Range])	Artery	Measure	Hypoxia (FiO ₂ [%], P _{ET} O ₂ [mmHg], or Altitude [m])	SpO ₂ (%)	Duration	Aim	Assessment of CA	Calculation of CA	Hypoxic effect?
Bailey et al., (2009)	18	26±6	MCAv	TCD	12 %	80–85	6 h	dCA, BBB function, and AMS	Spontaneous dCA - Rest	TFA	Yes
									Forced - Rapid thigh cuff deflation	RoR	Yes
Subudhi et al., (2009)	12 (6)	24–40	MCAv	TCD	12 %	85	10 min	Compare two methods of dCA assessment during NH	Forced dCA - Rapid thigh cuff deflation	ARI	Yes
									Spontaneous dCA - Rest	TFA	Yes
Nishimura et al., (2010)	13 (2)	28±7	MCAv	TCD	15 %	92	5 h	Assess hourly changes in dCA during NH	Spontaneous dCA - Rest	TFA	Yes
Ogoh et al., (2010)	9 (0)	23±6	MCAv	TCD	14 %	89 95	8 min	CO ₂ effect on dCA during hypoxia (IH and PH)	Forced dCA - Rapid thigh cuff deflation	RoR	Yes (IH) No (PH)
Subudhi et al., (2010)	55 (14)	29±7	MCAv	TCD	89 mmHg	77–80	4 h 9 h	Hypobaric chamber hypoxia and AMS.	Spontaneous dCA - Rest	TFA	Yes
Cochand et al., (2011)	18 (5)	29±9	MCAv	TCD	3,800 m	N/A	6 h	SL dCA score and AMS at HA	Forced dCA - Rapid thigh cuff deflation	ARI	N/A
Iwasaki et al., (2011)	11	23±4	MCAv	TCD	10.5 % 5,260 m	78 90	30 min 1 month	dCA during acute NH and acclimatization to HA	Spontaneous dCA - Rest	TFA	Yes
Ainslie et al., (2012)	10 (3)	28±8	MCAv	TCD	5,050 m	85	D3–10	Determine sympathoexcitation on dCA at HH	Spontaneous dCA - Rest	TFA	Yes
Querido et al., (2013)	11 (3)	29±5	MCAv	TCD	50 mmHg	81	20 min	dCA during hypoxia, effect of CO ₂ (IH and PH)	Forced dCA - Squat-to-stand at 0.10 Hz	Regression Slope	Yes (IH) No (PH)
	8 (4)	29±6	MCAv	TCD	50 mmHg P _{ET} CO ₂ clamped	82	20 min	Static CA during IH	Static CA - Sodium nitroprusside Static CA - Phenylephrine	Regression Slope	No Yes

Author (Year)	N (F)	Age (Years [Mean ± SD or Mean + Range])	Artery	Measure	Hypoxia (FiO ₂ [%], P _{ET} O ₂ [mmHg], or Altitude [m])	SpO ₂ (%)	Duration	Aim	Assessment of CA	Calculation of CA	Hypoxic effect?
Ogoh et al., (2014)	8 (0)	23±4	MCAv	TCD	12 %	82	8 min	Effects hypoxia on CO ₂ reactivity and dCA	Spontaneous dCA - Rest	TFA	No
Smirl et al., (2014)	16 (2) LLs 16 (0) HLs	30±7 33±15	MCAv PCAv	TCD	5,050 m	96 80 83	SL D2 Wk2	Acclimatization with LLs vs HLs on dCA	Spontaneous dCA - Rest	TFA	Yes
									Forced - Squat-to-stand at 0.05 Hz and 0.10 Hz	TFA	No
Subudhi et al., (2014)	21 (9)	21±1	MCAv	TCD	5,260m	N/A	D1 D16	Acclimatization, AMS, and dCA	Spontaneous dCA - Rest	TFA	Yes
Subudhi et al., (2015)	11 (6)	21±2	MCAv	TCD	3,424 m	90	D2 D13	Compare two methods of dCA assessment at during HA	Spontaneous dCA - Rest	TFA	No
									Forced dCA - Rapid thigh cuff deflation	ARI	Yes
Horiuchi et al., (2016)	11 (0)	23±2	CCAbf	Duplex	21 % 18 % 15 % 12 %	97 94 90 79	1 h	Effect of stepwise NH on dCA	Forced dCA - Rapid thigh cuff deflation	RoR	Yes
Ogoh et al., (2018)	14 (9)	22±1	MCAv	TCD	12 %	80	35 min	dCA during cognitive task with hypoxia	Spontaneous dCA - Rest	TFA	Yes
van Helmond et al., (2018)	10 (0)	32±6	MCAv CCAdia	TCD Duplex	12–15 %	85	5 min	Hypoxia during LBNP on dCA	Spontaneous dCA - During LBNP	TFA	Yes
Tymko et al., (2020)	13 (1)	28±7	ICAbf CCAbf	Duplex	11 %	70	1 h	dCA during acute NH Acclimatization HA with LLs vs HLs	Forced dCA - Rapid thigh cuff deflation	RoR	Yes (NH) Yes (HH)
					3,440 m 5,050 m	90 83	D5 D10				
Horiuchi et al., (2022)	12 (0)	21±2	ICAbf	Duplex	13 %	85	1 h	Dietary nitrate on dCA in hypoxia	Forced dCA - Rapid thigh cuff deflation	RoR	Yes

Table 2.1. Cerebral autoregulation during hypoxia. Abbreviations; AMS, acute mountain sickness; ARI, autoregulatory index; BBB, blood-brain barrier; CA, cerebral autoregulation; CCAbf, common carotid artery blood flow; CCAdia, common carotid artery diameter; D, day; dCA, dynamic cerebral autoregulation; EX, exercise; F, female; FiO₂, fraction of inspired oxygen; HA, high altitude; HH, hypobaric hypoxia; HLs, highlanders; ICAbf, internal carotid artery blood flow; IH, isocapnic hypoxia; LBNP, lower body negative pressure; LLs, lowlanders; MAP, mean arterial pressure; MCAv, middle cerebral artery velocity; NH, normobaric hypoxia; PCAv, posterior cerebral artery velocity; P_{ET}CO₂, partial pressure of end-tidal carbon dioxide; P_{ET}O₂, partial pressure of end-tidal oxygen; PH, poikilocapnic hypoxia; RoR, rate of regulation; TCD, transcranial Doppler ultrasound; TFA, transfer function analysis; Wk, Week.

Mechanisms of reduced cerebral autoregulation during hypoxia

Vasodilation of the cerebral conduit arteries account for the marked reduction in dynamic cerebral autoregulation during hypoxia, akin to that postulated with an acute bout of hypercapnia (Panerai et al., 1999). Indeed, the balance of alterations in vascular tone to hypoxia and the prevailing hypoxic ventilatory associated hypocapnia may regulate dynamic cerebral autoregulation during hypoxia. During isocapnic hypoxia, where the effects of hypoxia are isolated from hypocapnia, dynamic cerebral autoregulation is reduced (Ogoh et al., 2010; Querido et al., 2013). In contrast, dynamic cerebral autoregulation is maintained when exposed to poikilocapnic hypoxia and is likely related to the hypocapnic-induced vasoconstriction (increased vascular tone) counteracting the hypoxia-induced vasodilation (Ogoh et al., 2010; Querido et al., 2013). Supplemental hyperoxia has also been shown to restore dynamic cerebral autoregulation during acute hypoxia (Ainslie, Ogoh, et al., 2008), possibly due to a reversal of hypoxia-induced vasodilation.

Whilst the role of nitric oxide in dynamic cerebral autoregulation remains equivocal (White et al., 2000; R. Zhang et al., 1998), its integral role for hypoxia-induced vasodilation (Umbrello et al., 2013) makes it a prime candidate to contribute to the reduction in dynamic cerebral autoregulation during hypoxia. Elevated levels of sympathetic outflow at high altitude may also play a role by disrupting cerebral vascular regulation since blockade of sympathoexcitation improved dynamic cerebral autoregulation (Ainslie et al., 2012). Heightened autonomic nervous activity with hypoxia may compromise integrity of blood brain barrier, mediate increased cerebral perfusion, and impact dynamic cerebral autoregulation (Subudhi et al., 2009). However, whilst dynamic cerebral autoregulation is selectively reduced in acute mountain sickness positive individuals, there was no evidence for hyper-perfusion, blood brain barrier disruption, or neuronal-parenchymal damage, in comparison to acute mountain sickness

negative individuals who had no alteration to dynamic cerebral autoregulation (Bailey et al., 2009). Other mechanisms likely to be involved in the development of reduced dynamic cerebral autoregulation during hypoxia include metabolic factors, myogenic factors, intracranial nervous system, autonomic nervous system, and endothelial factors and have yet to be fully elucidated (Paulson et al., 1990).

2.6 Regional regulation of blood flow at the cerebral conduit arteries

The cerebral conduit arteries can be categorised by those that supply the anterior regions of the brain and those that supply the posterior regions of the brain. It is proposed that the posterior cerebral conduit arteries may regulate differently to the anterior cerebral conduit arteries to prioritise maintenance of cerebral blood flow to the posterior regions of the brain involved in homeostatic, autonomic, and cardiorespiratory function, e.g., pons, medulla oblongata, thalamus, brainstem, and cerebellum (Sato, Sadamoto, et al., 2012; Willie et al., 2012). Possible structural differences such as receptor density (Koep et al., 2022) may also contribute to segmental within-region (i.e., located in the anterior or posterior region) differences in regulation between the intracranial and extracranial arteries. To date, evidence of regional cerebral blood flow regulation between the anterior and posterior cerebral conduit arteries remains equivocal.

2.6.1 Regional cerebral autoregulation during normoxia

Whilst there are reports of no differences in dynamic cerebral autoregulation between the anterior and posterior regions in otherwise normal conditions (Labrecque et al., 2021; Reehal et al., 2021), there is evidence that the posterior cerebral artery has a lower damping capacity, and is more susceptible, to spontaneous oscillations in blood pressure compared to the middle cerebral artery (Haubrich et al., 2004; Nakagawa et al., 2009). A poorer dynamic cerebral autoregulation in the posterior circulation compared to the anterior circulation could be

resultant of a lower basal resting vascular tone at rest akin to that postulated with reductions in dynamic cerebral autoregulation during an acute bout of hypercapnia (Panerai et al., 1999). The lower basal resting vascular tone of the posterior cerebral arteries may be a consequence of an increased neuronal metabolic demand of the visual cortices, located in the occipital lobe and supplied blood flow by the posterior circulation, caused by individuals eyes being open during cerebrovascular assessments even without forced visual simulation (Nakagawa et al., 2009). Indeed, in comparison to measurements collected with eyes closed, eyes open caused a significant increase in TCD-derived blood velocity and higher transfer function gain (i.e., increased effect of transmission of blood pressure on cerebral blood flow) to spontaneous oscillations of blood pressure in the posterior cerebral artery than the middle cerebral artery (Nakagawa et al., 2009). Unfortunately, since these measurements were conducted with TCD, there was no direct measurement of intracranial or extracranial arterial diameter to confirm whether vascular tone differences are responsible for the observed anterior-posterior regional differences in dynamic cerebral autoregulation.

Direct measurements of anterior and posterior vascular tone and dynamic cerebral autoregulation of the extracranial arteries has been reported in response to head-up tilt using duplex ultrasound (Sato, Fisher, et al., 2012). That is, in response to a head-up tilt induced reduction in blood pressure, the vertebral artery maintained vascular tone and blood flow, whereas there was a vasoconstriction-induced reduction in blood flow in the internal carotid artery (Sato, Fisher, et al., 2012). Dynamic cerebral autoregulation was then assessed using the rapid thigh cuff deflation at supine and head-up tilt (Sato, Fisher, et al., 2012). During head-up tilt (where vascular tone and blood flow regulation differences were noted between the vertebral artery and internal carotid artery), the reduction in blood flow in the vertebral artery ($-32.2 \pm 1.7\%$) following cuff release was greater than the internal carotid artery ($-26.1 \pm 1.8\%$). Moreover, there was only a reduction in rate of regulation (the measure of dynamic

cerebral autoregulation) in the vertebral artery between supine and head-up tilt, whereas the rate of regulation was unchanged in the internal carotid artery (Sato, Fisher, et al., 2012). These differences in vascular tone, blood flow, and dynamic cerebral autoregulation indicate regional regulation between the anterior and posterior cerebral conduit arteries during orthostatic stress. Indeed, the attenuation in dynamic cerebral autoregulation during orthostasis only in the vertebral artery may be a consequential by-product of the reduced vascular tone in the posterior vascular beds compared to the anterior vascular beds to preferentially maintain blood flow to the posterior regions of the brain that are involved in systemic cardiorespiratory control.

Whilst studies investigating static cerebral autoregulation assess cerebral blood flow regulation *after* the autoregulatory response, these studies may also provide evidence of differences in cerebrovascular regulation between the anterior and posterior cerebral conduit arteries. Indeed, regional differences are reported in response to a cold pressor test-induced hypertension, with a greater relative blood velocity increase in middle cerebral artery than the posterior cerebral artery (Herrington et al., 2019), suggesting a protective regulation of the posterior circulation to acute increases in blood pressure. Evidence from extreme levels (-60 mmHg) of lower body negative pressure (Thrall et al., 2021) and sit-to-standing (Sorond et al., 2005) have shown that the posterior cerebral artery may be more susceptible to reductions in blood flow from acute hypotension than the middle cerebral artery, which may be related to differences in basal vascular tone augmenting the orthostatic-induced reductions in blood flow of the posterior cerebral conduit arteries (Sato, Fisher, et al., 2012). A reduction in internal carotid artery blood flow at all levels of increasing lower body negative pressure (-20 , -35 , -50 mmHg) whilst vertebral artery blood flow was maintained at all levels, further suggest that only at extreme (>50 mmHg) levels might posterior cerebral blood flow become compromised (Ogoh et al., 2015). Posterior cerebral blood flow reductions occurring at extreme levels of orthostasis may be a mechanism related to orthostatic tolerance. Those who maintain cerebral blood flow at the

posterior cerebral conduit arteries during lower body negative pressure are shown to have the highest tolerance to orthostasis (Kay & Rickards, 2016). One proposed mechanism for the regional regulation between the anterior and posterior regions during acute hypotension may be modulated by the associated levels of hypocapnia (Lewis et al., 2015) or hypercapnia (Herrington et al., 2019; Thrall et al., 2021), aligning with earlier findings of differences in carbon dioxide reactivities between the anterior and posterior regions in the cerebral conduit arteries (Sato, Sadamoto, et al., 2012; Willie et al., 2012).

In contrast, there are several studies which have failed to replicate reports of regional static cerebral autoregulation. Indeed, cold pressor test-induced hypertension elevations in cerebral blood velocity were shown not to be different between the middle cerebral artery and posterior cerebral artery (Washio et al., 2020). The follow-up to the Kay & Rickards (2016) study failed to replicate the maintained posterior cerebral artery blood velocity relative to reductions in middle cerebral artery during lower body negative pressure (Kay et al., 2017), and similar reductions in internal carotid and vertebral artery blood flow have been reported during incremental lower body negative pressure (Kaur et al., 2018). Furthermore, no difference in regulation between middle cerebral artery and posterior cerebral artery was reported during steady-state orthostasis-induced changes in blood pressure (i.e., supine, head-down tilt, and/or head-up tilt) superimposed on carbon dioxide reactivity (Tymko et al., 2015) or lower body negative pressure (Deegan et al., 2010; Tymko et al., 2016).

Whilst evidence of anterior-posterior regional differences during static cerebral autoregulation at the cerebral conduit arteries is equivocal, these reports regularly only measure cerebral blood velocity of the intracranial arteries. Capturing the vasoactive and volumetric regulation of the extracranial arteries is essential to identify regional cerebral autoregulation between the anterior and posterior cerebral conduit arteries, as previously demonstrated by Sato and colleagues (Sato, Fisher, et al., 2012). As such volumetric duplex ultrasound measurements

should be incorporated when assessing cerebral autoregulation, in addition to blood velocity measurements of the intracranial arteries, to provide the greatest understanding of the regional cerebral blood flow regulation.

2.6.2 Regional cerebral blood flow response to hypoxia

Acute hypoxia-induced increases in global cerebral blood flow are not uniform across the brain (Binks et al., 2008). For example, acute poikilocapnic hypoxia increases at the frontal lobes of the brain are concomitant with reductions in cerebral blood flow, a reversal of neurovascular coupling, and alterations to oxidative metabolism in the default mode network (Lawley et al., 2017; Rogan et al., 2022; Rossetti et al., 2020). In the cerebral conduit arteries, absolute reactivity slopes are largely dependent on baseline flow and since the internal carotid artery has an inherently larger baseline cerebral blood flow than the vertebral artery it is common to compare the relative reactivity slopes (Willie et al., 2012). In response to isocapnic hypoxia, the vertebral artery has a larger relative blood flow increase compared to the internal carotid artery, middle cerebral artery, and posterior cerebral artery (Willie et al., 2012). Moreover, whilst carbon dioxide tensions and hypocapnic-induced vasoconstriction may differ between poikilocapnic hypoxia exposures from different experiments, the vertebral artery was found to be the only artery to vasodilate (Ogoh et al., 2013) and to have a 20% larger blood flow increase than the internal carotid artery that persisted throughout the subsequent decline in cerebral blood flow with time of exposure (Lewis et al., 2014).

A greater hypoxic sensitivity in the vertebral arteries is proposed to maintain oxygen delivery to the posterior regions of the brain involved in homeostatic and cardiorespiratory centres that play a crucial role in the chemoreflex control, hypoxic ventilatory response, and autonomic control (Hoiland et al., 2015; Lewis et al., 2014; Ogoh et al., 2013; Willie et al., 2012). Indeed, a relationship between the hypoxic ventilatory decline during isocapnic hypoxia and reactivity

to hypoxia in the vertebral artery, but not internal carotid artery, may be related to carbon dioxide–[H⁺] washout modulating respiratory responses or alterations to peripheral chemoreceptor sensitivity (Hoiland et al., 2015). Preferential maintenance of blood flow to respiratory control centres in the posterior regions may only be required during the initial hypoxic ventilatory response that occurs within early hours or days of hypoxic exposure since prolonged exposure (7 to 14 days) to hypobaric hypoxia report no regional differences (Hoiland et al., 2018; Lafave et al., 2019; Willie, Smith, et al., 2014). Whilst a similar number of studies have failed to report anterior-posterior regional differences in blood flow regulation to hypoxia (Fernandes et al., 2018; Hoiland et al., 2017; Kellawan et al., 2017; Lafave et al., 2019), all of the present literature investigating the cerebral blood flow response to hypoxia are limited by small sample sizes (< 14 participants) and therefore it remains equivocal whether anterior-posterior regional differences exist during acute hypoxia.

Carbon dioxide reactivity during hypoxia is found to be regionally different between anterior and posterior regions (Sato, Sadamoto, et al., 2012; Willie et al., 2012). Sato, Sadamoto and colleagues (2012) reported that overall carbon dioxide reactivity (incremental through the hypocapnic and hypercapnic range) is lower in the vertebral and basilar arteries than the internal carotid and middle cerebral arteries, whereas Willie et al., (2012) reported greater hypocapnic reactivity in the vertebral artery than the internal carotid artery, with no reported differences in the hypercapnic range nor overall carbon dioxide reactivity. Carbon dioxide reactivity was also found to be segmentally different in both anterior and posterior regions, with the extracranial arteries found to be approximately 25% more sensitive than the intracranial arteries (Willie et al., 2012). Whilst these segmental regulation differences may be due to differences in reactivity calculations that are derived from cerebral blood flow in the extracranial arteries and blood velocity in the intracranial arteries, anterior-posterior regional differences in vascular regulation may occur at different segments of the cerebrovasculature

within a region and should be considered. Indeed, four-dimensional flow magnetic resonance imaging quantification of arterial cross-sectional area revealed that cerebral blood flow increases were similar between regions, but were mediated by vasodilation of the anterior cerebral conduit arteries and not the posterior cerebral conduit arteries, suggesting that site of vascular regulation in the posterior regions occur more downstream at the level of the pial arteries (Kellawan et al., 2017).

2.6.3 Regional cerebral autoregulation during hypoxia

Anterior and posterior regional differences in dynamic cerebral autoregulation during hypoxia could contribute to the development of acute mountain sickness. Symptoms of dizziness or vertigo, headaches, vomiting and nausea, imbalance, weakness, ataxia that are associated with alterations in blood flow to the posterior circulation (Neto et al., 2017; Savitz & Caplan, 2005) are akin to that experienced during acute mountain sickness (Roach et al., 2018). Further, associations between acute mountain sickness and cerebral haemodynamics, blood flow imbalances, and changes in vascular tone in the vertebral arteries are reported (Barclay et al., 2021; Bian et al., 2014). Whilst there is a lack of relationship between the reduction in dynamic cerebral autoregulation and severity of acute mountain sickness during hypoxia (Smirl et al., 2014; Subudhi et al., 2010, 2014, 2015; Ter Minassian et al., 2001; Tymko et al., 2020), these studies have only investigated dynamic cerebral autoregulation of cerebral conduit arteries that supply the anterior regions of the brain (i.e., MCA, CCA, and ICA).

To date, assessments of dynamic cerebral autoregulation during hypoxia in the extracranial arteries that measured volumetric blood flow and vascular tone are limited to the common carotid or internal carotid arteries, which only reflect delivery of cerebral blood flow to the anterior regions (Horiuchi et al., 2016, 2022; Tymko et al., 2020; van Helmond et al., 2018). In fact, there has been only one investigation of regional dynamic cerebral autoregulation in

hypobaric hypoxia, which is limited to blood velocity measurements of the intracranial arteries (Smirl et al., 2014). Compared to the middle cerebral artery, the authors report that the posterior cerebral artery had a decreased low frequency gain shift at day 2 and day 14 at high altitude to spontaneous oscillations in blood pressure, and an increased phase shift during repeated squat-to-stand manoeuvres (0.10 Hz) upon return to sea level from a fortnight at high altitude (Smirl et al., 2014). A decrease in gain and increase in phase shift reflects an improved dynamic cerebral autoregulation implies that the posterior cerebral artery has better ability to buffer changes in blood pressure compared to the middle cerebral artery. Whilst this study by Smirl and colleagues (2014) provides some evidence of the regional differences in dynamic cerebral autoregulation, the topic is largely unexplored, and therefore further research is required to fully investigate regional dynamic cerebral autoregulation during hypoxia within the intracranial and extracranial arteries.

2.6.4 Mechanisms of regional cerebral blood flow regulation

In animal models, differences in sensitivities to vasodilators and vasoconstrictors between the anterior and posterior cerebral conduit arteries are reported (Hamel et al., 1988). For example, in comparison to anteriorly-located arteries, the posterior cerebral conduit arteries have a greater density of β -adrenoceptor and its coupled response of adenylate cyclase (Ayajiki & Toda, 1992), as well as having a more sensitive activation of endothelial vasopressin receptors and the coupled nitric oxide synthase response (Katusic, 1992; Onoue et al., 1988; Suzuki et al., 1993). In addition, segmental regulation differences between the cerebral conduit arteries have been suggested with the extracranial portion of the vertebral artery found to be less sensitive than the intracranial portion of the vertebral artery (Suzuki et al., 1993).

In humans, heterogeneous regional regulation in vessel tone and blood flow between anterior and posterior circulations may be underpinned by these differences in sympathetic

adrenoreceptor subtype distribution and parasympathetic innervation to ensure that adequate blood flow to the brainstem is prioritized (Koep et al., 2022). Specifically, there is a greater density of $\alpha 1$ receptors in the anterior circulation in contrast to a greater density of $\beta 2$ receptors and Ca^{2+} channel receptors in the posterior circulation, as well as the presence of parasympathetic innervation in the vertebral arteries compared with the internal carotid arteries (Koep et al., 2022). In response to hypoxia, adenosine-triphosphate-sensitive K^+ channels were found to only mediate the hypoxia-induced increase at the internal carotid artery blood flow and were not involved at the vertebral artery blood flow (Rocha et al., 2020). Hypertensive patients, who have an impaired endothelium-dependent vasodilation, are shown to have a blunted increase in vertebral artery blood flow in comparison to the internal carotid artery when exposed to hypoxia, suggesting a functional vasodilatory signalling regional difference between the anterior and posterior circulations (Fernandes et al., 2018). Similarly, hypertensive patients have selective impairment of vertebral artery vasodilation compared to the internal carotid artery in response to L-arginine that may suggest a lower sensitivity to nitric oxide bioavailability in the posterior circulations (Vianna et al., 2018). However, cerebral blood flow and cerebrovascular tone regulation by nitric oxide synthase and nitric oxide bioavailability has been shown to be regionally uniform in anterior and posterior intracranial and extracranial arteries (K. J. Carter et al., 2021). Finally, the vertebral arteries are less sensitive to exacerbated reactive oxygen species and attenuated nitric oxide bioavailability that occurs during isocapnic hyperoxia as the vertebral artery can maintain blood flow whereas internal carotid artery blood flow is reduced (Mattos et al., 2019). Supplementation of vitamin C attenuated the reduction in internal carotid artery blood flow during isocapnic hyperoxia which may further suggest that the anterior circulation has a greater sensitivity to nitric oxide bioavailability than the posterior circulation (Mattos et al., 2020).

2.7 Thesis aims

The cerebral conduit arteries play an important role in the cerebral blood flow regulation. Current literature proposes an anterior-posterior regional difference in cerebral blood flow regulation at the cerebral conduit arteries, but with a lack of empirical research examining the posterior cerebral conduit arteries using vascular tone and volumetric measurements, evidence remains equivocal (Figure 2.9). Acute hypoxia elicits a reliable and repeatable stimulus that provides a suitable model to better understand the mechanisms involved in the regulation of cerebral blood flow during a compromised oxygen delivery.

Therefore, the aim of this thesis was to investigate regional blood flow regulation between the cerebral conduit arteries that source the anterior and posterior regions of the brain in acute poikilocapnic hypoxia.

The first study (Chapter 3) was conducted to establish a level of proficiency in Doppler ultrasound sonography for the subsequent empirical studies within this thesis. Specifically, between-day reliability studies were conducted to determine sonographer intra-rater reliability of cerebral haemodynamics of the intracranial and extracranial arteries as measured by TCD and duplex ultrasound, respectively.

The second study (Chapter 4) investigated the bilateral regional blood flow regulation in the extracranial cerebral conduit arteries to acute poikilocapnic hypoxia. Specifically, whether anatomical variabilities, vessel imbalances, and unilateral measurements of the internal carotid arteries and vertebral arteries may impact the regional blood flow and vascular tone regulation to acute poikilocapnic hypoxia (Figure 2.9. Q1, 2, & 3). The secondary aim of this study was to investigate whether unilateral measurements are reflective of the true bilateral cerebral blood

flow regulation given that lateral arteries are not always asymmetrical in size and blood flow (Figure 2.9. Q4).

The third study (Chapter 5) investigated regional dynamic cerebral autoregulation in the intracranial and extracranial cerebral conduit arteries in acute poikilocapnic hypoxia. Specifically, whether the posterior circulation has a poorer capability to dampen abrupt reductions in blood pressure than the anterior circulation in normoxia and acute poikilocapnic hypoxia (Figure 2.9. Q5).

The fourth study (Chapter 6) investigated the effect of the metabolic state of the visual cortices on regional extracranial vascular tone and dynamic cerebral autoregulation in the intracranial arteries in normoxia and acute poikilocapnic hypoxia. Specifically, whether, in normoxia and hypoxia, the differences in dynamic cerebral autoregulation between the anterior and posterior intracranial arteries may be a consequence of a lower basal vascular tone in the posterior circulation in response to an increased neuronal metabolic demand of the visual cortices caused by eyes being open during cerebrovascular assessments (Figure 2.9. Q6).

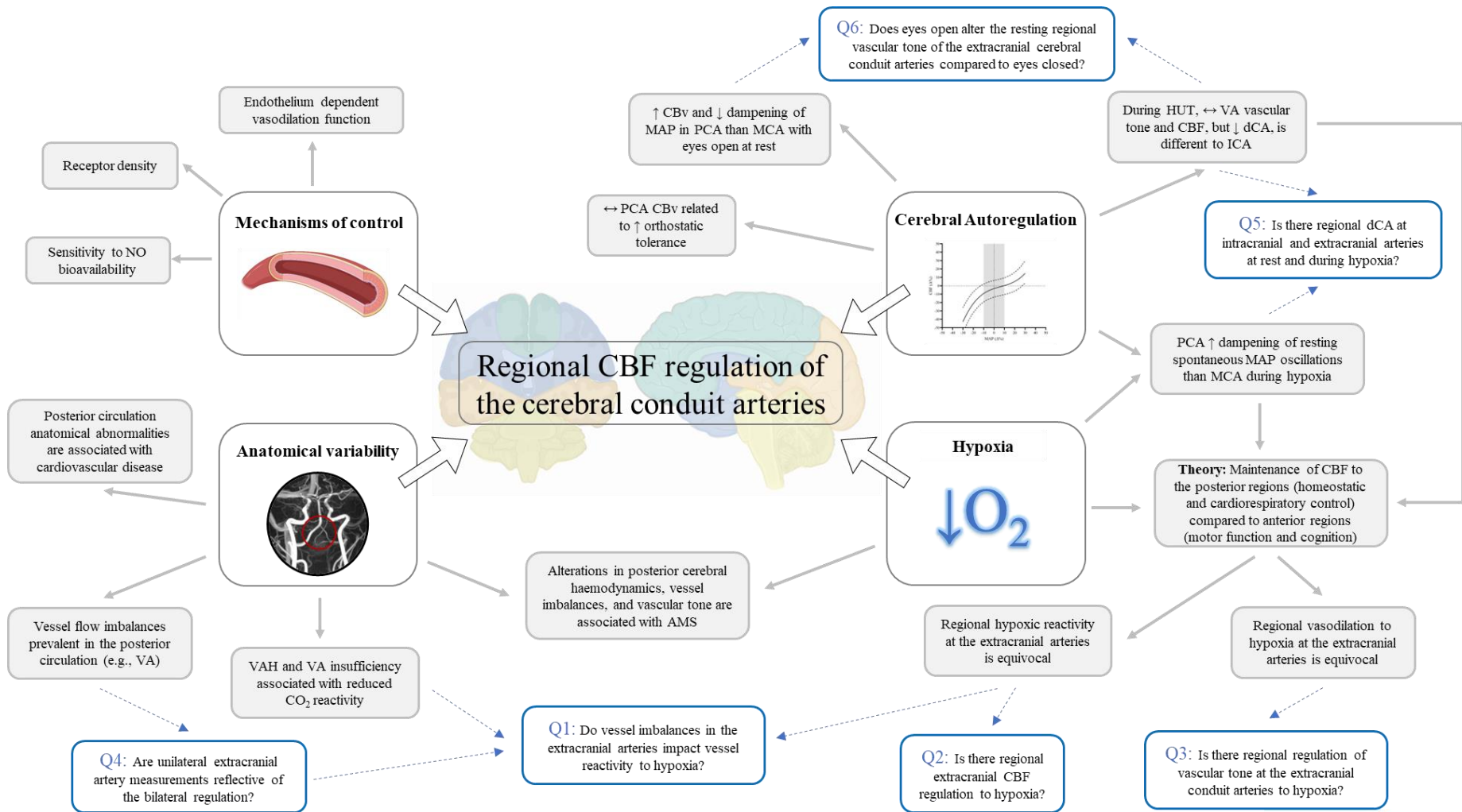


Figure 2.9. Summary of the evidence of anterior-posterior regional differences in the cerebral conduit arteries and the aims addressed in this thesis. *Chapter 4*) Anatomical variabilities, which are more prevalent in the posterior cerebral conduit arteries such as vessel flow imbalances and artery hypoplasia, are related to a reduced cerebrovascular function and may impact on regulation of posterior circulation to vasoactive stimuli, such as hypoxia, in comparison to the anterior circulation (Q1). It is proposed that cerebral blood flow regulation is different in the posterior cerebral conduit arteries compared to the anterior cerebral conduit arteries to hypoxia to preferentially maintain circulation of the posterior regions of the brain involved in homeostatic and cardiorespiratory control. However, due to small sample sizes, unilateral measurements of cerebral conduit arteries, and a limited number of studies which have directly measured vascular tone changes, evidence of regional differences in vascular tone and cerebral blood flow regulation between the anterior and posterior cerebral conduit arteries during hypoxia remains equivocal (Q2 & 3). Unilateral measurements of the posterior cerebral conduit arteries may not be reflective of the true bilateral cerebral blood flow regulation if lateral arteries are asymmetrical in size and blood flow (Q4). *Chapter 5*) Due to differences in vascular tone, the posterior circulation is proposed to have a greater capability to dampen fluctuations in blood pressure than the anterior circulation during normoxia at rest. To date, there is only one study that has explored regional intracranial artery regional dynamic cerebral autoregulation during hypoxia. Therefore, concurrent intracranial and extracranial artery regional dynamic cerebral autoregulation differences to capture volumetric and vasoactive regulation during hypoxia is yet to be explored (Q5). *Chapter 6*) The differences in dynamic cerebral autoregulation between the anterior and posterior cerebral conduit arteries may be a consequence of a lower resting vascular tone in the posterior circulation in response to an increased neuronal metabolic demand of the visual cortices caused by individuals eyes being open during cerebrovascular assessments (Q6). Abbreviations; AMS, acute mountain sickness; CBF, cerebral blood flow; CBv, cerebral blood velocity; dCA, dynamic cerebral autoregulation; HUT, head-up tilt; MAP, mean arterial pressure; MCA, middle cerebral artery; NO, nitric oxide; PCA, posterior cerebral artery; VA, vertebral artery; VAH, vertebral artery hypoplasia. Created with BioRender.com.

Chapter Three

Between-trial reliability of duplex and transcranial Doppler ultrasound measurements in the cerebral conduit arteries

3.1 Abstract

Haemodynamics of the cerebral conduit arteries can be measured using duplex and transcranial Doppler ultrasound (TCD) ultrasound. Reliability of these measurements is operator dependent, with guidelines suggesting that an intra-rater reliability assessment should be completed before investigative research. This study aimed to determine the between-trial reliability of cerebral haemodynamics acquired by duplex ultrasound and TCD. The relationship between logged hours of practice and reliability was also investigated. Thirty-five young healthy participants were recruited across four studies. Each study consisted of two trials of 10-min rest at the same time of day separated by a minimum of 24h. Blood velocity, vessel diameter, and blood flow of the common carotid artery, internal carotid artery, and vertebral artery were assessed from the *Siemens* (at 50h and 100h practice) and *Terason* (200h) duplex ultrasound. Blood velocity of the middle cerebral artery and the posterior cerebral artery were assessed from *Spencer Technologies* (50h) TCD. Reliability was determined by the coefficient of variation (CV) and intra-class coefficient (ICC). Reliability of blood flow for all arteries in the *Siemens* was improved with practice from poor–good at 50h (CV = 11–24 %, ICC = 0.39–0.78) to good–excellent at 100h (CV = 6–11%, ICC = 0.88–0.91). Excellent reliability was reported in the *Terason* (CV 4–8%, ICC >0.94). TCD also showed excellent reliability (CV 2–3%, ICC >0.98). In conclusion, excellent between-trial reliability of cerebral hemodynamic measures acquired by duplex and TCD ultrasound is achievable, although at least 100h practice is required.

3.2 Introduction

Doppler ultrasound is a non-invasive, portable technique with high temporal resolution that can be used to produce real-time measurements of cerebral haemodynamics (Ng & Swanevelder, 2011; Oglat et al., 2018). High-frequency sound waves are emitted from the transducer and propagate through soft tissue to be either absorbed by the tissue or reflected to the transducer. Within an insonated blood vessel, the velocities of all moving blood cells are presented as a spectral display forming the Doppler signal and are calculated from the difference between the received and transmitted pulses using the Doppler frequency shift formula below (Ng & Swanevelder, 2011; Oglat et al., 2018).

$$\text{Doppler Frequency Shift} = \frac{2 \times (\text{Velocity of Reflector (cm/s)} \times \text{Incident Frequency} \times \cos(\theta))}{\text{Propagation Speed}}$$

Propagation speed is dependent on the medium the ultrasound beam is emitted into, which for soft tissue is approximately 1541 m/s. Incident frequency is the transducer frequency and theta (θ) is the angle of insonation or Doppler angle between the ultrasound beam from the transducer and tissue or organ of interest. It is essential that the Doppler angle remains $\leq 60^\circ$ since cosine values at larger Doppler angles [e.g., $\cos(90^\circ) = 0$] cause large blood velocity overestimations (Oglat et al., 2018; M. Y. Park et al., 2012). For example, the error in blood flow volume calculation for a 5° deviation in Doppler angle from 60° leads to a 18.4% error (Thomas et al., 2015).

Transcranial Doppler ultrasound (TCD) is type of Doppler ultrasound which can be used to assess velocity of red blood cells in the conduit arteries within the cranium. Low frequency transducers (2.0–3.5 MHz) that can penetrate through thin portions of the temporal bone are secured to the skull with the addition of a headband enabling continuous measurements of beat-to-beat blood velocity. A variety of standardised acoustic windows are available to insonate a variety of conduit arteries within circle of Willis (Purkayastha & Sorond, 2012). TCD does not

provide an image of the vessel, therefore requires the sonographer to be experienced insonating the blood vessel by the visual Doppler spectra and audible Doppler shift, in addition to such vessel identification approaches like the transient carotid compression test.

Duplex ultrasound can concurrently measure blood velocity and blood vessel diameter to enable calculations of volumetric blood flow. Pulse wave Doppler imaging mode displays the spectral Doppler signal to calculate blood velocity of moving red blood cells. Brightness mode (B-Mode) offers a greyscale 2-dimensional image of the blood vessel, where the brightness of the image is based on the amplitude or intensity of each reflected sound wave and its depth and can be used to image an artery in the longitudinal axis to measure blood vessel diameter. B-mode imaging also ensures that the Doppler spectra waveform represents the flow profile of all moving red blood cells within the cerebral artery, often a parabolic-shaped laminar flow profile, by adjusting the Doppler gate to the width of the vessel (Oglat et al., 2018). Despite the benefits of duplex ultrasound, there is a known ‘trade-off’ between Doppler imaging and B-Mode imaging (Thomas et al., 2015). For optimal B-mode resolution the transducer should be orientated perpendicular to blood vessel, whereas for acceptable estimations of blood velocity the Doppler imaging angle must be $\leq 60^\circ$ which may require further transducer orientation (M. Y. Park et al., 2012; Thomas et al., 2015). The Doppler angle can be visualised on B-mode imaging and adjusted appropriately in relation to the blood vessel using an in-built beam steering function and various transducer manipulation skills. In an untrained sonographer, tiny alterations in a Doppler angle and/or a loss of resolution on the B-Mode image causing inaccuracies in diameter can cause gross deviations to flow volume estimations (Schöning et al., 1994; Thomas et al., 2015).

Doppler ultrasound techniques require highly skilled operators to acquire accurate high-quality images of the cerebral arteries. To achieve proficiency, novice sonographers should develop a full understanding of the cerebrovasculature anatomy, learn how best to visualise the cerebral

arteries using journal guides and video demonstrations of transducer manipulation and ultrasound machine-specific ‘knobology’, and should complete over > 150 scans of each artery of interest with guided feedback from a trained sonographer (Bahner et al., 2016; Ihnatsenka & Boezaart, 2010; Thomas et al., 2015). Before completing investigative research, assessments of intra-rater reliability should be conducted as evidence of proficiency in Doppler ultrasound techniques, such as the intra-class correlation coefficient (ICC) and the recommended coefficient of variation (CV) of < 10 % (Thomas et al., 2015).

The primary aim of this study was to determine the between-trial reliability of cerebral haemodynamics acquired by *Siemens and Terason* duplex ultrasound devices, and *Spencer Technologies* TCD. We also aimed to examine the relationship between logged hours of practice and reliability between the *Siemens* device at 50 h and 100 h. Three separate between-trial reliability studies using duplex ultrasound were completed in the common carotid arteries (CCA), the internal carotid arteries (ICA), and the vertebral arteries (VA); two using the *Siemens* (logged practice: 50 h and 100 h) and one using *Terason* (logged practice: 200 h). Reliability of *Spencer Technologies* TCD (logged practice: 50 h) was measured in the middle cerebral arteries (MCA) and the posterior cerebral arteries (PCA).

3.3 Methods

Ethical Approval

Ethical approval for these studies was obtained from Bangor University (*Siemens* duplex ultrasound: proposal number P07-18/19, accepted 05/03/2019, Appendix 1; *Terason* duplex ultrasound and *TCD*: proposal number P05-20/21, accepted 03/02/2021, Appendix 3) and was conducted following the standards of the *Declaration of Helsinki 2013*, except for registration in a database, with written informed consent obtained from all participants.

Participants

Sample cohort

Study	1	2	3	4
Device type	Duplex Ultrasound	Duplex Ultrasound	Duplex Ultrasound	TCD
Manufacturer	<i>Siemens</i>	<i>Siemens</i>	<i>Terason</i>	<i>Spencer Technologies</i>
Logged practice (h)	50	100	200	50
Sample size (N)	10	10	5	10
Male:Female	6:4	8:2	4:1	6:4
Age (yr)	26 ± 3	24 ± 4	30 ± 6	29 ± 5
Height (cm)	176.3 ± 9.2	179.0 ± 9.4	178.7 ± 6.0	175.5 ± 5.8
Weight (kg)	69.8 ± 9.5	68.3 ± 5.4	177.3 ± 11.5	76.9 ± 11.9

Participants were non-smokers, and free from cardiovascular, haematological, and neurological disease. Participants were instructed to refrain from consuming alcohol and from undertaking exhaustive exercise within 24 h of visiting the laboratory and were instructed to match their diet and supplement intake, including caffeinated beverages, before each trial.

Experimental design and measurements

For each between-trial reliability study, participants completed two trials at the same time of day separated by a minimum of 24 h and measurements were collected after 10-min period of rest by a single sonographer (AF).

Duplex ultrasound measurements

Three between-trial reliability studies were completed using duplex ultrasound, twice with the *Siemens* at 50 h and 100 h and once on with the *Terason* at 200 h. All duplex ultrasound measurements were collected in the supine position, at 30 frames per second, and as per recommended technical guidelines (Thomas et al., 2015). High-resolution B-mode images were used to measure vessel diameter. Flow velocity was measured using Doppler velocity spectrum with the cursor set in the centre of the vessel with a 60° angle of insonation with the

Doppler gate adjusted to fill the size of the vessel. The left and right artery of the CCA, ICA, and VA were measured by left- and right-handed assessments, respectively. The CCA were measured 2 cm proximal to the carotid bifurcation, the ICA were measured 1.0–1.5 cm distal to the carotid bifurcation, and the VA were measured between C3 and the subclavian artery. The location was chosen based on the position that ensured no turbulent or retrograde flow and that was most reproducible for each individual between trials.

Siemens: Two between-trial reliability studies were conducted, one at 50 h and one at 100 h of logged practice in order to examine the relationship between practice and reliability. Duplex ultrasound measurements were collected using a 12 MHz linear transducer (Siemens Acuson X300, Siemens Healthcare, GmbH; Erlangen: Germany). To improve the accuracy of the blood flow measurements and minimise the trade-off between B-mode and pulsed-wave Doppler mode (Thomas et al., 2015), vessel diameter and flow velocity measurements were collected in consecutive 30 s recordings with care taken to maintain the same position within the artery.

Terason: This between-trial reliability study was conducted after 200 h of logged practice. Systolic blood pressure, diastolic blood pressure, and calculated mean arterial pressure (MAP), were acquired from the brachial artery (Model M6 AC ME, Omron Healthcare Co., Ltd, Kyoto, Japan). Duplex ultrasound measurements were collected using a 15 MHz linear transducer (uSmart 3300, Terason, Burlington, MA, USA). Simultaneous B-mode and pulse wave mode imaging were used to measure each artery in consecutive 30 s recordings with care taken to maintain the same position within the artery.

Transcranial Doppler ultrasound measurements

This between-trial reliability study was conducted at 50 h of logged practice. Participants were positioned in a semi-recumbent position for TCD measurements. Beat-to-beat systolic blood pressure, diastolic blood pressure, and calculated MAP were measured from the finger arterial

waveform (Finometer Midi, Finapres Medical Systems, Netherlands). Cerebral blood velocity of the MCA and PCA were measured using two 2 MHz probes placed over the left and right transtemporal windows and secured in place via an adjustable head piece (PMD150, Spencer Technologies, Seattle, WA, USA). Insonation of each vessel was achieved using standardised procedures (Willie et al., 2011), with probe position and signal depth noted to replicate the placement between sessions. The MCA and PCA were assessed only on one side as determined by the strongest signal achievable. Confirmation of MCA and PCA were confirmed by responses to transient carotid compression test.

Data Processing

Duplex ultrasound

All duplex ultrasound data was captured and stored for subsequent offline analysis by an investigator blinded to the condition of the experimental trials. Offline analysis was adapted from standardised procedures described elsewhere (Hoiland et al., 2017; Ogoh et al., 2013). Blood flow was averaged from 10 cardiac cycles to minimise the impact of respiration and was calculated using the following equation:

$$\text{Blood flow (ml}\cdot\text{min}^{-1}\text{)} = [\text{TAMx (cm}\cdot\text{s}^{-1}\text{)}^2] \times [\pi \times (\text{mean artery diameter (cm)}^2)^2] \times 60$$

Where half of the time-averaged maximum velocity (TAMx; also known as peak envelope velocity) was used as an estimation of mean blood velocity (Seidel et al., 1999) and mean vessel diameter was measured using an automated edge-detection tracking software (Brachial Analyser, Medical Imaging Applications, Iowa, USA). Specifically, for the *Siemens* mean vessel diameter was calculated from a weighted average of the peak systolic and diastolic diameters across 10 cardiac cycles $[(\text{systolic diameter} \times \frac{1}{3}) + (\text{diastolic diameter} \times \frac{2}{3})]$, whereas for the *Terason* mean vessel diameter was calculated only from end-diastolic diameters across 10 cardiac cycles.

Transcranial Doppler ultrasound

Continuous beat-to-beat measurements of blood velocity of the MCA and PCA, and systolic and diastolic blood pressure were all acquired continuously at 1 kHz using an analog-to-digital converter (Powerlab 16/35; ADInstruments, Colorado Springs, CO, USA) and interfaced on a computer in real time using LabChart software (LabChart 8, ADInstruments). Resting time-averaged maximum values of MCAv and PCAv, and MAP were determined from each R-R interval and averaged over a five-minute period.

Statistical Analysis

Statistical analysis was conducted using SPSS Statistics v27 (IBM Corp., Armonk, NY, USA) and figures were created in GraphPad Prism (GraphPad Software, San Diego, CA, USA). Values are mean \pm standard deviation unless otherwise stated. Cardiovascular variables were analysed using a paired t-test and statistical significance was set at $P < 0.05$. For reliability studies, it is recommended to present the mean CV from individual CVs in the sample, rather than the sample CV (Atkinson & Nevill, 1998). Therefore, each artery within a participant was calculated with a CV using the following equation [(standard deviation of trial 1 and trial 2 / mean average of trial 1 and trial 2) multiplied by 100] and the mean CV from all participants was calculated as the operator between-trial reliability. The recommended CV for duplex ultrasound measurements is $< 10\%$ (Thomas et al., 2015). ICC was calculated as the absolute agreement using a two-way random model between trial 1 and trial 2. An ICC value ≤ 0.49 was considered poor reliability, 0.50–0.74 indicated moderate reliability, 0.75–0.89 indicated good reliability, ≥ 0.90 indicated excellent reliability (Koo & Li, 2016).

3.4 Results

MAP was measured during *Terason* duplex ultrasound and *Spencer Technologies* TCD studies only. MAP was similar on trial 1 (*Terason*: 84.2 ± 3.3 and *TCD*: 90.7 ± 5.6 mmHg) and trial 2 (82.0 ± 5.2 and 94.0 ± 12.5 mmHg, $P = 0.46$ and $P = 0.34$, respectively).

Duplex ultrasound

Resting values and the respective reliability indices of left and right CCA, ICA, VA vessel diameter, blood velocity, and blood flow measured by the *Siemens* duplex ultrasound are presented in Table 3.1. When the mean CV and ICC were calculated from the left and right arteries, *Siemens* 50 h CV for vessel diameter, blood velocity and blood flow, and ICC of blood flow showed poor–moderate reliability; CCA (CV = $3.7 \pm 2.6\%$, $8.3 \pm 8.0\%$, $10.9 \pm 11.2\%$ and ICC = 0.78), ICA (CV = $7.7 \pm 6.2\%$, $6.9 \pm 3.4\%$, $13.9 \pm 10.9\%$ and ICC = 0.61), and VA (CV = $9.0 \pm 14.0\%$, $9.6 \pm 8.6\%$, $23.7 \pm 21.8\%$, and ICC = 0.39). Reliability was improved with increasing hours of logged practice (Figure 3.1), as *Siemens* 100 h CV for vessel diameter, blood velocity, and blood flow, and ICC for blood flow showed good–excellent reliability; CCA (CV = $2.4 \pm 1.8\%$, $4.9 \pm 4.1\%$, $5.5 \pm 3.8\%$, and ICC = 0.91), ICA (CV = $4.0 \pm 3.1\%$, $7.2 \pm 5.1\%$, $11.2 \pm 8.8\%$ and ICC = 0.88), and VA (CV = $2.4 \pm 1.5\%$, $6.8 \pm 5.1\%$, $8.5 \pm 5.3\%$, and ICC = 0.91).

Resting values and the respective reliability indices of left and right CCA, ICA, VA vessel diameter, blood velocity and blood flow measured by the *Terason* duplex ultrasound are presented in Table 3.2. The *Terason* mean CV for vessel diameter, blood velocity, and blood flow, and ICC of blood flow showed excellent reliability; CCA (CV = $1.3 \pm 1.0\%$, $6.1 \pm 5.0\%$, $5.4 \pm 4.2\%$, and ICC = 0.94), ICA (CV = $1.1 \pm 1.0\%$, $3.1 \pm 2.9\%$, $4.1 \pm 3.5\%$ and ICC = 0.96), and VA (CV = $1.4 \pm 1.0\%$, $7.3 \pm 4.5\%$, $7.6 \pm 3.7\%$, and ICC = 0.95).

	Day 1	Day 2	CV (%)	ICC
Common carotid artery (left)				
Vessel diameter (mm)	6.46 ± 0.36	6.68 ± 0.34	2.9 ± 1.8	0.803
Blood velocity (cm·s ⁻¹)	46.2 ± 5.2	45.5 ± 6.2	3.1 ± 2.7	0.945
Blood flow (ml·min ⁻¹)	452 ± 44	478 ± 71	5.9 ± 4.7	0.755
Common carotid artery (right)				
Vessel diameter (mm)	6.60 ± 0.44	6.60 ± 0.26	1.9 ± 1.7	0.848
Blood velocity (cm·s ⁻¹)	47.8 ± 6.0	46.0 ± 4.4	6.6 ± 4.5	0.648
Blood flow (ml·min ⁻¹)	490 ± 67	472 ± 50	5.2 ± 3.0	0.877
Internal carotid artery (left)				
Vessel diameter (mm)	5.17 ± 0.59	5.05 ± 0.56	3.6 ± 2.7	0.907
Blood velocity (cm·s ⁻¹)	49.1 ± 5.6	47.1 ± 7.9	7.2 ± 4.0	0.805
Blood flow (ml·min ⁻¹)	310 ± 59	280 ± 47	11.5 ± 7.6	0.654
Internal carotid artery (right)				
Vessel diameter (mm)	5.01 ± 0.48	5.13 ± 0.53	4.4 ± 3.6	0.798
Blood velocity (cm·s ⁻¹)	50.3 ± 9.7	51.7 ± 10.6	7.1 ± 6.2	0.858
Blood flow (ml·min ⁻¹)	299 ± 78	316 ± 55	11.0 ± 10.2	0.716
Vertebral artery (left)				
Vessel diameter (mm)	3.86 ± 0.45	3.91 ± 0.44	2.1 ± 1.7	0.969
Blood velocity (cm·s ⁻¹)	29.4 ± 6.1	29.1 ± 7.0	7.2 ± 5.8	0.902
Blood flow (ml·min ⁻¹)	106 ± 36	107 ± 37	9.4 ± 5.8	0.939
Vertebral artery (right)				
Vessel diameter (mm)	3.55 ± 0.51	3.47 ± 0.45	2.6 ± 1.4	0.972
Blood velocity (cm·s ⁻¹)	27.8 ± 5.8	27.8 ± 6.3	6.3 ± 4.5	0.932
Blood flow (ml·min ⁻¹)	85 ± 33	80 ± 28	7.7 ± 4.8	0.967

Table 3.1. Between-trial variation of cerebrovascular haemodynamics of the extracranial arteries at rest using *Siemens* duplex ultrasound with 100 h of logged practice. Extracranial arteries were measured on two trials separated by at least 24 h. The left and right common carotid, internal carotid, and vertebral arteries were assessed by the left- and right-hand, respectively. The coefficient of variation (CV) and intra-class correlation (ICC) were calculated as an index of inter-rater reliability. Values are means ± standard deviation.

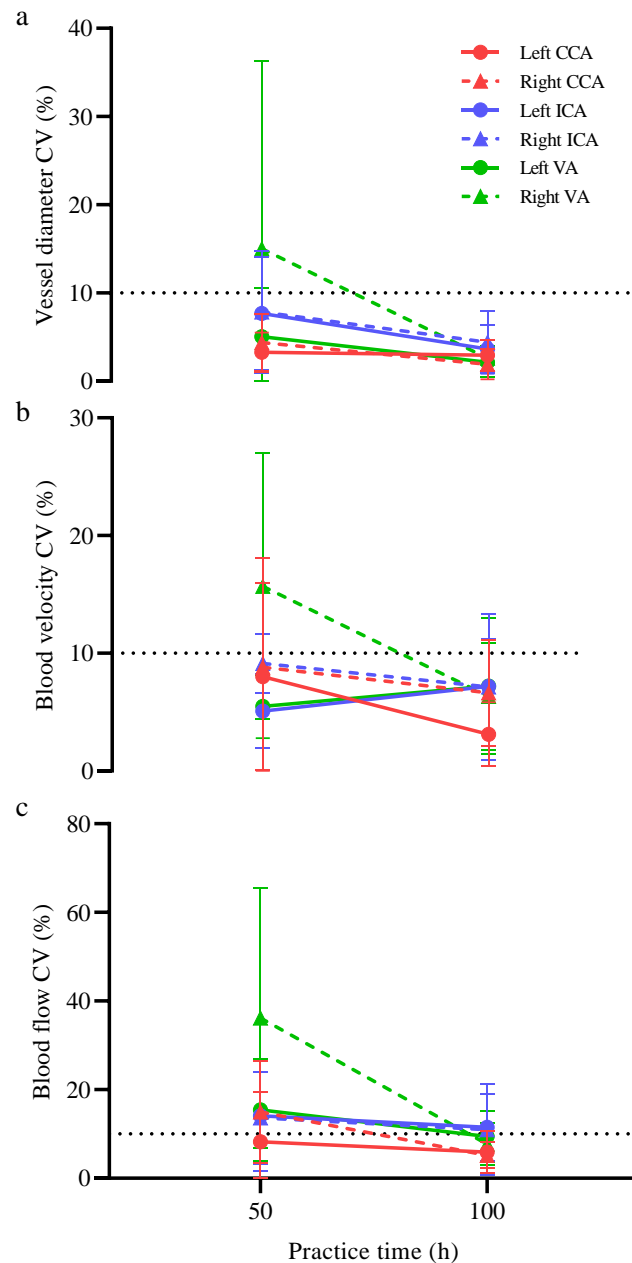


Figure 3.1. Coefficient of variation of the extracranial arteries measured using *Siemens* duplex ultrasound by logged hours of practice. Coefficient of variation of vessel diameter (a), blood velocity (b), and blood flow (c) in the left (circle) and right (triangle) common carotid artery (CCA, red), internal carotid artery (ICA, blue), and vertebral artery (VA, green) from repeat between-trial reliability studies with increasing hours of logged practice. Reliability was assessed at 50 h (left N = 6, right N = 4) and at 100 h (left and right N = 10) using the *Siemens* duplex ultrasound. A dotted line marked at 10% represents the recommended guidelines for proficiency in duplex ultrasound of the extracranial arteries (Thomas et al., 2015). Values are mean \pm standard deviation.

	Day 1	Day 2	CV (%)	ICC
Common carotid artery (left)				
Vessel diameter (mm)	6.80 ± 0.39	6.78 ± 0.45	0.9 ± 0.7	0.984
Blood velocity (cm·s ⁻¹)	43.7 ± 6.8	44.4 ± 2.4	6.4 ± 6.4	0.577
Blood flow (ml·min ⁻¹)	478 ± 89	482 ± 67	5.0 ± 4.9	0.930
Common carotid artery (right)				
Vessel diameter (mm)	6.93 ± 0.50	7.03 ± 0.52	1.6 ± 1.2	0.963
Blood velocity (cm·s ⁻¹)	42.4 ± 6.3	44.9 ± 7.5	5.7 ± 3.9	0.894
Blood flow (ml·min ⁻¹)	478 ± 77	522 ± 101	5.8 ± 3.9	0.915
Internal carotid artery (left)				
Vessel diameter (mm)	4.93 ± 0.36	4.97 ± 0.31	0.7 ± 0.7	0.992
Blood velocity (cm·s ⁻¹)	49.2 ± 9.4	48.5 ± 7.3	3.1 ± 3.3	0.995
Blood flow (ml·min ⁻¹)	285 ± 74	284 ± 64	3.3 ± 3.1	0.985
Internal carotid artery (right)				
Vessel diameter (mm)	5.03 ± 0.41	4.98 ± 0.44	1.5 ± 1.1	0.977
Blood velocity (cm·s ⁻¹)	47.6 ± 6.7	46.1 ± 8.1	3.0 ± 2.8	0.994
Blood flow (ml·min ⁻¹)	280 ± 24	269 ± 39	5.0 ± 3.9	0.884
Vertebral artery (left)				
Vessel diameter (mm)	3.93 ± 0.54	3.93 ± 0.43	1.7 ± 1.3	0.988
Blood velocity (cm·s ⁻¹)	28.0 ± 2.2	28.1 ± 4.5	7.0 ± 4.5	0.633
Blood flow (ml·min ⁻¹)	104 ± 33	103 ± 26	8.5 ± 4.1	0.932
Vertebral artery (right)				
Vessel diameter (mm)	3.50 ± 0.49	3.47 ± 0.45	1.1 ± 0.7	0.995
Blood velocity (cm·s ⁻¹)	27.8 ± 4.6	28.8 ± 6.1	7.6 ± 5.0	0.884
Blood flow (ml·min ⁻¹)	81 ± 25	84 ± 29	6.8 ± 3.4	0.980

Table 3.2. Between-trial variation of cerebrovascular haemodynamics of the extracranial arteries at rest using *Terason* duplex ultrasound with 200 h of logged practice. The extracranial arteries were measured on two trials separated by at least 24 h. The left and right common carotid, internal carotid, and vertebral arteries were assessed by the left- and right-hand, respectively. The coefficient of variation (CV) and intra-class correlation (ICC) were calculated as an index of inter-rater reliability. Values are means ± standard deviation.

Transcranial Doppler ultrasound

There was excellent reliability for blood velocity of the MCA (CV = 2.5 ± 2.6 %, ICC = 1.00, Table 3.3) and PCA (CV = 2.6 ± 3.0 %, ICC = 0.98).

	Trial 1	Trial 2	CV (%)	ICC
Middle cerebral artery				
Blood velocity (cm·s ⁻¹)	52.2 ± 14.9	51.8 ± 14.6	2.5 ± 2.6	0.996
Posterior cerebral artery				
Blood velocity (cm·s ⁻¹)	44.7 ± 10.5	44.1 ± 9.8	2.6 ± 3.0	0.979

Table 3.3. Between-trial variation of blood velocity of the intracranial arteries at rest using *Spencer Technologies* transcranial Doppler ultrasound. The intracranial arteries were measured on two trials separated by at least 24 h. The coefficient of variation (CV) and intra-class correlation (ICC) were calculated as an index of inter-rater reliability. Values are means ± standard deviation.

3.5 Discussion

Main findings

The primary aim of this study was to determine the between-trial intra-rater reliability of cerebral haemodynamics acquired by *Siemens* and *Terason* duplex ultrasound devices, and *Spencer Technologies* TCD. We also aimed to examine the relationship between logged hours of practice and reliability in the *Siemens* device. Reliability of blood flow in the *Siemens* was improved with practice from poor–good at 50 h (CV = 11–24 %, ICC = 0.39–0.78) to good–excellent at 100 h (CV = 6–11 %, ICC = 0.88–0.91). We report excellent reliability in the *Terason* for all extracranial arteries (CCA, ICA, and VA; CV < 7.6% and ICC > 0.94). We also reported excellent reliability in TCD measurements of the MCA and PCA blood velocity with an ICC > 0.98 and a CV < 3.0%.

Reliability of cerebral blood flow measurements

The resting cerebrovascular values for vessel diameter, blood velocity, and blood flow reported here are similar to that previously reported (Scheel, Ruge, & Schöning, 2000; Scheel, Ruge, Petruich, et al., 2000; Schöning et al., 1994). The CV varied depending on the cerebral haemodynamic variable of interest, with blood flow (CV = 7.6–11.2 %) having the largest CV (worst reliability) compared to vessel diameter (CV = 1.1–4.0 %) and blood velocity (CV = 3.1–7.2 %). The recommendation of achieving a CV < 10 % stated by Thomas et al., (2015) does not specify whether this is for measurements of vessel diameter, blood velocity, or blood flow. Blood flow is frequently the primary variable of interest when using duplex ultrasound, but since it is the product of vessel diameter and blood velocity, the CV of blood flow is reliant on the reliability of these two measurements. This study showed that to achieve a CV < 10% in blood flow, the range in CV across arteries for vessel diameter is narrower in comparison to the CV of blood velocity (Tables 3.1 and 3.2, Figure 3.1), which is expected as the non-linear relationship between Doppler angle and estimations of blood velocity by duplex ultrasound would cause more variability between repeated measurements. An excellent CV of vessel diameter ensures that measurements are reliable to detect alterations in vascular tone particularly during investigations where evidence is equivocal, such as exposure to acute hypoxia (Lewis et al., 2014; Ogoh et al., 2013). We advise that the CV for each cerebral haemodynamic variable of interest is reported for duplex ultrasound.

The reliability of blood velocity when measured in the MCA and PCA by TCD was better than duplex ultrasound (Table 3.3, CV < 3%) and may be explained by the fixed position of the Doppler probes on the headframe minimising movement and limited insonation windows that reduce possible insonation and measurement variability. Fixation of Doppler probes in duplex ultrasound has been applied during prolonged procedures, such as flow mediated dilation of

the brachial artery, and might be explored in future with an aim to reduce duplex ultrasound measurement of the cerebral haemodynamics.

Practice and duplex ultrasound machine type

Between-trial reliability of cerebral haemodynamics measurements acquired by duplex ultrasound is improved with practice where reliability is poor–moderate at 50 h improving to good–excellent at 100 h. Moreover, not all extracranial arteries require the same hours of practice to achieve a good reliability in duplex ultrasound measurements of blood flow (Figure 3.1). Location differences between the cerebral arteries likely impact the necessary practice and skill required to image each artery successfully and justify the recommendation to scan the artery of interest a minimum of 150 times (Thomas et al., 2015). Accessibility to the ICA can be obstructed by the jawbone and reliable measurements of blood flow may be restricted due to the positioning of the carotid bifurcation and its corresponding turbulent flow. Similarly, producing clear images of the VA diameter may be impacted by the positioning of the vertebrae and signal strength may be reduced due to its deeper location in the tissue. Anatomical variability within a cerebral artery is a topic of many investigations (Hart, 2016; Sato et al., 2015; Warnert, Hart, et al., 2016; Warnert, Rodrigues, et al., 2016) and can cause large variability in image quality between individuals as seen with a large standard deviation in the VA at 50 h (Figure 3.1). To ensure reliable and accurate images of arteries are collected, pre-screening participants before experimental trials has become common practice (Hoiland et al., 2017). We also advise that a separate reliability CV is reported for each artery of interest.

The reliability of TCD had benefited from the previous practice of the duplex ultrasound since the logged hours of TCD practice were considerably less (approx. 50 h). Transferable skills between duplex ultrasound and TCD is not unexpected since both require a full understanding

of the cerebrovasculature anatomy, transducer manipulation skills, and ultrasound machine-specific settings.

In addition to increased logged hours of practice, differences in hardware and software between the *Siemens* and *Terason* will have contributed to improvements in reliability. The *Terason* uses a higher transducer frequency for better image resolution in B-mode, can alter the screen size ratio used by B-mode and pulse wave mode, and has a greater capacity to collect measurements with concurrent B-mode and pulse wave mode imaging (triplex mode). When measuring in triplex mode in the *Siemens*, the processing capacity of the ultrasound is split, with the transducer frequency in B-mode reduced to accommodate the overwriting Doppler spectra in pulse wave mode. In turn, the Doppler scale (as determined by the pulse repetition frequency) is limited, so high blood velocity traces (such as in the CCA) can cause aliasing. Therefore, to overcome this trade-off and ensure accurate vessel diameter and blood velocity measurements the *Siemens* required consecutive collections. In contrast, the *Terason* has a higher ceiling before this is an issue and therefore can measure vessel diameter and blood velocity concurrently, which is essential for non-steady state measurements e.g., rapid thigh cuff deflation for assessments of dynamic cerebral autoregulation.

Conclusions

In conclusion, duplex and TCD ultrasound acquired measurements of cerebral haemodynamics in the extracranial and intracranial arteries had excellent between-trial reliability. To achieve excellent between-trial reliability of cerebral haemodynamics acquired by duplex ultrasound requires at least 100 h of practice.

Author contributions and acknowledgments

Authors: Alexander T. Friend, Gabriella M.K. Rossetti, Aamer Sandoo, Jamie H. Macdonald, and Samuel J. Oliver. AF and SO conceived and designed the study. All authors contributed to

the acquisition, analysis, or interpretation of data for the work. AF and SO drafted the manuscript, with all remaining authors reviewing and providing critical feedback important for intellectual content.

We would like to thank the participants for their time and effort in this study. We also thank Liam Joyce and Harry Nicholson for their contribution to data collection.

Chapter Four

Bilateral regional extracranial blood flow regulation to hypoxia and unilateral duplex ultrasound measurement error

4.1 Abstract

Whether blood flow regulation to hypoxia is similar between left and right internal carotid arteries (ICA) and vertebral arteries (VA) is unclear. Extracranial blood flow is regularly calculated by doubling a unilateral assessment; however, lateral artery differences may lead to measurement error. This study aimed to determine extracranial blood flow regulation to hypoxia when factoring for vessel type (ICA or VA) and vessel side (left or right) effects, and investigate unilateral assessment measurement error compared to bilateral assessment. In a repeated-measures crossover design, extracranial arteries of 44 participants were assessed bilaterally by duplex ultrasound during 90 min of normoxic and poikilocapnic hypoxic (12.0% fraction of inspired oxygen) conditions. Linear mixed model analyses revealed no ‘Condition’ × ‘Vessel Type’ × ‘Vessel Side’ interaction for blood flow, vessel diameter, and flow velocity (all $P > 0.05$) indicating left and right ICA and VA blood flow regulation to hypoxia was similar. Bilateral hypoxic reactivity was comparable [ICA, 1.4 (1.0) vs VA, 1.7 (1.1) $\Delta\% \cdot \Delta\text{SpO}_2^{-1}$; $P = 0.12$]. Compared to bilateral assessment, unilateral mean measurement error of the relative blood flow response to hypoxia was up to 5%, but individual errors reached 37% and were greatest in ICA and VA with the smaller resting blood flow due to a ratio-scaling problem. In conclusion, left and right ICA and VA regulation to hypoxia is comparable when factoring for vessel type and vessel side. Assessing the ICA and VA vessels with the larger resting blood flow, not the left or right vessel, reduces unilateral measurement error.

4.2 Introduction

Cerebral blood flow regulation is critical to support oxygen delivery to match the high metabolic demand of the brain and to maintain normal neurovascular function (Ogoh, 2017; Willie, Tzeng, et al., 2014). During acute hypoxia when arterial oxygen content is reduced, global cerebral blood flow increases (Hoiland et al., 2018). However, hypoxia-induced changes in blood flow are not uniform across the brain (Lawley et al., 2017; Rossetti et al., 2020), which may in part relate to different regulation of blood flow at the extracranial arteries (Lewis et al., 2014; Ogoh et al., 2013; Subudhi et al., 2014; Willie et al., 2012).

Regional extracranial blood flow regulation can be measured non-invasively by duplex ultrasound of the vertebral arteries (VA) that feed the homeostatic posterior brain regions, and the internal carotid arteries (ICA) that feed the more functional anterior brain regions. In response to hypoxia, absolute increases in blood flow within the ICA are greater than the VA (Lafave et al., 2019). When indexed as a relative response some evidence indicates that the blood flow increase to hypoxia in the VA is greater than in the ICA (Lewis et al., 2014; Ogoh et al., 2013; Subudhi et al., 2014; Willie et al., 2012). Although the majority of literature reporting differences between ICA and VA blood flow regulation has been in response to hypoxia, the greater relative response in the VA has also been observed in response to other stressors including carbon dioxide, orthostasis, and exercise, and is proposed as a mechanism to preferentially maintain posterior blood flow to the homeostatic brain regions (Sato et al., 2016; Sato, Fisher, et al., 2012; Sato, Sadamoto, et al., 2012). Despite this compelling argument, a disparity exists within the literature with a similar number of studies failing to report differences between the ICA and VA blood flow regulation to hypoxia (Hoiland et al., 2017; Lafave et al., 2019; Willie, Smith, et al., 2014). It is also contentious whether the increase in blood flow to hypoxia at the extracranial arteries is regulated by a change in vessel diameter (Lewis et al., 2014) or not (Ogoh et al., 2013).

In contrast to the study of ICA (anterior) versus VA (posterior) extracranial regional blood flow response to hypoxia, the effect of vessel side has yet to be considered in studies using duplex ultrasound. Regulation of extracranial blood flow to hypoxia is typically assessed by doubling unilateral measurements of the ICA and VA. Reports suggest that at rest the left and right ICA have equal blood flow, whereas the right VA has 20–30% less blood flow than the left VA as a consequence of its smaller resting vessel diameter (Khan et al., 2017; Schöning et al., 1994). Anatomical variations in the aortic branching that alter shear stress and vascular resistance between arteries have been proposed as a possible mechanism for the difference in lateral extracranial blood flow (Hu et al., 2013; van Campen et al., 2018). Moreover, intra- and extracranial cerebrovasculature have the capacity for compensatory collateral flow as demonstrated during and after vessel occlusion (Romero et al., 2010; J. Wang et al., 2019), and immediately after endarterectomy (Aleksic & Brunkwall, 2009; J. Wang et al., 2019). Therefore, the interplay between extracranial artery vessel type (ICA or VA) *and* vessel side (left or right) should be considered when investigating the global haemodynamic response to a stressor.

Another possible explanation for the equivocal findings in regional extracranial blood flow regulation to hypoxia is the method by which extracranial blood flow data is acquired and expressed. In assessments of brachial artery vascular function by flow-mediated dilation (FMD), a negative correlation between resting brachial artery diameter and the percentage change in diameter suggests that the calculation of diameter percentage change in smaller brachial arteries overestimates the relative FMD response (Atkinson et al., 2013; Atkinson & Batterham, 2013a, 2013b). Further, brachial arteries with smaller diameters displayed more varied responses than those with large diameters. Consequently, the relatively larger blood flow increase to hypoxia in the VA compared to ICA previously reported (Lewis et al., 2014; Ogoh et al., 2013; Subudhi et al., 2014; Willie et al., 2012) may be a product of a ratio-scaling

problem arising from random intra-individual lateral anatomical and resting blood flow differences, more prominent in the VA than the ICA, when unilateral rather than bilateral measurements are used.

The primary aim of this study was to determine the extracranial blood flow regulation to acute poikilcapnic hypoxia when factoring for vessel type (ICA or VA) and vessel side (left or right) effects. In this study, we assessed left and right ICA and VA blood flow, vessel diameter, and flow velocity by duplex ultrasound. We hypothesised that when factoring for vessel type and vessel side extracranial blood flow regulation to hypoxia would be similar in left and right ICA and VA. The secondary aim of this study was to investigate the measurement error in unilateral compared to bilateral calculations of extracranial blood flow. Although other stimuli might be used (e.g. carbon dioxide, exercise), we chose to examine the extracranial measurement error to acute poikilcapnic hypoxia as it has previously been shown to increase cerebral blood flow by approximately 30% for a 1–2 h period (Lewis et al., 2014; Morris et al., 2017). Based on the previously identified ratio-scaling problem with FMD, we hypothesised that a negative relationship would exist between extracranial artery resting normoxic blood flow and the relative blood flow response to hypoxia. We also expected that extracranial arteries with the smaller resting blood flow would have a more varied relative blood flow response to hypoxia than those arteries with larger resting blood flows. Consequently, the measurement error to the relative blood flow response to hypoxia was hypothesised to be greater when calculated from doubling a unilateral measurement of the lateral extracranial artery with the smaller resting blood flow.

4.3 Methods

Ethical Approval

Ethical approval for this study was obtained from Bangor University (proposal number 2019-16489, accepted 11/03/2019, Appendix 2) and was conducted following the standards of the *Declaration of Helsinki 2013*, except for registration in a database, with written informed consent obtained from all study volunteers.

Participants

Forty-four young healthy participants were recruited in this study [17 female, 24 (5) yr, 177 (9) cm, 72 (9) kg, haemoglobin 15 (1) g·dL⁻¹, haematocrit 44 (4) %]. Participants were non-smokers, and free from cardiovascular, haematological, and neurological disease. Participants had not resided overnight at an altitude of > 2500 m within the last six months. Participants were screened for vascular abnormalities to ensure reliable ICA and VA ultrasound images could be acquired. To minimise the impact of fluctuations in sex hormones on blood flow measurements (Krejza et al., 2001) female participants were included if they had contraceptive-induced amenorrhea or a regular menstruating cycle. Participants with a regular menstrual cycle were tested during the early follicular phase (day 1 to 7) or the placebo phase of the oral contraceptive. Participants were instructed to refrain from consuming alcohol and from undertaking exhaustive exercise within 24 h of experimental trials. Experimental trials were completed at the same time of day and participants were encouraged to match their diet and supplement intake, including caffeinated beverages, before arrival at the laboratory.

Study Design

A repeated-measures, crossover design was used where each participant completed two experimental trials separated by a minimum of 48 h. Experimental trials consisted of a 90 min

exposure to either normoxia (fraction of inspired oxygen [FiO_2] = 20.9%) or poikilocapnic hypoxia (FiO_2 = 12.0%) in a temperature [26 (2) °C] and humidity [30 (4) %] controlled environmental chamber (Hypoxico Inc, New York, USA).

Experimental procedures

On entry to the chamber, participants were instrumented with a 3-lead electrocardiogram, pulse oximeter, and a blood-pressure cuff to measure heart rate, peripheral arterial oxygen saturation (SpO_2 ; Model 9590 Oximeter; Nonin Medical Inc. Minnesota, USA), and mean arterial blood pressure (MAP; Model M6 AC ME, Omron Healthcare Co., Ltd, Kyoto, Japan), respectively. After 20 min participants lay supine for 10 min before a facemask was attached to measure the partial pressure of end-tidal carbon dioxide ($P_{ET}CO_2$) and minute ventilation ($\dot{V}E$) for 5 min (Metalyzer 3B, CORTEX Biophysik, GmbH; Leipzig; Germany). Following this, blood flow measurements of the left and right ICA and VA were completed by duplex ultrasound. Cardiovascular measurements were obtained at 30 min intervals and respiratory measurements were obtained at minute 30 and 90.

Duplex ultrasound acquisition and analysis

All extracranial blood flow measurements were collected by the same operator (ATF), using duplex ultrasound with a 12 MHz linear transducer (Acuson X300, Siemens Healthcare, GmbH; Erlangen: Germany) at 30 frames per second, and per recommended technical guidelines (Thomas et al., 2015). Bilateral ICA and VA blood flow was calculated from consecutive left and right measurements. To improve the accuracy of the blood flow measurements and minimise the trade-off between B-mode and pulsed-wave Doppler mode (Thomas et al., 2015), vessel diameter and flow velocity measurements were collected in consecutive 30 s recordings with care taken to maintain the same position within the vessel. High-resolution B-mode images were used to measure vessel diameter. Flow velocity was

measured using Doppler velocity spectrum with the cursor set in the centre of the vessel with a 60° angle of insonation with the Doppler gate adjusted to fill the size of the vessel. ICA were measured 1.0–1.5 cm distal to the carotid bifurcation and VA were measured between C3 and the subclavian artery. The order of imaging was (1) VA right, (2) ICA right, (3) VA left, and (4) ICA left. In a separate day-to-day reproducibility study (N = 10) completed by the same operator (ATF), the coefficient of variation (CV) of this technique for blood flow, vessel diameter, and flow velocity of the ICA (11%, 4%, and 7%) and VA (9%, 2%, and 7%) were comparable with recommended guidelines (Thomas et al., 2015).

All data was captured and stored for subsequent offline analysis by an investigator blinded to the condition of the experimental trials. Following a conservative image quality check, data and statistical analysis were completed on 33 ICA pairs (24 male, 9 female) and 43 VA pairs (26 male, 17 female). The 11 ICA exclusions were due to lack of clear insonation and poor image quality whilst the 1 VA exclusion was due to the presence of an unidentified branching vessel. Offline analysis was adapted from standardised procedures described elsewhere (Hoiland et al., 2017; Ogoh et al., 2013). Specifically, mean flow velocity was calculated using half the time-averaged maximum velocity (TAMx) and was averaged from 10 cardiac cycles to minimise the impact of respiration. Mean vessel diameter was measured using an automated edge-detection tracking software (Brachial Analyser, Medical Imaging Applications, Iowa, USA) and was calculated from a weighted average of the peak systolic and diastolic diameters across 10 cardiac cycles [(systolic diameter \times 1/3) + (diastolic diameter \times 2/3)]. Subsequently, blood flow was calculated using the following equation:

$$\text{Blood flow (ml} \cdot \text{min}^{-1} = \\ [TAMx (cm \cdot s^{-1})/2] \times [\pi \times (\text{mean artery diameter (cm)/2})^2] \times 60$$

Absolute and relative change in blood flow was calculated as the change in blood flow from normoxia to hypoxia at the same time point using the following equations:

$$\begin{aligned} & \textit{Absolute change in blood flow to hypoxia (ml} \cdot \textit{min}^{-1}\textit{)} \\ & = \textit{hypoxic blood flow (ml} \cdot \textit{min}^{-1}\textit{)} - \textit{normoxic blood flow (ml} \\ & \quad \cdot \textit{min}^{-1}\textit{)} \end{aligned}$$

$$\begin{aligned} & \textit{Relative change in blood flow to hypoxia (\%)} \\ & = [(\textit{hypoxic blood flow (ml} \cdot \textit{min}^{-1}\textit{)} - \textit{normoxic blood flow (ml} \\ & \quad \cdot \textit{min}^{-1}\textit{)}) / \textit{normoxic blood flow (ml} \cdot \textit{min}^{-1}\textit{)}] \times 100 \end{aligned}$$

To control for differences between individual responses to poikilocapnic hypoxia, an index of absolute and relative hypoxic blood flow reactivity was calculated by normalising these values to the absolute change in SpO₂ (Δ SpO₂).

To calculate the difference in resting normoxic blood flow between lateral arteries of the ICA and VA, the following equation was used:

$$\begin{aligned} & \textit{Lateral artery difference in resting normoxic blood flow (\%)} \\ & = [(\textit{Larger blood flow (ml} \cdot \textit{min}^{-1}\textit{)} - \textit{smaller blood flow (ml} \\ & \quad \cdot \textit{min}^{-1}\textit{)}) / \textit{smaller blood flow (ml} \cdot \textit{min}^{-1}\textit{)}] \times 100 \end{aligned}$$

Extracranial arteries were also identified and grouped by the lateral vessel (left or right) with the larger resting normoxic blood flow.

Statistical Analysis

No sample size estimation was completed for this study however, the number recruited is greater than the previous research to examine and report differences in extracranial blood flow response to hypoxia (sample sizes of 6 to 21) (Hoiland et al., 2017, 2018; Kellawan et al., 2017;

Lafave et al., 2019; Lewis et al., 2014; Morris et al., 2017; Ogoh et al., 2013; Subudhi et al., 2014; Willie et al., 2012; Willie, Smith, et al., 2014).

Statistical analysis was conducted using SPSS Statistics v25 (IBM Corp., Armonk, NY, USA).

Values are mean (SD) unless otherwise stated and statistical significance was set at $P < 0.05$.

To determine any differences in cardiorespiratory variables during normoxia and hypoxia a linear mixed model (LMM) was used. Fixed effects of interest were 'Condition' (normoxia or hypoxia), 'Time' (30, 60, or 90 min), as well as the interaction ('Condition' \times 'Time'), with 'Participant ID' added as a random effect. Baseline data were not included as these measurements were collected during seated rest before entry to the environmental chamber.

To determine whether there are resting normoxic blood flow differences between left and right ICA and VA, a LMM was used with fixed effects of interest 'Vessel Type' (ICA or VA), and 'Vessel Side' (left or right), as well as the interaction ('Vessel Type' \times 'Vessel Side'), adding 'Participant ID' added as a random effect.

To determine whether there are differences in blood flow regulation to hypoxia between the four extracranial arteries, a LMM was used to examine left and right ICA and VA absolute blood flow, vessel diameter, and flow velocity in normoxia and hypoxia. Specifically, fixed effects of interest were 'Condition', 'Vessel Type', and 'Vessel Side', with 'Participant ID' as added as a random effect. The primary outcome of interest was the interaction ('Condition' \times 'Vessel Type' \times 'Vessel Side'). In addition, for conventional purposes, a LMM was used to examine the absolute change and relative change in blood flow, vessel diameter, and flow velocity regulation to hypoxia (i.e. change from normoxia) between the ICA and VA with 'Vessel Type', and 'Vessel Side' and their interaction ('Vessel Type' \times 'Vessel Side') as fixed effects of interest, adding 'Participant ID' as a random effect. Values from LMM analysis are reported as estimated marginal means and an estimated SD which was derived from the

standard error (SE), where n is the sample size [$Estimated\ SD = SE \times (\sqrt{n})$] (Shenouda et al., 2017).

To determine the measurement error in unilateral compared to bilateral calculations of relative extracranial blood flow response to hypoxia, we investigated whether a ratio-scaling problem exists and quantified the measurement error by Bland-Altman analysis (Bland & Altman, 1986). Disproportionate ratio-scaling in the calculation of relative change ratios has been described extensively elsewhere (Atkinson et al., 2013; Atkinson & Batterham, 2013a, 2013b). For clarity, the analysis used in the present study is described. Pearson's correlation was used to determine whether a negative relationship between resting normoxic blood flow and the relative blood flow response to hypoxia existed in the left and right arteries of the ICA and VA. To confirm that the relationships between resting normoxic blood flow and the relative blood flow response to hypoxia were statistically different from the relationships between resting normoxic blood flow and the absolute blood flow response to hypoxia, correlation coefficients were compared using Fisher's Z transformation via the cocor online software (Diedenhofen & Musch, 2015). Then, appropriate ratio-scaling was applied to the ICA and VA to calculate the 'corrected' ICA and VA blood flow response to hypoxia. The calculation of the regression slope between logarithmically-transformed normoxic blood flow and hypoxic blood flow was used to determine whether hypoxic blood flow scales disproportionately for the range of values of normoxic blood flow, with an upper confidence limit [95%CI] being less than 1.0 indicating this to be true. An analysis of covariance analysis (ANCOVA) model was used to determine group differences between unilateral and bilateral calculations of logged-scale change in blood flow (Δ blood flow), with logarithmically-transformed normoxic blood flow as a covariate. Back-transformation of covariate-adjusted Δ blood flow were converted to $\Delta\%$ blood flow as the final corrected, and more conventional, calculation of the relative blood flow response to hypoxia. Bland-Altman analysis was used to determine the level of agreement between

unilateral and bilateral calculations of the relative blood flow response to hypoxia for the ICA and VA. Unilateral measurements were determined by resting normoxic blood flow (smaller or larger) or vessel side (left or right) and doubled before calculating the relative blood flow response to hypoxia. The mean difference between unilateral and bilateral calculations of the relative blood flow response to hypoxia was determined as the measurement bias (error), with the respective 95% confidence intervals, and the 95% limits of agreement.

4.4 Results

Cardiorespiratory responses to hypoxia

There were no interactions for cardiorespiratory responses during the period of supine rest (Table 4.1, all $P > 0.05$). Compared to normoxia, acute poikilocapnic hypoxia increased heart rate [Main effect of ‘Condition’; +11 (6) bpm; $P < 0.001$], MAP [+1 (4) mmHg; $P < 0.05$] and $\dot{V}E$ [+0.9 (1.4) L·min⁻¹; $P < 0.001$], and decreased $P_{ET}CO_2$ [-3.9 (2.1) mmHg; $P < 0.001$] and SpO_2 [-20 (3) %; $P < 0.001$] during supine rest. Cardiorespiratory responses were stable between 30–90 min with the exception of an increase in MAP [Main effect of ‘Time’; +2 (4) mmHg, 90 vs 60 min; $P < 0.01$] and a decline in $\dot{V}E$ [-0.5 (1.5) L·min⁻¹, 90 vs 30 min; $P < 0.05$] in both conditions. Acute poikilocapnic hypoxia did not induce acute mountain sickness (Appendix 5.2).

Resting extracranial artery characteristics

There was no ‘Vessel Type’ × ‘Vessel Side’ interaction ($P = 0.17$), nor a main effect of ‘Vessel Side’ ($P = 0.74$), in resting normoxic blood flow between the left and right ICA [299 (43) and 288 (43) mL·min⁻¹, 4%] and left and right VA [103 (43) and 95 (43) mL·min⁻¹, 8%], but there was a main effect of ‘Vessel Type’ ($P < 0.001$). The difference in resting normoxic blood flow between lateral arteries ranged from 1 to 91% for the ICA and 0 to 400% for the VA. More

participants had a larger resting normoxic blood flow in the right ICA (14 left, 19 right) and VA (21 left, 22 right) than left.

Extracranial artery blood flow regulation to hypoxia

LMM analyses revealed no ‘Condition’ × ‘Vessel Type’ × ‘Vessel Side’ interaction for blood flow (Figure 4.1a; $P = 0.62$), vessel diameter (Figure 4.1b; $P = 0.70$), and flow velocity (Figure 4.1c; $P = 0.64$), indicating that ICA and VA blood flow regulation to acute poikilocapnic hypoxia did not differ as a function of vessel type and vessel side.

There was also no ‘Condition’ × ‘Vessel Side’ interaction for vessel diameter ($P = 0.32$), flow velocity ($P = 0.18$), blood flow ($P = 0.86$), and the volume of left and right extracranial blood flow were similar in hypoxia [left ICA + VA, 495 (93) mL·min⁻¹ vs right ICA + VA, 501 (93) mL·min⁻¹; $P = 0.89$].

Due to the ICA and VA differences at normoxic baseline, there was a ‘Condition’ × ‘Vessel Type’ interaction for blood flow ($P < 0.001$). Subsequently, to account for the large discrepancy between ICA and VA blood flow at normoxic baseline, this variable was analysed using the conventionally reported change scores from normoxia. LMM analysis revealed no ‘Vessel Type’ × ‘Vessel Side’ interaction for the absolute and relative blood flow response to hypoxia between the left and right ICA and VA (Figure 4.2a, 4.2c, 4.2e, 4.2g, all $P > 0.05$) and reaffirmed that there was no main effect of ‘Vessel Side’ for these blood flow variables (all $P > 0.05$). As expected, a main effect of ‘Vessel Type’ (i.e. when data was pooled as the bilateral value) revealed that the ICA had a greater absolute blood flow response to hypoxia [Figure 4.2b; 155 (63) vs 57 (65) ΔmL·min⁻¹, $P < 0.001$], and absolute hypoxic reactivity [Figure 4.2d, 8.0 (3.3) vs 3.0 (3.4) ΔmL·min⁻¹·ΔSpO₂⁻¹; $P < 0.001$] than the VA. Whereas, there was no main effect of ‘Vessel Type’ for the relative blood flow response to hypoxia [Figure 4.2f, 26.6 (21.6) vs 33.2 (22.6) Δ%; $P = 0.053$] and relative hypoxic reactivity [Figure 4.2h, 1.4 (1.0) vs

1.7 (1.1) $\Delta\% \cdot \Delta\text{SpO}_2^{-1}$; $P = 0.12$]. When calculated bilaterally, acute poikilocapnic hypoxia increased global blood flow by 29.1 (18.1) % [776 (124) vs 995 (124) $\text{mL} \cdot \text{min}^{-1}$; $P < 0.001$]. There was no ‘Condition’ \times ‘Vessel Type’ interaction for vessel diameter ($P = 0.29$) and flow velocity ($P = 0.37$), which had a similar relative vessel diameter response to hypoxia [ICA 6.9 (3.7) vs VA 7.0 (3.8) %; $P = 0.83$] and relative flow velocity response to hypoxia [ICA 11.2 (15.7) vs VA 15.6 (16.1) %; $P = 0.09$] between bilateral calculations of the ICA and VA.

	Normoxia				Hypoxia				<i>P</i>		
	Baseline	30 min	60 min	90 min	Baseline	30 min	60 min	90 min	Condition	Time	Interaction
SpO ₂ (%)	98 (1)	98 (1)	99 (1)	99 (1)	99 (1)	80 (5)	78 (6)	78 (6)	<0.001	0.70	0.13
Heart Rate (bpm)	71 (14)	63 (10)	60 (9)	60 (10)	68 (12)	73 (14)	71 (12)	72 (12)	<0.001	0.30	0.84
MAP (mmHg)	90 (7)	84 (7)	83 (7)	85 (7)	91 (6)	85 (9)	85 (8)	86 (8)	<0.05	<0.01	0.71
P _{ET} CO ₂ (mmHg)	-	37.5 (3.6)	-	37.4 (3.6)	-	34.2 (3.2)	-	32.6 (3.7)	<0.001	0.12	0.06
$\dot{V}E$ (L·min ⁻¹)	-	9.5 (1.7)	-	8.6 (1.3)	-	10.3 (1.9)	-	9.6 (1.9)	<0.001	<0.05	0.45

Table 4.1. Cardiorespiratory responses to normoxia and acute poikilocapnic hypoxia. Data were collected during a seated baseline and during supine rest between 30–90 min in a temperature [26 (2) °C] and humidity [30 (4) %] controlled environmental chamber during normoxia (fraction of inspired oxygen [FiO₂] = 20.9%) and acute poikilocapnic hypoxia (FiO₂ = 12.0%). Linear mixed model analysis was completed for the period of supine rest. Values are mean (SD). Abbreviations: SpO₂, peripheral arterial oxygen saturation; MAP, mean arterial pressure; P_{ET}CO₂, partial pressure of end-tidal carbon dioxide; $\dot{V}E$, minute ventilation.

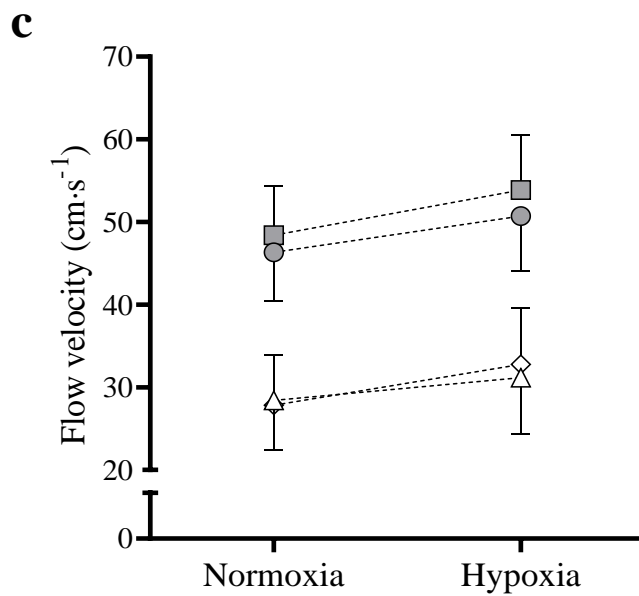
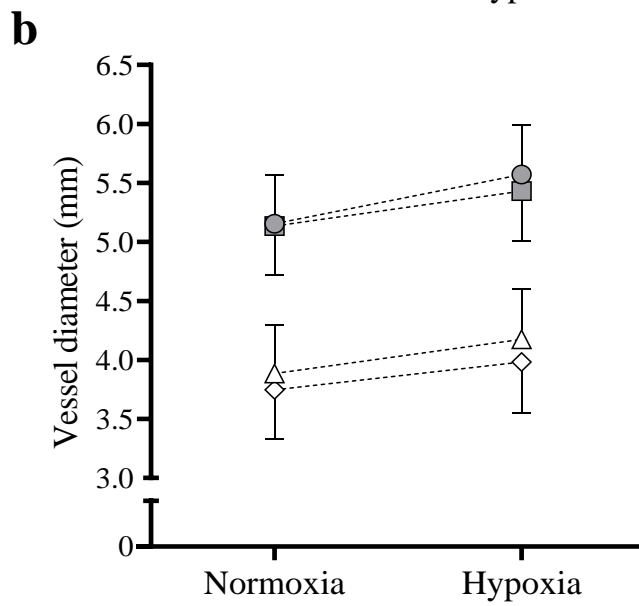
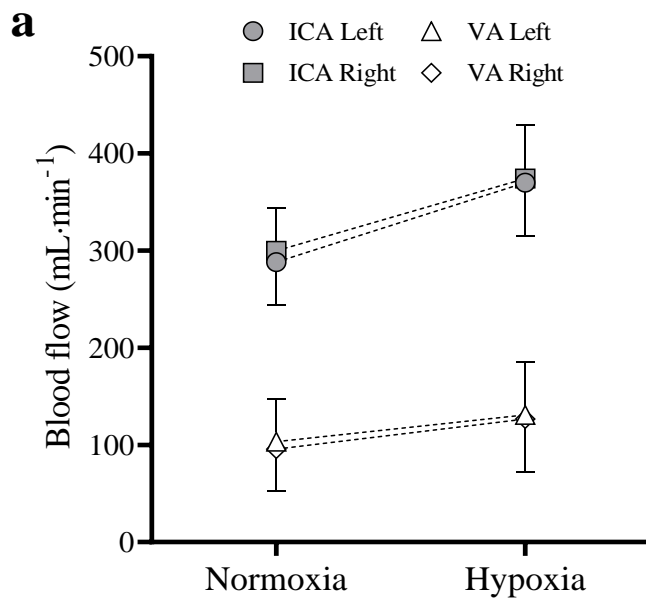


Figure 4.1. Extracranial artery blood flow regulation in normoxia and acute poikilocapnic hypoxia. Left and right internal carotid artery (ICA) and vertebral artery (VA) blood flow regulation was measured from normoxia (fraction of inspired oxygen [FiO_2] = 20.9%) to acute poikilocapnic hypoxia ($\text{FiO}_2 = 12.0\%$). Linear mixed model analysis revealed no ‘Condition’ (normoxia or hypoxia) \times ‘Vessel Type’ (ICA or VA) \times ‘Vessel Side’ (left or right) interaction for blood flow (a, $\text{mL}\cdot\text{min}^{-1}$; $P = 0.62$), vessel diameter (b, mm; $P = 0.70$), and flow velocity (c, $\text{cm}\cdot\text{s}^{-1}$; $P = 0.64$), adding ‘Participant ID’ as a random effect. Data points are estimated marginal means (estimated SD) from LMM analysis. Raw mean (SD) data are presented in Table 4.2.

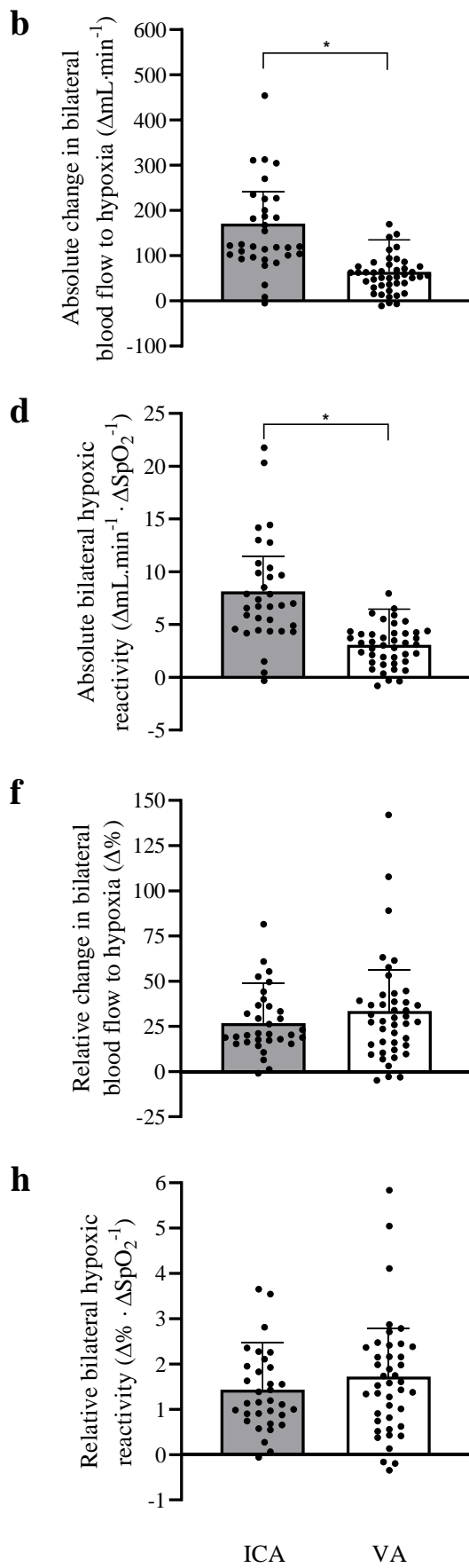
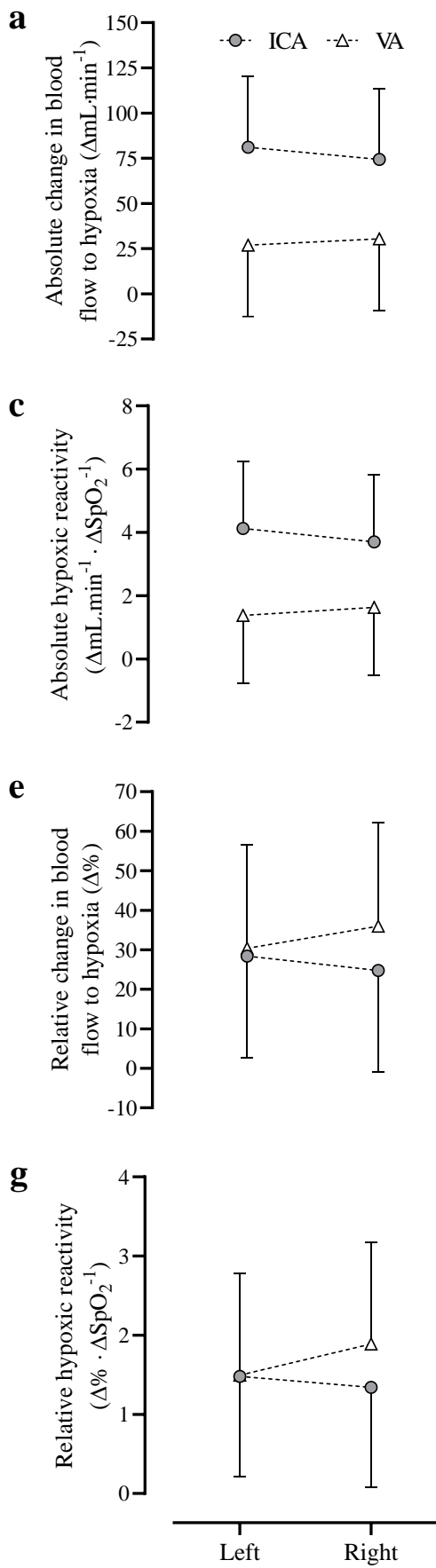


Figure 4.2. Extracranial artery blood flow response and reactivity to acute poikilocapnic hypoxia. Left and right internal carotid artery (ICA; grey circle or bars) and vertebral artery (VA; white triangle or bars) blood flow response to acute poikilocapnic hypoxia (fraction of inspired oxygen [FiO_2] = 12.0%). Linear mixed model (LMM) analysis revealed no ‘Vessel Type’ (ICA or VA) \times ‘Vessel Side’ (left or right) interaction for the absolute change in blood flow to hypoxia (a, $\Delta mL \cdot min^{-1}$; $P = 0.32$), absolute hypoxic reactivity (c, $\Delta mL \cdot min^{-1} \cdot \Delta SpO_2^{-1}$; $P = 0.37$), the relative change in blood flow to hypoxia (e, $\Delta\%$; $P = 0.15$), or relative hypoxic reactivity (g, $\Delta\% \cdot \Delta SpO_2^{-1}$; $P = 0.13$). There were no main effects of ‘Vessel Side’ for these blood flow variables (all $P > 0.05$). Main effects of ‘Vessel Type’ were revealed for the absolute change in bilateral blood flow to hypoxia (b; $P < 0.001$), absolute bilateral hypoxic reactivity (d; $P < 0.001$), but not for the relative change in bilateral blood flow to hypoxia (f; $P = 0.053$), or relative bilateral hypoxic reactivity (h; $P = 0.12$). * $P < 0.001$ between ICA and VA. Data points represent individuals' ICA and VA blood flow responses to acute hypoxia. Bars are estimated marginal means (estimated SD) from LMM analysis.

The relationship between resting normoxic blood flow and the blood flow response to hypoxia

No relationship was observed between resting normoxic blood flow and the absolute blood flow response to hypoxia (Figures 4.3a and 4.3b). However, negative relationships were identified between resting normoxic blood flow and the relative ICA and VA blood flow response to hypoxia (Figures 4.3c and 4.3d, $r = -0.33$ and -0.37 , respectively; $P < 0.001$). These relationships were statistically different from the relationships observed between resting normoxic blood flow and the absolute blood flow response to hypoxia (both $P < 0.001$). These relationships indicated that vessels with smaller resting blood flow were associated with a greater and more varied relative blood flow change to hypoxia. As negative relationships were identified between normoxic blood flow and the relative blood flow response to hypoxia, ratio-scaling was conducted. The regression slopes between logarithmically-transformed resting normoxic blood flow and hypoxic blood flow were 0.70 (95%CI [0.49 to 0.91]) for the ICA and 0.79 (95%CI [0.67 to 0.91]) for the VA with each upper confidence limit of less than 1.0, indicating that vessels with smaller resting blood flow were associated with a disproportionately large relative change in hypoxic blood flow. The covariate-adjusted group means for the relative blood flow response to hypoxia after ANCOVA analysis indicated smaller differences between left and right calculations of the ICA [27.5 (16.8) and 25.1 (16.8) %] and VA [28.3 (22.5) and 32.4 (22.5) %] compared with non-corrected values of the relative blood flow response to hypoxia (Table 4.2).

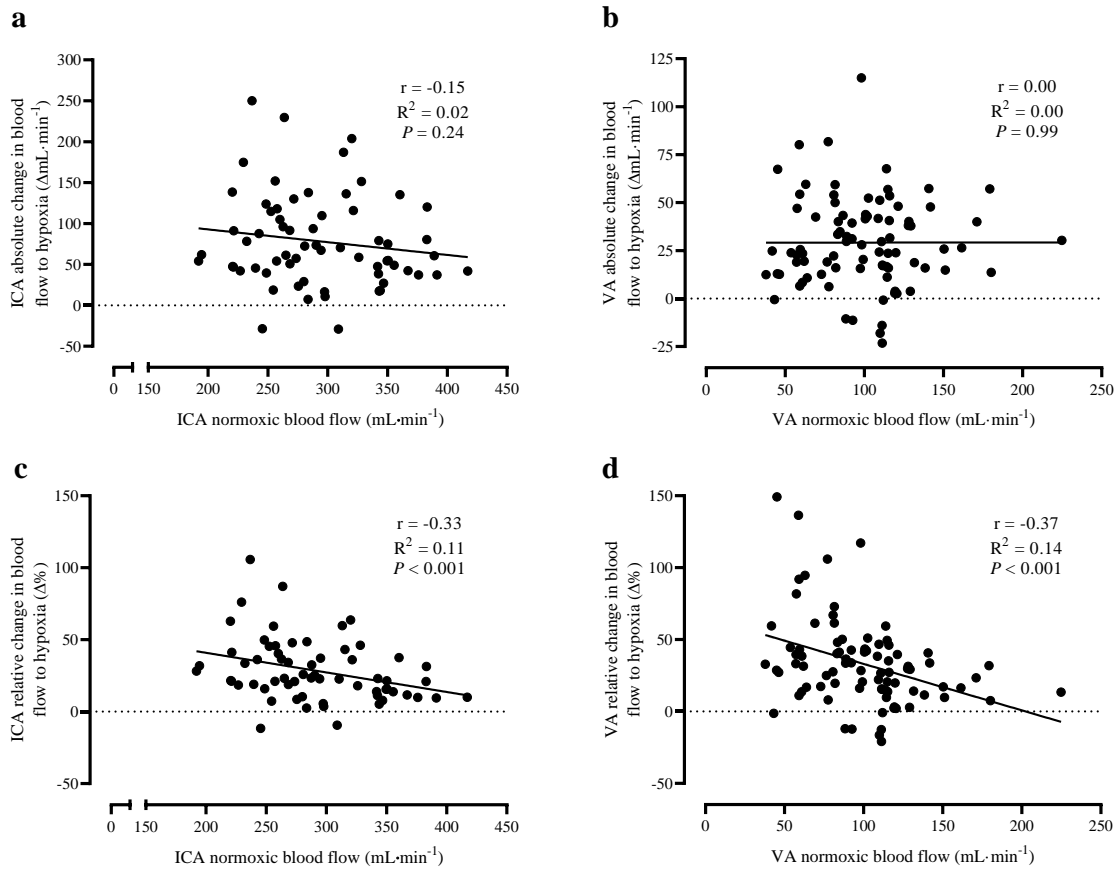


Figure 4.3. Relationships between resting normoxic blood flow and the absolute or relative blood flow response to acute poikilocapnic hypoxia in the extracranial arteries. Internal carotid arteries (ICA) and vertebral arteries (VA) blood flow response were assessed from normoxia (fraction of inspired oxygen [FiO_2] = 20.9%) to acute poikilocapnic hypoxia (FiO_2 = 12.0%). The blood flow response to hypoxia is presented as the absolute change ($\Delta\text{mL}\cdot\text{min}^{-1}$; a and b) and the relative change ($\Delta\%$; c and d) from resting normoxic blood flow ($\text{mL}\cdot\text{min}^{-1}$). Data plots include the left and right vessels of the ICA and the VA.

	Normoxia	Hypoxia	Δ	$\Delta\%$
<u>Blood flow (mL·min⁻¹) *</u>				
Internal carotid artery				
Left only	575 (94)	738 (130)	163 (108)	29.7 (21.6)
Right only	598 (117)	747 (155)	149 (117)	26.1 (21.7)
Bilateral	587 (79)	743 (117)	156 (97)	27.3 (17.8)
Vertebral artery				
Left only	206 (64)	261 (83)	55 (53)	30.6 (33.0)
Right only	190 (76)	252 (86)	62 (40)	36.2 (28.3)
Bilateral	198 (44)	256 (50)	58 (40)	32.5 (28.4)
<u>Vessel diameter (mm)</u>				
Internal carotid artery				
Left only	5.16 (0.37)	5.58 (0.39)	0.42 (0.26)	8.24 (5.24)
Right only	5.14 (0.40)	5.43 (0.43)	0.30 (0.23)	5.86 (4.62)
Mean average	5.15 (0.31)	5.50 (0.34)	0.36 (0.21)	7.00 (4.14)
Vertebral artery				
Left only	3.88 (0.42)	4.17 (0.44)	0.29 (0.17)	7.57 (4.38)
Right only	3.75 (0.49)	3.98 (0.47)	0.23 (0.16)	6.50 (4.69)
Mean average	3.82 (0.28)	4.08 (0.27)	0.26 (0.13)	6.98 (3.66)
<u>Flow velocity (cm·s⁻¹)</u>				
Internal carotid artery				
Left only	46.0 (7.2)	50.4 (7.3)	4.4 (7.3)	10.8 (17.9)
Right only	48.1 (7.9)	53.5 (8.6)	5.4 (8.5)	12.7 (18.9)
Mean average	47.1 (7.0)	52.0 (6.9)	4.9 (6.8)	11.6 (15.5)
Vertebral artery				
Left only	28.3 (5.4)	31.1 (5.6)	2.8 (5.5)	11.9 (21.8)
Right only	27.7 (5.6)	32.7 (5.9)	4.9 (4.8)	19.7 (20.2)
Mean average	28.0 (4.6)	31.9 (4.6)	3.8 (4.5)	15.4 (19.0)

Table 4.2. Extracranial artery blood flow, vessel diameter, and flow velocity in normoxia and acute poikilocapnic hypoxia. Blood flow ($\text{mL}\cdot\text{min}^{-1}$), vessel diameter (mm), and flow velocity (time-averaged maximum velocity; $\text{cm}\cdot\text{s}^{-1}$) were assessed in the left and right internal carotid arteries (ICA) and vertebral arteries (VA) during normoxia (fraction of inspired oxygen $[\text{FiO}_2] = 20.9\%$) and acute poikilocapnic hypoxia ($\text{FiO}_2 = 12.0\%$). Left and right vessel blood flows were calculated by doubling unilateral measurements, whereas bilateral blood flow was calculated as the sum of left and right unilateral measurements. Data are mean (SD) of the raw values, with the absolute (Δ) and relative change ($\Delta\%$) from normoxia. Linear mixed model analysis revealed no ‘Condition’ (normoxia or hypoxia) \times ‘Vessel Type’ (ICA or VA) \times ‘Vessel Side’ (left or right) interaction for blood flow (a, $\text{mL}\cdot\text{min}^{-1}$; $P = 0.62$), vessel diameter (b, mm; $P = 0.70$), and flow velocity (c, $\text{cm}\cdot\text{s}^{-1}$; $P = 0.64$), with ‘Participant ID’ as a random effect. LMM revealed no ‘Condition’ \times ‘Vessel Side’ interactions. * Interaction effect of ‘Condition’ \times ‘Vessel Type’ ($P < 0.001$).

Measurement bias between unilateral and bilateral calculations of the relative blood flow response to hypoxia

Bland-Altman analysis revealed doubling unilateral ICA measurements from the vessel with the smaller resting normoxic blood flow overestimated the relative ICA blood flow response to hypoxia by 5% (95%CI [1 to 9], limits of agreement: -19 to +29%) compared to bilateral calculations (Figure 4.4a). Doubling unilateral ICA measurements from the vessel with the larger resting normoxic blood flow underestimated the relative ICA blood flow response to hypoxia by 4% (95%CI [-7 to 0], limits of agreement: -23 to +16%) compared to bilateral calculations (Figure 4.4b). There was no significant bias in the relative VA blood flow response to hypoxia from doubling unilateral VA measurements from the vessel with the smaller or larger resting normoxic blood flow compared to bilateral calculations (Figure 4.4c and 4.4d). However, the vessel with the larger resting normoxic blood flow had the lowest measurement bias and narrowest limits of agreement to the relative VA blood flow response to hypoxia compared to doubling bilateral calculations (Figure 4.4d).

Bland-Altman analysis revealed no significant bias in the relative ICA blood flow response to hypoxia from doubling left or right unilateral ICA measurements compared to bilateral calculations (Figures 4.5a and 4.5b). Bland-Altman analysis revealed doubling unilateral right VA measurements overestimated the relative VA blood flow response to hypoxia by 4% (95%CI [0 to 7], limits of agreement: -21 to +28%) compared to bilateral calculations (Figure 4.5d). In contrast, there was no significant bias in the relative VA blood flow response to hypoxia from doubling unilateral left VA measurements compared to bilateral calculations (Figure 4.5c).

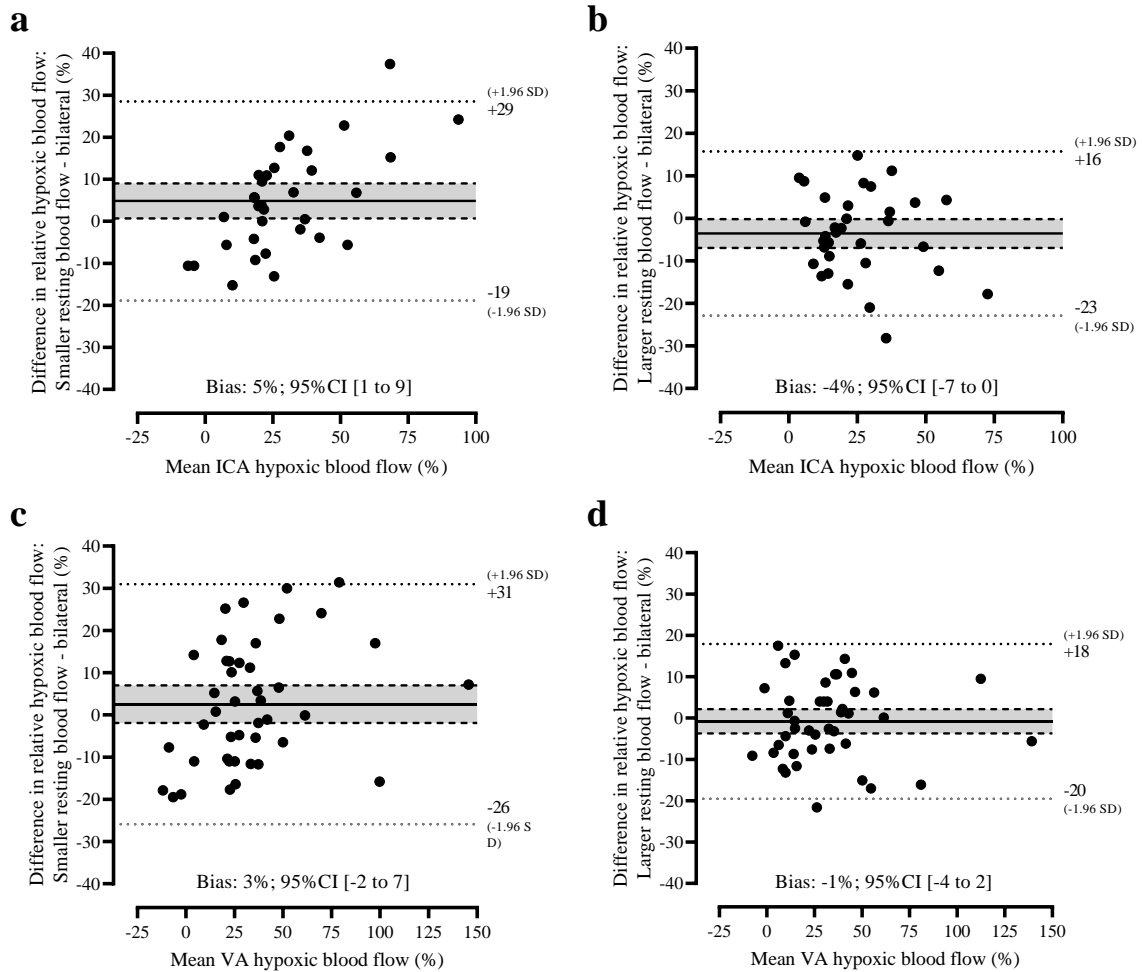


Figure 4.4. Bland-Altman plots of the measurement bias between a unilateral assessment of the vessel with the smaller or larger resting normoxic blood flow and the bilateral calculation of the relative change in blood flow from normoxia to acute poikilocapnic hypoxia of the extracranial arteries. Internal carotid arteries (ICA) and vertebral arteries (VA) relative blood flow response from normoxia (fraction of inspired oxygen [FiO_2] = 20.9%) to acute poikilocapnic hypoxia (FiO_2 = 12.0%) were calculated from doubling unilateral measurements of the vessel with the smaller (a and c) or larger (b and d) resting normoxic blood flow and compared to the bilateral calculation of the relative blood flow response to hypoxia. Average bias (solid black line) is reported with respective 95% confidence intervals (dashed black lines), and $\pm 1.96SD$ limits of agreement (dotted black lines).

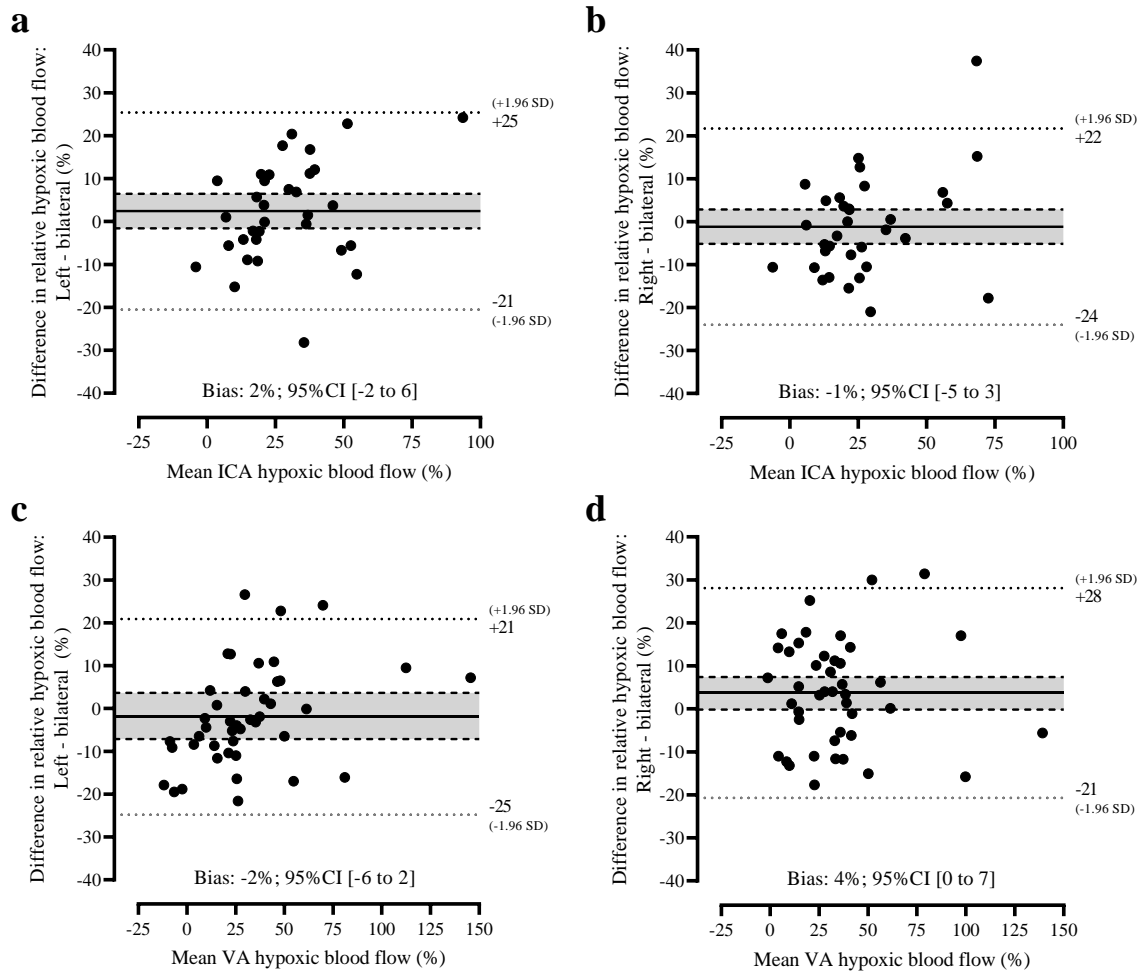


Figure 4.5. Bland-Altman plots of the measurement bias between a unilateral assessment of the left or right vessel and the bilateral calculation of the relative change in blood flow from normoxia to acute poikilocapnic hypoxia of the extracranial arteries. Internal carotid arteries (ICA) and vertebral arteries (VA) relative blood flow response from normoxia (fraction of inspired oxygen [FiO_2] = 20.9%) to acute poikilocapnic hypoxia (FiO_2 = 12.0%) were calculated from doubling unilateral measurements of the left (a and c) or right (b and d) side and compared to the bilateral calculation of the relative blood flow response to hypoxia. Average bias (solid black line) is reported with respective 95% confidence intervals (dashed black lines), and $\pm 1.96\text{SD}$ limits of agreement (dotted black lines).

4.5 Discussion

Main findings

The principal finding of this study was that extracranial blood flow regulation to hypoxia is comparable (Figure 4.1) when factoring for vessel type (ICA or VA) and vessel side (left or right). The increase in blood flow to hypoxia was regulated by an increase in vessel diameter and flow velocity in all extracranial vessels. Global extracranial blood flow to hypoxia increased from 776 (124) to 995 (124) mL·min⁻¹ (29.1%, $P < 0.001$) that was equally distributed between the left and right sides [left ICA + VA, 495 (93) vs right ICA + VA, 501 (93) mL·min⁻¹; $P = 0.89$]. When conventionally reported as the change score from normoxia, the bilateral absolute blood flow response to hypoxia was greater in the ICA than the VA (Figure 4.2b and 4.2d), whereas the bilateral relative blood flow response to hypoxia was comparable between the ICA and VA (Figure 4.2f and 4.2h). We are unaware of previous duplex ultrasound investigations that have assessed bilateral extracranial blood flow regulation to hypoxia, nor considered the effect of vessel type and vessel side.

This study also identified negative relationships between extracranial artery resting normoxic blood flow and the relative blood flow response to hypoxia for the ICA and VA (Figure 4.3c and 4.3d), which illustrated a ratio-scaling problem akin to that previously described with FMD assessment of brachial artery vascular function (Atkinson et al., 2013; Atkinson & Batterham, 2013a, 2013b). Compared with bilateral measurement of relative blood flow change to hypoxia, the common practice of doubling unilateral measurements led to average errors of up to 5%, and individual errors of up to 37%, which were greatest and more varied in the extracranial arteries with smaller resting normoxic blood flow (Figure 4.4a – 4.5d).

Bilateral extracranial blood flow regulation to hypoxia

When assessed bilaterally, acute poikilocapnic hypoxia caused the same vasodilation [ICA 6.9 (3.7) vs VA 7.0 (3.8) %; $P = 0.87$] and comparable relative increases in blood flow and blood flow reactivity in the ICA and VA (Figure 4.2f and 4.2h). These regional blood flow responses to acute hypoxia are similar to those previously reported from studies employing the typical method of doubling unilateral measurements (Lewis et al., 2014; Morris et al., 2017; Willie et al., 2012). There are as many studies reporting that the increase in blood flow to hypoxia is mediated by vasodilation in both ICA and VA to extreme ($< 80\%$ SpO₂) poikilocapnic hypoxia (Lewis et al., 2014; Morris et al., 2017) or isocapnic hypoxia (Fernandes et al., 2018; Hoiland et al., 2017) as there are reporting no vasodilation (Lafave et al., 2019; Ogoh et al., 2013; Willie et al., 2012; Willie, Smith, et al., 2014), with others suggesting regionally-specific vasodilation (Kellawan et al., 2017; Subudhi et al., 2014). Notwithstanding the methodological differences of inducing hypoxia that is known to affect the cerebrovascular response, such as the clamping of carbon dioxide (Kellawan et al., 2017; Ogoh et al., 2013; Willie et al., 2012), exposure to high-altitude hypobaric hypoxia (Hoiland et al., 2017; Lafave et al., 2019; Subudhi et al., 2014; Willie, Smith, et al., 2014) and length of exposure (Lewis et al., 2014), the aforementioned studies are often limited by their sample size and therefore sensitivity to detect small differences where high inter-individual variability with exposure to acute severe hypoxia is notable (Willie, Smith, et al., 2014). Compared to previous literature, the present study was conducted in a relatively large cohort and is strengthened by bilateral measurement of the blood flow response to hypoxia which provides more certainty that blood flow is similarly regulated in ICA and VA in response to acute poikilocapnic hypoxia.

Extracranial artery blood flow measurement error

The absolute increase in blood flow to hypoxia was comparable within ICA (Figure 4.3a) and VA (Figure 4.3b) irrespective of the resting blood flow. In contrast, significant negative relationships were identified between resting blood flow and the relative blood flow response to hypoxia in both the ICA and VA, where vessels with smaller resting blood flow had greater relative blood flow responses to hypoxia (Figure 4.3c and 4.3d). This indicated the same ratio-scaling problem in extracranial arteries as has previously been described with FMD assessment of the brachial artery vascular function (Atkinson et al., 2013; Atkinson & Batterham, 2013a, 2013b). In brief, Atkinson and Batterham describe this relationship to be a fundamental ratio-scaling problem when using relative change ratios (i.e. $\Delta\%FMD = [\text{peak diameter} - \text{resting diameter}] / \text{resting diameter} \times 100$) where the numerator (i.e. difference in diameter) does not scale proportionately for the range of denominator values (i.e. resting diameter). The negative relationships also indicated that the relative change in blood flow to hypoxia were more varied in vessels with smaller resting normoxic blood flow. This skewness towards the group with the smaller scores (i.e. smaller resting normoxic blood flow) is common with ratio indices since ratios cause the outcome data to be non-normally distributed even when the two ratios are normally distributed (Atkinson & Batterham, 2013b; Vickers, 2001). This relationship highlights a mathematical, rather than physiological, source of measurement error when adopting a unilateral rather than bilateral assessment.

When compared to the bilateral calculation, doubling of a unilateral extracranial measurement of the relative blood flow response to hypoxia from the vessel with the smaller resting blood flow led to a greater mean measurement bias (5%) and wider limits of agreement (up to 31%) than from the vessel with the larger resting blood flow (Figure 4.4). Despite the mean bias of a unilateral measurement compared to the bilateral measurement being small (3 to 5%), it is misleading to judge the measurement error of a unilateral assessment from this metric alone.

To fully examine measurement error, mean bias, the width of the limits of agreement, and visual inspection of the Bland-Altman plots for a constant or proportional bias should be completed (Giavarina, 2015). Here, the limits of agreement of a unilateral measurement were -26 to 31% (Figure 4.4), which can be considered significant when considering the magnitude is similar to the mean extracranial relative blood flow response to hypoxia. These wide limits of agreement indicate a low level of precision in unilateral measurements, compared to bilateral measurements, which may lead to erroneous interpretation of data particularly in small sample cohorts. Moreover, the Bland-Altman analysis revealed a proportional measurement bias that was more prominent in the vessels with the smaller blood flow (i.e., Figure 4.4a). Therefore, doubling a unilateral extracranial measurement from the vessel with the smaller resting normoxic blood flow is the least comparable, and causes the greatest measurement error, to the true bilateral relative blood flow response to hypoxia.

In investigations of extracranial blood flow regulation to hypoxia, a unilateral measurement of the right VA is overwhelmingly favoured (Fernandes et al., 2018; Hoiland et al., 2017; Lafave et al., 2019; Lewis et al., 2014; Morris et al., 2017; Ogoh et al., 2013; Willie et al., 2012) compared to the left VA (Subudhi et al., 2014; Willie, Smith, et al., 2014). The rationale often stated for the right side being chosen is to account for the 20–30% smaller blood flow in the right VA compared to the left VA such that absolute calculations of regional and global blood flow are an underestimation (Lewis et al., 2014; Ogoh et al., 2013). However, due to the stark differences in resting blood flow between the ICA and VA, regional blood flow response to stressors such as hypoxia are commonly reported relative to resting blood flow (Willie et al., 2012). Disproportionate scaling in the calculation of blood flow relative change may, in part, have contributed to conclusions of preferential blood flow regulation to the posterior circulation compared to anterior circulation in previous research (Lewis et al., 2014; Ogoh et al., 2013; Subudhi et al., 2014; Willie et al., 2012). In these studies, the relative blood flow

response to hypoxia was greater in the VA (posterior) than ICA (anterior) based on unilateral measures from the right VA (Lewis et al., 2014; Ogoh et al., 2013; Willie et al., 2012). In the current study, when unilateral extracranial measurements were selected on the vessel side, right VA measurements overestimated the relative blood flow response to the greatest degree (4%; Figure 4d) and had the widest limits of agreement (-21 to 28%) compared to the bilateral calculation. This finding is particularly noteworthy given that many investigators choose to scan the right rather than the left VA presuming that the right VA is the conservative option when doubling a unilateral measurement. But, as detailed in this study, vessels with the smaller resting blood flow are more susceptible to greater and more varied measurement errors due to the ratio-scaling problem when describing a relative blood flow response.

Perspectives and application

In this study, there was no statistical difference in resting blood flow between the left and right vessels of the ICA (4%) and VA (8%). Therefore, we may have underestimated the group mean measurement error of unilateral compared to bilateral assessment that may be found in future studies. This is particularly likely for the VA as the left-to-right blood flow difference in the VA is typically reported in the range of 20–30% (Khan et al., 2017; Schöning et al., 1994). The heterogeneity between individuals in the magnitude of difference between left and right extracranial arteries blood flow (ICA: 1 to 91% and VA: 0 to 400%) means that without examining the contralateral vessel there is an increased likelihood of substantial measurement error in the calculation of the relative blood flow response to hypoxia.

To eliminate measurement error in the relative blood flow response to hypoxia, bilateral measurements should be used. However, if this is infeasible, we advise the ICA and VA vessel with the larger resting normoxic blood flow be measured for each participant following pre-screening of both the left and right vessels based on two inferences. Firstly, vessels with the

smaller resting normoxic blood flow were associated with a greater and more varied relative blood flow response to hypoxia (Figure 4.2). This is also supported by the Bland-Altman analysis that identified the greatest measurement bias and limits of agreement, and the presence of a proportional bias is caused by unilateral measurements of the extracranial vessel with the smaller blood flow (Figure 4.4). Secondly from a practical aspect, successfully imaging a vessel, maintaining consistent flow velocity with a centrally-positioned Doppler gate, and accurately measuring vessel diameter (whether manual or automated) are all easier in the vessel containing the larger blood flow. Moreover, to improve efficiency and feasibility of identifying the vessel with the larger resting normoxic blood flow before experimental trials, the left and right vessel diameter could be measured using the standard built-in caliper method available in ultrasound devices as a strong index of vessel blood flow (Cipolla, 2009). Where simultaneous insonation of two extracranial arteries is necessary this is normally achieved by contralateral measurements due to ultrasound interference and physical probe space limitations (Sato et al., 2016). In this instance, the extracranial artery (ICA or VA) with the widest difference in resting normoxic blood flow between the left and right vessels should be prioritised in imaging to minimise measurement error. We advise these methods to be applied when measuring extracranial blood flow to other vasoactive stimuli such as carbon dioxide, orthostasis, and exercise.

Methodological considerations

The interaction of oxygen and carbon dioxide tensions are key factors in the overall change in cerebral blood flow during exposure to hypoxia (Bruce et al., 2016; Friend et al., 2019; Lucas et al., 2011). The single bout of poikilocapnic hypoxia used here resulted in a range of SpO_2 , $\dot{V}E$ and, $P_{ET}CO_2$ between participants, therefore not all individuals had similar systemic hypoxia. However, when the relative blood flow response to hypoxia was corrected for the differences in SpO_2 as an index of relative hypoxic reactivity the ICA and VA were found to

remain similar (Figure 4.2h). Future research should use stepwise gas manipulations to investigate the regulation of extracranial arteries through the range of hypoxic severities typically experienced. Bilateral calculations of blood flow were derived from consecutive rather than simultaneous measurements of the left and right arteries as we only had access to a single ultrasound. However, the short time difference introduced by using consecutive left and right measurements likely had limited influence on the interpretation of our findings as the ICA and VA measurements were obtained whilst participants were rested. A wide range of methodological techniques are currently employed to measure cerebral blood flow at rest and in response to stressors, each with its advantages and disadvantages (Tymko et al., 2018). Duplex ultrasound offers a non-invasive, volumetric measurement of intravascular blood flow with excellent temporal resolution important for the assessment of cerebral blood flow to dynamic stressors (e.g., hypoxia, carbon dioxide, orthostasis, and exercise). However, to obtain accurate and reliable (~10 % day-to-day CV) measurements considerable ultrasound training is required (Thomas et al., 2015). Notwithstanding this, the results presented here reveal a source of previously under-recognised measurement error in the assessments of unilateral extracranial relative blood flow response to vasoactive stimuli and provides a systematically approached consensus for the selection of unilateral extracranial measurements to minimise this measurement error when bilateral measurement is infeasible.

Conclusions

ICA and VA blood flow regulation to hypoxia is comparable when factoring for vessel type (ICA or VA) and vessel side (left or right) effects. Bilateral calculations of the ICA and VA indicated the same degree of vasodilation and comparable increases in relative blood flow to acute poikilocapnic hypoxia. Compared to bilateral assessment of the relative blood flow response to hypoxia, individual unilateral measurement error reached 37%, and were greatest in ICA and VA with the smaller resting blood flow due to a ratio-scaling problem. Where

bilateral assessment is infeasible assessing the ICA and VA vessels with the larger resting blood flow, not the left or right vessel, reduces unilateral measurement error.

Author contributions and acknowledgments

Authors: Alexander T. Friend, Matthew Rogan, Gabriella M.K. Rossetti, Justin S. Lawley, Paul G. Mullins, Aamer Sandoo, Jamie H. Macdonald, and Samuel J. Oliver. AF and SO conceived and designed the study. All authors contributed to the acquisition, analysis, or interpretation of data for the work. AF and SO drafted the manuscript, with all remaining authors reviewing and providing critical feedback important for intellectual content.

We would like to thank the participants for their time and effort in this study. We also thank Poppy Barsby, Liam Joyce, and Harry Nicholson for their contribution to data collection.

Chapter Five

Regional dynamic cerebral autoregulation in acute poikilocapnic hypoxia

5.1 Abstract

Hypoxia reduces dynamic cerebral autoregulation (dCA), but evidence is limited to the anterior circulation. As dCA is poorer in the posterior compared to anterior circulation in normoxia, possibly due to a lower basal vascular tone, we hypothesised hypoxia would cause an exacerbated reduction in dCA of the posterior compared to the anterior circulation. In a random order, twenty participants (14 men) were exposed to 120-min of normoxia and poikilocapnic hypoxia (12.5% fraction of inspired oxygen). Regional dCA was assessed in the internal carotid artery (ICA, anterior circulation) and vertebral artery (VA, posterior circulation) as the rate of regulation (RoR) of volumetric vascular conductance to acute hypotension induced by the thigh cuff method. In the mixed cohort, ICA and VA RoR were comparable in normoxia and hypoxia. In secondary analysis, accounting for sex and improving the statistical model, hypoxia reduced VA RoR $[-0.15 (0.19) \text{ s}^{-1}, p=0.012]$, but not ICA RoR $[-0.07 (0.19) \text{ s}^{-1}, p=0.198]$ in men. Hypoxia induced vasodilation of the ICA $[+0.30 (0.32) \text{ mm}, p=0.009]$, but not the VA $[+0.08 (0.33) \text{ mm}, p=0.398]$ in men. In conclusion, dCA of the cerebral conduit arteries to hypoxia is regionally different in men and may not be influenced by changes in vascular tone.

5.2 Introduction

Dynamic cerebral autoregulation (dCA) is an intrinsic mechanism that regulates cerebral blood flow to fluctuations in arterial blood pressure within a few seconds via changes in vascular tone to maintain a constant delivery of oxygen to the brain (Brassard et al., 2021; Claassen et al., 2021; Lucas et al., 2010). Arterial vascular tone and, in turn, cerebral blood flow, is regulated by the vascular smooth muscle that lines the cerebral arterial circulation (Brozovich et al., 2016). The type, density, and distribution of receptors and channels present on the arterial vascular wall and its sensitivity to vasoactive agents are key mediators responsible for the regulation of vascular tone (Hayes et al., 2022), and variability within these mechanisms between the anterior and posterior cerebral circulation may underpin the observed regional cerebral blood flow regulation during systemic physiological stress, such as orthostasis (Sato, Fisher, et al., 2012), hypoxia (Kellawan et al., 2017; Lewis et al., 2014; Ogoh et al., 2013; Willie et al., 2012), hyperthermia (Bain et al., 2013; Caldwell et al., 2020), and alterations in end-tidal carbon dioxide (Sato, Sadamoto, et al., 2012; Willie et al., 2012). Indeed, distinctive sympathetic adrenoceptor subtype distribution and parasympathetic innervation between the anterior and posterior cerebral conduit arteries have been identified (Koep et al., 2022), and may explain early reports of opposing vasoactive responses to norepinephrine between anterior and posterior bovine cerebral conduit arteries (Ayajiki & Toda, 1992). Further, a lower sensitivity to vasoactive agents, such as reactive oxygen species and nitric oxide bioavailability, has been reported in the posterior circulation compared to the anterior circulation (Mattos et al., 2019, 2020; Vianna et al., 2018).

These observed regional differences in cerebral blood flow regulation may be a necessity to maintain a lower basal vascular tone in the posterior compared to anterior circulation. Such differences may preferentially maintain blood flow to the posterior regions of the brain involved in systemic cardiorespiratory control, particularly during times of systemic

physiological stress (Sato, Fisher, et al., 2012), and/or to meet the neurometabolic demand of the occipital lobes to visual stimulation since assessments are normally conducted with eyes open (Hermes et al., 2007; Matsutomo et al., 2023; Nakagawa et al., 2009). The influence of vessel tone on dCA has been seldom studied in humans perhaps due to the difficulty of manipulating and measuring vessel tone before and during dCA assessment. However, using an elegant-design, one study to examine the role of vessel tone demonstrated regionally specific dCA (Sato, Fisher, et al., 2012). Specifically, in response to an orthostatic-induced reduction in blood pressure caused by head-up tilt, cerebral blood flow reductions were attenuated in the vertebral artery (VA) compared to the internal carotid artery (ICA), which are the upstream conduit arteries that supply blood to the posterior and anterior circulations, respectively. This was attributed to an unchanged vascular tone in the VA that contrasted with the increased vascular tone of the ICA (Sato, Fisher, et al., 2012). Volumetric dCA was then assessed by the rapid thigh cuff method during the head-up tilt, and it was reported that compared to supine the VA had a greater reduction in blood flow and a slower rate of regulation (RoR) of vascular conductance to the abrupt reduction in blood pressure caused by the thigh cuff deflation than the ICA (Sato, Fisher, et al., 2012). It was proposed that a lower basal vascular tone of the VA is necessary to preferentially attenuate the orthostatic-induced reduction in cerebral blood flow to the posterior regions of the brain, but this is at the expense of a reduced dCA (i.e., more pressure-passive). Further evidence of a more pressure-passive disposition of the posterior compared to the anterior circulation to acute reductions in blood pressure is reported elsewhere (Lewis et al., 2015; Sorond et al., 2005; Thrall et al., 2021; Washio et al., 2018).

Exposure to acute hypoxia has been shown to reduce dCA (Bailey et al., 2009; Horiuchi et al., 2016, 2022; Iwasaki et al., 2007; Levine et al., 1999; Nishimura et al., 2010; Ogoh et al., 2010; Subudhi et al., 2009; Tymko et al., 2020). This has been attributed to the reduction in vascular tone of the cerebrovasculature, which is a compensatory response in a low oxygen environment

to increase cerebral blood flow to maintain cerebral oxygen delivery (Ogoh et al., 2010; Querido et al., 2013). However, studies that have assessed vascular tone and volumetric blood flow simultaneously during assessments of dCA in hypoxia are limited to the cerebral conduit arteries that feed the anterior regions of the brain (Horiuchi et al., 2016, 2022; Tymko et al., 2020), and therefore whether hypoxia causes regional differences in dCA remains to be determined. It is important to establish the effect of hypoxia on dCA of the posterior circulation because regional differences in dCA may also explain the stronger association of the posterior than anterior circulation with orthostatic (in)tolerance (Kay & Rickards, 2016), acute mountain sickness (Barclay et al., 2021; Bian et al., 2014), and cerebral small vessel disease (Liu et al., 2016).

This study compared volumetric dCA of the anterior and posterior cerebral conduit arteries in a mixed cohort of men and women in normoxia and in acute poikilocapnic hypoxia. As previous research indicates the posterior circulation is more pressure-passive than the anterior circulation (Haubrich et al., 2004; Rosengarten & Kaps, 2002; Sato, Fisher, et al., 2012; Sorond et al., 2005), and the magnitude of hypoxia-induced vasodilation is similar between the anterior and posterior cerebral conduit arteries (Friend et al., 2021; Lewis et al., 2014), we hypothesised the dCA reduction to large abrupt reductions in blood pressure in acute hypoxia would be exacerbated in the posterior compared to anterior circulation.

5.3 Methods

Ethical Approval

Ethical approval for this study was obtained from Ethics Committee of the School of Sport, Health, and Exercise Sciences at Bangor University (Ethics ID: P05-2021, Appendix 3) and was conducted following the standards of the *Declaration of Helsinki 2013*, except for registration in a database, with written informed consent obtained from all participants.

Participants

Twenty young healthy participants were recruited in this study 14 men, 6 women, 25 (7) yr, 175.8 (8.5) cm, 71.3 (11.3) kg, body fat 15.8 (6.4) %, haemoglobin 14.2 (2.0) g·dL⁻¹, haematocrit 42 (6) %, mean (standard deviation)]. Participants were non-smokers, free from cardiovascular, haematological, and neurological disease, not at an increased risk of COVID-19 as defined by the Welsh Government and had not resided overnight at an altitude of > 2500 m within the last six months. Women were included if they had a regular menstruating cycle or were taking an oral contraceptive pill which included inactive/placebo days. Participants with a regular menstrual cycle were tested during the onset of menses and the early follicular phase (day 1 to 5) and participants on the oral contraceptive pill were tested during their withdrawal bleed (Elliott-Sale et al., 2021). Menstrual subphase identification was completed by a forward counting self-report method (Allen et al., 2016). Participants were instructed to refrain from consuming alcohol and from undertaking exhaustive exercise within 24 h of visiting the laboratory. Participants were familiarised with the experimental procedures and screened for vascular abnormalities before completing the experimental trials. Each experimental trial was completed at the same time of day and participants were instructed to match their diet and supplement intake, and prohibited from consuming caffeinated beverages, on the day of each trial.

Experimental Design

This study followed a single-blind, repeated-measures, counterbalanced crossover design with each participant completing two experimental trials separated by at least 48 h. Experimental trials consisted of a 120-min exposure to either normoxia (fraction of inspired oxygen [FiO₂] = 20.9 %) or acute poikilocapnic hypoxia (FiO₂ = 12.5 %) in a temperature [25.6 (0.8) °C] and humidity [30.3 (5.0) %] controlled environmental chamber (Hypoxico Inc, New York, USA).

Experimental Measurements

Cardiorespiratory

Peripheral arterial oxygen saturation was measured via pulse oximetry (S_pO_2 , Model 7500 Oximeter, Nonin Medical Inc. Minnesota, USA). Beat-to-beat heart rate was measured with a Lead II electrocardiogram and blood pressure was measured by finger photoplethysmography (Finometer Midi, Finapres Medical Systems, Netherlands). Measurements of systolic blood pressure, diastolic blood pressure, and mean arterial pressure (MAP) were calculated from the finger arterial waveform and calibrated to the average of three automated brachial blood pressure measurements (Tango+, SunTech, Morrisville, NC, USA). The partial pressure of end-tidal oxygen ($P_{ET}O_2$) and partial pressure of end-tidal carbon dioxide ($P_{ET}CO_2$) were recorded breath-by-breath by a gas analyser (ML206, ADInstruments, Colorado, CO, USA).

Extracranial arteries

Blood flow of the ICA and VA were collected using duplex ultrasound with a 15 MHz linear transducer at 30 Hz (uSmart 3300, Terason, Burlington, MA, USA). High-resolution images of vessel diameter were acquired using B-mode imaging whilst pulse wave mode was used to simultaneously measure the Doppler velocity spectra. Care was taken to ensure the strongest Doppler velocity spectrum signal by positioning the Doppler gate in the centre of the artery with a 60° angle of insonation and adjusting to fill the artery lumen as per recommended technical guidelines (Thomas et al., 2015). The ICA was measured at least 1.0–1.5 cm distal to the carotid bifurcation and the VA was measured between C3 and the subclavian artery.

Intracranial arteries

Blood velocity of the MCA and PCA were measured by transcranial Doppler ultrasound (TCD) using two 2 MHz probes placed over the left and right transtemporal windows and secured in place via an adjustable head piece (PMD150, Spencer Technologies, Seattle, WA, USA).

Insonation of each artery was achieved using standardised procedures (Willie et al., 2011), with probe position, signal depth and gain settings recorded to replicate the placement between sessions. All TCD measurements were collected by the same operator (ATF). Pairs of MCA and ICA, and PCA and VA were measured on the same side of the participant as determined by the most reliable and reproducible signals.

In two separate day-to-day reproducibility studies completed by the same operator (ATF), the coefficient of variation for duplex ultrasound (N = 5) measurements of blood flow, vessel diameter, and blood velocity of the ICA (4%, 1%, and 3%) and VA (8%, 1%, and 7%) and TCD (N = 10) blood velocity measurements of the MCA (3%) and PCA (3%) were comparable with recommended guidelines (Thomas et al., 2015).

Experimental Procedures

Rapid thigh cuff deflation induced hypotension

dCA was assessed (elapsed time: 60 min) using the standardised rapid thigh cuff method that causes transient abrupt hypotension (Aaslid et al., 1989). Participants were instrumented with bilateral thigh cuffs (CC17, Hokanson, Bellevue, WA, USA) connected to a rapid deflator (E20 Rapid Cuff Inflator, Hokanson), seated comfortably in an upright position, and asked to rest for a two-minute baseline. After the bilateral thigh cuffs were inflated to 200 mmHg for three minutes. Participants were instructed to remain relaxed and were not given feedback regarding the elapsed time of thigh cuff occlusion. Immediately after the three-minute inflation period both thigh cuffs were rapidly deflated (< 1 s), causing a transient fall in MAP, and participants were instructed to remain still for one-minute thereafter. Measurements of heart rate, MAP, S_pO_2 , $P_{ET}O_2$, $P_{ET}CO_2$ and blood velocity of the MCA and PCA were recorded continuously throughout each rapid thigh cuff deflation. Simultaneous ICA and VA measurements were recorded for 30 s pre- and post-deflation. A minimum of four thigh cuff deflations were

completed per participant to enable a minimum of two recordings each of the ICA and VA. Whilst participants may have required more than four deflations [5 deflations (N=9), 6 deflations (N=4), 7 deflations (N=1)], the impact of repeated thigh cuff deflations on dCA, such as occurs with acute remote ischaemic preconditioning, are thought to be negligible (H. Carter et al., 2020).

Data Processing

Measurements of blood velocity of the MCA and PCA, heart rate, systolic and diastolic blood pressure, S_pO_2 , $P_{ET}O_2$ and $P_{ET}CO_2$ were all acquired continuously at 1 kHz using an analog-to-digital converter (Powerlab 16/30, ADInstruments) and interfaced on a computer in real time using LabChart software (Chart 8, ADInstruments). Real time beat-to-beat MAP and time-averaged maximum values of blood velocity of the MCA or PCA were determined from each R-R interval. All duplex ultrasound data was captured and stored for subsequent offline analysis by an investigator blinded to the condition of the experimental trials. Concurrent measurements of vessel diameter and time-averaged maximum velocity (TAMx) were acquired using an automated edge-detection tracking software (Brachial Analyser, Vascular Research Tools 6, Medical Imaging Applications, Coralville, IA, USA). Subsequently, blood flow was calculated using the following equation:

$$\text{Blood flow (ml}\cdot\text{min}^{-1}) = [\text{TAMx (cm}\cdot\text{s}^{-1})^2] \times [\pi \times (\text{mean vessel diameter (cm)/2})^2] \times 60$$

Following a conservative quality check, data and statistical analysis were completed on (normoxia: hypoxia); 18:17 ICA (13:12 male, 5:5 female), 17:19 VA (12:13 male, 5:6 female), 19:19 MCA (13:13 male, 6:6 female), and 16:16 PCA (10:10 male, 6:6 female). The exclusions were due to a poor image or signal quality of the extra- and intracranial arteries.

Data Analysis

Cardiorespiratory

Continuous beat-to-beat heart rate, systolic blood pressure, diastolic blood pressure, MAP, S_{pO_2} , $P_{ET}O_2$, and $P_{ET}CO_2$, were calculated from a two-minute average before the rapid thigh cuff method.

Cerebrovascular

In accordance with previous methods (Labrecque et al., 2021), dCA after rapid thigh cuff deflation was characterised by the following metrics (Figure 5.1): 1) maximal reduction, 2) time to counter-regulation, and 3) rate of regulation (RoR).

The absolute and relative maximum reduction following rapid thigh cuff deflation in MAP, blood flow, blood velocity, vessel diameter, and cerebrovascular conductance (CVC = blood flow/MAP) or index (CVCi = blood velocity/MAP) values, were calculated as the difference from their respective pre-deflation mean that was defined as the four seconds immediately before thigh cuff release. The time taken from thigh cuff deflation to the nadir in MAP and CVC or CVCi were individually determined and defined as the time to first MAP nadir and time to CVC or CVCi counter-regulation, respectively. RoR was calculated from CVC or CVCi. Post thigh cuff deflation responses were normalised to their concomitant pre-deflation values. RoR was calculated using the following equation:

$$[\text{RoR} = (\Delta\text{conductance}/\Delta\text{time}) / \Delta\text{MAP}]$$

where $\Delta\text{conductance}/\Delta\text{time}$ is the slope of the regression line between normalised CVC or CVCi and the time of CVC or CVCi counter-regulation plus 2.5 s from thigh cuff release, and ΔMAP , is the magnitude of the reduction in normalised MAP during thigh cuff release during the same 2.5 s phase.

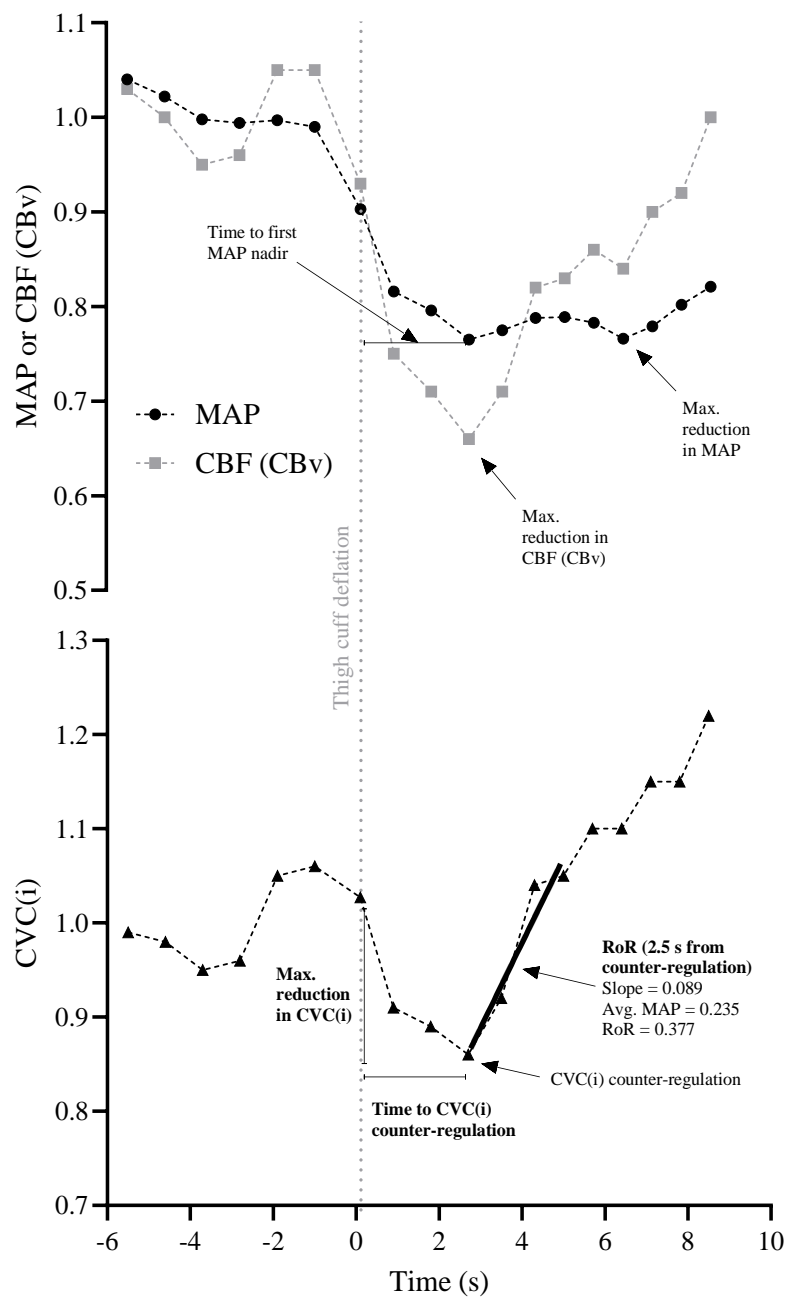


Figure 5.1. Representative illustration of the dynamic cerebral autoregulation metrics after rapid thigh cuff deflation induced hypotension. Mean arterial pressure (MAP, circle), cerebral blood flow (CBF) or velocity (CBv, square), and cerebrovascular conductance (CVC) or index (CVCi, triangle) after rapid thigh cuff method assessment of dynamic cerebral autoregulation. Data were normalised relative to their respective means during the four seconds immediately before the thigh cuff release. In accordance with previous methods (Labrecque et al., 2021), dCA after rapid thigh cuff deflation was characterised as the following metrics: 1) maximal reduction, 2) time to counter-regulation, and 3) rate of regulation (RoR).

Statistical Analysis

A sample size estimation [G*Power 3.1.9, (Faul et al., 2009)] for the primary analysis using ANOVA indicated that 12 participants were needed to detect a statistical difference between dynamic cerebral autoregulation in the internal carotid and vertebral arteries. This was estimated using standard α (0.05), power (0.80), and a Cohen's F effect size of 0.48, which was calculated from the only other previous study to compare dynamic cerebral autoregulation in anterior and posterior extracranial arteries (Sato, Fisher, et al., 2012). Since planning the study, we learnt of the superiority of linear mixed models and have adopted these methods to analyse data, e.g., (Friend et al., 2021). Moreover, the number recruited in our study is also greater than included in the limited previous research to examine and report differences in volumetric dynamic cerebral autoregulation to physiological stressors (sample sizes of 6 to 13) (Horiuchi et al., 2016, 2022; Sato, Fisher, et al., 2012; Tymko et al., 2020).

Statistical analysis was conducted using SPSS Statistics v27 (IBM Corp., Armonk, NY, USA) and figures were created in GraphPad Prism (GraphPad Prism 9, San Diego, CA, USA). The primary statistical test was to compare dCA of the anterior and posterior cerebral conduit arteries in a mixed cohort of men and women in normoxia and hypoxia. Therefore, dCA metrics following rapid thigh cuff deflation were analysed by a linear mixed model (LMM) with fixed effects of condition (normoxia and hypoxia) and region (anterior and posterior), adding participant as a random effect, with the interaction the primary effect of interest. Secondary analyses included the additional fixed effects of interest of sex or $P_{ET}CO_2$, given their known influence on dCA (Barnes & Charkoudian, 2021; Ogoh et al., 2010), as well as basal blood flow, blood velocity, and vessel diameter. The model fit of each LMM with additional fixed effects was compared to the original model using the Chi-square likelihood ratio test. Cardiorespiratory and cerebrovascular variables before rapid thigh cuff method were analysed by a LMM with condition the primary fixed effect of interest, participant as a random effect,

and additional fixed effects of interest of region, sex, or $P_{ET}CO_2$. Raw data are mean (standard deviation) unless otherwise stated and statistical significance was set at $p < 0.05$. Bonferroni corrected-multiple pairwise comparisons were conducted when significant main or interactions effects were detected. Values from LMM pairwise comparison analysis are reported as estimated marginal means and an estimated standard deviation (Friend et al., 2021; Shenouda et al., 2017).

5.4 Results

Cardiorespiratory response in normoxia and hypoxia before thigh cuff deflation induced hypotension

Compared to normoxia, acute poikilocapnic hypoxia reduced S_pO_2 [estimated marginal means (estimated standard deviation), -14.6 (3.7) %, main effect of condition, $p < 0.001$, Table 5.1], $P_{ET}O_2$ [-57.0 (4.8) mmHg, $p < 0.001$], $P_{ET}CO_2$ [-2.7 (3.6) mmHg, $p = 0.004$], diastolic blood pressure [-5.1 (8.6) mmHg, $p = 0.014$], and MAP [-4.5 (7.4) mmHg, $p = 0.013$], and increased heart rate [$+7.0$ (7.6) bpm, $p = 0.001$]. Acute poikilocapnic hypoxia did not induce acute mountain sickness (Appendix 5.2).

Haemodynamic response in normoxia and hypoxia to thigh cuff deflation induced hypotension

The rapid thigh cuff deflation caused comparable time to first MAP nadir and absolute maximum reduction in MAP in normoxia and hypoxia (both $p > 0.05$, Table 5.2). Due to lower pre-thigh cuff deflation MAP in hypoxia than normoxia (Table 5.1), the relative maximum reduction in MAP was greater in hypoxia than normoxia (main effect of condition, $p = 0.048$). The relative maximum reduction to the thigh cuff induced hypotension in blood velocity, vessel diameter, blood flow in normoxia and hypoxia were regionally comparable within the extracranial (ICA and VA) and intracranial (MCA and PCA) arteries (condition \times region interaction, all $p > 0.05$).

	Condition		<i>p</i> value Condition
	Normoxia	Hypoxia	
Cardiorespiratory			
S _p O ₂ (%)	96.8 (1.0)	82.1 (3.7)	<0.001
Heart rate (bpm)	66.0 (8.2)	73.0 (10.4)	0.001
Systolic blood pressure (mmHg)	117.1 (11.4)	113.8 (12.6)	0.076
Diastolic blood pressure (mmHg)	73.3 (8.2)	68.2 (10.8)	0.014
Mean arterial pressure (mmHg)	87.9 (8.1)	83.4 (10.3)	0.013
P _{ET} O ₂ (mmHg)	106.0 (4.4)	49.0 (3.9)	<0.001
P _{ET} CO ₂ (mmHg)	37.9 (3.4)	35.3 (2.8)	0.004
Extracranial blood flow (ml·min⁻¹)			
Internal carotid artery	260.2 (58.8)	289.5 (68.3)	0.129
Vertebral artery	107.0 (33.3)	115.1 (54.3)	0.357
Extracranial vessel diameter (mm)			
Internal carotid artery	5.03 (0.70)	5.41 (0.61)	0.002
Vertebral artery	3.69 (0.51)	3.87 (0.52)	0.075
Extracranial blood velocity (cm·s⁻¹)			
Internal carotid artery	45.0 (9.7)	42.2 (8.1)	0.279
Vertebral artery	32.8 (6.7)	31.9 (7.5)	0.450
Intracranial blood velocity (cm·s⁻¹)			
Middle cerebral artery	54.3 (13.3)	56.1 (13.6)	0.338
Posterior cerebral artery	43.4 (9.8)	45.3 (10.5)	0.355

Table 5.1. Cardiorespiratory and cerebrovascular responses before the rapid thigh cuff method in normoxia and hypoxia. Data were analysed by linear mixed model analysis. The primary outcome of interest for these cardiorespiratory and cerebrovascular variables was the effect of condition (normoxia and acute poikilocapnic hypoxia). Abbreviations: P_{ET}CO₂, partial pressure of end-tidal carbon dioxide; P_{ET}O₂, partial pressure of end-tidal oxygen; S_pO₂, peripheral arterial oxygen saturation. Data are raw means (standard deviation).

	Condition		<i>p</i> values
	Normoxia	Hypoxia	Condition
Mean arterial pressure (MAP)			
Time to MAP first nadir (s)	4.5 (1.0)	4.5 (0.9)	0.846
Max. Δ MAP (mmHg)	-21.3 (6.0)	-22.6 (2.8)	0.383
Max. Δ MAP (%)	-23.3 (6.3)	-26.2 (3.7)	0.048
Extracranial max. Δ blood flow (%)			
Internal carotid artery	-33.9 (8.2)	-32.2 (9.4)	0.426
Vertebral artery	-34.3 (8.6)	-33.2 (8.2)	0.423
Extracranial max. Δ vessel diameter (%)			
Internal carotid artery	-6.3 (2.7)	-7.7 (3.1)	0.089
Vertebral artery	-7.2 (3.9)	-7.9 (4.9)	0.804
Extracranial max. Δ blood velocity (%)			
Internal carotid artery	-26.5 (7.3)	-22.9 (8.7)	0.096
Vertebral artery	-26.6 (8.2)	-24.4 (6.2)	0.226
Intracranial max. Δ blood velocity (%)			
Middle cerebral artery	-26.6 (6.2)	-25.8 (5.5)	0.429
Posterior cerebral artery	-26.2 (4.3)	-24.9 (6.0)	0.452

Table 5.2. Haemodynamic responses to the rapid thigh cuff deflation induced hypotension in normoxia and hypoxia. Data were analysed by linear mixed model analysis. The primary outcome of interest for mean arterial pressure and cerebrovascular variables was the effect of condition (normoxia and acute poikilocapnic hypoxia). Data are raw means (standard deviation).

Regional dynamic cerebral autoregulation in normoxia and hypoxia

In our mixed cohort of men and women, ICA RoR and VA RoR in normoxia [0.42 (0.23) s^{-1} and 0.41 (0.13) s^{-1} , respectively] and hypoxia [0.35 (0.12) s^{-1} and 0.36 (0.19) s^{-1} , condition \times region interaction effect, $p = 0.975$, Figure 5.2a] were comparable and not reduced in hypoxia (main effect of condition, $p = 0.119$). However, the inclusion of sex as an additional fixed factor (condition \times region \times sex interaction) improved the model fit ($p < 0.05$), and revealed that hypoxia reduced VA RoR in men [normoxia, 0.44 (0.18) s^{-1} , $N = 12$, and hypoxia, 0.30 (0.13) s^{-1} , $N = 13$, pairwise comparison, $p = 0.012$], whilst in women VA RoR remained unchanged [normoxia, 0.36 (0.18) s^{-1} , $N = 5$, and hypoxia, 0.50 (0.13) s^{-1} , $N = 6$, $p = 0.094$]. ICA RoR was comparable in normoxia and hypoxia in men [normoxia, 0.41 (0.18) s^{-1} , $N = 13$, and hypoxia, 0.34 (0.12) s^{-1} , $N = 12$, $p = 0.198$] and women [normoxia, 0.42 (0.18) s^{-1} , $N = 5$, and hypoxia, 0.40 (0.13) s^{-1} , $N = 5$, $p = 0.810$]. In men only, compared with normoxia, ICA RoR was maintained (-0.07 (0.21) s^{-1} , $p = 0.264$, Figure 5.3a) in hypoxia, whereas VA RoR was reduced in hypoxia (-0.15 (0.19) s^{-1} , $p = 0.012$, Figure 5.3c).

Hypoxia increased ICA vessel diameter (reduced vascular tone) but did not significantly increase VA vessel diameter before thigh cuff deflation induced hypotension in the mixed cohort (Table 5.1). These findings were consistent when examined in men only, with a hypoxia induced reduction in vascular tone of the ICA [$+0.30$ (0.32) mm, main effect of condition, $p = 0.009$, Figure 5.3b], but not the VA [$+0.08$ (0.33) mm, $p = 0.398$, Figure 5.3d]. Blood flow and blood velocity of the ICA and VA in the mixed cohort, and in men only, were unchanged to hypoxia (all $p > 0.05$). The addition of P_{ETCO_2} to the LMM did not change the statistical outcome for any variable.

There was no condition \times region interaction for any other dCA metric from the rapid thigh cuff deflation including, MCA RoR and PCA RoR (Figure 5.2b), and maximal reduction in CVC

or CVCi (Figure 5.4a and 5.4b) and time to CVC or CVCi counter-regulation (Figure 5.4c and 5.4d) in the extracranial or intracranial arteries (all $p > 0.05$). The addition of sex, P_{ETCO_2} , basal blood flow, blood velocity, or vessel diameter to the LMM did not change the statistical outcome for any cerebrovascular variable.

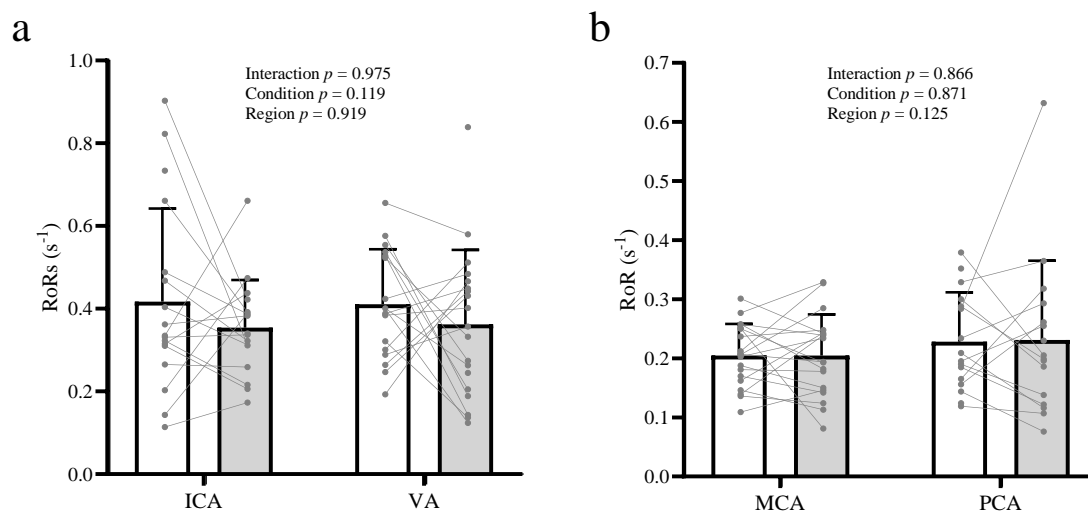


Figure 5.2. Rate of regulation following rapid thigh cuff deflation induced hypotension in normoxia and hypoxia. Rate of regulation (RoR) of the extracranial internal carotid (ICA) and vertebral (VA) arteries (a) and of the intracranial middle cerebral (MCA) and posterior cerebral (PCA) arteries (b) in normoxia (white bars, fraction of inspired oxygen [FiO_2] = 20.9%) and acute poikilocapnic hypoxia (grey bars, FiO_2 = 12.5%). Data are raw means (standard deviation) and are presented with individual responses of a mixed cohort of men and women. Data were analysed by linear mixed model analysis.

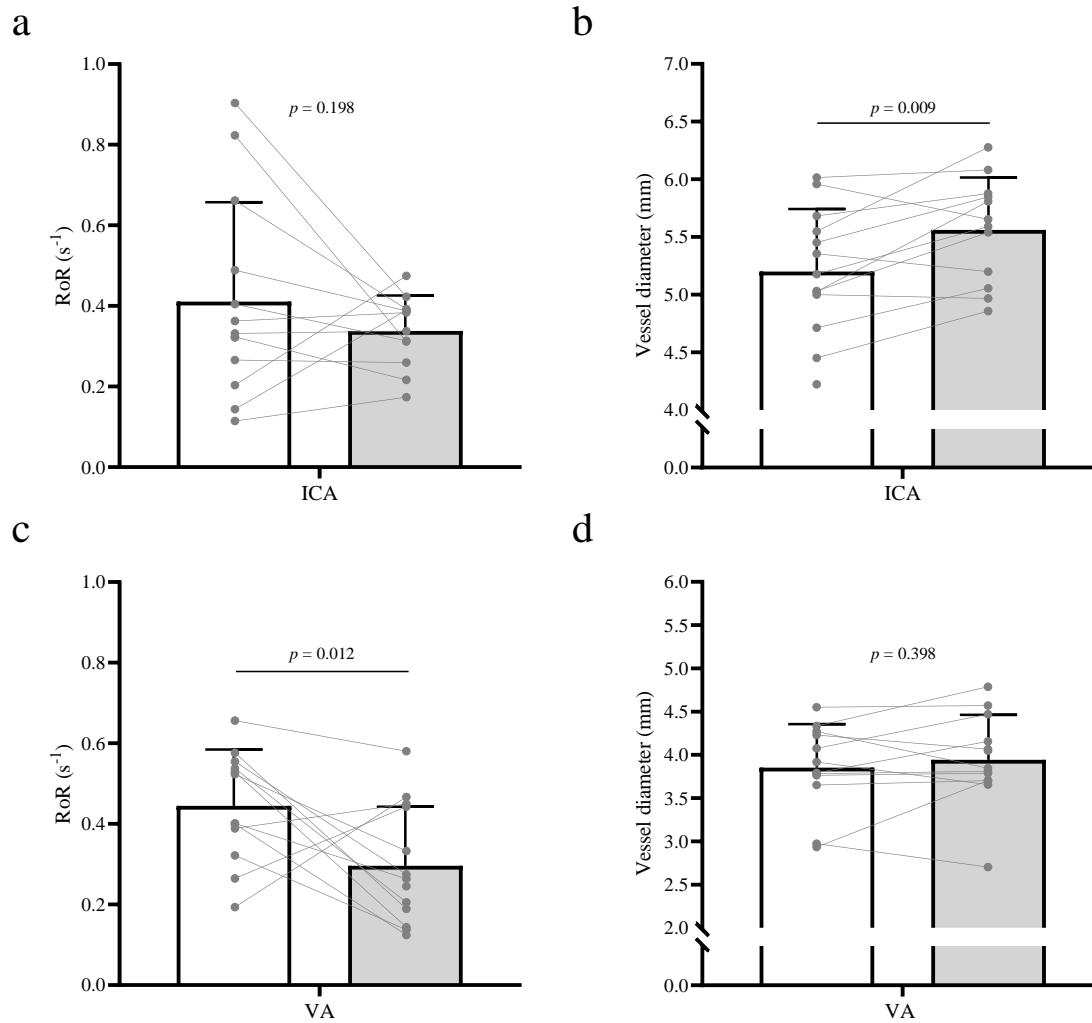


Figure 5.3. Rate of regulation following rapid thigh cuff deflation induced hypotension and pre-thigh cuff deflation vessel diameter in normoxia and hypoxia in men. Rate of regulation (RoR) and vessel diameter of the ICA (a and b) and VA (c and d) in normoxia (white bars, fraction of inspired oxygen [FiO_2] = 20.9%) and acute poikilocapnic hypoxia (grey bars, FiO_2 = 12.5%) in men (N = 13). Data are raw means (standard deviation) and are presented with individual responses. Data were analysed by linear mixed model analysis.

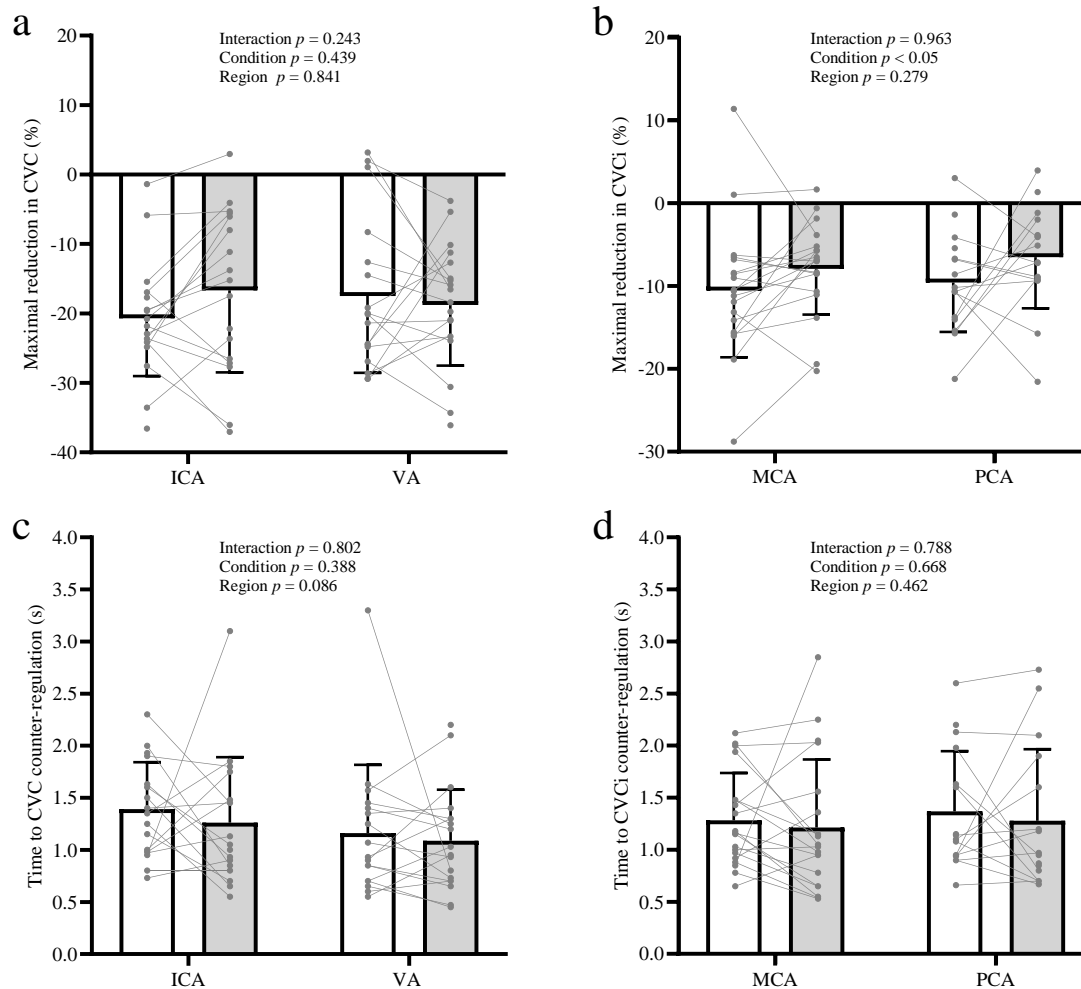


Figure 5.4. Cerebrovascular responses after thigh cuff deflation induced hypotension in normoxia and hypoxia. Maximal relative reduction in cerebrovascular conductance (CVC) or index (CVCi) and time to CVC or CVCi counter-regulation in the extracranial (a and c) internal carotid (ICA) and vertebral (VA) arteries and the intracranial (b and d) middle cerebral (MCA) and posterior cerebral (PCA) arteries in normoxia (white bars, fraction of inspired oxygen [FiO_2] = 20.9%) and acute poikilocapnic hypoxia (grey bars, FiO_2 = 12.5%). Data are raw means (standard deviation) and are presented with individual responses of a mixed cohort of men and women. Data were analysed by linear mixed model analysis.

5.5 Discussion

This study compared for the first time volumetric dCA of the anterior and posterior cerebral conduit arteries in normoxia and acute poikilocapnic hypoxia. We report in a mixed cohort of men and women that dCA of the intracranial and extracranial cerebral conduit arteries were regionally comparable during normoxia and hypoxia and were unexpectedly not reduced in hypoxia compared to normoxia. However, secondary analysis accounting for sex, and which importantly improved the statistical model, revealed hypoxia reduced dCA (i.e., more pressure-passive) of the posterior circulation in men, indicated by a reduction in VA RoR. In contrast, dCA of the ICA in men was similar in normoxia and hypoxia. We also observed that immediately before the dCA assessment hypoxia caused vasodilation (reduced vascular tone) of the ICA in men, but not the VA, which suggests an alternative mechanism to hypoxia-induced reduction in conduit artery vascular tone is responsible for the regional dCA responses observed in this study.

Dynamic cerebral autoregulation in hypoxia is region specific in men

We report for the first time, using volumetric blood flow RoR methods, the dCA of the cerebral conduit arteries to hypoxia is regionally different in men. Although region specific dCA has not previously been shown in acute hypoxia, our findings are consistent with those by Sato and colleagues that reported reduced VA RoR but not ICA RoR in a male-only cohort in response to large reductions in blood pressure caused by a combination of the thigh cuff method superimposed on head-up tilt (Sato, Fisher, et al., 2012). Furthermore, the magnitude of the reduction in dCA of the posterior circulation in men [VA RoR -0.15 (0.19) s^{-1}] is consistent with reductions in volumetric dCA of the anterior circulation previously reported in hypoxia, e.g., [ICA RoR -0.15 (0.26) s^{-1}] (Tymko et al., 2020).

The prevailing explanation for reduced dCA in the VA than ICA during systemic physiological stress is a lower basal vascular tone of the posterior circulation is necessary to maintain blood flow to the cardiorespiratory control centres of the brain (Sato, Fisher, et al., 2012). Regional differences in key mediators of cerebrovascular regulation may be linked to the reduced dCA of VA, such as differences in the CO₂ sensitivity. The VA has previously been shown to be more sensitive than the ICA to changes in hypotension and hypocapnia (Lewis et al., 2015). However, whilst we report a hypoxia-induced hypocapnia during the rapid thigh cuff method, incorporating P_{ET}CO₂ into our analyses did not influence the interpretation of the study findings, and so it is unlikely to explain the observed region specific dCA to acute hypoxia. Other plausible explanations for the reduced dCA of the VA compared to the ICA may be underpinned by an increased metabolic state of the visual cortices (Hermes et al., 2007; Matsutomo et al., 2023; Nakagawa et al., 2009), distinctive autonomic innervation (Koep et al., 2022), and different sensitivities to vasoactive agents, such as reactive oxygen species, and nitric oxide bioavailability (Mattos et al., 2019, 2020; Vianna et al., 2018). Our findings in a mixed cohort of men and women expand on the work by Sato and colleagues (Sato, Fisher, et al., 2012) by identifying that region specific dCA, and likely the mechanisms underpinning it, is influenced by biological sex, since we only found a regional difference in dCA in men.

Postural-induced differences in peripheral arterial blood pressure may influence dynamic cerebral autoregulation in hypoxia

The lack of a reduction in anterior circulation dCA to acute hypoxia in the present study was unexpected as the severity of hypoxia was similar to the three other previous studies to report reductions in anterior circulation volumetric dCA in hypoxia (Horiuchi et al., 2016, 2022; Tymko et al., 2020). A possible explanation for these contrasting reports is the difference in the peripheral arterial blood pressure response to the hypoxia before the thigh cuff method, since in previous studies MAP was either increased or unchanged (Horiuchi et al., 2016, 2022;

Tymko et al., 2020), whereas we report a reduction in MAP. The differences in arterial blood pressure responses to acute hypoxia can be explained by posture differences as in the current study, participants were sat upright, which contrasts the semi-reclined and supine positions in previous studies (Horiuchi et al., 2016, 2022; Tymko et al., 2020). Posture differences are also known to impact the magnitude of cerebral blood flow reduction to rapid thigh cuff method (Deegan et al., 2010), which may also partly explain our contrasting response in dCA of the ICA to the literature. Whilst we induced a comparable reduction in MAP by the rapid thigh cuff deflation, we induced a greater reduction in blood flow (-34% vs max. -22%) to that reported previously (Horiuchi et al., 2016, 2022; Tymko et al., 2020). Our reduction in blood flow was more akin to the reduction reported during large abrupt reductions in blood pressure induced by a combination of head-up tilt and the thigh cuff method (-32%), which also reported a reduction in dCA of the VA but not ICA (Sato, Fisher, et al., 2012). Taken together, it could be speculated that an exacerbated reduction in dCA of the VA to acute hypoxia compared to the ICA, as which we had originally hypothesised, may occur during a relative hypoxia-induced hypertension in the upright position; however, this requires confirmation in future research.

Reductions in dynamic cerebral autoregulation in hypoxia may not be attributable to hypoxia-induced vasodilation

We report differences in the acute hypoxia-induced vasodilation between the anterior and posterior cerebral conduit arteries. Specifically, in men, hypoxia caused vasodilation of the ICA but not the VA (Figure 5.3). Combined with the hypoxia-induced reduction in dCA of the VA but not the ICA in men, our study provides evidence to contrast the prevailing hypothesis that a lowered vascular tone is the mechanism that reduces dCA in acute hypoxia (Ogoh et al., 2010; Querido et al., 2013). Therefore, in agreement with other reports of an unchanged vessel diameter but reduced dCA in hypoxia (Tymko et al., 2020) and head-up tilt (Sato, Fisher, et al., 2012), other mechanisms are likely responsible for the reduction in posterior dCA in acute

hypoxia in the present study, for example, our proposed effect of basal blood pressure differences before the dCA assessment and posture. This explanation may also extend to previous research that primarily attributes the reduction in dCA by hypercapnia to the vasodilatory effect of CO₂ (Panerai et al., 1999), whilst our findings suggest the reduction of dCA may be due to the hypertensive effects of hypercapnia. Another possible explanation for lack of association between lowered vascular tone and reduced dCA in the extracranial arteries in our study is that the large vasculature is less vasoactive in the regulation of dCA with most of the regulation of vascular resistance occurring in the downstream arteries and arterioles. Whilst the large arteries do contribute to vascular resistance (Liu et al., 2013), segmental differences in innervation and regulation of the vasculature suggests that a large proportion of vasodilation-induced reductions in dCA occur in the microvasculature (Cipolla, 2009; Duffin et al., 2021; Koep et al., 2022).

Methodological considerations and future directions

We report that intracranial dCA of MCA and PCA blood velocity were comparable in normoxia and hypoxia and between sexes, which contrasts our volumetric extracranial findings in this study. Whilst measurements of the extracranial arteries are limited as they may not reflect downstream vascular regulation, particular caution is needed when interpreting intracranial findings acquired by TCD as they do not account for vessel diameter changes. TCD has previously been shown to underestimate dCA compared to duplex ultrasound (Liu et al., 2013) and the importance of capturing vessel diameter, particularly during experimental methods that are known to change vessel tone such as hypoxia, is highlighted here since it was only when RoR was derived from volumetric blood flow measurements obtained at the extracranial arteries that the hypothesised regional dCA response was found. These findings support the view that dCA responses between different methods are not comparable and highlights the importance of capturing vessel diameter to calculate volumetric blood flow to have the most

confidence in the physiological interpretation of cerebrovascular function (Brassard et al., 2021).

Whilst there remains no gold standard measurement of dCA, and with evidence of poor agreement between different metrics of dCA (Tzeng et al., 2012), we believe our careful approach to dCA strengthens our findings (Figure 5.1). We used the standardised rapid thigh cuff deflation method (Aaslid et al., 1989) and duplex ultrasonography to assess dCA volumetrically to abrupt changes in blood pressure (< 4 s). To the authors' knowledge there is no other method than duplex ultrasonography with sufficient temporal resolution to examine dCA volumetrically to abrupt changes in blood pressure (< 4 s). Our approach to analysis involved metrics of dCA that have revealed regional differences previously, including the relative reduction in haemodynamics (Lewis et al., 2015), onset of recovery (Rosengarten & Kaps, 2002), and RoR (Horiuchi et al., 2016, 2022; Sato, Fisher, et al., 2012; Tymko et al., 2020). Whilst our adjustment to the RoR curves from the onset of recovery is different from previous hypoxia investigations (Horiuchi et al., 2016, 2022; Sato, Fisher, et al., 2012; Tymko et al., 2020), this approach accounts for individual differences (Labrecque et al., 2021), and enables the inclusion of the other metrics to provide a complete description of the cerebrovascular response to abrupt reduction in blood pressure. Moreover, the onset of recovery in CVC (1.4 s maximum, Figure 5.4) was within the time to first nadir in MAP (4.5 s on average, Table 5.2), so it is unlikely that our RoR metric included any MAP-mediated counter-regulation. Our careful approach to dCA analysis enabled us to isolate that it was the RoR, rather than the magnitude or time to counter-regulation, that was different between conduit cerebral arteries, which may suggest that RoR is a more sensitive dCA metric following rapid thigh cuff deflation induced hypotension.

The inclusion of sex as an additional fixed factor significantly improved the model fit and suggests biological sex may influence dCA of the extracranial arteries to abrupt reductions in

blood pressure. Whilst hypoxia induced regional dCA between the extracranial arteries in men, we are cautious in our interpretation of the findings in women due to the small sample size (N = 6). Women in our study completed repeat assessments in a menstrual or non-active pill phase associated with the lowest levels of oestrogen and progesterone to reduce the variability of sex hormones, which are known to influence cerebrovascular function (Barnes & Charkoudian, 2021; Krejza et al., 2001, 2003, 2013; Peltonen et al., 2016). Here we show that this approach may not reduce variability between men and women and that sex differences in dCA may persist even when female sex hormones are at their lowest. Indeed, including a mixed cohort of men and women with uneven group sizes, as in this study (14 men, 6 women), may complicate the interpretation of cerebrovascular regulation mechanisms, particularly when hypotheses are generated from previous studies that have almost entirely been generated in men (Horiuchi et al., 2016, 2022; Sato, Fisher, et al., 2012; Tymko et al., 2020). It is perhaps not surprising to observe sex differences in cerebral blood flow regulation given the differences between men and women in resting cerebral perfusion (Alisch et al., 2021; Daniel et al., 1989; Rodriguez et al., 1988) and blood pressure regulation (Hart et al., 2009). Our finding highlights that simplifying the variability between men and women to only differences in female sex hormones is insufficient as an experimental control and should serve as a cautionary example for future cerebrovascular research studies planning to use mixed men and women cohorts. Future research should employ rigorous methodologies to unravel the present contrasting and inconsistent reports of sex differences in dCA (Barnes & Charkoudian, 2021).

Conclusions

In a mixed cohort of men and women, the dCA of the intracranial and extracranial cerebral conduit arteries were regionally comparable during normoxia and acute poikilocapnic hypoxia. Further analysis, accounting for sex and improving the statistical model, revealed hypoxia reduced the dCA of the VA, but not the ICA in men. Hypoxia caused vasodilation of the ICA,

but not the VA, suggesting alterations in vascular tone may not be responsible for the reduction in dCA of the VA observed in men in hypoxia.

Author contributions and acknowledgments

Authors: Alexander T. Friend, Michiel Ewalts, Masahiro Horiuchi, Gabriella M.K. Rossetti, Aamer Sandoo, Jamie H. Macdonald, and Samuel J. Oliver. AF and SO conceived and designed the study. All authors contributed to the acquisition, analysis, or interpretation of data for the work. AF and SO drafted the manuscript, with all remaining authors reviewing and providing critical feedback important for intellectual content.

We would like to thank the participants for their time and effort in this study. We would like to thank Guto Hughes, Jonathan O'Duffy, Flynn Owen, Ferrida Ponce, and Sophia Wakefield for their contribution to data collection.

Chapter Six

Effect of the metabolic state of the visual cortices on regional vascular tone and dynamic cerebral autoregulation in normoxia and acute hypoxia

6.1 Abstract

Metabolic activation of the visual cortices from ambient light when measurements are completed with eyes open is proposed to lower basal vascular tone of the posterior cerebral circulation and contribute to the reduced dynamic cerebral autoregulation (dCA) of the posterior circulation compared to the anterior circulation. We hypothesised that, in normoxia and hypoxia, dCA of the posterior cerebral artery (PCA) and vascular tone of the vertebral artery (VA) would be reduced with 10-min of high (lights on – eyes open) compared to low visual input (lights off – eyes closed), whereas the middle cerebral artery (MCA) and internal carotid artery (ICA) would be unchanged. In twenty participants (14 men), vascular tone was measured using duplex ultrasound and dCA was derived from transfer function analysis of transcranial Doppler ultrasound measurements during spontaneous oscillations in blood pressure at rest. Visual stimulation reduced very low-frequency phase of the PCA [high, 1.00 (0.23) vs low, 1.24 (0.28), $P<0.01$], but not the MCA, [high, 1.25 (0.23) vs low, 1.22 (0.28), $P=0.72$] in normoxia, indicating a reduced posterior dCA, whereas there was no regional difference in dCA with visual stimulation in hypoxia. Visual stimulation increased blood velocity of the PCA and VA compared to MCA and ICA, but extracranial vascular tone was unchanged, in normoxia and hypoxia. In conclusion, visual stimulation elicited a regional intracranial and extracranial blood velocity increase in normoxia and hypoxia but did not reduce extracranial vessel tone, suggesting other mechanisms are responsible for the regional differences in intracranial dCA to visual stimulation.

6.2 Introduction

Cerebral blood flow is regulated by alterations in vascular tone of the cerebral arterial circulation to deliver oxygen and nutrients to match metabolic demand of the brain and remove cellular waste (Brozovich et al., 2016; Claassen et al., 2021). Dynamic cerebral autoregulation (dCA) is an intrinsic mechanism of the cerebral circulation that regulates cerebral blood flow via changes in vascular tone to fluctuations in arterial blood pressure within a few seconds (Brassard et al., 2021; Claassen et al., 2021; Lucas et al., 2010). Reduced vascular tone is a predominant mechanism that reduces dCA, such as during hypoxia and hypercapnia (Ogoh et al., 2010; Panerai et al., 1999). However, dCA is seldom studied in humans in response to physiological stress perhaps due to the difficulty of manipulating and measuring vessel tone before and during dCA assessment.

The posterior cerebral circulation is reported to regulate cerebral blood flow differently to the anterior circulation, particularly during times of physiological stress, such as in hypoxia (Kellawan et al., 2017; Lewis et al., 2014; Ogoh et al., 2013), orthostasis (Sato, Fisher, et al., 2012), hyperthermia (Bain et al., 2013; Caldwell et al., 2020) and alterations in carbon dioxide (Sato, Sadamoto, et al., 2012; Willie et al., 2012). Evidence from beat-to-beat transcranial Doppler ultrasound (TCD) derived measurements of blood velocity in the middle cerebral artery (MCA) and posterior cerebral artery (PCA) report that the posterior circulation has a poorer dCA compared to the anterior circulation and is more pressure-passive to fluctuations in arterial blood pressure (Haubrich et al., 2004; Sorond et al., 2005). In addition, previous research that assessed dCA with duplex ultrasound volumetric measurements has shown posterior dCA measured at the vertebral artery (VA) to be poorer compared to anterior dCA measured at the internal carotid artery (ICA) (Sato, Fisher, et al., 2012). The authors also elegantly demonstrated, using direct measurements of extracranial vessel diameter and the layering acute hypotension on top of orthostasis, that a lower vascular tone in the VA compared

to the ICA may be a mechanism for the more pressure-passive dCA of the posterior circulation (Sato, Fisher, et al., 2012). It is proposed that this lower vascular tone in the posterior circulation is necessary to preferentially maintain blood flow to brain regions involved in systemic cardiorespiratory control, particularly during times of systemic physiological stress where cerebral metabolic demand is increased, and/or to match neurometabolic demand of the visual cortices since assessments are regularly conducted with eyes open (Sato, Fisher, et al., 2012).

As is well-documented with the increase in blood velocity of the PCA during neurovascular coupling (Phillips et al., 2016), stimulation of the visual cortices reduces vascular tone of the posterior circulation compared to the anterior circulation (Bizeau et al., 2018; Masamoto & Vazquez, 2018). Neurovascular coupling paradigms often involve on-off cycles of visual stimuli a few centimetres from the face, such as a flashing screen, reading, or eye tracking of a moving object (Phillips et al., 2016). Visual stimulation-induced alterations in posterior compared to the anterior cerebrovascular haemodynamics have also been shown with more subtle ambient light and eyes open/closed manipulations (Hermes et al., 2007; Matsutomo et al., 2023). Less studied, owing to the limited methods available, is how subtle visual stimuli influences dCA. The only such study that has reported regional differences in dCA found that the dCA of the PCA is reduced when assessments at rest were completed in ambient light with eyes open compared to with eyes closed, whereas the dCA of the MCA was unchanged (Nakagawa et al., 2009). This demonstrates that increased neural activation of the visual cortices from ambient light with eyes open may modulate vascular tone and consequently dCA of the conduit arteries in the posterior circulation differently to the anterior circulation. However, since cerebral haemodynamics measurements in this study were limited to TCD (Nakagawa et al., 2009), the influence of eyes open stimulus on cerebral vascular tone and volumetric cerebral blood flow was not determined to confirm this hypothesis. Recently, it has

been reported that neurovascular coupling induces vasodilation and increased volumetric blood flow in the posterior cerebral conduit arteries, measured extracranially in the VA, which supports that visual stimulation may reduce the vascular tone of the posterior circulation (Samora et al., 2020). This also suggests that duplex ultrasound measurements of the ICA and VA can provide an indication of the vascular tone of the anterior and posterior circulations during visual stimulation that can be utilised to elucidate the role of vessel tone in underpinning the regional differences in dCA between lights on/eyes open vs lights off/eyes closed assessments.

Whilst there is evidence to suggest a regional cerebral blood flow regulation to hypoxia (Kellawan et al., 2017; Lewis et al., 2014; Ogoh et al., 2013), whether hypoxia leads to a regional difference in dCA has received little investigation. Hypoxia reduces dCA compared to normoxia (Bailey et al., 2009; Horiuchi et al., 2016; Subudhi et al., 2009; Tymko et al., 2020) and the prevailing explanation is that hypoxia-induced reductions in vascular tone causes the cerebral circulation to be more pressure-passive (Ogoh et al., 2010; Querido et al., 2013); however, these reports are limited to the cerebral conduit arteries of the anterior circulation. The limited research available that has investigated regional dCA in hypoxia is conflicting, with some suggesting that dCA of the posterior circulation may be reduced (Thesis Chapter 4) or improved (Smirl et al., 2014) compared to the anterior circulation to hypoxia. The effect of visual stimulation on dCA in hypoxia has not been previously investigated.

This study aimed to determine, in normoxia and hypoxia, the influence of low and high ambient visual input on regional cerebral haemodynamics, vascular tone, and dynamic cerebral autoregulation. We hypothesised that in normoxia and hypoxia; 1) intracranial blood velocity and extracranial blood velocity and blood flow of the posterior circulation would be greater with high compared to low visual input, whilst the anterior circulation would be unchanged; 2) extracranial vascular tone of the posterior circulation would be reduced with high compared to

low visual input, whilst the anterior circulation would be unchanged; 3) dCA of the posterior circulation would be reduced compared to the anterior circulation with high visual input, but comparable with low visual input.

6.3 Methods

Ethical Approval

Ethical approval for this study was obtained from Bangor University (proposal number P05-2021, Appendix 3) and was conducted following the standards of the *Declaration of Helsinki 2013*, except for registration in a database, with written informed consent obtained from all participants.

Participants

Twenty young healthy participants were recruited to this study [6 female, 25 (7) yr, 175.8 (8.5) cm, 71.3 (11.3) kg, body fat 15.8 (6.4) %, haemoglobin 14.2 (2.0) g·dL⁻¹, haematocrit 42 (6) %]. Participants were non-smokers, free from cardiovascular, haematological, and neurological disease, not at an increased risk of COVID-19 as defined by the Welsh Government and had not resided overnight at an altitude of > 2500 m within the last six months. Female participants were included if they had a regular menstruating cycle or were taking an oral contraceptive pill that included inactive/placebo days. Participants with a regular menstrual cycle were tested during the onset of menses and the early follicular phase (days 1 to 5) and participants on the oral contraceptive pill were tested during their withdrawal bleed (Elliott-Sale et al., 2021). Menstrual subphase identification was completed by a forward counting self-report method (Allen et al., 2016). Participants were instructed to refrain from consuming alcohol and from undertaking exhaustive exercise within 24 h of visiting the laboratory. Participants were familiarised with the experimental procedures and screened for vascular abnormalities before completing the experimental trials. Each experimental trial was completed at the same time of

day and participants were instructed to match their diet and supplement intake, and prohibited from consuming caffeinated beverages, on the day of the trial.

Experimental Design

This study followed a single-blind, repeated-measures, counterbalanced crossover design with each participant completing two experimental trials; a high visual input trial (lights on – eyes open) and low visual input trial (lights off – eyes closed).

The two experimental trials were completed in two experimental conditions also in a single-blind, repeated-measures, counterbalanced crossover design consisting of a 60 min exposure to either normoxia (fraction of inspired oxygen [FiO_2] = 20.9%) or poikilocapnic hypoxia (FiO_2 = 12.5%) in a temperature [25.6 (0.8) °C] and humidity [30.3 (5.0) %] controlled environmental chamber (Hypoxico Inc, New York, USA) separated by at least 48 h.

Experimental Measurements

Room illuminance

Laboratory illuminance was determined at eye level from a handheld light meter (RS-92, RS Components Ltd., Northamptonshire, UK).

Cardiorespiratory

Peripheral arterial oxygen saturation was measured via pulse oximetry (SpO_2 ; Model 7500 Oximeter; Nonin Medical Inc. Minnesota, USA). Beat-to-beat heart rate was measured with a Lead II electrocardiogram and blood pressure was measured by finger photoplethysmography (Finometer Midi, Finapres Medical Systems, Netherlands). Measurements of systolic blood pressure, diastolic blood pressure and mean arterial pressure (MAP) were calculated from the finger arterial waveform that was calibrated to the average of three automated brachial blood pressure measurements (Tango+, SunTech, Morrisville, NC, USA). The partial pressure of

end-tidal oxygen ($P_{ET}O_2$) and partial pressure of end-tidal carbon dioxide ($P_{ET}CO_2$) were recorded breath-by-breath from the mouth using a gas analyser (ML206, ADInstruments, Colorado, CO).

Extracranial arteries

Blood flow of the ICA and VA were collected using duplex ultrasound with a 15 MHz linear transducer at 30 Hz (uSmart 3300, Terason, Burlington, MA, USA). High-resolution images of vessel diameter were acquired using B-mode imaging whilst pulse wave mode was used to simultaneously measure the Doppler velocity spectra. Care was taken to ensure the strongest Doppler velocity spectrum signal was recorded by positioning the Doppler gate in the centre of the artery with a 60° angle of insonation and adjusting to fill the artery lumen as per recommended technical guidelines (Thomas et al., 2015). The ICA was measured at least 1.0–1.5 cm distal to the carotid bifurcation and the VA was measured between C3 and the subclavian artery. The location was chosen based on the position that was most reproducible within each individual and this position was repeated between trials. Pairs of MCA and ICA, and PCA and VA were measured on the same side of the participant as determined by the most reliable and reproducible signals.

Intracranial arteries

Blood velocity of the MCA and PCA were measured by transcranial Doppler ultrasound (TCD) using two 2 MHz probes placed over the left and right transtemporal windows and secured in place via an adjustable headpiece (PMD150, Spencer Technologies, Seattle, WA, USA). Insonation of each artery was achieved using standardised procedures (Willie et al., 2011), with probe position, signal depth and gain settings recorded to replicate the placement during trials. All participant measurements were collected by the same operator (ATF).

In two separate day-to-day reproducibility studies (each N = 5) completed by the same operator (ATF), the coefficient of variation for duplex ultrasound assessments of blood flow, vessel diameter, and blood velocity of the ICA (4%, 1%, and 3%) and VA (8%, 1%, and 7%) and TCD blood velocity assessments of the MCA (3%) and PCA (3%) were comparable with recommended guidelines (Thomas et al., 2015).

Experimental Procedures

Participants completed an initial TCD instrumentation breathing normal room air outside of the environmental chamber. On entry to the chamber, participants were seated comfortably instrumented with the remaining measures, and rested for 15 min. In a randomised counter-balanced order, participants were then instructed to rest quietly and minimise movement for a two 10 min periods, once with their eyes closed and laboratory lights turned off (low visual input), and once with their eyes open and laboratory lights switched on (high visual input), whilst resting cardiorespiratory and TCD measurements were collected for the assessment spontaneous dCA. Resting duplex ultrasound measurements of the ICA and VA were collected immediately after each 10 min period.

Data Processing

Measurements of blood velocity of the MCA and PCA, heart rate, MAP, SpO₂, PETO₂ and PETCO₂ were all acquired continuously at 1 kHz using an analog-to-digital converter (Powerlab 16/30; ADInstruments) and interfaced on a computer in real time using LabChart software (LabChart 8, ADInstruments). Real time beat-to-beat mean value of MAP and time-averaged maximum values of blood velocity of the MCA or PCA were determined from each R-R interval.

All Duplex ultrasound data were captured and stored for subsequent offline analysis by an investigator blinded to the condition of the experimental trials. Concurrent measurements of

vessel diameter and time-averaged maximum velocity (TAMx) were acquired using an automated edge-detection tracking software (Brachial Analyser, Vascular Research Tools 6, Medical Imaging Applications, Coralville, IA, USA). Subsequently, extracranial blood flow was calculated using the following equation:

$$\text{Blood flow (ml}\cdot\text{min}^{-1}) = [\text{TAMx (cm}\cdot\text{s}^{-1})/2] \times [\pi \times (\text{mean vessel diameter (cm)/2})^2] \times 60$$

Data Analysis

Continuous beat-to-beat resting blood velocity of the MCA and PCA, heart rate, MAP, SpO₂ and PETCO₂ were calculated from a five-minute average during the period of spontaneous dCA measurement. Resting beat-to-beat ICA and VA blood flow were averaged from a 30s period.

Transfer function analysis

Spontaneous cerebral autoregulation during rest was analysed using Ensemble (Version 1.0.0.14, Elucimed, Wellington, New Zealand). In accordance with the recommendations of the Cerebral Autoregulation Research Network (CARNet) 500 s of beat-to-beat blood pressure and blood velocity of the MCA or PCA data were resampled at 4 Hz for spectral and transfer function analysis based on the Welch method (Panerai et al., 2023). This involved subdividing each data epoch into nine successive 100 s window segments that overlapped by 50%. Each window segment was linearly detrended and passed through a Hanning window for linear transfer function analysis. Incidents of phase wrap-around were excluded from the analysis. In this study, MAP and blood velocity of the MCA or PCA power spectrum density, and the mean values of transfer function analysis coherence, phase (radians), absolute gain (cm s⁻¹/mmHg), and normalized gain (%/mmHg) were calculated across the very low (0.02–0.07 Hz), low (0.07–0.2 Hz) and high (0.2–0.5 Hz) frequency ranges, where the corresponding coherence reached the a-priori defined 95% statistical significance level (coherence > 0.42).

Statistical Analysis

No sample size estimation was completed for this chapter as the data presented here was part of a larger study that investigated differences in dCA between the internal carotid and vertebral arteries (Chapter 5). Statistical analysis was conducted using SPSS Statistics v27 (IBM Corp., Armonk, NY, USA) and figures were created in GraphPad Prism (GraphPad Prism 9, San Diego, CA, USA). All analysis was completed using linear mixed models. To confirm that acute poikilocapnic hypoxia exposure was achieved, absolute values of cardiorespiratory and cerebrovascular variables at rest were analysed with fixed effects of visual input (low and high) and condition (normoxia and hypoxia), adding participant as a random effect, with the main effect of condition the primary outcome effect of interest. Absolute values of cardiorespiratory and cerebrovascular variables at rest and metrics from transfer function analysis in normoxia and hypoxia were analysed by a linear mixed model with visual input and, were appropriate for cerebrovascular variables, the interaction with region (anterior and posterior), adding participant as a random effect. To better examine regional differences in cerebrovascular variables at rest with high or low visual input in normoxia and hypoxia by accounting for differences in baseline values, the relative change values (from low visual input to high visual input) of cerebrovascular variables were analysed with region the fixed effect of interest, adding the participant as a random effect. Sex and P_{ETCO_2} was also added to each linear mixed model as a fixed effect of interest and each additive model fit was compared to the original model using the Chi-square likelihood ratio test. Raw data are mean (standard deviation) unless otherwise stated and statistical significance was set at $P < 0.05$. Bonferroni corrected-multiple pairwise comparisons were conducted when significant main effects or interactions were detected. Values from linear mixed model pairwise comparison analysis are reported as estimated marginal means and an estimated standard deviation that was derived from the standard error, where n is the sample size (estimated standard deviation = standard error $\times \sqrt{n}$)

(Friend et al., 2021; Shenouda et al., 2017). Given the potential for uneven group sizes where the coherence threshold was not reached, values from linear mixed model pairwise comparison analysis are reported as estimated marginal means and an estimated standard deviation and differ from the raw data.

6.4 Results

Ambient laboratory light was greater in high compared to low visual input

Laboratory luminance measured at eye-level was greater with high visual input compared to low visual input in both normoxia [Low, 11.1 (17.6) and High, 366.1 (75.1), $P < 0.001$] and hypoxia [Low, 18.0 (23.0) and High, 361.0 (72.6), $P < 0.001$].

Visual stimulation elicited an attenuated reduction in intracranial posterior cerebral blood velocity compared to the anterior circulation in normoxia

Heart rate, systolic blood pressure, diastolic blood pressure, MAP, SpO₂ were not influenced by visual stimulation in normoxia (all $P > 0.05$, Table 6.1). P_{ET}O₂ was increased [estimated marginal mean (estimated standard deviation); +5.6 (5.8) mmHg, $P < 0.01$], and P_{ET}CO₂ was decreased [-2.9 (2.8) mmHg, $P < 0.001$] in high compared to low visual input.

In the intracranial arteries, changing from a low to high visual input reduced blood velocity of the MCA and the PCA; however, the reduction was attenuated in the PCA [MCA, -5.2 (8.1) % and PCA, -2.6 (7.6) %, $P = 0.02$, Figure 6.1a]. In the extracranial arteries, there was a statistical trend for the relative change from low to high visual input in blood velocity [VA, +5.9 (15.3) % and ICA, -2.4 (13.7) %, $P = 0.08$, Figure 6.1b]. In contrast, vessel diameter ($P = 0.23$, Figure 6.1c), and blood flow ($P = 0.31$, Figure 6.1d) changes from low to high visual input were regionally comparable in the ICA and VA. The addition of P_{ET}CO₂ or sex either did not improve the model fit or, whilst may have improved the model fit, did not unveil a regional

difference in cerebrovascular blood flow regulation between the anterior and posterior regions from low to high visual input.

Visual stimulation in normoxia reduced dynamic cerebral autoregulation to spontaneous oscillation in blood pressure in the intracranial posterior but not the anterior circulation

The number of data sets that exceeded the required coherence value of 0.42 for the MCA and PCA were between 7 – 14 in the VLF range, 17 – 18 in the LF range, and 4 – 8 in the HF range (Table 6.2). Reduced posterior dCA was indicated by a visual input x region interaction modelled with P_{ETCO_2} that revealed VLF phase of the PCA was reduced in high compared to low visual input [estimated marginal mean (estimated standard deviation); High, 1.00 (0.23) radians, N = 9 and Low, 1.24 (0.28) radians, N = 12, $P < 0.01$, Figure 6.2] whereas, VLF phase of the MCA was unchanged between high and low visual input [High, 1.25 (0.23) rad, N = 7 and Low, 1.22 (0.28) rad, N = 14, $P = 0.72$], which is indicative of no change in anterior dCA. VLF phase of the PCA in high visual input was also lower than VLF phase of the MCA in either low or high visual input ($P < 0.01$), thus revealing a reduced dCA. There was no interaction (visual input x region) effect for LF or HF transfer function metrics. The addition of P_{ETCO_2} or sex did not improve the model fit or unveil a regional difference in regulation from low to high visual input.

	Low visual input	High visual input
Cardiorespiratory		
SpO ₂ (%) *	96.2 (1.2)	96.6 (1.2)
Heart rate (bpm)	67.1 (6.9)	69.4 (7.7)
Systolic blood pressure (mmHg)	114.6 (13.5)	115.7 (12.9)
Diastolic blood pressure (mmHg)	67.5 (10.0)	68.5 (6.9)
Mean arterial pressure (mmHg)	83.2 (9.4)	84.2 (6.5)
P _{ET} O ₂ (mmHg) *	106.2 (6.8)	112.3 (8.1)
P _{ET} CO ₂ (mmHg) *	38.5 (4.3)	35.4 (5.4)
Intracranial blood velocity (cm·s ⁻¹) †		
Middle cerebral artery	53.7 (14.1)	50.4 (11.9)
Posterior cerebral artery	39.9 (8.7)	38.6 (7.8)
Extracranial blood flow (ml·min ⁻¹) †		
Internal carotid artery	265.0 (62.8)	251.7 (56.1)
Vertebral artery	92.3 (42.2)	96.3 (41.5)
Extracranial vessel diameter (mm) †		
Internal carotid artery	5.17 (0.76)	5.13 (0.75)
Vertebral artery	3.65 (0.63)	3.63 (0.63)
Extracranial blood velocity (cm·s ⁻¹) †		
Internal carotid artery	42.5 (8.3)	41.6 (10.3)
Vertebral artery	27.7 (6.4)	29.5 (6.7)

Table 6.1. Cardiorespiratory and cerebrovascular responses to low (lights off – eyes closed) and high (lights on – eyes open) visual input in normoxia (fraction of inspired oxygen = 20.9%). Data were analysed by a linear mixed model analysis. The primary outcome of interest for cardiorespiratory variables was the effect of visual input (low and high). The primary outcome of interest for cerebrovascular variables was the effect of interaction of visual input and region (anterior and posterior) with the intracranial (middle cerebral artery and posterior cerebral artery) or extracranial arteries (internal carotid artery and vertebral artery). There was no interaction effect between condition and region for any intracranial or extracranial cerebrovascular variable (all $P > 0.05$). * Main effect of condition ($P < 0.05$) † Main effect of region ($P < 0.05$). Additional fixed effects of interest (e.g., sex or P_{ETCO_2}) did not change the statistical outcome for any other variable. Abbreviations: P_{ETCO_2} , partial pressure of end tidal carbon dioxide; P_{ETO_2} , partial pressure of end tidal oxygen; S_pO_2 , peripheral oxygen saturation. Values are raw data means (standard deviation).

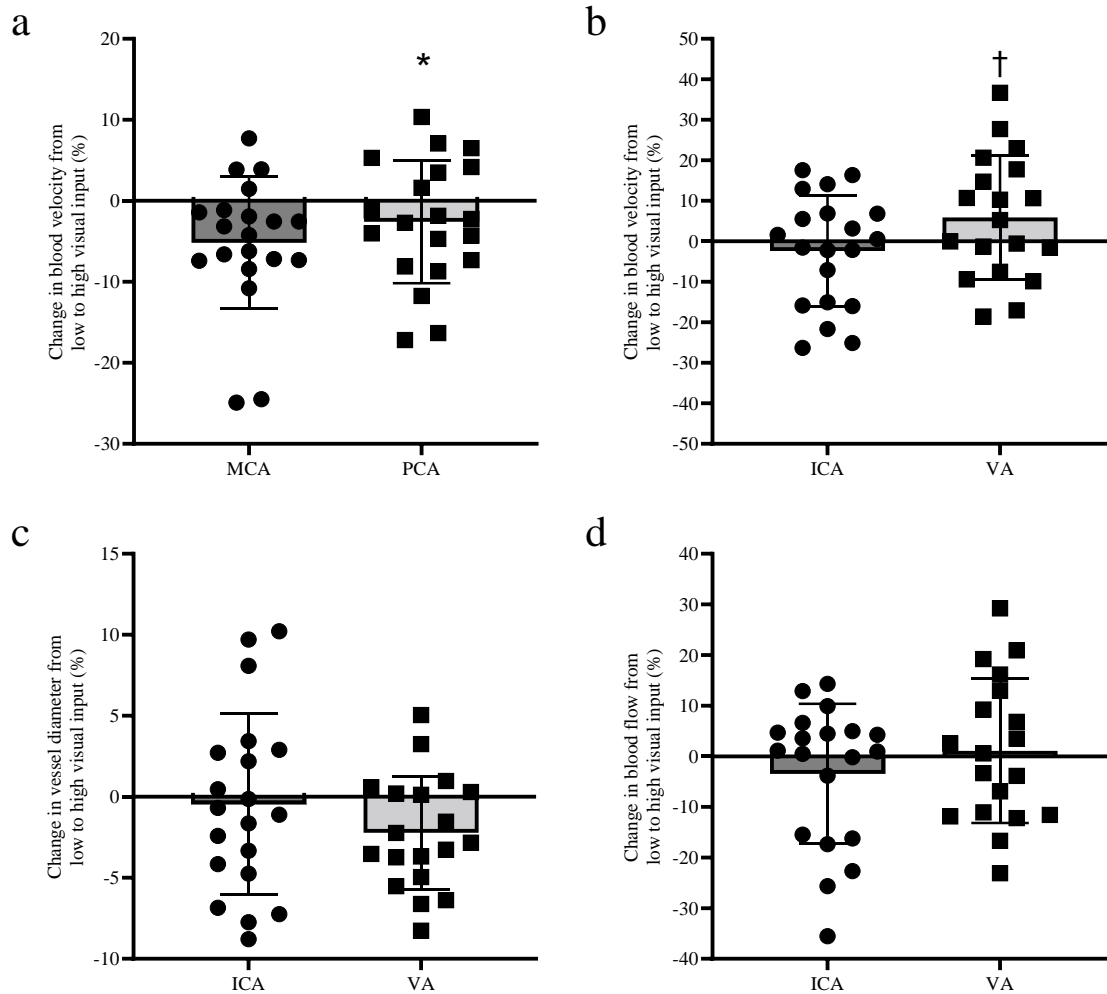


Figure 6.1. Cerebrovascular response from low to high visual input in the intracranial and extracranial arteries in normoxia. Relative change from low (lights off – eyes closed) to high (lights on – eyes open) visual input in blood velocity (a, $P = 0.02$) of the middle cerebral artery (MCA) and posterior cerebral artery (PCA), and blood velocity (b, $P = 0.08$), vessel diameter (c, $P = 0.23$), and blood flow (d, $P = 0.31$) of the internal carotid artery (ICA) and vertebral artery (VA) in normoxia (fraction of inspired oxygen = 20.9%). Variables were analysed by a linear mixed model analysis with the primary outcome of interest was the effect of region, adding participant as random effect. Additional fixed effects of interest (e.g., sex or P_{ETCO_2}) did not change the statistical outcome for any other variable. Data are raw data means (standard deviation) with individual data points. * $P < 0.05$ between regions. † $P < 0.08$ between regions.

	Middle cerebral artery		Posterior cerebral artery	
	Low visual input	High visual input	Low visual input	High visual input
Very low frequency (0.02–0.07 Hz)	(N = 14)		(N = 12)	
MAP power (mmHg ² /Hz) *	19.79 (18.96)	14.25 (10.19)	21.39 (20.04)	22.69 (23.49)
CBv power ([cm/s] ² /Hz)	9.76 (8.18)	5.86 (5.47)	8.17 (9.02)	5.47 (4.27)
Coherence (Index) *	0.57 (0.12)	0.54 (0.07)	0.60 (0.09)	0.51 (0.07)
Phase (radians) a	1.15 (0.31) ‡	1.43 (0.28)	1.18 (0.31)	1.13 (0.37)
Gain (cm/s/mmHg) *	0.74 (0.46)	0.59 (0.22)	0.62 (0.41)	0.50 (0.24)
nGain (%/mmHg)	1.29 (0.52)	1.07 (0.38)	1.44 (0.63)	1.23 (0.68)
Low frequency (0.07–0.2 Hz)	(N = 18)		(N = 18)	
MAP power (mmHg ² /Hz) b	18.98 (25.40)	19.08 (22.08)	18.98 (25.40)	19.19 (22.80)
CBv power ([cm/s] ² /Hz) †	7.14 (3.81)	6.01 (3.81)	4.61 (2.47)	4.89 (4.08)
Coherence (Index)	0.71 (0.14)	0.70 (0.12)	0.70 (0.14)	0.70 (0.10)
Phase (radians)	1.47 (0.24)	1.51 (0.20)	1.52 (0.25)	1.51 (0.18)
Gain (cm/s/mmHg) †	0.76 (0.35)	0.66 (0.25)	0.61 (0.30)	0.57 (0.23)
nGain (%/mmHg)	1.40 (0.61)	1.32 (0.49)	1.49 (0.63)	1.49 (0.57)
High frequency (0.2–0.5 Hz)	(N = 5)		(N = 4)	
MAP power (mmHg ² /Hz)	2.08 (1.60)	2.20 (1.59)	0.97 (0.56)	2.33 (1.60)
CBv power ([cm/s] ² /Hz) c	2.22 (1.93)	2.80 (2.14)	1.29 (1.59)	1.81 (1.29)
Coherence (Index) *†	0.58 (0.12)	0.53 (0.10)	0.55 (0.12)	0.50 (0.09)
Phase (radians)	1.52 (0.21)	1.53 (0.27)	1.56 (0.09)	1.61 (0.30)
Gain (cm/s/mmHg) b c	0.99 (0.37)	1.05 (0.47)	0.91 (0.37)	0.79 (0.30)
nGain (%/mmHg) b	2.06 (0.76)	2.12 (0.67)	2.46 (0.94)	2.07 (0.69)

Table 6.2. Transfer function analysis of the intracranial arteries during spontaneous oscillations in blood pressure in low (lights off – eyes closed) and high (lights on – eyes open) visual input in normoxia. Transfer function metrics of the middle cerebral artery and posterior cerebral artery at very low (0.02–0.07 Hz), low (0.07–0.2 Hz), and high (0.2–0.5 Hz) frequencies were collected during a period of seated rest with low and high visual input in normoxia (fraction of inspired oxygen = 20.9%). To accommodate for uneven group sizes, data were analysed by a linear mixed model analysis. The primary outcome of interest was the interaction effect of visual input (low and high) and region (middle cerebral artery and posterior cerebral artery), adding participant as random effect. Partial pressure of end-tidal carbon dioxide (P_{ETCO_2}) at rest was also added into the model as a covariate for each variable and model fits were compared using the Chi-square likelihood ratio test. The model which had the best fit is reported for each variable. * Main effect of visual input ($P < 0.05$). † Main effect of region ($P < 0.05$). ^a Interaction effect when modelled with P_{ETCO_2} ($P < 0.05$). ^b Main effect of visual input when modelled with P_{ETCO_2} ($P < 0.05$). ^c Main effect of region when modelled with P_{ETCO_2} ($P < 0.05$). Additional fixed effects of interest (e.g., sex or P_{ETCO_2}) did not change the statistical outcome for any other variable. Abbreviations: CBV, cerebral blood velocity; MAP, mean arterial pressure; nGain, normalised gain. Values are raw data means (standard deviation).

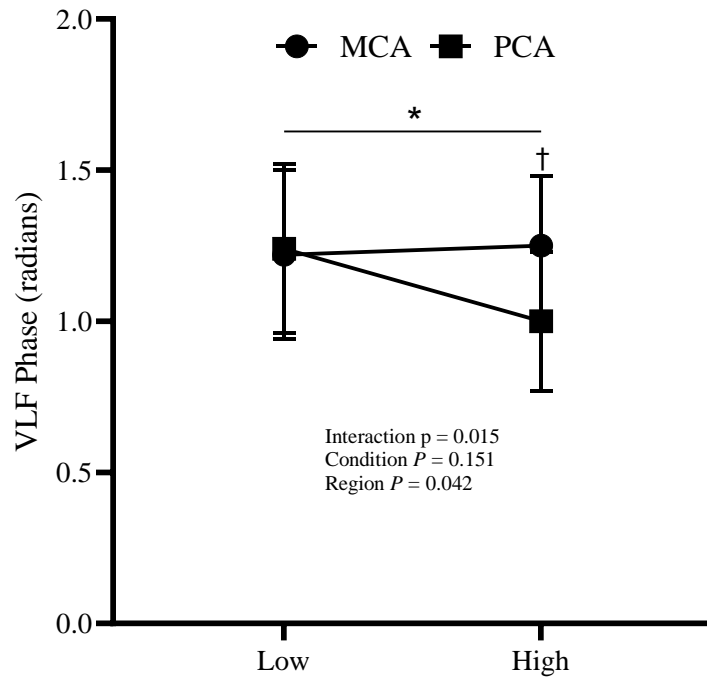


Figure 6.2. Visual stimulation in normoxia reduced dynamic cerebral autoregulation in the posterior but not anterior circulation. Very low frequency (VLF) phase of blood velocity in the middle cerebral artery (MCA) and posterior cerebral artery (PCA) during spontaneous oscillations in blood pressure at rest in low (lights off – eyes closed) to high (lights on – eyes open) visual input in normoxia (fraction of inspired oxygen = 20.9%). Variables were analysed by a linear mixed model analysis with the primary outcome of interest the interaction effect of visual input (low and high) and region (MCA and PCA), adding participant as random effect and partial pressure of end-tidal carbon dioxide (P_{ETCO_2}) at rest since it that improved the model fit using the Chi-square likelihood ratio test. Data are presented as estimated marginal mean (estimated standard deviation). * $P < 0.05$ between low and high visual input for PCA. † $P < 0.05$ between region.

Cardiorespiratory and cerebrovascular responses to acute poikilocapnic hypoxia

Irrespective of visual stimulation (i.e., main effect of condition), hypoxia elicited reductions in S_pO_2 [estimated marginal mean (estimated standard deviation); -14.3 (2.3) %], $P_{ET}O_2$ [-58.1 (3.7) mmHg], and diastolic blood pressure [-3.9 (5.4) mmHg], and increased heart rate [$+7.1$ (4.4) bpm] and systolic blood pressure [$+3.4$ (6.4) mmHg] (all $P < 0.05$), but MAP was unchanged [-1.5 (4.2) mmHg, $P = 0.114$]. Poikilocapnia was confirmed as $P_{ET}CO_2$ was reduced in hypoxia [-1.2 (2.0) mmHg, $P < 0.05$]. Acute poikilocapnic hypoxia did not induce acute mountain sickness (Appendix 5.2).

Acute poikilocapnic hypoxia increased (all $P < 0.05$) blood velocity of the intracranial arteries [MCA, $+3.1$ (5.1) $cm \cdot s^{-1}$ and PCA, $+3.4$ (3.3) $cm \cdot s^{-1}$], and extracranial vessel diameter [VA, $+0.21$ (0.11) mm and ICA, $+0.31$ (0.21) mm] and blood flow [VA, $+12.5$ (11.6) $ml \cdot min^{-1}$ and ICA, $+30.5$ (33.4) $ml \cdot min^{-1}$]. Compared to normoxia, hypoxia decreased VLF and LF phase of the MCA and PCA intracranial arteries, indicating a reduction in dCA, and decreased VLF and LF normalised gain (all $P < 0.05$), which is indicative of increased dCA.

Visual stimulation increased blood velocity in the posterior circulation but not the anterior circulation in acute poikilocapnic hypoxia

$P_{ET}O_2$, $P_{ET}CO_2$, diastolic blood pressure, S_pO_2 were not influenced by visual stimulation in hypoxia (all $P > 0.05$, Table 6.1). Systolic blood pressure [estimated marginal mean (estimated standard deviation); -4.5 (8.4) mmHg, $P < 0.05$], MAP [-3.2 (6.4) mmHg, $P < 0.05$], and heart rate [-1.9 (4.1) bpm, $P < 0.05$] decreased from low to high visual input.

In acute poikilocapnic hypoxia, the increase in blood velocity of the PCA from low to high visual input was greater compared to the MCA [PCA, $+6.3$ (10.5) % and MCA, $+1.5$ (8.5) %; $P < 0.05$, Figure 6.3a]. The greater increase from low to high visual input in posterior blood velocity was consistent in the extracranial arteries, with the increase in blood velocity of the

VA greater compared to the ICA [VA, +8.9 (15.0) % and ICA, +0.2 (10.5) %; $P < 0.05$, Figure 3b]. The addition of sex as a fixed factor to this variable improved the model fit and unveiled that this regional difference was present in men only [Men; ICA, -1.7 (11.3) % and VA +13.5 (14.8) %, $P < 0.05$, Women; ICA, +4.7 (7.4) % and VA, -1.1 (10.2) %, $P = 0.39$]. In addition, extracranial blood flow response to visual stimulation tended to be greater in the VA than ICA [VA +6.6 (14.5) % and ICA, -1.7 (14.3) %, $P = 0.08$, Figure 6.3d], whereas vessel diameter response was regionally comparable [$P = 0.98$, Figure 6.3c]. The addition of P_{ETCO_2} or sex to blood flow or vessel diameter did not improve the model fit or unveil a regional difference in regulation from low to high visual input.

No influence of visual stimulation on regional dynamic cerebral autoregulation to spontaneous oscillation in blood pressure in acute poikilocapnic hypoxia

The number of data sets that exceeded the required coherence value of 0.42 for the MCA and PCA were between 11 – 17 in the VLF range, 16 – 19 in the LF range, and 4 – 5 in the HF range (Table 6.4). There was no visual input x region interaction effect for any VLF, LF, or HF transfer function metrics, with or without the addition of P_{ETCO_2} or sex (in the LF range only) as an additional fixed factor.

	Low visual input	High visual input
Cardiorespiratory		
SpO ₂ (%)	82.0 (4.1)	82.6 (4.7)
Heart rate (beats per min) *	76.3 (9.8)	74.4 (10.4)
Systolic blood pressure (mmHg)	120.8 (16.6)	116.3 (14.0)
Diastolic blood pressure (mmHg)	65.4 (8.6)	62.8 (11.4)
Mean arterial pressure (mmHg) *	83.8 (9.7)	80.6 (10.5)
P _{ET} O ₂ (mmHg)	50.7 (4.6)	51.2 (6.5)
P _{ET} CO ₂ (mmHg)	36.0 (3.1)	35.5 (3.3)
Intracranial blood velocity (cm·s ⁻¹) †		
Middle cerebral artery	55.3 (13.9)	56.2 (15.2)
Posterior cerebral artery	41.8 (11.3)	43.6 (11.1)
Extracranial blood flow (ml·min ⁻¹) †		
Internal carotid artery	291.3 (63.2)	286.5 (75.6)
Vertebral artery	101.5 (43.4)	112.1 (45.3)
Extracranial vessel diameter (mm) †		
Internal carotid artery	5.50 (0.62)	5.43 (0.61)
Vertebral artery	3.83 (0.71)	3.85 (0.61)
Extracranial blood velocity (cm·s ⁻¹) †		
Internal carotid artery	41.2 (8.0)	41.3 (9.2)
Vertebral artery	28.2 (5.5)	31.0 (6.8)

Table 6.3. Cardiorespiratory and cerebrovascular responses to low (lights off – eyes closed) and high (lights on – eyes open) visual input in acute poikilocapnic hypoxia (fraction of inspired oxygen = 12.5%). Data were analysed by a linear mixed model analysis. The primary outcome of interest for cardiorespiratory variables was the effect of visual input (low and high). The primary outcome of interest for cerebrovascular variables was the effect of interaction of visual input and region (anterior and posterior) with the intracranial (middle cerebral artery and posterior cerebral artery) or extracranial arteries (internal carotid artery and vertebral artery). There was no interaction effect between condition and region for any intracranial or extracranial cerebrovascular variable (all $P > 0.05$). * Main effect of condition ($P < 0.05$) † Main effect of region ($P < 0.05$). Additional fixed effects of interest (e.g., sex or P_{ETCO_2}) did not change the statistical outcome for any other variable. Abbreviations: P_{ETCO_2} , partial pressure of end tidal carbon dioxide; P_{ETO_2} , partial pressure of end tidal oxygen; S_pO_2 , peripheral oxygen saturation. Values are raw data means (standard deviation).

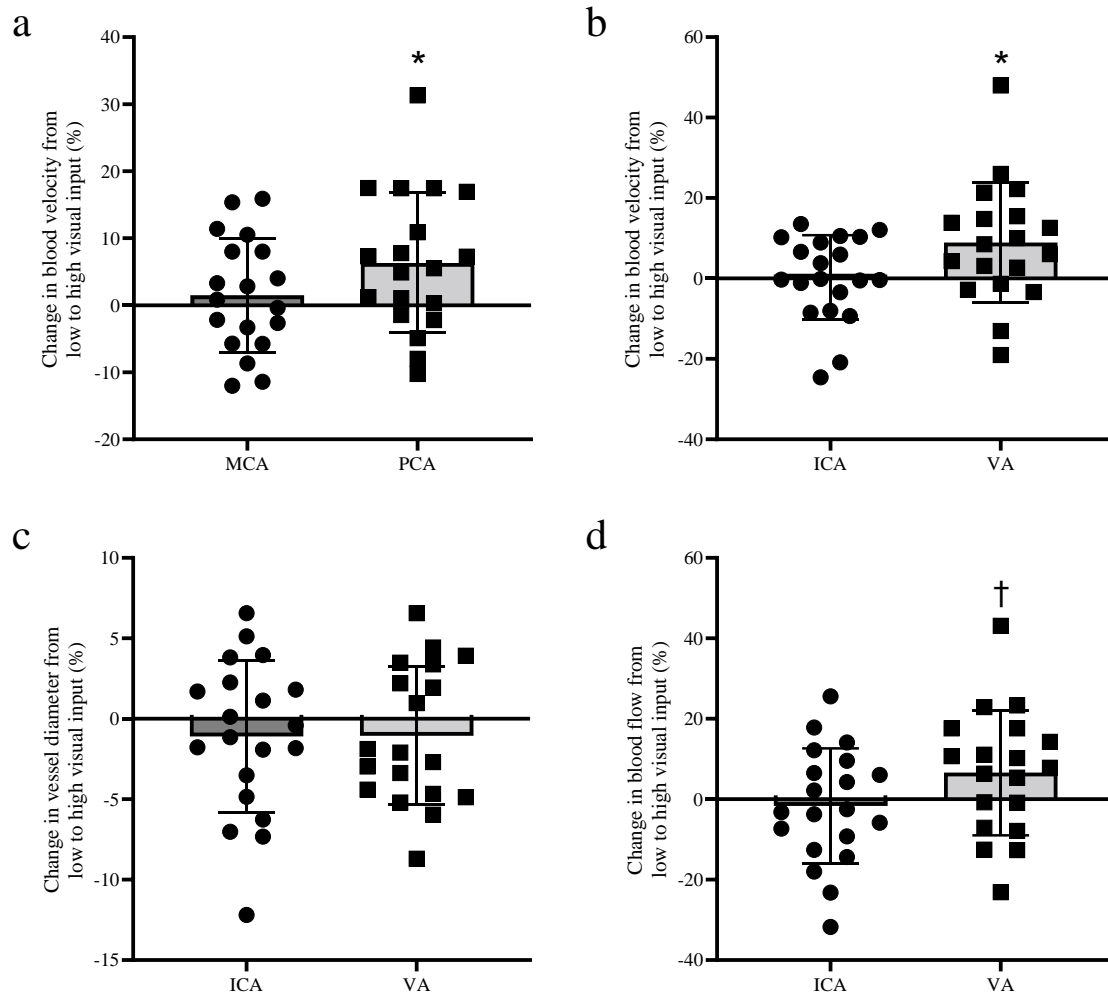


Figure 6.3. Cerebrovascular response from low to high visual input in the intracranial and extracranial arteries in acute hypoxia. Relative change from low (lights off – eyes closed) to high (lights on – eyes open) visual input in blood velocity (a, $P < 0.05$) of the middle cerebral artery (MCA) and posterior cerebral artery (PCA), and blood velocity (b, $P < 0.05$), vessel diameter (c, $P = 0.98$), and blood flow (d, $P = 0.08$) of the internal carotid artery (ICA) and vertebral artery (VA) in normoxia (fraction of inspired oxygen = 20.9%). Variables were analysed by a linear mixed model analysis with the primary outcome of interest was the effect of region, adding participant as random effect. The addition of sex as a fixed factor to the change in blood velocity of the extracranial arteries improved the model fit and revealed that this regional difference was present in men only [Men; ICA, -1.7 (11.3) % and VA, 13.5 (14.8) %, $P < 0.05$, Women; ICA, 4.7 (7.4) % and VA, -1.1 (10.2) %, $P = 0.39$]. Data are raw data means (standard deviation) with individual data points. * $P < 0.05$ between regions. † $P < 0.08$ between region.

	Middle cerebral artery		Posterior cerebral artery	
	Low visual input	High visual input	Low visual input	High visual input
Very low frequency (0.02–0.07 Hz)	<i>(N = 13)</i>		<i>(N = 11)</i>	
MAP power (mmHg ² /Hz) b	35.11 (29.42)	37.79 (36.33)	31.66 (27.05)	40.79 (35.88)
CBv power ([cm/s] ² /Hz) c	14.70 (9.84)	17.21 (17.39)	8.17 (7.48)	13.15 (11.49)
Coherence (Index)	0.58 (0.11)	0.58 (0.12)	0.58 (0.10)	0.57 (0.10)
Phase (radians)	0.74 (0.26)	0.86 (0.35)	0.91 (0.33)	0.82 (0.41)
Gain (cm/s/mmHg) †	0.60 (0.31)	0.60 (0.30)	0.45 (0.25)	0.52 (0.30)
nGain (%/mmHg)	0.96 (0.36)	1.07 (0.40)	1.00 (0.33)	1.07 (0.45)
Low frequency (0.07–0.2 Hz)	<i>(N = 17)</i>		<i>(N = 16)</i>	
MAP power (mmHg ² /Hz)	25.97 (25.11)	25.23 (21.51)	27.15 (25.44)	24.22 (21.66)
CBv power ([cm/s] ² /Hz)	10.67 (10.32)	11.04 (18.12)	6.90 (7.14)	10.08 (14.98)
Coherence (Index)	0.66 (0.13)	0.64 (0.14)	0.65 (0.13)	0.64 (0.12)
Phase (radians)	1.31 (0.26)	1.35 (0.27)	1.40 (0.30)	1.36 (0.33)
Gain (cm/s/mmHg)	0.65 (0.34)	0.62 (0.29)	0.55 (0.33)	0.61 (0.30)
nGain (%/mmHg)	1.14 (0.46)	1.15 (0.50)	1.23 (0.50)	1.30 (0.51)
High frequency (0.2–0.5 Hz)	<i>(N = 5)</i>		<i>(N = 5)</i>	
MAP power (mmHg ² /Hz)	3.40 (3.05)	1.68 (1.31)	2.86 (3.28)	2.12 (1.36)
CBv power ([cm/s] ² /Hz)	3.23 (1.89)	2.14 (1.12)	2.09 (1.65)	2.33 (1.25)
Coherence (Index)	0.52 (0.12)	0.53 (0.09)	0.51 (0.07)	0.49 (0.02)
Phase (radians) *	1.46 (0.29)	1.59 (0.41)	1.39 (0.21)	1.61 (0.16)
Gain (cm/s/mmHg)	0.89 (0.15)	1.07 (0.57)	0.81 (0.36)	1.12 (0.74)
nGain (%/mmHg)	1.75 (0.38)	2.15 (1.05)	1.81 (0.58)	2.21 (1.05)

Table 6.4. Transfer function analysis of the intracranial arteries during spontaneous oscillations in blood pressure in low (lights off – eyes closed) and high (lights on – eyes open) visual input in acute poikilocapnic hypoxia. Transfer function metrics of the middle cerebral artery and posterior cerebral artery at very low (0.02–0.07 Hz), low (0.07–0.2 Hz), and high (0.2–0.5 Hz) frequencies were collected during a period of seated rest with low and high visual input in acute poikilocapnic hypoxia (fraction of inspired oxygen = 12.5%). To accommodate for uneven group sizes, data were analysed by a linear mixed model analysis with the primary outcome of interest the interaction effect of visual input (low and high) and region (middle cerebral artery and posterior cerebral artery), adding participant as random effect. Partial pressure of end-tidal carbon dioxide (P_{ETCO_2}) at rest was also added into the model as a covariate for each variable and model fits were compared using the Chi-square likelihood ratio test. The model which had the best fit is reported for each variable. * Main effect of visual input ($P < 0.05$). † Main effect of region ($P < 0.05$). ^a Interaction effect when modelled with P_{ETCO_2} ($P < 0.05$). ^b Main effect of visual input when modelled with P_{ETCO_2} ($P < 0.05$). ^c Main effect of region when modelled with P_{ETCO_2} ($P < 0.05$). Additional fixed effects of interest (e.g., sex or P_{ETCO_2}) did not change the statistical outcome for any other variable. Abbreviations: CBV, cerebral blood velocity; MAP, mean arterial pressure; nGain, normalised gain. Values are raw data means (standard deviation).

6.5 Discussion

Main findings

This study aimed to determine the influence of low and high ambient visual input on regional cerebral haemodynamics, vascular tone, and dynamic cerebral autoregulation in normoxia and hypoxia. We report that high visual input compared to low visual input caused a greater intracranial blood velocity and extracranial blood velocity of the posterior circulation compared to anterior circulation in normoxia, whereas extracranial vascular tone was unchanged in both circulations. Furthermore, in normoxia, posterior intracranial dCA to spontaneous oscillations in blood pressure at rest was reduced in high compared to low visual input, whereas visual stimulation did not influence anterior dCA. In hypoxia, visual stimulation elicited a greater blood velocity and blood flow of the posterior intracranial and extracranial circulation compared to the anterior circulation but did not influence extracranial vascular tone or intracranial dCA. These findings suggest reductions in posterior intracranial dCA induced by ambient visual stimulation in normoxia are not mediated by changes in extracranial vascular tone and may indicate that the responsible mechanisms for the regional dCA occur downstream.

Ambient visual stimulation does elicit regional blood velocity and blood flow responses of the intracranial and extracranial cerebral conduit arteries

In agreement with previous studies (Hermes et al., 2007; Matsutomo et al., 2023), we successfully evoked a greater response in blood velocity of the PCA compared to the MCA with high ambient visual input (lights on – eyes open) compared to low ambient visual input (lights off – eyes closed) in normoxia, indicating an increased metabolic state of the visual cortex. Moreover, we demonstrated that this intracranial regional response from low to high ambient visual input occurs in acute poikilocapnic hypoxia, extending previous literature that

has used neurovascular coupling paradigms involving on-off cycles of visual stimuli (Caldwell et al., 2017, 2018; Leacy et al., 2018). We also provide support to previous literature (Samora et al., 2020) that these regional responses occur upstream at the extracranial arteries, with a larger increase in blood velocity of the VA compared to the ICA in normoxia ($P = 0.08$) and, for the first time to the authors knowledge, in blood velocity ($P < 0.05$) and blood flow ($P < 0.08$) of the VA compared to the ICA in hypoxia.

Dynamic cerebral autoregulation of the posterior circulation is reduced with ambient visual stimulation in normoxia but not hypoxia

Here we report that ambient visual stimulation reduced VLF phase of the PCA, but not the MCA, in normoxia, representing a smaller shift in time between blood pressure and blood velocity that results in blood velocity having a greater tendency to follow fluctuations in blood pressure and, therefore, is an indication of a reduced dCA of the PCA (i.e., more pressure-passive) (Claassen et al., 2021). Our findings strengthen the single previous report in normoxia showing reduced posterior dCA, but not anterior dCA, to spontaneous oscillations in blood pressure with eyes open compared to eyes closed (Nakagawa et al., 2009). This previous study reported an increased transfer function gain in the PCA to eyes opens compared to eyes closed (Nakagawa et al., 2009), which also indicates a reduced dCA since it reflects a lower buffering capacity of the posterior circulation to blood pressure fluctuations. Our findings extend these findings as transfer function phase rather than gain has been suggested as the primary criterion for evaluating dCA (Ogoh et al., 2018; R. Zhang et al., 1998). Taken together, these findings indicate that increased metabolic state of the visual cortices with ambient visual stimulation in normoxia does induce a reduction in dCA of the posterior conduit artery (i.e., PCA), possibly reflecting a more localised pressure-passive and vulnerable microcirculation in the posterior regions of the brain.

Acute hypoxia induced vasodilation and reduced intracranial dCA as indicated by reduction in LF phase of MCA and PCA compared to normoxia. However, in contrast to normoxia, visual stimulation did not induce regional differences in dCA for any transfer function metric in hypoxia. It is plausible that acute hypoxia will have drained the vasodilatory reserve of the cerebrovasculature (Horiuchi et al., 2022). That is, the cerebrovasculature was maximally dilated by hypoxia, and therefore any additional negative effects of high visual stimulation (i.e., further reductions in dCA of the PCA) would have been overwhelmed by the global effects of acute hypoxia. However, as visual stimulation did induce a positive regional difference in blood velocity between the MCA and PCA in acute hypoxia, this may suggest that the posterior microcirculation was not maximally dilated and still has a vasodilatory reserve. Therefore, it is somewhat surprising to have not seen any regional differences in MCA and PCA transfer function metrics to spontaneous oscillations in blood pressure, as we did in normoxia in this study, if measurements of the intracranial arteries are reflective of downstream microvasculature haemodynamics. Possible explanations for this inconsistency are that dCA changes in the intracranial arteries are not reflective of downstream vascular bed, and that a localised alteration in vascular tone in the posterior microcirculation is not related to, or are not translated to, the change in dCA at the intracranial arteries, and/or the reduction in dCA of the cerebral conduit arteries was already maximal due to the hypoxia.

Ambient visual stimulation does not modulate regional vascular tone of the extracranial cerebral conduit arteries

In contrast with our hypothesis and recent reports (Samora et al., 2020), visual stimulation did not evoke an increase in VA diameter in normoxia. The presence of an unexpected hypocapnia in response to visual stimulation in normoxia may have modified the cerebrovascular response of the cerebral conduit arteries. Whilst we successfully elicited a regional response between blood velocity of the PCA and MCA to visual stimulation in normoxia, the impact of a

hypocapnia associated cerebral vasoconstriction likely attenuated a positive increase in intracranial blood velocity to visual stimulation and may have also blunted any increase in VA blood flow and vessel diameter. Indeed, hypocapnia is shown to attenuate the NVC response in the posterior circulation (Bader et al., 2021; Szabo et al., 2011). When P_{ETCO_2} is similar between low and high visual input conditions, as occurred in acute hypoxia in this study, the blood velocity of the PCA and VA were positive compared to the MCA and ICA, respectively, and there was a statistical trend for the increase in blood flow of the VA compared to the ICA, supporting previous work that visual stimulation evokes an increase in blood flow of the VA (Samora et al., 2020). Another possible reason for the lack of vessel diameter change in the VA to visual stimulation in this study is that the extracranial arteries are not sensitive with alterations in visual stimulation. It is likely that the cerebrovascular response to visual stimulation at the cerebral conduit arteries is driven by a localised downstream vasodilation of the large- (e.g., PCA) and micro- (e.g., pial arteries) vasculature more proximal to the visual cortices (Bizeau et al., 2018; Masamoto & Vazquez, 2018). Indeed, our findings suggest that modulation of upstream extracranial cerebral conduit artery vascular tone are not responsible for the regional dCA to spontaneous oscillations in blood pressure at rest reported here in normoxia, and therefore other mechanisms induced by visual stimulation primarily determine dCA outcome. Further investigations that control for fluctuation in P_{ETCO_2} are required to fully determine whether, if at all, the extracranial cerebral conduit arteries are vasoactive in response to a visual stimulation induced increase in the metabolic state of the visual cortices, and, in turn, impact dCA.

Comparison between the intracranial and extracranial arteries

Previous reports have shown that the magnitude of VA blood flow response to visual stimulation was smaller than PCA blood velocity response, and this was attributed to the anatomical location of the VA that feeds other branching arteries before the basilar artery and

intracranial branches (i.e., PCA) that source the visual cortices (Samora et al., 2020). Recently, it has been shown that there is a heterogeneous haemodynamic response in the posterior cerebral circulation, with the PCA found to have larger cerebrovascular resistance response and a stronger association to alterations in $P_{ET}CO_2$ than the VA during isometric exercise (Washio et al., 2022). Taken together, and in combination with distinctive subtype, distribution, and density of adrenoceptors between the extracranial and intracranial arteries (Koep et al., 2022), these findings indicate site-specific regulatory mechanisms in the posterior circulation between the PCA and VA. Here, in contrast to reports (Samora et al., 2020), we show that VA blood velocity and VA blood flow had a larger or similar response to PCA blood velocity in normoxia and hypoxia. It is plausible that the increased sensitivity to $P_{ET}CO_2$ in the PCA (Washio et al., 2022), and an unexpected hypocapnia in normoxia in our study, may have caused an attenuated blood velocity response in the PCA compared to VA to visual stimulation.

Methodological considerations

In agreement with previous reports using magnetic resonance imaging (Hermes et al., 2007; Matsutomo et al., 2023), we show that prolonged alterations in ambient laboratory visual stimulation between lights on–eyes open or lights off–eyes closed do evoke a robust metabolic activation of the visual cortices and, furthermore, we extend these reports that this haemodynamic response can be captured in the cerebral conduit arteries by duplex and transcranial Doppler ultrasound. Our findings provide a simple alternative method to the more conventionally used visual stimulation paradigms that involve on-off cycles of a visual stimuli a few centimetres from the face, such as a flashing screen, reading, or eye tracking of a moving object (Phillips et al., 2016; Samora et al., 2020), for inducing a regional difference in the haemodynamic response between the cerebral conduit arteries.

The impact of the metabolic state of the visual cortices with visual stimulation on dCA may contribute to the observations of a reduced dCA in the PCA compared to MCA under normal physiological conditions that are likely to have completed assessments in a laboratory with lights on—eyes open (Haubrich et al., 2004; Sorond et al., 2005). Therefore, our findings extend the recommended guidelines for transfer function analysis of dCA (Claassen et al., 2016; Panerai et al., 2023), by evidencing that the standardised conditions should not only minimise visual disturbances (for example, people entering or leaving a room), but also consider the basal visual stimulation. Such recommendations for a darkened room to minimise visual stimulation are suggested in the standardised assessment of flow-mediated dilation of a conduit artery (Thijssen et al., 2011).

We followed the recommendations of the Cerebral Autoregulation Research Network (CARNet) for transfer function analysis of dCA (Claassen et al., 2016; Panerai et al., 2023) and used the commercially available Ensemble software in our assessment of dCA. To maximise the number of trials that reached the coherence threshold, we increased the duration of recording and number of windows from the conventional 300 s and 5 windows to 500 s and 9 windows. However, whilst this adjustment preserved 80% of our data in the LF range, 65% of data in the VLF range and 80% of the data in HF range were lost and limited our ability for any interpretation in the VLF and HF range. We acknowledge that assessing the relationship between spontaneous oscillations in blood pressure and cerebral blood velocity is beneficial for the translation to clinical populations, however, using driven oscillations in blood pressure, such as sit-to-stand or squat-to-stand, would produce greater coherence values (> 0.99) and would maximize the signal-to-noise ratio of the blood pressure-cerebral haemodynamic relationship and may provide a better model for transfer function analysis of regional dCA to visual stimulation (Burma et al., 2021).

Neurovascular coupling assessments are often measured as a ratio-scaled increase in blood velocity (i.e., relative change). A ratio-scaling problem has been previously reported during assessment of the extracranial arteries blood flow response to hypoxia [Chapter 4 (Friend et al., 2021)], akin to that previously identified with FMD assessment of the brachial artery vascular function (Atkinson et al., 2013; Atkinson & Batterham, 2013a, 2013b), and describes a skewness towards the vessels with smaller values to have the largest and most varied measurement error. Consequently, with the possibility of inter- and intra-individual lateral resting blood velocity differences between pairs of the MCA and PCA, investigation for a ratio-scaling problem in neurovascular coupling assessments is warranted to minimise a mathematical, rather than physiological, source of measurement error.

Upon including sex as an exploratory fixed factor, we found a greater increase in blood velocity in the VA than ICA to hypoxia in men. Whilst we are cautious in our interpretation of our findings in women due to the small sample size ($N = 6$), this may provide some insight and impetus for investigation of the regulation of the extracranial arteries to visual stimulation between men and women, particularly as to date studies examining the influence of sex to cerebral responses to visual stimulation have been limited to the intracranial arteries (Koep et al., 2023; Leacy et al., 2022).

Conclusions

In conclusion, visual stimulation reduced dCA of the PCA, but not the MCA, to spontaneous oscillations in blood pressure at rest in normoxia, whereas there was no regional difference in dCA to visual stimulation in hypoxia. Visual stimulation elicited a greater blood velocity in the PCA and VA compared to the MCA and ICA, but did not reduce extracranial vessel tone, in normoxia and hypoxia, suggesting other mechanisms are responsible for the reduction in dCA of the posterior circulation to visual stimulation in normoxia.

Author contributions and acknowledgments

Authors: Alexander T. Friend, Michiel Ewalts, Masahiro Horiuchi, Gabriella M.K. Rossetti, Aamer Sandoo, Jamie H. Macdonald, and Samuel J. Oliver. AF and SO conceived and designed the study. All authors contributed to the acquisition, analysis, or interpretation of data for the work. AF and SO drafted the manuscript, with all remaining authors reviewing and providing critical feedback important for intellectual content.

We would like to thank the participants for their time and effort in this study. We would like to thank Guto Hughes, Jonathan O'Duffy, Flynn Owen, Ferrida Ponce, and Sophia Wakefield for their contribution to data collection.

Chapter Seven

General discussion

7.1 Summary of main findings

This PhD aimed to investigate regional cerebral conduit artery blood flow regulation in acute poikilocapnic hypoxia. The first study (Chapter 4) found that the bilateral vessel diameter and blood flow response to hypoxia was comparable between the internal carotid artery (ICA) and vertebral artery (VA). This study also provided evidence to recommend that assessing the vessel with the larger resting blood flow, rather than the left or right vessel, reduces unilateral measurement error compared to the bilateral measurement. The second study (Chapter 5) reported a regional difference in dynamic cerebral autoregulation (dCA) in men during hypoxia compared to normoxia. Specifically, VA rate of regulation (RoR) to abrupt reductions in blood pressure in men was reduced in hypoxia, whereas ICA RoR was maintained. There was also evidence which suggested that dCA was not influenced by hypoxia-induced reductions in vascular tone. The third study (Chapter 6) found that ambient visual stimulation does not modulate regional extracranial vascular tone of the cerebral conduit arteries, and therefore is unlikely to explain the reduced intracranial dCA to spontaneous oscillations in blood pressure in the posterior circulation in normoxia. Further, the study extended reports that visual stimulation does induce a regional difference in detectable haemodynamics in the extracranial arteries in normoxia and hypoxia. In conclusion, the findings of this thesis suggest regional differences between the anterior and posterior cerebral conduit arteries exists in dCA in hypoxia and with visual stimulation in normoxia, but not the blood flow response to hypoxia. This thesis also emphasises the importance of capturing vascular tone and volumetric blood flow measurements to fully understand the regional regulation of the cerebral circulation.

7.2 Regional regulation of the cerebral conduit arteries

In this thesis, regional differences between the anterior and posterior cerebral conduit arteries were reported in dCA in hypoxia and with visual stimulation in normoxia, but not blood flow response to hypoxia.

7.2.1 Regional dynamic cerebral autoregulation of the cerebral conduit arteries to acute poikilocapnic hypoxia and with visual stimulation

This thesis provides evidence of heterogeneous dCA between the cerebral conduit arteries that feed the anterior and posterior regions of the brain. In Chapter 5, volumetric dCA to abrupt reductions in blood pressure of the extracranial arteries in hypoxia was reduced (i.e., more pressure-passive) in the VA, but not the ICA, extending the existing literature that has solely investigated dCA to hypoxia in the anterior circulation using volumetric (Horiuchi et al., 2016, 2022; Tymko et al., 2020) or blood velocity measurements (Levine et al., 1999; Ogoh et al., 2010; Subudhi et al., 2009). In Chapter 6, dCA to spontaneous oscillations in blood pressure of the intracranial arteries with ambient visual stimulation in normoxia was reduced in the posterior cerebral artery (PCA), but not middle cerebral artery (MCA), and provides support to, to our knowledge, the only other study which reports of regional dCA to ambient visual stimulation (Nakagawa et al., 2009). The results from Chapter 6 provide a potential mechanism for previously reported regional differences in dCA at rest, since it is likely that these reports were conducted with ambient visual stimulation from laboratory light (Haubrich et al., 2004; Sorond et al., 2005). This thesis provides direct evidence that investigating cerebrovascular regulation (particularly dCA) with a single measurement (e.g., MCA) as a marker of global cerebral haemodynamics is insufficient and that future studies should incorporate measurements that reflect the vasculature that feed both the anterior and posterior regions of the brain.

This results from this thesis are strengthened by the multimodal and multimetric approach to assessing dCA that aligns with recent recommendations of best practice for investigating the cerebral pressure-flow relationship (Brassard et al., 2023). Indeed, the standardised rapid thigh cuff method in Chapter 5 is the best method available to assess dCA to abrupt changes in blood pressure by volumetric blood flow measurements of the extracranial arteries. Pairing upstream extracranial (ICA and VA) volumetric measurements with downstream intracranial (MCA and PCA) blood velocity measurements during the rapid thigh cuff method in hypoxia enabled a comparison between methods of assessing cerebral haemodynamics. The lack of regional difference in dCA to abrupt changes in blood pressure between the intracranial arteries highlights the importance of assessing the cerebrovasculature using vascular tone and volumetric measurements to fully understand regional differences in cerebral blood flow regulation. Since completion of Chapter 5 of this thesis, others have stated that adopting volumetric cerebral blood flow measurements is an important next step to develop the research field of dCA (Brassard et al., 2023). Notwithstanding, the findings in Chapter 6 of a regional difference in dCA to spontaneous oscillations in blood pressure between the MCA and PCA with visual stimulation in normoxia complement the findings in Chapter 5 by providing a measurement of the cerebrovascular regulation downstream of the extracranial arteries. Collectively these Chapters 5 and 6 provide evidence that regional differences in dCA exists between the anterior and posterior circulations;

- 1) at the extracranial and intracranial segments of the cerebrovasculature,
- 2) using both volumetric blood flow and blood velocity measurements, and
- 3) in response to small and large fluctuations in blood pressure, reflecting two distinct points on the autoregulatory curve, i.e., spontaneous oscillations and driven abrupt reductions in blood pressure.

7.2.2 Visual stimulation elicits regional blood velocity and blood flow responses in the cerebral conduit arteries

The findings in Chapter 6 provide evidence of a regional blood velocity and blood flow response in the extra- and intra-cranial arteries to visual stimulation. A regionally greater blood velocity in PCA compared to MCA to ambient visual stimulation reported in Chapter 6 supports the existing literature (Hermes et al., 2007; Matsutomo et al., 2023; Nakagawa et al., 2009) and is akin to those found in studies of neurovascular coupling that modulate neurometabolic activity with cyclical light-on and light-off protocols (Caldwell et al., 2017, 2018; Phillips et al., 2016). Moreover, the findings from Chapter 6 also extends literature showing that this regional difference in haemodynamics to visual stimulation occurs at the level of the extracranial arteries (ICA and VA) and is detectable by duplex ultrasound measurements of blood velocity and blood flow (Samora et al., 2020). Finally, the observation of a regional difference in intracranial blood velocity responses in acute hypoxia despite the hypoxia-induced vasodilation aligns with previous reports of an intact neurovascular coupling response to acute hypoxia (Caldwell et al., 2017, 2018; Leacy et al., 2018).

Despite these visual stimulation-induced changes in blood velocity and blood flow, and in contrast to our proposed mechanistic hypothesis, visual stimulation did not reduce extracranial vessel tone in either normoxia or hypoxia. Therefore, mechanisms other than reductions in extracranial vascular tone likely explain the expected reductions in dCA of PCA, but not MCA, with visual stimulation in normoxia. It can be likely that as there is an increase in blood velocity at the VA and PCA, but not extracranial vessel diameter, the vascular tone reductions in the posterior circulation are likely mediated downstream. Indeed, the data in acute hypoxia from Chapter 6 suggests that the microvasculature still had a capacity to accommodate visual stimulation-induced increases in demand, despite a hypoxia-induced vasodilation of the extracranial conduit arteries. Evidence of segmental modulation of vascular tone throughout

the large- (e.g., PCA) and micro- (e.g., pial arteries) vasculature that is more proximal to the visual cortices has been reported previously (Bizeau et al., 2018; Masamoto & Vazquez, 2018). Curiously, if the posterior microcirculation downstream of the extracranial conduit arteries had been further dilated with visual stimulation in hypoxia (a stressor known to reduce vascular tone), then it might be expected that dCA of the PCA, but not MCA, to be further reduced if vascular tone reductions are related to reduced dCA. The lack of this observation in hypoxia in Chapter 6 suggests reductions of dCA at the intracranial cerebral conduit arteries were already maximal due to the hypoxia and/or are not reflective of microvasculature dCA. Further investigations are required to determine whether resting vascular tone is different between the microvasculature that feed the anterior and posterior regions and how this may explain the differences in dCA observed.

7.2.3 Comparable regional cerebral conduit artery haemodynamics to acute hypoxia

The relatively large cohorts in Chapter 4, 5 and 6, and the bilateral assessment to measure the ‘true’ response in Chapter 4, provides a consistent finding that regulation in vascular tone and volumetric blood flow between the ICA and VA to acute poikilocapnic hypoxia is comparable. This comparable extracranial regulation to acute hypoxia throughout this thesis contrasts the regional difference in extracranial and intracranial dCA reported in Chapters 5 and 6. Whilst the mechanisms underpinning regulation of the cerebrovasculature to alterations in partial pressure of oxygen, visual stimulation, or blood pressure likely work as an integrative system and share functional pathways (Ainslie & Duffin, 2009; Claassen et al., 2021), there may be regional sensitivities to these stimuli as shown in this thesis. Acute hypoxia elicits a large global sustained stimulus to the cerebral circulation, whereas visual stimulation or assessments of dCA elicits localised and/or transient responses to the cerebral circulation. An example of the complexity of these mechanisms was demonstrated in Chapter 6 with the combined assessment

of dCA with visual stimulation in acute hypoxia. Indeed, the observation of a reduced dCA to spontaneous oscillations in blood pressure in the PCA compared to MCA with visual stimulation in normoxia, was not replicated in acute hypoxia. It is likely that any additional negative effects of visual stimulation (i.e., further reductions in dCA of the PCA) were overwhelmed by the global effects of acute hypoxia, possibly as acute hypoxia will have drained the vasodilatory reserve of the cerebrovasculature (Horiuchi et al., 2022). However, this does not explain why in Chapter 5 there was a reduced dCA of the VA, but not ICA, to abrupt reductions in blood pressure to acute hypoxia, and is likely a result of the added complications between methods of quantifying dCA (see 7.5.2).

Summary

The findings from this thesis provide robust empirical evidence of regional differences between the anterior and posterior cerebral conduit arteries in dCA in acute hypoxia and with visual stimulation in normoxia, but not the blood flow response to acute hypoxia. Future studies should investigate the mechanistic underpinning that are producing these regional differences in the cerebral circulation (see section 7.6.2).

7.3 Importance of volumetric flow measures of cerebrovascular regulation

Cerebral arteries are lined with vascular smooth muscle that enables them to regulate cerebral blood flow through modulation vascular tone (Brozovich et al., 2016), which have the greatest influence in the calculation of blood flow. This thesis emphasises the importance capturing vessel diameter and volumetric flow to fully understand the regional cerebrovascular response to environmental stress that otherwise would have been missed if only measured using measurements of blood velocity.

7.3.1 Cerebral conduit extracranial arteries do vasodilate to acute poikilocapnic hypoxia

Each of the empirical chapters in this thesis used an exposure to acute poikilocapnic hypoxia. Volumetric (and vessel diameter) measurements of the extracranial arteries were central to the investigation in each of these repeat exposures and the findings across the chapters of this thesis provide evidence that the extracranial cerebral conduit arteries do regulate blood flow by reducing vascular tone to hypoxia. Indeed, in Chapter 4, there were comparable increases in vessel diameter of the ICA and VA to hypoxia when measured bilaterally. In Chapter 5 and Chapter 6 the cerebral blood flow response to hypoxia of the extracranial arteries was also mediated solely by a change in vessel diameter, not blood velocity, providing further support to the importance of assessing vessel diameter. The comparable vessel diameter responses between the ICA and VA to hypoxia were present despite differences in posture between Chapters 4 (supine) and Chapters 5 and 6 (seated), and these differences in posture may have contributed to the different blood velocity responses between chapters. The findings in this thesis that the extracranial conduit arteries actively modulate vascular tone to acute poikilocapnic hypoxia provides clarity to existing inconsistent evidence (Lewis et al., 2014; Ogoh et al., 2013). Specifically this is consistent with some previous studies (Fernandes et al., 2018; Hoiland et al., 2017; Lewis et al., 2014; Morris et al., 2017) but contrasts with others (Lafave et al., 2019; Ogoh et al., 2013; Willie et al., 2012; Willie, Smith, et al., 2014). These findings from Chapter 4, 5, and 6 supports the importance of using volumetric measurements to fully understand the how the cerebrovascular regulates blood flow to environmental stress.

7.3.2 Reduced posterior dCA in hypoxia was only identified with volumetric flow measurements of the extracranial arteries

In Chapter 5 a multimodal approach was used to assess the cerebrovascular response to abrupt reductions in blood pressure using a combination of TCD and duplex ultrasound (Labrecque et

al., 2021). The primary finding in Chapter 5 of a reduced dCA to abrupt reductions in blood pressure of the posterior, but not anterior, circulation in men to hypoxia was only identified from the measurement of volumetric (i.e., vascular conductance) RoR of the extracranial arteries. In contrast, RoR derived from blood velocity (i.e., vascular conductance index) of the MCA and PCA showed no regional difference to hypoxia. To our knowledge this is the first study of reduced volumetric RoR in the VA in acute hypoxia, with existing volumetric reports only focusing on the ICA (Horiuchi et al., 2016, 2022; Tymko et al., 2020). Therefore, the data from Chapter 5 further supports the importance of using volumetric measurements to fully understand regional cerebrovascular regulation.

7.3.3 The regional haemodynamic response to visual stimulation is detected with volumetric blood flow measurements of the extracranial arteries

In Chapter 6, volumetric measurements of the extracranial arteries captured a regional difference in haemodynamics between the anterior and posterior circulation in response to visual stimulation. Indeed, whilst the vascular tone of the extracranial arteries was not modulated by visual stimulation, the observation of a regional increase in blood velocity and flow in VA, but not ICA, during normoxia and acute hypoxia, suggests that the extracranial arteries are also sensitive to detect haemodynamic alterations to visual stimulation. Furthermore, this regional haemodynamic response between the ICA and VA was of a similar degree to the response in the MCA and PCA and therefore also likely reflects the regularly attributed localised microvascular response that occurs with visual stimulation (Hermes et al., 2007; Matsutomo et al., 2023). This observation of a regional haemodynamic response in the extracranial arteries demonstrates the utility of using duplex ultrasound over TCD because it captures vessel diameter and volumetric blood flow in addition to blood velocity. Therefore,

duplex ultrasound may be advantageous for investigations where vascular tone is known to change, e.g., visual stimulation with hypoxia-induced vasodilation.

Summary

This thesis shows the importance of capturing vascular tone and volumetric measurements to fully understand cerebrovascular regulation. Indeed, duplex ultrasound measurements of volumetric blood flow revealed findings that would have been missed from measurements of blood velocity from TCD. Future studies should implement volumetric measurements when investigating regional differences in the cerebral circulation (see section 7.6.1).

7.4 Unilateral volumetric assessments of cerebral conduit arteries

In Chapter 4, a systematically approached consensus was established for duplex ultrasound volumetric measurements that assessing the vessel with the larger resting blood flow, rather than the left or right vessel, reduces unilateral measurement error compared to the bilateral measurement. Throughout the remaining empirical chapters of the thesis (Chapters 5 and 6), the recommendation of selecting the vessel with the greatest resting blood flow from Chapter 4 is reinforced. Indeed, in Chapter 5 and Chapter 6, each study was designed to capture ipsilateral duplex ultrasound and transcranial Doppler ultrasound assessments of the ICA/MCA and VA/PCA to investigate dCA at both the intracranial and extracranial arteries to hypoxia. The most stable TCD signal that could be sustained for a prolonged period was prioritised in Chapters 5 and 6, so it was not always feasible to follow the recommendation from Chapter 4. However, the duplex ultrasound volumetric blood flow measurements of the extracranial arteries were the only measurement that revealed a regional difference in dCA to acute hypoxia, whereas TCD blood velocity measurements did not reveal regional differences (Chapter 5). Furthermore, duplex ultrasound volumetric blood flow measurements were also sensitive to detect the regional haemodynamic response to the visual stimulation, matching the TCD blood

velocity measurements (Chapter 6). Considering these findings, the duplex ultrasound measurement recommendation from Chapter 4 should be prioritised over TCD since duplex ultrasound was the most informative about cerebrovascular regulation. The findings from this thesis to prioritise volumetric blood flow when assessing mechanisms of blood flow regulation (i.e., dCA) align with recent recommendations (Brassard et al., 2021, 2023).

In Chapter 4 we investigated how anatomical variance in artery resting blood flow (i.e., size) may impact cerebrovascular regulation to environmental stress. Anatomical variances and/or imbalances of resting blood flow between lateral pairs of arteries have a higher incidence rate in the VA than ICA (Gaigalaite et al., 2016; Jeng & Yip, 2004; Katsanos et al., 2013). A VA with a resting blood flow $< 40 \text{ ml}\cdot\text{min}^{-1}$ is termed VA hypoplasia and has an incidence rate ranging from 10 to 31 % (Chen et al., 2010; Gaigalaite et al., 2016). If severe enough, VA hypoplasia can cause a reduction in net vertebral artery blood flow ($< 100 \text{ ml}\cdot\text{min}^{-1}$) in a condition called vertebrobasilar insufficiency. These anatomical variances in the posterior circulation have been related to reduced cerebrovascular function (Sato et al., 2015) and the manifestation of cerebrovascular and cardiovascular disease (Chuang et al., 2012; Hart, 2016; Katsanos et al., 2013; Seidel et al., 1999; Warnert, Rodrigues, et al., 2016). In Chapter 4, there was only one case (out of 86) of VA hypoplasia. Whilst this restricts our interpretation of the present data and cannot specifically be applied to these anatomical variants, we found no relationship between artery resting blood flow and the absolute blood flow response to acute hypoxia (Chapter 4, Figure 4.4b), which suggests that artery resting blood flow is not related to the magnitude of change in blood flow to a stressor (i.e., acute hypoxia). Furthermore, the negative relationship between artery resting blood flow and the relative blood flow response to acute hypoxia suggests that the arteries with lowest resting blood flow have the greatest relative response, which was explained by a ratio-scaling problem. Therefore, whilst this data is unable to fully explore the impact of VA hypoplasia on cerebrovascular function, the recommendation

in Chapter 4 of choosing the artery with the largest resting blood flow to minimise measurement error will not be impacted by the possibility of a different cerebrovascular regulation of a hypoplastic artery.

7.5 Thesis methodological considerations

7.5.1 End-tidal CO₂ control

Regional sensitivity to the partial pressure of end-tidal carbon dioxide (P_{ET}CO₂) between the anterior and posterior cerebral conduit arteries is well established (Sato, Sadamoto, et al., 2012; Willie et al., 2012). Therefore, an important methodological consideration for this thesis was the presence of alterations in P_{ET}CO₂. All studies used poikilocapnic hypoxia as an experimental manipulation to induce a robust environmental stimulus that raises blood flow by 20–30% during a 1–2 h of exposure. In Chapter 4 a 3.9 (±2.1) mmHg decrease in P_{ET}CO₂, and the associated vasoconstriction, did not impact the regionally comparable hypoxia-induced vasodilation of the ICA and VA. In contrast, in Chapter 5 and Chapter 6, the presence of hypocapnia-induced vasoconstriction likely had a greater impact on the results. Indeed, in Chapter 5, a 2.7 (±3.6) mmHg decrease in P_{ET}CO₂ may explain the lack of reduction in ICA, MCA and PCA RoR given its known effect to attenuate, and even abolish, hypoxia-induced reductions in dCA (Ogoh et al., 2010; Querido et al., 2013). However, existing literature in poikilocapnic hypoxia reports reduced volumetric ICA RoR (Horiuchi et al., 2016; Tymko et al., 2020) and therefore it is surprising to not have emulated this reduction in anterior dCA too. In Chapter 6, in contrast to previous literature (Nakagawa et al., 2009), there was a hypocapnia [2.9 (±2.8) mmHg decrease in P_{ET}CO₂] in the high visual input group in normoxia only. A visual stimulation associated hypocapnia in normoxia likely explains the negative change scores in cerebral haemodynamics from low to high visual input. Despite the negative values, there was still the presence of a regional difference in the blood velocity and blood flow

response to visual stimulation, with an attenuated reduction in PCA and VA haemodynamics compared to MCA and ICA, suggesting that the cerebrovasculature was not fully overwhelmed by the hypocapnic vasoconstriction as it could still respond to the addition of visual stimulation. Conversely, the similar $P_{ET}CO_2$ between the high and low visual input trials in hypoxia in Chapter 6 revealed the expected positive increase in posterior haemodynamics compared to anterior haemodynamics. Therefore, the differing haemodynamic responses (negative vs positive change scores) to visual stimulation in normoxia and hypoxia in Chapter 6 demonstrate the impact of uncontrolled $P_{ET}CO_2$ alterations between repeat trials. Whilst $P_{ET}CO_2$ was included as a fixed factor in the linear mixed model analysis to examine the impact of fluctuations in $P_{ET}CO_2$ on cerebrovascular regulation, it did not always improve the model fit. Future studies should aim to minimise fluctuations in $P_{ET}CO_2$ by using methods such as volitionally or metronome controlled respiratory rates and/or end-tidal gas clamping systems (Fisher & Mikulis, 2021; Mardimae et al., 2012; Ogoh et al., 2010; Querido et al., 2013).

7.5.2 Complexities of measuring dynamic cerebral autoregulation

Whilst there has been a successful decade of methodological advances and consensuses within the field of dCA research (Claassen et al., 2016; Panerai et al., 2023), the complexity to quantify dCA still remains a topic of discussion (Brassard et al., 2023; Tzeng et al., 2012). This thesis used the advised multimodal and multimetric approach to assess dCA (Brassard et al., 2023; Labrecque et al., 2021) and reports a regional difference in dCA between the anterior and posterior intracranial and extracranial cerebral conduit arteries. However, the findings in this thesis were not without some inconsistencies and complexities. In Chapter 5, acute poikilocapnic hypoxia induced a regional difference in dCA to abrupt reductions in blood pressure at the extracranial arteries, with a reduced VA, but not ICA, whereas there was no reduced dCA in either intracranial artery (MCA or PCA). The results from Chapter 5 supports

the view that dCA responses between different methods (e.g., duplex and TCD) are not comparable (Brassard et al., 2023; Tzeng et al., 2012). In Chapter 6, dCA to spontaneous oscillations in blood pressure in the PCA was reduced with visual stimulation; however, a high proportion of the data was lost by not achieving the appropriate coherence thresholds set out by standardised guidelines for transfer function analysis (Claassen et al., 2016; Panerai et al., 2023). Using sit-stand/squat-stand induced oscillations in blood pressure may provide an alternative to explore as these manoeuvres have been shown to improve coherence values (> 0.90) to have a greatest confidence in the transfer function metrics (Burma et al., 2021). Standardisation of the movement depth (Batterham et al., 2020) and the use of force sensors (Brassard et al., 2023) for the squat-stand/sit-stand manoeuvres have recently emerged and may help the manoeuvres become agreed upon technique for assessment of dCA. As highlighted in a recent review (Brassard et al., 2023), until there is an agreed upon gold standard method, researchers should implement the variety of multimodal and multimetric tools available for a holistic physiological interpretation of dCA.

7.6 Future directions

7.6.1 Implementation of volumetric regional assessment to mechanisms of cerebrovascular regulation

This thesis highlights that the cerebral conduit arteries play an important role in the regulation of cerebral blood flow. This thesis also suggests that mechanisms of blood flow regulation (e.g., dCA) be completed at multiple arteries of the cerebral circulation to capture possible regional differences in cerebrovascular regulation. Furthermore, in line with recent recommendations (Brassard et al., 2023), volumetric measurements should be central to investigations of cerebrovascular regulation to continue to progress the field forward. Throughout this thesis, volumetric measurements detected the same cerebrovascular response,

or was the only method that revealed a regional cerebrovascular response, as the more conventional and widely used blood velocity-derived TCD measurements. Duplex ultrasound is a valuable measurement tool that offers a non-invasive, cheaper, and portable volumetric measurement alternative to magnetic resonance imaging or positron emission tomography, that also has the benefit of an excellent temporal resolution for the assessment of cerebral blood flow to a variety of dynamic stressors in the laboratory or in the field (e.g., hypoxia, dCA, orthostasis). This thesis also shows that approximately 100 h of training is required to obtain accurate and reliable duplex ultrasound volumetric measurements (Chapter 3). Future studies should aim to implement duplex ultrasound volumetric measurements to assess regional regulation of the cerebrovasculature.

7.6.2 Identifying possible cellular mechanisms that underpin the regional difference in cerebral conduit artery regulation

The primary findings in this thesis relate to the regional differences in cerebrovascular regulation between posterior and anterior conduit arteries. One proposed mechanism for the regional differences in dCA is that the posterior circulation has a lower vascular tone at rest compared to anterior brain regions (Sato, Sadamoto, et al., 2012). In Chapter 6, we investigated whether the lower basal vascular tone of the posterior region was due to increased metabolic activity caused by visual stimulation by directly measuring vessel diameter of the extracranial cerebral conduit arteries using duplex ultrasound. It was reported that vascular tone was unchanged in the extracranial cerebral conduit arteries to visual stimulation, but a change in cerebral blood velocity and cerebral blood flow of the PCA and VA, respectively, suggests that the modulation to visual stimulation is downstream of the cerebral conduit arteries. As has been adopted previously (Bizeau et al., 2018), future studies could utilise magnetic resonance

imaging of the downstream microcirculation to investigate where in the posterior circulation ambient visual stimulation modulates vascular tone.

Other proposed possible mechanisms for lower basal vascular tone of the posterior circulation could be related to differences in sympathoexcitation, postural control, gravitational stress, autonomic innervations, and reactivity to reactive oxygen species (Sato, Sadamoto, et al., 2012). Regional heterogeneity in receptor densities identified between the anterior and posterior circulations has been established recently (Koep et al., 2022) and now require future investigations to translate how these structural differences impact cerebrovascular regulation, for example through the use of various blockades (e.g., cholinergic, beta adrenergic, sympathetic). Recent studies have already revealed evidence of mechanistic differences in control of cerebral blood flow between the anterior-posterior circulations, including adenosine-triphosphate-sensitive K⁺ channel activation (Rocha et al., 2020), endothelium-dependent vasodilation (Fernandes et al., 2018), and sensitivity to nitric oxide bioavailability and reactive oxygen species (Mattos et al., 2019, 2020; Vianna et al., 2018). Future research should continue to build upon these recent advancements to better understand the mechanisms underpinning the regional differences in cerebral conduit artery regulation.

7.6.3 Regional regulation of the cerebral conduit arteries in the development of pathophysiology

This thesis shows that the cerebral conduit arteries that supply the brain tissue are involved in the regulation of cerebral blood flow to physiological stress and this regulation may also be region-specific. This region-specific cerebral blood flow regulation at the cerebral conduit arteries is remarkably like the region-specific reductions in tissue perfusion at the posterior cingulate, temporal, parietal, and hippocampal cortices, which are associated with neurodegenerative diseases such as Alzheimer's disease (Korte et al., 2020; Swinford et al.,

2023; H. Zhang et al., 2021). Region-specific alterations in cerebral blood flow and/or cerebrovascular function have also been associated with psychological disorders (Baruah and Vasudevan 2019). Therefore, measuring cerebral haemodynamic and function at the cerebral conduit arteries could contribute to understanding the development of these pathophysiological conditions.

The regional differences in dCA reported in this thesis may be a mechanism to explain the stronger association of the posterior circulation than anterior circulation with orthostatic (in)tolerance (Kay & Rickards, 2016), acute mountain sickness (Barclay et al., 2021; Bian et al., 2014), and cerebral small vessel disease (Liu et al., 2016). Similarly, anatomical variants in the posterior cerebral conduit artery circulation are related to symptoms of headache, migraine, vertigo, and syncope migraine (Chuang et al., 2012; Gaigalaite et al., 2016; Katsanos et al., 2013; J. H. Park et al., 2007; Y. Wang et al., 2009) and are thought to be involved in development of hypertension (Hart, 2016; Warnert, Hart, et al., 2016; Warnert, Rodrigues, et al., 2016). Further, recent work in clinical populations has revealed that hypertensive patients have a blunted increase in VA blood flow to acute hypoxia (Fernandes et al., 2018), and L-arginine increased nitric oxide bioavailability (Vianna et al., 2018). Whilst reduced dCA of the cerebral conduit arteries in autonomic disorders has also been explored in a recent review (Brassard et al., 2021), it does highlight the common drawback that most research at the cerebral conduit arteries is limited to a single index of cerebral haemodynamics (i.e., MCA blood velocity) as a representation of global cerebral function. Future research should continue to build upon the recent associations between alterations in cerebral conduit artery function and pathophysiology by measuring arteries that are representative of the anterior and posterior circulations.

7.6.4 Regional cerebral blood flow regulation and sex

All studies in the thesis used a mixed cohort of men and women. In Chapter 5, including sex as a fixed factor in the linear mixed model analysis improved the model fit and revealed a regional difference in volumetric extracranial dCA in men only to acute poikilocapnic hypoxia. There are inconsistent findings with examining cerebral conduit artery haemodynamics and dCA within women (Deegan et al., 2010, 2011; Edgell et al., 2012; Favre et al., 2020; Favre & Serrador, 2019; Labrecque et al., 2021; Vavilala et al., 2005; Y. J. Wang et al., 2010). This lack of clarity is suggested to be largely a consequence of the differences in measurement techniques, primarily TCD-derived blood velocity, and standardisation of control and classification of menstrual cycle (Barnes & Charkoudian, 2021). Indeed, hormonal profiles of estrogen and progesterone between men and women are commonly reported to explain sex differences in cerebrovascular function, because these hormones are known to influence the cerebrovasculature (Krejza et al., 2001, 2003, 2013; Peltonen et al., 2016; Robison et al., 2019). However, the suggestion of sex-specific differences in Chapter 5 remained despite women completing repeat assessments during the menstrual or non-active pill phase associated with the lowest levels of oestrogen and progesterone to reduce the variability of sex hormones. Consequently, completing cerebrovascular assessment in women during the lower hormone phase of the cycle is not an appropriate method when using mixed cohort of men and women and suggests that mechanisms other than resting sex hormone differences likely explain the observed regional differences in dCA between men and women.

Women are underrepresented in physiology research (James et al., 2023). Sex differences are prominent in brain structure and cerebral blood flow across the lifespan between men and women, and this rapidly growing body of evidence is changing the previous status quo, which considered sex differences to be negligible (Kaczurkin et al., 2018). Indeed, sex and gender differences in intrinsic biological risk factors are increasingly prominent for the development

of Alzheimer's disease between men and women (Zhu et al., 2021). Furthermore, orthostatic symptoms and/or intolerance are worse in women (Cheng et al., 2011; Fu et al., 2005), particularly with increasing age (Newman et al., 2022). The incidence of migraine is greater in women compared to men (Al-Hassany et al., 2020), and the risk of cerebrovascular diseases, such as stroke, are lower in young premenopausal women compared to men but then is reversed following menopause (Robison et al., 2019). Other possible sex-specific mechanisms that have been explored, in addition to differences in sex hormone profiles, include; the greater resting cerebral perfusion in women (Alisch et al., 2021; Daniel et al., 1989; Rodriguez et al., 1988), dissimilarities in brain structure (Kaczurkin et al., 2018) and cerebral conduit artery size (Müller et al., 1991; Scheel, Ruge, & Schöning, 2000), distinct autonomic responses at rest (Hart et al., 2009) and during orthostasis (Robertson et al., 2020), and differences in cerebrovascular function, e.g., myogenic, endothelium-dependent, and -independent mechanisms (Pabbidi et al., 2018). Chapter 5 adds to the mounting evidence supporting sex differences in cerebrovascular function. Given this evidence, researchers developing studies into cerebrovascular function that include women, particularly as a mixed cohort, should be cautious when hypotheses are derived from research that was conducted almost entirely in men. Indeed, future studies of cerebrovascular regulation should carefully consider the methodological approaches to studying men and women. Only when studies are conducted with such methodological approaches in mind can research help understand potential sex-related differences in biology, health, and disease (Rich-Edwards et al., 2018).

7.7 Conclusions

The major conclusions from this thesis include:

1. The cerebral conduit arteries vasodilate and increase blood flow comparably between the anterior and posterior circulations in acute hypoxia.
2. Dynamic cerebral autoregulation to abrupt reductions in blood pressure of the extracranial arteries in acute hypoxia and to spontaneous oscillations in blood pressure of the intracranial arteries with visual stimulation in normoxia is reduced in the posterior circulation compared to the anterior circulation.
3. Visual stimulation does not modulate extracranial cerebral conduit artery vascular tone and is unlikely to be a mechanism for the reduced dynamic cerebral autoregulation observed in the intracranial posterior circulation.
4. Unilateral duplex volumetric measurements of the extracranial arteries should be prioritised over transcranial Doppler ultrasound blood velocity-only measurements of the intracranial arteries as volumetric measurements provide a clearer interpretation of cerebrovascular regulation.
5. Unilateral volumetric measurements of the extracranial arteries should be assessed in the artery exhibiting the largest resting blood flow of a lateral pairing to reduce error when compared to a bilateral measurement.

References

- Aaslid, R. (1987). Visually evoked dynamic blood flow response of the human cerebral circulation. *Stroke*, *18*(4), 771–775. <https://doi.org/10.1161/01.STR.18.4.771>
- Aaslid, R., Lindegaard, K. F., Sorteberg, W., & Nornes, H. (1989). Cerebral autoregulation dynamics in humans. *Stroke*, *20*(1), 45–52. <https://doi.org/10.1161/01.STR.20.1.45>
- Aaslid, R., Markwalder, T. M., & Nornes, H. (1982). Noninvasive transcranial Doppler ultrasound recording of flow velocity in basal cerebral arteries. *Journal of Neurosurgery*, *57*(6), 769–774. <https://doi.org/10.3171/JNS.1982.57.6.0769>
- Acar, M., Degirmenci, B., Yucel, A., Albayrak, R., & Haktanir, A. (2005). An evaluation of internal carotid artery and cerebral blood flow volume using color duplex sonography in patients with vertebral artery hypoplasia. *European Journal of Radiology*, *53*(3), 450–453. <https://doi.org/10.1016/J.EJRAD.2004.05.010>
- Ainslie, P. N., Barach, A., Murrell, C., Hamlin, M., Hellemans, J., & Ogoh, S. (2007). Alterations in cerebral autoregulation and cerebral blood flow velocity during acute hypoxia: rest and exercise. *American Journal of Physiology-Heart and Circulatory Physiology*, *292*(2), H976–H983. <https://doi.org/10.1152/ajpheart.00639.2006>
- Ainslie, P. N., & Brassard, P. (2014). Why is the neural control of cerebral autoregulation so controversial. *F1000Prime Reports*, *6*(14). <https://doi.org/10.12703/P6-14>
- Ainslie, P. N., & Duffin, J. (2009). Integration of cerebrovascular CO₂ reactivity and chemoreflex control of breathing: mechanisms of regulation, measurement, and interpretation. *American Journal of Physiology. Regulatory, Integrative and Comparative Physiology*, *296*(5), R1473–R1495. <https://doi.org/10.1152/ajpregu.91008.2008>
- Ainslie, P. N., Hamlin, M., Hellemans, J., Rasmussen, P., & Ogoh, S. (2008). Cerebral hypoperfusion during hypoxic exercise following two different hypoxic exposures: independence from changes in dynamic autoregulation and reactivity. *American Journal of Physiology. Regulatory, Integrative and Comparative Physiology*, *295*(5), R1613–R1622. <https://doi.org/10.1152/AJPREGU.90420.2008>
- Ainslie, P. N., & Hoiland, R. L. (2014). Transcranial Doppler ultrasound: valid, invalid, or both? *Journal of Applied Physiology (Bethesda, Md. : 1985)*, *117*(10), 1081–1083. <https://doi.org/10.1152/JAPPLPHYSIOL.00854.2014>
- Ainslie, P. N., Hoiland, R. L., & Bailey, D. M. (2016). Lessons from the laboratory; integrated regulation of cerebral blood flow during hypoxia. *Experimental Physiology*, *101*(9), 1160–1166. <https://doi.org/10.1113/EP085671>
- Ainslie, P. N., Lucas, S. J. E., Fan, J. L., Thomas, K. N., Cotter, J. D., Tzeng, Y. C., & Burgess, K. R. (2012). Influence of sympathoexcitation at high altitude on cerebrovascular function and ventilatory control in humans. *Journal of Applied Physiology (Bethesda, Md. : 1985)*, *113*(7), 1058–1067. <https://doi.org/10.1152/JAPPLPHYSIOL.00463.2012>
- Ainslie, P. N., Ogoh, S., Burgess, K., Celi, L., McGrattan, K., Peebles, K., Murrell, C., Subedi, P., & Burgess, K. R. (2008). Differential effects of acute hypoxia and high altitude on cerebral blood flow velocity and dynamic cerebral autoregulation: alterations with hyperoxia. *Journal of Applied Physiology (Bethesda, Md. : 1985)*, *104*(2), 490–498. <https://doi.org/10.1152/JAPPLPHYSIOL.00778.2007>
- Ainslie, P. N., & Poulin, M. J. (2004). Ventilatory, cerebrovascular, and cardiovascular interactions in acute hypoxia: regulation by carbon dioxide. *Journal of Applied Physiology (Bethesda, Md. : 1985)*, *97*(1), 149–159. <https://doi.org/10.1152/JAPPLPHYSIOL.01385.2003>

- Ainslie, P. N., Shaw, A. D., Smith, K. J., Willie, C. K., Ikeda, K., Graham, J., & Macleod, D. B. (2014). Stability of cerebral metabolism and substrate availability in humans during hypoxia and hyperoxia. *Clinical Science (London, England : 1979)*, *126*(9), 661–670. <https://doi.org/10.1042/CS20130343>
- Al-Hassany, L., Haas, J., Piccininni, M., Kurth, T., Maassen Van Den Brink, A., & Rohmann, J. L. (2020). Giving researchers a headache – sex and gender differences in migraine. *Frontiers in Neurology*, *11*, 549038. <https://doi.org/10.3389/FNEUR.2020.549038>
- Aleksic, M., & Brunkwall, J. (2009). Extracranial blood flow distribution during carotid surgery. *European Journal of Vascular and Endovascular Surgery*, *38*(5), 552–555. <https://doi.org/doi:10.1016/j.ejvs.2009.06.023>
- Alisch, J. S. R., Khattar, N., Kim, R. W., Cortina, L. E., Rejimon, A. C., Qian, W., Ferrucci, L., Resnick, S. M., Spencer, R. G., & Bouhrara, M. (2021). Sex and age-related differences in cerebral blood flow investigated using pseudo-continuous arterial spin labeling magnetic resonance imaging. *Aging*, *13*(4), 4911–4925. <https://doi.org/10.18632/AGING.202673>
- Allen, A. M., McRae-Clark, A. L., Carlson, S., Saladin, M. E., Gray, K. M., Wetherington, C. L., McKee, S. A., & Allen, S. S. (2016). Determining menstrual phase in human biobehavioral research: a review with recommendations. *Experimental and Clinical Psychopharmacology*, *24*(1), 1–11. <https://doi.org/10.1037/PHA0000057>
- Arngim, N., Schytz, H. W., Britze, J., Amin, F. M., Vestergaard, M. B., Hougaard, A., Wolfram, F., de Koning, P. J. H., Olsen, K. S., Secher, N. H., Larsson, H. B. W., Olesen, J., & Ashina, M. (2016). Migraine induced by hypoxia: an MRI spectroscopy and angiography study. *Brain : A Journal of Neurology*, *139*(Pt 3), 723–737. <https://doi.org/10.1093/BRAIN/AWV359>
- Ashby, J. W., & Mack, J. J. (2021). Endothelial control of cerebral blood flow. *The American Journal of Pathology*, *191*(11), 1906–1916. <https://doi.org/10.1016/J.AJP.2021.02.023>
- Atkinson, G., & Batterham, A. M. (2013a). Allometric scaling of diameter change in the original flow-mediated dilation protocol. *Atherosclerosis*, *226*(2), 425–427. <https://doi.org/10.1016/j.atherosclerosis.2012.11.027>
- Atkinson, G., & Batterham, A. M. (2013b). The percentage flow-mediated dilation index: A large-sample investigation of its appropriateness, potential for bias and causal nexus in vascular medicine. *Vascular Medicine*, *18*(6), 354–365. <https://doi.org/10.1177/1358863X13508446>
- Atkinson, G., Batterham, A. M., Thijssen, D. H. J., & Green, D. J. (2013). A new approach to improve the specificity of flow-mediated dilation for indicating endothelial function in cardiovascular research. *Journal of Hypertension*, *31*(2), 287–291. <https://doi.org/10.1097/HJH.0b013e32835b8164>
- Atkinson, G., & Nevill, A. M. (1998). Statistical methods for assessing measurement error (reliability) in variables relevant to sports medicine. *Sports Medicine (Auckland, N.Z.)*, *26*(4), 217–238. <https://doi.org/10.2165/00007256-199826040-00002>
- Ayajiki, K., & Toda, N. (1992). Regional difference in the response mediated by beta 1-adrenoceptor subtype in bovine cerebral arteries. *Journal of Cerebral Blood Flow and Metabolism*, *12*(3), 507–513. <https://doi.org/10.1038/JCBFM.1992.69>
- Bader, T. J., Leacy, J. K., Keough, J. R. G., Ciorogariu-Ivan, A. M., Donald, J. R., Marullo, A. L., O'Halloran, K. D., Jendzjowsky, N. G., Wilson, R. J. A., & Day, T. A. (2021). The effects of acute incremental hypocapnia on the magnitude of neurovascular coupling in healthy participants. *Physiological Reports*, *9*(15), e14952. <https://doi.org/10.14814/PHY2.14952>
- Bahner, D. P., Blickendorf, J. M., Bockbrader, M., Adkins, E., Vira, A., Boulger, C., & Panchal, A. R. (2016). Language of transducer manipulation: codifying terms for effective teaching. *Journal of*

- Bailey, D. M., Evans, K. A., James, P. E., McEneny, J., Young, I. S., Fall, L., Gutowski, M., Kewley, E., McCord, J. M., Møller, K., & Ainslie, P. N. (2009). Altered free radical metabolism in acute mountain sickness: implications for dynamic cerebral autoregulation and blood-brain barrier function. *The Journal of Physiology*, 587(1), 73–85. <https://doi.org/10.1113/JPHYSIOL.2008.159855>
- Bain, A. R., Smith, K. J., Lewis, N. C., Foster, G. E., Wildfong, K. W., Willie, C. K., Hartley, G. L., Cheung, S. S., & Ainslie, P. N. (2013). Regional changes in brain blood flow during severe passive hyperthermia: effects of PaCO₂ and extracranial blood flow. *Journal of Applied Physiology (Bethesda, Md. : 1985)*, 115(5), 653–659. <https://doi.org/10.1152/JAPPLPHYSIOL.00394.2013>
- Barclay, H., Mukerji, S., Kayser, B., O'Donnell, T., Tzeng, Y. C., Hill, S., Knapp, K., Legg, S., Frei, D., & Fan, J. L. (2021). Respiratory alkalization and posterior cerebral artery dilatation predict acute mountain sickness severity during 10 h normobaric hypoxia. *Experimental Physiology*, 106(1), 175–190. <https://doi.org/10.1113/EP088938>
- Barnes, J. N., & Charkoudian, N. (2021). Integrative cardiovascular control in women: regulation of blood pressure, body temperature, and cerebrovascular responsiveness. *FASEB J.*, 35(2), e21143. <https://doi.org/10.1096/FJ.202001387R>
- Batterham, A. P., Panerai, R. B., Robinson, T. G., & Haunton, V. J. (2020). Does depth of squat-stand maneuver affect estimates of dynamic cerebral autoregulation? *Physiological Reports*, 8(16), e14549. <https://doi.org/10.14814/PHY2.14549>
- Bian, S. Z., Jin, J., Li, Q. N., Qin, J., Zhang, J. H., Yu, S. Y., Chen, J. F., Tang, C. F., & Huang, L. (2014). Cerebral hemodynamic characteristics of acute mountain sickness upon acute high-altitude exposure at 3,700 m in young Chinese men. *European Journal of Applied Physiology*, 114(10), 2193–2200. <https://doi.org/10.1007/S00421-014-2934-6>
- Binks, A. P., Cunningham, V. J., Adams, L., & Banzett, R. B. (2008). Gray matter blood flow change is unevenly distributed during moderate isocapnic hypoxia in humans. *Journal of Applied Physiology (Bethesda, Md. : 1985)*, 104(1), 212–217. <https://doi.org/10.1152/JAPPLPHYSIOL.00069.2007>
- Bizeau, A., Gilbert, G., Bernier, M., Huynh, M. T., Bocti, C., Descoteaux, M., & Whittingstall, K. (2018). Stimulus-evoked changes in cerebral vessel diameter: a study in healthy humans. *Journal of Cerebral Blood Flow & Metabolism*, 38(3), 528–539. <https://doi.org/10.1177/0271678X17701948>
- Blaber, A. P., Hartley, T., & Pretorius, P. J. (2003). Effect of acute exposure to 3660 m altitude on orthostatic responses and tolerance. *Journal of Applied Physiology (Bethesda, Md. : 1985)*, 95(2), 591–601. <https://doi.org/10.1152/JAPPLPHYSIOL.00749.2002>
- Bland, J. M., & Altman, D. G. (1986). Statistical methods for assessing agreement between two methods of clinical measurement. *The Lancet*, 327(8476), 307–310. [https://doi.org/10.1016/S0140-6736\(86\)90837-8](https://doi.org/10.1016/S0140-6736(86)90837-8)
- Brassard, P., Labrecque, L., Smirl, J. D., Tymko, M. M., Caldwell, H. G., Hoiland, R. L., Lucas, S. J. E., Denault, A. Y., Couture, E. J., & Ainslie, P. N. (2021). Losing the dogmatic view of cerebral autoregulation. *Physiological Reports*, 9(15), e14982. <https://doi.org/10.14814/PHY2.14982>
- Brassard, P., Roy, M. A., Burma, J. S., Labrecque, L., & Smirl, J. D. (2023). Quantification of dynamic cerebral autoregulation: welcome to the jungle! *Clinical Autonomic Research* 2023, 1–20. <https://doi.org/10.1007/S10286-023-00986-2>
- Brassard, P., Tymko, M. M., & Ainslie, P. N. (2017). Sympathetic control of the brain circulation:

- appreciating the complexities to better understand the controversy. *Autonomic Neuroscience : Basic & Clinical*, 207, 37–47. <https://doi.org/10.1016/J.AUTNEU.2017.05.003>
- Brisset, M., Boutouyrie, P., Pico, F., Zhu, Y., Zureik, M., Schilling, S., Dufouil, C., Mazoyer, B., Laurent, S., Tzourio, C., & Debette, S. (2013). Large-vessel correlates of cerebral small-vessel disease. *Neurology*, 80(7), 662–669. <https://doi.org/10.1212/WNL.0B013E318281CCC2>
- Brozovich, F. V., Nicholson, C. J., Degen, C. V., Gao, Y. Z., Aggarwal, M., & Morgan, K. G. (2016). Mechanisms of vascular smooth muscle contraction and the basis for pharmacologic treatment of smooth muscle disorders. *Pharmacological Reviews*, 68(2), 476–532. <https://doi.org/10.1124/PR.115.010652>
- Bruce, C. D., Steinback, C. D., Chauhan, U. V., Pfoh, J. R., Abrosimova, M., Vanden Berg, E. R., Skow, R. J., Davenport, M. H., & Day, T. A. (2016). Quantifying cerebrovascular reactivity in anterior and posterior cerebral circulations during voluntary breath holding. *Experimental Physiology*, 101(12), 1517–1527. <https://doi.org/10.1113/EP085764>
- Buck, A., Schirlo, C., Jasinsky, V., Weber, B., Burger, C., von Schulthess, G. K., Koller, E. A., & Pavlicek, V. (1998). Changes of cerebral blood flow during short-term exposure to normobaric hypoxia. *Journal of Cerebral Blood Flow and Metabolism*, 18(8), 906–910. <https://doi.org/10.1097/00004647-199808000-00011>
- Burma, J. S., Kennedy, C. M., Penner, L. C., Miutz, L. N., Galea, O. A., Ainslie, P. N., & Smirl, J. D. (2021). Long-term heart transplant recipients: heart rate-related effects on augmented transfer function coherence during repeated squat-stand maneuvers in males. *American Journal of Physiology - Regulatory Integrative and Comparative Physiology*, 321(6), R925–R937. <https://doi.org/10.1152/AJPREGU.00177.2021>
- Caldwell, H. G., Ainslie, P. N., Ellis, L. A., Phillips, A. A., & Flück, D. (2017). Stability in neurovascular function at 3800m. *Physiology & Behavior*, 182, 62–68. <https://doi.org/10.1016/J.PHYSBEH.2017.09.023>
- Caldwell, H. G., Coombs, G. B., Howe, C. A., Hoiland, R. L., Patrician, A., Lucas, S. J. E., & Ainslie, P. N. (2020). Evidence for temperature-mediated regional increases in cerebral blood flow during exercise. *The Journal of Physiology*, 598(8), 1459–1473. <https://doi.org/10.1113/JP278827>
- Caldwell, H. G., Coombs, G. B., Tymko, M. M., Nowak-Flück, D., & Ainslie, P. N. (2018). Severity-dependent influence of isocapnic hypoxia on reaction time is independent of neurovascular coupling. *Physiology & Behavior*, 188, 262–269. <https://doi.org/10.1016/J.PHYSBEH.2018.02.035>
- Carr, J. M. J. R., Hoiland, R. L., Fernandes, I. A., Schrage, W. G., & Ainslie, P. N. (2023). Recent insights into mechanisms of hypoxia-induced vasodilatation in the human brain. *The Journal of Physiology*, 0(0), 1–18. <https://doi.org/10.1113/JP284608>
- Carter, H. H., Maxwell, J. D., Hellsten, Y., Thompson, A., Andrew, D., Thijssen, H. J., & Jones, H. (2020). The impact of acute remote ischaemic preconditioning on cerebrovascular function. *European Journal of Applied Physiology*, 120(3), 603–612. <https://doi.org/10.1007/s00421-019-04297-1>
- Carter, K. J., Ward, A. T., Kellawan, J. M., Eldridge, M. W., Al-Subu, A., Walker, B. J., Lee, J. W., Wieben, O., & Schrage, W. G. (2021). Nitric oxide synthase inhibition in healthy adults reduces regional and total cerebral macrovascular blood flow and microvascular perfusion. *The Journal of Physiology*, 599(22), 4973–4989. <https://doi.org/10.1113/JP281975>
- Chen, Y. Y., Chao, A. C., Hsu, H. Y., Chung, C. P., & Hu, H. H. (2010). Vertebral artery hypoplasia is associated with a decrease in net vertebral flow volume. *Ultrasound in Medicine & Biology*, 36(1), 38–43. <https://doi.org/10.1016/J.ULTRASMEDBIO.2009.08.012>

- Cheng, Y. C., Vyas, A., Hymen, E., & Perlmutter, L. C. (2011). Gender differences in orthostatic hypotension. *The American Journal of the Medical Sciences*, *342*(3), 221–225. <https://doi.org/10.1097/MAJ.0B013E318208752B>
- Chuang, Y.-M., Chan, L., Wu, H.-M., Lee, S.-P., & Chu, Y.-T. (2012). The clinical relevance of vertebral artery hypoplasia. *Acta Neurologica Taiwanica*, *21*(1), 1–7.
- Chuang, Y.-M., Liu, C.-Y., Pan, P.-J., & Lin, C.-P. (2008). Posterior communicating artery hypoplasia as a risk factor for acute ischemic stroke in the absence of carotid artery occlusion. *Journal of Clinical Neuroscience*, *15*(12), 1376–1381. <https://doi.org/10.1016/J.JOCN.2008.02.002>
- Cipolla, M. J. (2009). The cerebral circulation. *Colloquium Series on Integrated Systems Physiology: From Molecule to Function*, *1*(1), 1–59. <https://doi.org/10.4199/C00005ED1V01Y200912ISP002>
- Claassen, J. A. H. R., Meel-van den Abeelen, A. S., Simpson, D. M., Panerai, R. B., & (CARNet), international C. A. R. N. (2016). Transfer function analysis of dynamic cerebral autoregulation: a white paper from the international Cerebral Autoregulation Research Network. *Journal of Cerebral Blood Flow & Metabolism*, *36*(4), 665–680. <https://doi.org/10.1177/0271678X15626425>
- Claassen, J. A. H. R., Thijssen, D. H. J., Panerai, R. B., & Faraci, F. M. (2021). Regulation of cerebral blood flow in humans: physiology and clinical implications of autoregulation. *Physiological Reviews*, *101*(4), 1487–1559. <https://doi.org/10.1152/physrev.00022.2020>
- Cochand, N. J., Wild, M., Brugniaux, J. V., Davies, P. J., Evans, K. A., Wise, R. G., & Bailey, D. M. (2011). Sea-level assessment of dynamic cerebral autoregulation predicts susceptibility to acute mountain sickness at high altitude. *Stroke*, *42*(12), 3628–3630. <https://doi.org/10.1161/STROKEAHA.111.621714>
- Cohen, P. J., Alexander, S. C., Smith, T. C., Reivich, M., & Wollman, H. (1967). Effects of hypoxia and normocarbina on cerebral blood flow and metabolism in conscious man. *Journal of Applied Physiology*, *23*(2), 183–189. <https://doi.org/10.1152/JAPPL.1967.23.2.183>
- Coverdale, N. S., Gati, J. S., Opalevych, O., Perrotta, A., & Shoemaker, J. K. (2014). Cerebral blood flow velocity underestimates cerebral blood flow during modest hypercapnia and hypocapnia. *Journal of Applied Physiology (Bethesda, Md. : 1985)*, *117*(10), 1090–1096. <https://doi.org/10.1152/JAPPLPHYSIOL.00285.2014>
- Daniel, D. G., Mathew, R. J., & Wilson, W. H. (1989). Sex roles and regional cerebral blood flow. *Psychiatry Research*, *27*(1), 55–64. [https://doi.org/10.1016/0165-1781\(89\)90009-7](https://doi.org/10.1016/0165-1781(89)90009-7)
- Deegan, B. M., Devine, E. R., Geraghty, M. C., Jones, E., Ó'Laighin, G., & Serrador, J. M. (2010). The relationship between cardiac output and dynamic cerebral autoregulation in humans. *Journal of Applied Physiology (Bethesda, Md. : 1985)*, *109*(5), 1424–1431. <https://doi.org/10.1152/JAPPLPHYSIOL.01262.2009>
- Deegan, B. M., Sorond, F. A., Galica, A., Lipsitz, L. A., O'Laighin, G., & Serrador, J. M. (2011). Elderly women regulate brain blood flow better than men do. *Stroke*, *42*(7), 1988–1993. <https://doi.org/10.1161/STROKEAHA.110.605618>
- Diedenhofen, B., & Musch, J. (2015). cocor: a comprehensive solution for the statistical comparison of correlations. *PLOS ONE*, *10*(4), e0121945. <https://doi.org/10.1371/journal.pone.0121945>
- Diehl, R. R., Linden, D., Lücke, D., & Berlitz, P. (1995). Phase relationship between cerebral blood flow velocity and blood pressure. *Stroke*, *26*(10), 1801–1804. <https://doi.org/10.1161/01.STR.26.10.1801>
- Duffin, J., Mikulis, D. J., & Fisher, J. A. (2021). Control of cerebral blood flow by blood gases.

- Edgell, H., Robertson, A. D., & Hughson, R. L. (2012). Hemodynamics and brain blood flow during posture change in younger women and postmenopausal women compared with age-matched men. *Journal of Applied Physiology (Bethesda, Md. : 1985)*, 112(9), 1482–1493. <https://doi.org/10.1152/JAPPLPHYSIOL.01204.2011>
- Elliott-Sale, K. J., Minahan, C. L., de Jonge, X. A. K. J., Ackerman, K. E., Sipilä, S., Constantini, N. W., Lebrun, C. M., & Hackney, A. C. (2021). Methodological considerations for studies in sport and exercise science with women as participants: a working guide for standards of practice for research on women. *Sports Medicine (Auckland, N.Z.)*, 51(5), 843–861. <https://doi.org/10.1007/S40279-021-01435-8>
- Fan, A. P., Jahanian, H., Holdsworth, S. J., & Zaharchuk, G. (2016). Comparison of cerebral blood flow measurement with [15O]-water positron emission tomography and arterial spin labeling magnetic resonance imaging: a systematic review. *Journal of Cerebral Blood Flow & Metabolism*, 36(5), 842–861. <https://doi.org/10.1177/0271678X16636393>
- Faraci, F. M., Heistad, D. D., & Mayhan, W. G. (1987). Role of large arteries in regulation of blood flow to brain stem in cats. *The Journal of Physiology*, 387(1), 115–123. <https://doi.org/10.1113/JPHYSIOL.1987.SP016566>
- Faul, F., Erdfelder, E., Buchner, A., & Lang, A. G. (2009). Statistical power analyses using G*Power 3.1: Tests for correlation and regression analyses. *Behavior Research Methods*, 41(4), 1149–1160. <https://doi.org/10.3758/BRM.41.4.1149/METRICS>
- Favre, M. E., Lim, V., Falvo, M. J., & Serrador, J. M. (2020). Cerebrovascular reactivity and cerebral autoregulation are improved in the supine posture compared to upright in healthy men and women. *PloS One*, 15(3). <https://doi.org/10.1371/JOURNAL.PONE.0229049>
- Favre, M. E., & Serrador, J. M. (2019). Sex differences in cerebral autoregulation are unaffected by menstrual cycle phase in young, healthy women. *American Journal of Physiology. Heart and Circulatory Physiology*, 316(4), H920–H933. <https://doi.org/10.1152/AJPHEART.00474.2018>
- Fernandes, I. A., Mattos, J. D., Campos, M. O., Machado, A. C., Rocha, M. P., Rocha, N. G., Vianna, L. C., & Nobrega, A. C. L. (2016). Selective α 1-adrenergic blockade disturbs the regional distribution of cerebral blood flow during static handgrip exercise. *American Journal of Physiology. Heart and Circulatory Physiology*, 310(11), H1541–H1548. <https://doi.org/10.1152/AJPHEART.00125.2016>
- Fernandes, I. A., Rocha, M. P., Campos, M. O., Mattos, J. D., Mansur, D. E., Rocha, H. N. M., Terra, P. A. C., Garcia, V. P., Rocha, N. G., Secher, N. H., & Nóbrega, A. C. L. (2018). Reduced arterial vasodilatation in response to hypoxia impairs cerebral and peripheral oxygen delivery in hypertensive men. *Journal of Physiology*, 596(7), 1167–1179. <https://doi.org/10.1113/JP275545>
- Fisher, J. A. (2016). The CO₂ stimulus for cerebrovascular reactivity: fixing inspired concentrations vs. targeting end-tidal partial pressures. *Journal of Cerebral Blood Flow and Metabolism*, 36(6), 1004–1011. <https://doi.org/10.1177/0271678X16639326>
- Fisher, J. A., & Mikulis, D. J. (2021). Cerebrovascular reactivity: purpose, optimizing methods, and limitations to Interpretation - a personal 20-Year odyssey of (re)searching. *Frontiers in Physiology*, 12(629651). <https://doi.org/10.3389/FPHYS.2021.629651>
- Friend, A. T., Balanos, G. M., & Lucas, S. J. E. (2019). Isolating the independent effects of hypoxia and hyperventilation-induced hypocapnia on cerebral haemodynamics and cognitive function. *Experimental Physiology*, 104(10), 1482–1493. <https://doi.org/10.1113/EP087602>
- Friend, A. T., Rogan, M., Rossetti, G. M. K., Lawley, J. S., Mullins, P. G., Sandoo, A., Macdonald, J. H., & Oliver, S. J. (2021). Bilateral regional extracranial blood flow regulation to hypoxia and

- unilateral duplex ultrasound measurement error. *Experimental Physiology*, *106*(7), 1535–1548. <https://doi.org/10.1113/EP089196>
- Fu, Q., Witkowski, S., Okazaki, K., & Levine, B. D. (2005). Effects of gender and hypovolemia on sympathetic neural responses to orthostatic stress. *American Journal of Physiology. Regulatory, Integrative and Comparative Physiology*, *289*(1). <https://doi.org/10.1152/AJPREGU.00013.2005>
- Gaigalaite, V., Vilimas, A., Ozeraitiene, V., Dementaviciene, J., Janilionis, R., Kalibatiene, D., & Rocka, S. (2016). Association between vertebral artery hypoplasia and posterior circulation stroke. *BMC Neurology*, *16*(118). <https://doi.org/10.1186/s12883-016-0644-x>
- Giavarina, D. (2015). Understanding Bland Altman analysis. *Biochemia Medica*, *25*(2), 141–151. <https://doi.org/10.11613/BM.2015.015>
- Glover, G. H. (2011). Overview of functional magnetic resonance imaging. *Neurosurgery Clinics of North America*, *22*(2), 133–139. <https://doi.org/10.1016/J.NEC.2010.11.001>
- Hainsworth, R., Drinkhill, M. J., & Rivera-Chira, M. (2007). The autonomic nervous system at high altitude. *Clinical Autonomic Research*, *17*(1), 13–19. <https://doi.org/10.1007/S10286-006-0395-7>
- Hamel, E., Edvinsson, L., & MacKenzie, E. T. (1988). Heterogeneous vasomotor responses of anatomically distinct feline cerebral arteries. *British Journal of Pharmacology*, *94*(2), 423–436. <https://doi.org/10.1111/J.1476-5381.1988.TB11544.X>
- Harrell, J. W., Peltonen, G. L., & Schrage, W. G. (2019). Reactive oxygen species and cyclooxygenase products explain the majority of hypoxic cerebral vasodilation in healthy humans. *Acta Physiologica (Oxford, England)*, *226*(4), e13288. <https://doi.org/10.1111/APHA.13288>
- Harris, A. D., Murphy, K., Diaz, C. M., Saxena, N., Hall, J. E., Liu, T. T., & Wise, R. G. (2013). Cerebral blood flow response to acute hypoxic hypoxia. *NMR in Biomedicine*, *26*(12), 1844–1852. <https://doi.org/10.1002/NBM.3026>
- Hart, E. C. (2016). Human hypertension, sympathetic activity and the selfish brain. *Experimental Physiology*, *101*(12), 1451–1462. <https://doi.org/10.1113/EP085775>
- Hart, E. C., Charkoudian, N., Wallin, B. G., Curry, T. B., Eisenach, J. H., & Joyner, M. J. (2009). Sex differences in sympathetic neural-hemodynamic balance: implications for human blood pressure regulation. *Hypertension*, *53*(3), 571–576. <https://doi.org/10.1161/HYPERTENSIONAHA.108.126391>
- Haubrich, C., Wendt, A., Diehl, R. R., & Klötzsch, C. (2004). Dynamic autoregulation testing in the posterior cerebral artery. *Stroke*, *35*(4), 848–852. <https://doi.org/10.1161/01.STR.0000120729.99039.B6>
- Hayes, G., Pinto, J., Sparks, S. N., Wang, C., Suri, S., & Bulte, D. P. (2022). Vascular smooth muscle cell dysfunction in neurodegeneration. *Frontiers in Neuroscience*, *16*, 1010164. <https://doi.org/10.3389/FNINS.2022.1010164>
- Heistad, D. D., Marcus, M. L., & Abboud, F. M. (1978). Role of large arteries in regulation of cerebral blood flow in dogs. *The Journal of Clinical Investigation*, *62*(4), 761–768. <https://doi.org/10.1172/JCI109187>
- Hermes, M., Hagemann, D., Britz, P., Lieser, S., Rock, J., Naumann, E., & Walter, C. (2007). Reproducibility of continuous arterial spin labeling perfusion MRI after 7 weeks. *Magma (New York, N.Y.)*, *20*(2), 103–115. <https://doi.org/10.1007/S10334-007-0073-3>
- Herrington, B. A., Thrall, S. F., Mann, L. M., Tymko, M. M., & Day, T. A. (2019). The effect of steady-state CO₂ on regional brain blood flow responses to increases in blood pressure via the

- cold pressor test. *Autonomic Neuroscience : Basic & Clinical*, 222(102581).
<https://doi.org/10.1016/J.AUTNEU.2019.102581>
- Hoiland, R. L., Ainslie, P. N., Wildfong, K. W., Smith, K. J., Bain, A. R., Willie, C. K., Foster, G., Monteleone, B., & Day, T. A. (2015). Indomethacin-induced impairment of regional cerebrovascular reactivity: implications for respiratory control. *The Journal of Physiology*, 593(5), 1291–1306. <https://doi.org/10.1113/JPHYSIOL.2014.284521>
- Hoiland, R. L., Bain, A. R., Rieger, M. G., Bailey, D. M., & Ainslie, P. N. (2016). Oxygen as a regulator of biological systems: hypoxemia, oxygen content, and the regulation of cerebral blood flow. *American Journal of Physiology - Regulatory, Integrative and Comparative Physiology*, 310(5), R398. <https://doi.org/10.1152/AJPREGU.00270.2015>
- Hoiland, R. L., Bain, A. R., Tymko, M. M., Rieger, M. G., Howe, C. A., Willie, C. K., Hansen, A. B., Flück, D., Wildfong, K. W., Stembridge, M., Subedi, P., Anholm, J., & Ainslie, P. N. (2017). Adenosine receptor-dependent signaling is not obligatory for normobaric and hypobaric hypoxia-induced cerebral vasodilation in humans. *Journal of Applied Physiology*, 122(4), 795–808. <https://doi.org/10.1152/jappphysiol.00840.2016>
- Hoiland, R. L., Caldwell, H. G., Howe, C. A., Nowak-Flück, D., Stacey, B. S., Bailey, D. M., Paton, J. F. R., Green, D. J., Sekhon, M. S., Macleod, D. B., & Ainslie, P. N. (2020). Nitric oxide is fundamental to neurovascular coupling in humans. *The Journal of Physiology*, 598(21), 4927–4939. <https://doi.org/10.1113/JP280162>
- Hoiland, R. L., Fisher, J. A., & Ainslie, P. N. (2019). Regulation of the cerebral circulation by arterial carbon dioxide. *Comprehensive Physiology*, 9(3), 1101–1154.
<https://doi.org/10.1002/CPHY.C180021>
- Hoiland, R. L., Howe, C. A., Coombs, G. B., & Ainslie, P. N. (2018). Ventilatory and cerebrovascular regulation and integration at high-altitude. *Clinical Autonomic Research*, 28(4), 423–435.
<https://doi.org/10.1007/s10286-018-0522-2>
- Hoiland, R. L., MacLeod, D. B., Stacey, B. S., Caldwell, H. G., Howe, C. A., Nowak-Flück, D., Carr, J. M. J. R., Tymko, M. M., Coombs, G. B., Patrician, A., Tremblay, J. C., Van Mierlo, M., Gasho, C., Stembridge, M., Sekhon, M. S., Bailey, D. M., & Ainslie, P. N. (2023). Hemoglobin and cerebral hypoxic vasodilation in humans: evidence for nitric oxide-dependent and S-nitrosothiol mediated signal transduction. *Journal of Cerebral Blood Flow and Metabolism*, 43(9), 1519–1531. <https://doi.org/10.1177/0271678X231169579>
- Horiuchi, M., Endo, J., Dobashi, S., Kiuchi, M., Koyama, K., & Subudhi, A. W. (2016). Effect of progressive normobaric hypoxia on dynamic cerebral autoregulation. *Experimental Physiology*, 101(10), 1276–1284. <https://doi.org/10.1113/EP085789>
- Horiuchi, M., Rossetti, G. M. K., & Oliver, S. J. (2022). Dietary nitrate supplementation effect on dynamic cerebral autoregulation in normoxia and acute hypoxia. *Journal of Cerebral Blood Flow & Metabolism*, 42(3), 486–494. <https://doi.org/10.1177/0271678X20910053>
- Hu, X. Y., Li, Z. X., Liu, H. Q., Zhang, M., Wei, M. L., Fang, S., Chen, W., Pan, H., Huang, J. X., Zhu, Y. M., & Liu, J. R. (2013). Relationship between vertebral artery hypoplasia and posterior circulation stroke in Chinese patients. *Neuroradiology*, 55(3), 291–295.
<https://doi.org/10.1007/s00234-012-1112-y>
- Huang, S. Y., Moore, L. G., McCullough, R. E., Micco, A. J., Fulco, C., Cymerman, A., Manco-Johnson, M., Weil, J. V., & Reeves, J. T. (1987). Internal carotid and vertebral arterial flow velocity in men at high altitude. *Journal of Applied Physiology (Bethesda, Md. : 1985)*, 63(1), 395–400. <https://doi.org/10.1152/JAPPL.1987.63.1.395>
- Hwaung, P., Heo, M., Bourgeois, B., Kennedy, S., Shepherd, J., & Heymsfield, S. B. (2019). Greater height is associated with a larger carotid lumen diameter. *Medicines*, 6(2), 57.

<https://doi.org/10.3390/MEDICINES6020057>

- Ihnatsenka, B., & Boezaart, A. P. (2010). Ultrasound: basic understanding and learning the language. *International Journal of Shoulder Surgery*, 4(3), 55–62. <https://doi.org/10.4103/0973-6042.76960>
- Iwasaki, K. I., Ogawa, Y., Shibata, S., & Aoki, K. (2007). Acute exposure to normobaric mild hypoxia alters dynamic relationships between blood pressure and cerebral blood flow at very low frequency. *Journal of Cerebral Blood Flow and Metabolism*, 27(4), 776–784. <https://doi.org/10.1038/SJ.JCBFM.9600384>
- Iwasaki, K. I., Zhang, R., Zuckerman, J. H., Ogawa, Y., Hansen, L. H., & Levine, B. D. (2011). Impaired dynamic cerebral autoregulation at extreme high altitude even after acclimatization. *Journal of Cerebral Blood Flow and Metabolism*, 31(1), 283–292. <https://doi.org/10.1038/JCBFM.2010.88>
- James, J. J., Klevenow, E. A., Atkinson, M. A., Vosters, E. E., Bueckers, E. P., Quinn, M. E., Kindy, S. L., Mason, A. P., Nelson, S. K., Rainwater, K. A. H., Taylor, P. V., Zippel, E. P., & Hunter, S. K. (2023). Underrepresentation of women in exercise science and physiology research is associated with authorship gender. *Journal of Applied Physiology*, 135(4), 932–942. <https://doi.org/10.1152/jappphysiol.00377.2023>
- Jansen, G. F. A., Krins, A., Basnyat, B., Bosch, A., & Odoom, J. A. (2000). Cerebral autoregulation in subjects adapted and not adapted to high altitude. *Stroke*, 31(10), 2314–2318. <https://doi.org/10.1161/01.STR.31.10.2314>
- Jansen, G. F. A., Krins, A., Basnyat, B., Odoom, J. A., & Ince, C. (2007). Role of the altitude level on cerebral autoregulation in residents at high altitude. *Journal of Applied Physiology (Bethesda, Md. : 1985)*, 103(2), 518–523. <https://doi.org/10.1152/JAPPLPHYSIOL.01429.2006>
- Jeng, J. S., & Yip, P. K. (2004). Evaluation of vertebral artery hypoplasia and asymmetry by color-coded duplex ultrasonography. *Ultrasound in Medicine and Biology*, 30(5), 605–609. <https://doi.org/10.1016/j.ultrasmedbio.2004.03.004>
- Kaczurkin, A. N., Raznahan, A., & Satterthwaite, T. D. (2018). Sex differences in the developing brain: insights from multimodal neuroimaging. *Neuropsychopharmacology* 2018 44:1, 44(1), 71–85. <https://doi.org/10.1038/s41386-018-0111-z>
- Kane, A. D., Kothmann, E., & Giussani, D. A. (2020). Detection and response to acute systemic hypoxia. *BJA Education*, 20(2), 58–64. <https://doi.org/10.1016/J.BJAE.2019.10.004>
- Katsanos, A. H., Kosmidou, M., Kyritsis, A. P., & Giannopoulos, S. (2013). Is vertebral artery hypoplasia a predisposing factor for posterior circulation cerebral ischemic events? A comprehensive review. *European Neurology*, 70(1–2), 78–83. <https://doi.org/10.1159/000351786>
- Katusic, Z. S. (1992). Endothelial L-arginine pathway and regional cerebral arterial reactivity to vasopressin. *The American Journal of Physiology*, 262(5 Pt 2), H1557–H1562. <https://doi.org/10.1152/AJPHEART.1992.262.5.H1557>
- Kaur, J., Vranish, J. R., Barbosa, T. C., Washio, T., Young, B. E., Stephens, B. Y., Matthew Brothers, R., Ogoh, S., & Fadel, P. J. (2018). Regulation of regional cerebral blood flow during graded reflex-mediated sympathetic activation via lower body negative pressure. *Journal of Applied Physiology (Bethesda, Md. : 1985)*, 125(6), 1779–1786. <https://doi.org/10.1152/JAPPLPHYSIOL.00623.2018>
- Kay, V. L., & Rickards, C. A. (2016). The role of cerebral oxygenation and regional cerebral blood flow on tolerance to central hypovolemia. *American Journal of Physiology - Regulatory Integrative and Comparative Physiology*, 310(4), R375–R383.

<https://doi.org/10.1152/ajpregu.00367.2015>

- Kay, V. L., Sprick, J. D., & Rickards, C. A. (2017). Cerebral oxygenation and regional cerebral perfusion responses with resistance breathing during central hypovolemia. *American Journal of Physiology. Regulatory, Integrative and Comparative Physiology*, *313*(2), R132–R139. <https://doi.org/10.1152/AJPREGU.00385.2016>
- Kellawan, J. M., Harrell, J. W., Roldan-Alzate, A., Wieben, O., & Schrage, W. G. (2017). Regional hypoxic cerebral vasodilation facilitated by diameter changes primarily in anterior versus posterior circulation. *Journal of Cerebral Blood Flow and Metabolism*, *37*(6), 2025–2034. <https://doi.org/10.1177/0271678X16659497>
- Kellawan, J. M., Peltonen, G. L., Harrell, J. W., Roldan-Alzate, A., Wieben, O., & Schrage, W. G. (2020). Differential contribution of cyclooxygenase to basal cerebral blood flow and hypoxic cerebral vasodilation. *American Journal of Physiology. Regulatory, Integrative and Comparative Physiology*, *318*(2), R468–R479. <https://doi.org/10.1152/AJPREGU.00132.2019>
- Kety, S. S., & Schmidt, C. F. (1945). The determination of cerebral blood flow in man by the use of nitrous oxide in low concentrations. *American Journal of Physiology - Legacy Content*, *143*(1), 53–66. <https://doi.org/10.1152/AJPLEGACY.1945.143.1.53>
- Khan, M. A., Liu, J., Tarumi, T., Lawley, J. S., Liu, P., Zhu, D. C., Lu, H., & Zhang, R. (2017). Measurement of cerebral blood flow using phase contrast magnetic resonance imaging and duplex ultrasonography. *Journal of Cerebral Blood Flow and Metabolism*, *37*(2), 541–549. <https://doi.org/10.1177/0271678X16631149>
- Koep, J. L., Bond, B., Barker, A. R., Ruediger, S. L., Pizzey, F. K., Coombes, J. S., & Bailey, T. G. (2023). Sex modifies the relationship between age and neurovascular coupling in healthy adults. *Journal of Cerebral Blood Flow & Metabolism*, *43*(8), 1254–1266. <https://doi.org/10.1177/0271678X231167753>
- Koep, J. L., Taylor, C. E., Coombes, J. S., Bond, B., Ainslie, P. N., & Bailey, T. G. (2022). Autonomic control of cerebral blood flow: fundamental comparisons between peripheral and cerebrovascular circulations in humans. *The Journal of Physiology*, *600*(1), 15–39. <https://doi.org/10.1113/JP281058>
- Koo, T. K., & Li, M. Y. (2016). A guideline of selecting and reporting intraclass correlation coefficients for reliability research. *Journal of Chiropractic Medicine*, *15*(2), 155–163. <https://doi.org/10.1016/J.JCM.2016.02.012>
- Korte, N., Nortley, R., & Attwell, D. (2020). Cerebral blood flow decrease as an early pathological mechanism in Alzheimer's disease. *Acta Neuropathologica*, *140*(6), 793–810. <https://doi.org/10.1007/S00401-020-02215-W>
- Krabbe-Hartkamp, M. J., Van Der Grond, J., De Leeuw, F. E., De Groot, J. C., Algra, A., Hillen, B., Breteler, M. M. B., & Mali, W. P. T. M. (1998). Circle of Willis: morphologic variation on three-dimensional time-of-flight MR angiograms. *Radiology*, *207*(1), 103–112. <https://doi.org/10.1148/RADIOLOGY.207.1.9530305>
- Krejza, J., Arkuszewski, M., Kasner, S. E., Weigele, J., Ustymowicz, A., Hurst, R. W., Cucchiara, B. L., & Messe, S. R. (2006). Carotid artery diameter in men and women and the relation to body and neck size. *Stroke*, *37*(4), 1103–1105. <https://doi.org/10.1161/01.STR.0000206440.48756.F7>
- Krejza, J., Mariak, Z., Huba, M., Wolczynski, S., & Lewko, J. (2001). Effect of endogenous estrogen on blood flow through carotid arteries. *Stroke*, *32*(1), 30–36. <https://doi.org/10.1161/01.str.32.1.30>
- Krejza, J., Rudzinski, W., Arkuszewski, M., Onuoha, O., & Melhem, E. R. (2013). Cerebrovascular reactivity across the menstrual cycle in young healthy women. *The Neuroradiology Journal*,

26(4), 413–419. <https://doi.org/10.1177/197140091302600406>

- Krejza, J., Siemkowicz, J., Sawicka, M., Szylak, A., Kochanowicz, J., Mariak, Z., Lewko, J., Spektor, V., Babikian, V., & Bert, R. (2003). Oscillations of cerebrovascular resistance throughout the menstrual cycle in healthy women. *Ultrasound in Obstetrics & Gynecology*, 22(6), 627–632. <https://doi.org/10.1002/UOG.907>
- Labrecque, L., Drapeau, A., Rahimaly, K., Imhoff, S., & Brassard, P. (2021). Dynamic cerebral autoregulation and cerebrovascular carbon dioxide reactivity in middle and posterior cerebral arteries in young endurance-trained women. *Journal of Applied Physiology (Bethesda, Md. : 1985)*, 130(6), 1724–1735. <https://doi.org/10.1152/JAPPLPHYSIOL.00963.2020>
- Lafave, H. C., Zouboules, S. M., James, M. A., Purdy, G. M., Rees, J. L., Steinback, C. D., Ondrus, P., Brutsaert, T. D., Nysten, H. E., Nysten, C. E., Hoiland, R. L., Sherpa, M. T., & Day, T. A. (2019). Steady-state cerebral blood flow regulation at altitude: interaction between oxygen and carbon dioxide. *European Journal of Applied Physiology*, 119(11–12), 2529–2544. <https://doi.org/10.1007/s00421-019-04206-6>
- Lassen, N. A. (1959). Cerebral blood flow and oxygen consumption in man. *Physiological Reviews*, 39(2), 183–238. <https://doi.org/10.1152/PHYSREV.1959.39.2.183>
- Lawley, J. S., Macdonald, J. H., Oliver, S. J., & Mullins, P. G. (2017). Unexpected reductions in regional cerebral perfusion during prolonged hypoxia. *Journal of Physiology*, 595(3), 935–947. <https://doi.org/10.1113/JP272557>
- Leacy, J. K., Johnson, E. M., Lavoie, L. R., Macilwraith, D. N., Bambury, M., Martin, J. A., Lucking, E. F., Linares, A. M., Saran, G., Sheehan, D. P., Sharma, N., Day, T. A., & O'Halloran, K. D. (2022). Variation within the visually evoked neurovascular coupling response of the posterior cerebral artery is not influenced by age or sex. *Journal of Applied Physiology (Bethesda, Md. : 1985)*, 133(2), 335–348. <https://doi.org/10.1152/JAPPLPHYSIOL.00292.2021>
- Leacy, J. K., Zouboules, S. M., Mann, C. R., Peltonen, J. D. B., Saran, G., Nysten, C. E., Nysten, H. E., Brutsaert, T. D., O'Halloran, K. D., Sherpa, M. T., & Day, T. A. (2018). Neurovascular coupling remains intact during incremental ascent to high altitude (4240 m) in acclimatized healthy volunteers. *Frontiers in Physiology*, 9. <https://doi.org/10.3389/FPHYS.2018.01691>
- Levine, B. D., Zhang, R., & Roach, R. C. (1999). Dynamic cerebral autoregulation at high altitude. *Advances in Experimental Medicine and Biology*, 474, 319–322. https://doi.org/10.1007/978-1-4615-4711-2_24
- Lewis, N. C. S., Messinger, L., Monteleone, B., & Ainslie, P. N. (2014). Effect of acute hypoxia on regional cerebral blood flow: effect of sympathetic nerve activity. *Journal of Applied Physiology*, 116(9), 1189–1196. <https://doi.org/10.1152/jappphysiol.00114.2014>
- Lewis, N. C. S., Smith, K. J., Bain, A. R., Wildfong, K. W., Numan, T., & Ainslie, P. N. (2015). Impact of transient hypotension on regional cerebral blood flow in humans. *Clinical Science*, 129(2), 169–178. <https://doi.org/10.1042/CS20140751>
- Liu, J., Tseng, B. Y., Khan, M. A., Tarumi, T., Hill, C., Mirshams, N., Hodics, T. M., Hynan, L. S., & Zhang, R. (2016). Individual variability of cerebral autoregulation, posterior cerebral circulation and white matter hyperintensity. *The Journal of Physiology*, 594(11), 3141–3155. <https://doi.org/10.1113/JP271068>
- Liu, J., Zhu, Y. S., Hill, C., Armstrong, K., Tarumi, T., Hodics, T., Hynan, L. S., & Zhang, R. (2013). Cerebral autoregulation of blood velocity and volumetric flow during steady-state changes in arterial pressure. *Hypertension*, 62(5), 973–979. <https://doi.org/10.1161/HYPERTENSIONAHA.113.01867>
- Lucas, S. J. E., Burgess, K. R., Thomas, K. N., Donnelly, J., Peebles, K. C., Lucas, R. A. I., Fan, J.-L.,

- Cotter, J. D., Basnyat, R., & Ainslie, P. N. (2011). Alterations in cerebral blood flow and cerebrovascular reactivity during 14 days at 5050 m. *The Journal of Physiology*, *589*(3), 741–753. <https://doi.org/10.1113/jphysiol.2010.192534>
- Lucas, S. J. E., Tzeng, Y. C., Galvin, S. D., Thomas, K. N., Ogoh, S., & Ainslie, P. N. (2010). Influence of changes in blood pressure on cerebral perfusion and oxygenation. *Hypertension*, *55*(3), 698–705. <https://doi.org/10.1161/HYPERTENSIONAHA.109.146290>
- Mardimae, A., Balaban, D. Y., Machina, M. A., Han, J. S., Katznelson, R., Minkovich, L. L., Fedorko, L., Murphy, P. M., Wasowicz, M., Naughton, F., Meineri, M., Fisher, J. A., & Duffin, J. (2012). The interaction of carbon dioxide and hypoxia in the control of cerebral blood flow. *Pflugers Archiv : European Journal of Physiology*, *464*(4), 345–351. <https://doi.org/10.1007/S00424-012-1148-1>
- Masamoto, K., & Vazquez, A. (2018). Optical imaging and modulation of neurovascular responses. *Journal of Cerebral Blood Flow and Metabolism*, *38*(12), 2057–2072. <https://doi.org/10.1177/0271678X18803372>
- Matsutomo, N., Fukami, M., Kobayashi, K., Endo, Y., Kuhara, S., & Yamamoto, T. (2023). Effects of eyes-closed resting and eyes-open conditions on cerebral blood flow measurement using arterial spin labeling magnetic resonance imaging. *Neurology and Clinical Neuroscience*, *11*(1), 10–16. <https://doi.org/10.1111/NCN3.12674>
- Mattos, J. D., Campos, M. O., Rocha, M. P., Mansur, D. E., Rocha, H. N. M., Garcia, V. P., Batista, G., Alvares, T. S., Oliveira, G. V., Souza, M. V., Videira, R. L. R., Rocha, N. G., Secher, N. H., Nóbrega, A. C. L., & Fernandes, I. A. (2019). Human brain blood flow and metabolism during isocapnic hyperoxia: the role of reactive oxygen species. *The Journal of Physiology*, *597*(3), 741–755. <https://doi.org/10.1113/JP277122>
- Mattos, J. D., Campos, M. O., Rocha, M. P., Mansur, D. E., Rocha, H. N. M., Garcia, V. P., Rocha, N. G., Alvares, T. S., Secher, N. H., Nóbrega, A. C. L., & Fernandes, I. A. (2020). Differential vasomotor responses to isocapnic hyperoxia: cerebral versus peripheral circulation. *American Journal of Physiology - Regulatory Integrative and Comparative Physiology*, *318*(1), R182–R187. <https://doi.org/10.1152/ajpregu.00248.2019>
- Mazioti, A., Economopoulos, N., Papakonstantinou, O., Kontopoulou, C., Filippiadis, D., Maratsos, A., Kelekis, N., & Alexopoulou, E. (2013). High resolution MR angiography of the posterior cerebral circulation: variants, incidence and clinical impact. *Open Journal of Radiology*, *2013*(04), 209–214. <https://doi.org/10.4236/OJRAD.2013.34034>
- Min, J. H., & Lee, Y. S. (2007). Transcranial Doppler ultrasonographic evaluation of vertebral artery hypoplasia and aplasia. *Journal of the Neurological Sciences*, *260*(1–2), 183–187. <https://doi.org/10.1016/J.JNS.2007.05.001>
- Morris, L. E., Flück, D., Ainslie, P. N., & McManus, A. M. (2017). Cerebrovascular and ventilatory responses to acute normobaric hypoxia in girls and women. *Physiological Reports*, *5*(15), e13372. <https://doi.org/10.14814/phy2.13372>
- Müller, H. R., Brunhölzl, C., Radü, E. W., & Buser, M. (1991). Sex and side differences of cerebral arterial caliber. *Neuroradiology*, *33*(3), 212–216. <https://doi.org/10.1007/BF00588220>
- Nakagawa, K., Serrador, J. M., Larose, S. L., Moslehi, F., Lipsitz, L. A., & Sorond, F. A. (2009). Autoregulation in the posterior circulation is altered by the metabolic state of the visual cortex. *Stroke*, *40*(6), 2062–2067. <https://doi.org/10.1161/STROKEAHA.108.545285>
- Neto, A. C. L., Bittar, R., Gattas, G. S., Bor-Seng-Shu, E., de Lima Oliveira, M., da Costa Monsanto, R., & Bittar, L. F. (2017). Pathophysiology and diagnosis of vertebrobasilar insufficiency: a review of the literature. *International Archives of Otorhinolaryngology*, *21*(3), 302–307. <https://doi.org/10.1055/S-0036-1593448>

- Newman, L., O'Connor, J. D., Nolan, H., Reilly, R. B., & Kenny, R. A. (2022). Age and sex related differences in orthostatic cerebral oxygenation: findings from 2764 older adults in the Irish Longitudinal Study on Ageing (TILDA). *Experimental Gerontology*, *167*, 111903. <https://doi.org/10.1016/J.EXGER.2022.111903>
- Ng, A., & Swanevelder, J. (2011). Resolution in ultrasound imaging. *Continuing Education in Anaesthesia Critical Care & Pain*, *11*(5), 186–192. <https://doi.org/10.1093/BJACEACCP/MKR030>
- Nicolau, C., Gilabert, R., García, A., Blasco, J., Chamorro, A., & Brú, C. (2001). Effect of internal carotid artery occlusion on vertebral artery blood flow: a duplex ultrasonographic evaluation. *Journal of Ultrasound in Medicine*, *20*(2), 105–111. <https://doi.org/10.7863/JUM.2001.20.2.105>
- Nishimura, N., Iwasaki, K. I., Ogawa, Y., & Aoki, K. (2010). Decreased steady-state cerebral blood flow velocity and altered dynamic cerebral autoregulation during 5-h sustained 15% O₂ hypoxia. *Journal of Applied Physiology (Bethesda, Md. : 1985)*, *108*(5), 1154–1161. <https://doi.org/10.1152/JAPPLPHYSIOL.00656.2009>
- Oglat, A. A., Matjafri, M. Z., Suardi, N., Oqlat, M. A., Abdelrahman, M. A., & Oqlat, A. A. (2018). A review of medical Doppler ultrasonography of blood flow in general and especially in common carotid artery. *Journal of Medical Ultrasound*, *26*(1), 3–13. https://doi.org/10.4103/JMU.JMU_11_17
- Ogoh, S. (2017). Relationship between cognitive function and regulation of cerebral blood flow. *Journal of Physiological Sciences*, *67*(3), 345–351. <https://doi.org/10.1007/s12576-017-0525-0>
- Ogoh, S., Hirasawa, A., Raven, P. B., Rebuffat, T., Denise, P., Lericollais, R., Sugawara, J., & Normand, H. (2015). Effect of an acute increase in central blood volume on cerebral hemodynamics. *American Journal of Physiology. Regulatory, Integrative and Comparative Physiology*, *309*(8), R902–R911. <https://doi.org/10.1152/AJPREGU.00137.2015>
- Ogoh, S., Nakahara, H., Ainslie, P. N., & Miyamoto, T. (2010). The effect of oxygen on dynamic cerebral autoregulation: critical role of hypocapnia. *Journal of Applied Physiology (Bethesda, Md. : 1985)*, *108*(3), 538–543. <https://doi.org/10.1152/JAPPLPHYSIOL.01235.2009>
- Ogoh, S., Nakahara, H., Ueda, S., Okazaki, K., Shibasaki, M., Subudhi, A. W., & Miyamoto, T. (2014). Effects of acute hypoxia on cerebrovascular responses to carbon dioxide. *Experimental Physiology*, *99*(6), 849–858. <https://doi.org/10.1113/EXPPHYSIOL.2013.076802>
- Ogoh, S., Nakata, H., Miyamoto, T., Bailey, D. M., & Shibasaki, M. (2018). Dynamic cerebral autoregulation during cognitive task: effect of hypoxia. *Journal of Applied Physiology (Bethesda, Md. : 1985)*, *124*(6), 1413–1419. <https://doi.org/10.1152/JAPPLPHYSIOL.00909.2017>
- Ogoh, S., Sato, K., Nakahara, H., Okazaki, K., Subudhi, A. W., & Miyamoto, T. (2013). Effect of acute hypoxia on blood flow in vertebral and internal carotid arteries. *Experimental Physiology*, *98*(3), 692–698. <https://doi.org/10.1113/expphysiol.2012.068015>
- Olesen, N. D., Nielsen, H. B., Olsen, N. V., & Secher, N. H. (2019). The age-related reduction in cerebral blood flow affects vertebral artery more than internal carotid artery blood flow. *Clinical Physiology and Functional Imaging*, *39*(4), 255–260. <https://doi.org/10.1111/CPF.12568>
- Onoue, H., Nakamura, N., & Toda, N. (1988). Endothelium-dependent and -independent responses to vasodilators of isolated dog cerebral arteries. *Stroke*, *19*(11), 1388–1394. <https://doi.org/10.1161/01.STR.19.11.1388>
- Pabbidi, M. R., Kuppusamy, M., Didion, S. P., Sanapureddy, P., Reed, J. T., & Sontakke, S. P. (2018). Sex differences in the vascular function and related mechanisms: role of 17 β -estradiol. *American Journal of Physiology. Heart and Circulatory Physiology*, *315*(6), H1499–H1518.

<https://doi.org/10.1152/AJPHEART.00194.2018>

- Pamenter, M. E., & Powell, F. L. (2016). Time domains of the hypoxic ventilatory response and their molecular basis. *Comprehensive Physiology*, 6(3), 1345–1385. <https://doi.org/10.1002/CPHY.C150026>
- Panerai, R. B. (2008). Cerebral autoregulation: from models to clinical applications. *Cardiovascular Engineering*, 8(1), 42–59. <https://doi.org/10.1007/S10558-007-9044-6/METRICS>
- Panerai, R. B., Brassard, P., Burma, J. S., Castro, P., Claassen, J. A. H. R., van Lieshout, J. J., Liu, J., Lucas, S. J. E., Minhas, J. S., Mitsis, G. D., Nogueira, R. C., Ogoh, S., Payne, S. J., Rickards, C. A., Robertson, A. D., Rodrigues, G. D., Smirl, J. D., & Simpson, D. M. (2023). Transfer function analysis of dynamic cerebral autoregulation: a CARNET white paper 2022 update. *Journal of Cerebral Blood Flow and Metabolism*, 43(1), 3–25. <https://doi.org/10.1177/0271678X221119760>
- Panerai, R. B., Deverson, S. T., Mahony, P., Hayes, P., & Evans, D. H. (1999). Effects of CO₂ on dynamic cerebral autoregulation measurement. *Physiological Measurement*, 20(3), 265–275. <https://doi.org/10.1088/0967-3334/20/3/304>
- Park, J. H., Kim, J. M., & Roh, J. K. (2007). Hypoplastic vertebral artery: frequency and associations with ischaemic stroke territory. *Journal of Neurology, Neurosurgery, and Psychiatry*, 78(9), 954–958. <https://doi.org/10.1136/JNNP.2006.105767>
- Park, M. Y., Jung, S. E., Byun, J. Y., Kim, J. H., & Joo, G. E. (2012). Effect of beam-flow angle on velocity measurements in modern Doppler ultrasound systems. *AJR. American Journal of Roentgenology*, 198(5), 1139–1143. <https://doi.org/10.2214/AJR.11.7475>
- Paulson, O., Strandgaard, S., & Edvinsson, L. (1990). Cerebral autoregulation. *Cerebrovasc Brain Metab Rev.*, 2(2), 161–192.
- Peltonen, G. L., Harrell, J. W., Aleckson, B. P., LaPlante, K. M., Crain, M. K., & Schrage, W. G. (2016). Cerebral blood flow regulation in women across menstrual phase: differential contribution of cyclooxygenase to basal, hypoxic, and hypercapnic vascular tone. *American Journal of Physiology. Regulatory, Integrative and Comparative Physiology*, 311(2), R222–R231. <https://doi.org/10.1152/AJPREGU.00106.2016>
- Peltonen, G. L., Harrell, J. W., Rousseau, C. L., Ernst, B. S., Marino, M. L., Crain, M. K., & Schrage, W. G. (2015). Cerebrovascular regulation in men and women: stimulus-specific role of cyclooxygenase. *Physiological Reports*, 3(7), e12451. <https://doi.org/10.14814/PHY2.12451>
- Peterson, E. C., Wang, Z., & Britz, G. (2011). Regulation of cerebral blood flow. *International Journal of Vascular Medicine*, 2011. <https://doi.org/10.1155/2011/823525>
- Phillips, A. A., Chan, F. H., Zheng, M. M. Z., Krassioukov, A. V., & Ainslie, P. N. (2016). Neurovascular coupling in humans: physiology, methodological advances and clinical implications. *Journal of Cerebral Blood Flow & Metabolism*, 36(4), 647–664. <https://doi.org/10.1177/0271678X15617954>
- Poulin, M. J., Fatemian, M., Tansley, J. G., O'Connor, D. F., & Robbins, P. A. (2002). Changes in cerebral blood flow during and after 48 h of both isocapnic and poikilocapnic hypoxia in humans. *Experimental Physiology*, 87(5), 633–642. <https://doi.org/10.1113/EPH8702437>
- Poulin, M. J., Liang, P. J., & Robbins, P. A. (1996). Dynamics of the cerebral blood flow response to step changes in end-tidal PCO₂ and PO₂ in humans. *Journal of Applied Physiology (Bethesda, Md. : 1985)*, 81(3), 1084–1095. <https://doi.org/10.1152/JAPPL.1996.81.3.1084>
- Powell, F. L., Milsom, W. K., & Mitchell, G. S. (1998). Time domains of the hypoxic ventilatory response. *Respiration Physiology*, 112(2), 123–134. [https://doi.org/10.1016/S0034-5687\(98\)00026-7](https://doi.org/10.1016/S0034-5687(98)00026-7)

- Purkayastha, S., & Sorond, F. (2012). Transcranial Doppler ultrasound: technique and application. *Seminars in Neurology*, 32(4), 411–420. <https://doi.org/10.1055/S-0032-1331812>
- Querido, J. S., Ainslie, P. N., Foster, G. E., Henderson, W. R., Halliwill, J. R., Ayas, N. T., & Sheel, A. W. (2013). Dynamic cerebral autoregulation during and following acute hypoxia: role of carbon dioxide. *Journal of Applied Physiology (Bethesda, Md. : 1985)*, 114(9), 1183–1190. <https://doi.org/10.1152/JAPPLPHYSIOL.00024.2013>
- Raichle, M. E., & Gusnard, D. A. (2002). Appraising the brain's energy budget. *Proceedings of the National Academy of Sciences of the United States of America*, 99(16), 10237–10239. <https://doi.org/10.1073/PNAS.172399499>
- Reehal, N., Cummings, S., Mullen, M. T., Baker, W. B., Kung, D., Tackett, W., & Favilla, C. G. (2021). Differentiating dynamic cerebral autoregulation across vascular territories. *Frontiers in Neurology*, 12, 653167. <https://doi.org/10.3389/FNEUR.2021.653167/BIBTEX>
- Rich-Edwards, J. W., Kaiser, U. B., Chen, G. L., Manson, J. A. E., & Goldstein, J. M. (2018). Sex and gender differences research design for basic, clinical, and population studies: essentials for investigators. *Endocrine Reviews*, 39(4), 424–439. <https://doi.org/10.1210/ER.2017-00246>
- Riggs, H. E., & Rupp, C. (1963). Variation in form of circle of Willis: The relation of the variations to collateral circulation: Anatomic analysis. *Archives of Neurology*, 8(1), 8–14. <https://doi.org/10.1001/ARCHNEUR.1963.00460010024002>
- Roach, R. C., Hackett, P. H., Oelz, O., Bärtsch, P., Luks, A. M., MacInnis, M. J., Baillie, J. K., Achatz, E., Albert, E., Zafren, K., Yaron, M., Willmann, G., Wilkes, M., West, J. B., Wang, S. H., Wagner, D. R., Voituron, N., Ulrich, S., Twomey, R., ... Andrews, J. S. (2018). The 2018 Lake Louise acute mountain sickness score. *High Altitude Medicine & Biology*, 19(1), 4–6. <https://doi.org/10.1089/HAM.2017.0164>
- Robertson, A. D., Papadhima, I., & Edgell, H. (2020). Sex differences in the autonomic and cerebrovascular responses to upright tilt. *Autonomic Neuroscience*, 229, 102742. <https://doi.org/10.1016/J.AUTNEU.2020.102742>
- Robison, L. S., Gannon, O. J., Salinero, A. E., & Zuloaga, K. L. (2019). Contributions of sex to cerebrovascular function and pathology. *Brain Research*, 1710, 43–60. <https://doi.org/10.1016/J.BRAINRES.2018.12.030>
- Rocha, M. P., Campos, M. O., Mattos, J. D., Mansur, D. E., Rocha, H. N. M., Secher, N. H., Nóbrega, A. C. L., & Fernandes, I. A. (2020). KATP channels modulate cerebral blood flow and oxygen delivery during isocapnic hypoxia in humans. *The Journal of Physiology*, 598(16), 3343–3356. <https://doi.org/10.1113/JP279751>
- Rodriguez, G., Warkentin, S., Risberg, J., & Rosadini, G. (1988). Sex differences in regional cerebral blood flow. *Journal of Cerebral Blood Flow and Metabolism*, 8(6), 783–789. <https://doi.org/10.1038/JCBFM.1988.133>
- Rogan, M., Friend, A. T., Rossetti, G. M., Edden, R., Mikkelsen, M., Oliver, S. J., Macdonald, J. H., & Mullins, P. G. (2022). Hypoxia alters posterior cingulate cortex metabolism during a memory task: a 1H fMRS study. *NeuroImage*, 260. <https://doi.org/10.1016/J.NEUROIMAGE.2022.119397>
- Romero, J. R., Pikula, A., Nguyen, T. N., Nien, Y. L., Norbash, A., & Babikian, V. L. (2010). Cerebral collateral circulation in carotid artery disease. *Current Cardiology Reviews*, 5(4), 279–288. <https://doi.org/10.2174/157340309789317887>
- Rosengarten, B., & Kaps, M. (2002). Cerebral autoregulation in middle cerebral artery territory precedes that of posterior cerebral artery in human cortex. *Cerebrovascular Diseases (Basel, Switzerland)*, 13(1), 21–25. <https://doi.org/10.1159/000047741>

- Rossetti, G. M., D'Avossa, G., Rogan, M., Macdonald, J. H., Oliver, S. J., & Mullins, P. G. (2020). Reversal of neurovascular coupling in the default mode network: evidence from hypoxia. *Journal of Cerebral Blood Flow & Metabolism*, 0271678X2093082. <https://doi.org/10.1177/0271678X20930827>
- Ryan, D. J., Byrne, S., Dunne, R., Harmon, M., & Harbison, J. (2015). White matter disease and an incomplete circle of Willis. *International Journal of Stroke*, 10(4), 547–552. <https://doi.org/10.1111/IJS.12042>
- Samora, M., Vianna, L. C., Carmo, J. C., Macedo, V., Dawes, M., Phillips, A. A., Paton, J. F. R., & Fisher, J. P. (2020). Neurovascular coupling is not influenced by lower body negative pressure in humans. *American Journal of Physiology. Heart and Circulatory Physiology*, 319(1), H2–H31. <https://doi.org/10.1152/AJPHEART.00076.2020>
- Sato, K., Fisher, J. P., Seifert, T., Overgaard, M., Secher, N. H., & Ogoh, S. (2012). Blood flow in internal carotid and vertebral arteries during orthostatic stress. *Experimental Physiology*, 97(12), 1272–1280. <https://doi.org/10.1113/expphysiol.2012.064774>
- Sato, K., Oue, A., Yoneya, M., Sadamoto, T., & Ogoh, S. (2016). Heat stress redistributes blood flow in arteries of the brain during dynamic exercise. *Journal of Applied Physiology*, 120(7), 766–773. <https://doi.org/10.1152/jappphysiol.00353.2015>
- Sato, K., Sadamoto, T., Hirasawa, A., Oue, A., Subudhi, A. W., Miyazawa, T., & Ogoh, S. (2012). Differential blood flow responses to CO₂ in human internal and external carotid and vertebral arteries. *Journal of Physiology*, 590(14), 3277–3290. <https://doi.org/10.1113/jphysiol.2012.230425>
- Sato, K., Yoneya, M., Otsuki, A., Sadamoto, T., & Ogoh, S. (2015). Anatomical vertebral artery hypoplasia and insufficiency impairs dynamic blood flow regulation. *Clinical Physiology and Functional Imaging*, 35(6), 485–489. <https://doi.org/10.1111/CPF.12179>
- Savitz, S., & Caplan, L. (2005). Vertebrobasilar disease. *The New England Journal of Medicine*, 352(25), 131–140. <https://doi.org/10.1056/NEJMRA041544>
- Scheel, P., Ruge, C., Petruich, U. R., & Schöning, M. (2000). Color duplex measurement of cerebral blood flow volume in healthy adults. *Stroke*, 31(1), 147–150. <https://doi.org/10.1161/01.STR.31.1.147>
- Scheel, P., Ruge, C., & Schöning, M. (2000). Flow velocity and flow volume measurements in the extracranial carotid and vertebral arteries in healthy adults: reference data and the effects of age. *Ultrasound in Medicine & Biology*, 26(8), 1261–1266. [https://doi.org/10.1016/S0301-5629\(00\)00293-3](https://doi.org/10.1016/S0301-5629(00)00293-3)
- Schöning, M., Walter, J., & Scheel, P. (1994). Estimation of cerebral blood flow through color duplex sonography of the carotid and vertebral arteries in healthy adults. *Stroke*, 25(1), 17–22. <https://doi.org/10.1161/01.str.25.1.17>
- Seidel, E., Eicke, B. M., Tettenborn, B., & Krummenauer, F. (1999). Reference values for vertebral artery flow volume by duplex sonography in young and elderly adults. *Stroke*, 30(12), 2692–2696. <https://doi.org/10.1161/01.STR.30.12.2692>
- Shenouda, N., Gillen, J. B., Gibala, M. J., & MacDonald, M. J. (2017). Changes in brachial artery endothelial function and resting diameter with moderate-intensity continuous but not sprint interval training in sedentary men. *Journal of Applied Physiology*, 123(4), 773–780. <https://doi.org/10.1152/jappphysiol.00058.2017>
- Silverman, A., & Petersen, N. H. (2023). Physiology, cerebral autoregulation. *StatPearls*. <https://www.ncbi.nlm.nih.gov/books/NBK553183/>
- Smirl, J. D., Lucas, S. J. E., Lewis, N. C. S., Dumanior, G. R., Smith, K. J., Bakker, A., Basnyat, A.

- S., & Ainslie, P. N. (2014). Cerebral pressure-flow relationship in lowlanders and natives at high altitude. *Journal of Cerebral Blood Flow and Metabolism*, *34*(2), 248–257. <https://doi.org/10.1038/JCBFM.2013.178>
- Sorond, F. A., Khavari, R., Serrador, J. M., & Lipsitz, L. A. (2005). Regional cerebral autoregulation during orthostatic stress: age-related differences. *The Journals of Gerontology. Series A, Biological Sciences and Medical Sciences*, *60*(11), 1484–1487. <https://doi.org/10.1093/GERONA/60.11.1484>
- Strandgaard, S., & Paulson, O. B. (1984). Cerebral autoregulation. *Stroke*, *15*(3), 161–192. <https://doi.org/10.1161/01.STR.15.3.413>
- Strandgaard, S., & Sigurdsson, S. T. (2008). Point:Counterpoint: sympathetic activity does/does not influence cerebral blood flow. Counterpoint: sympathetic nerve activity does not influence cerebral blood flow. *Journal of Applied Physiology (Bethesda, Md. : 1985)*, *105*(4), 1366–1367. <https://doi.org/10.1152/JAPPLPHYSIOL.90597.2008A>
- Subudhi, A. W., Fan, J. L., Evero, O., Bourdillon, N., Kayser, B., Julian, C. G., Lovering, A. T., & Roach, R. C. (2014). AltitudeOmics: Effect of ascent and acclimatization to 5260 m on regional cerebral oxygen delivery. *Experimental Physiology*, *99*(5), 772–781. <https://doi.org/10.1113/expphysiol.2013.075184>
- Subudhi, A. W., Grajzel, K., Langolf, R. J., Roach, R. C., Panerai, R. B., & Davis, J. E. (2015). Cerebral autoregulation index at high altitude assessed by thigh-cuff and transfer function analysis techniques. *Experimental Physiology*, *100*(2), 173–181. <https://doi.org/10.1113/EXPPHYSIOL.2014.082479>
- Subudhi, A. W., Panerai, R. B., & Roach, R. C. (2009). Acute hypoxia impairs dynamic cerebral autoregulation: results from two independent techniques. *Journal of Applied Physiology*, *107*(4), 1165–1171. <https://doi.org/10.1152/JAPPLPHYSIOL.00498.2009>
- Subudhi, A. W., Panerai, R. B., & Roach, R. C. (2010). Effects of hypobaric hypoxia on cerebral autoregulation. *Stroke*, *41*(4), 641–646. <https://doi.org/10.1161/STROKEAHA.109.574749>
- Suzuki, Y., Satoh, S. I., Oyama, H., Takayasu, M., & Shibuya, M. (1993). Regional differences in the vasodilator response to vasopressin in canine cerebral arteries in vivo. *Stroke*, *24*(7), 1049–1053. <https://doi.org/10.1161/01.STR.24.7.1049>
- Swinford, C. G., Risacher, S. L., Wu, Y. C., Apostolova, L. G., Gao, S., Bice, P. J., & Saykin, A. J. (2023). Altered cerebral blood flow in older adults with alzheimer’s disease: a systematic review. *Brain Imaging and Behavior*, *17*(2), 223–256. <https://doi.org/10.1007/S11682-022-00750-6>
- Szabo, K., Lako, E., Juhasz, T., Rosengarten, B., Csiba, L., & Olah, L. (2011). Hypocapnia induced vasoconstriction significantly inhibits the neurovascular coupling in humans. *Journal of the Neurological Sciences*, *309*(1–2), 58–62. <https://doi.org/10.1016/J.JNS.2011.07.026>
- Tarumi, T., & Zhang, R. (2018). Cerebral blood flow in normal aging adults: cardiovascular determinants, clinical implications, and aerobic fitness. *Journal of Neurochemistry*, *144*(5), 595–608. <https://doi.org/10.1111/JNC.14234>
- ter Laan, M., Van Dijk, J. M. C., Elting, J. W. J., Staal, M. J., & Absalom, A. R. (2013). Sympathetic regulation of cerebral blood flow in humans: a review. *British Journal of Anaesthesia*, *111*(3), 361–367. <https://doi.org/10.1093/BJA/AET122>
- Ter Minassian, A., Beydon, L., Ursino, M., Gardette, B., Gortan, C., & Richalet, J. P. (2001). Doppler study of middle cerebral artery blood flow velocity and cerebral autoregulation during a simulated ascent of Mount Everest. *Wilderness & Environmental Medicine*, *12*(3), 175–183. [https://doi.org/10.1580/1080-6032\(2001\)012\[0175:dsomca\]2.0.co;2](https://doi.org/10.1580/1080-6032(2001)012[0175:dsomca]2.0.co;2)

- Thierfelder, K. M., Baumann, A. B., Sommer, W. H., Armbruster, M., Opherk, C., Janssen, H., Reiser, M. F., Straube, A., & von Baumgarten, L. (2014). Vertebral artery hypoplasia: Frequency and effect on cerebellar blood flow characteristics. *Stroke*, *45*(5), 1363–1368. <https://doi.org/10.1161/STROKEAHA.113.004188>
- Thijssen, D. H. J., Black, M. A., Pyke, K. E., Padilla, J., Atkinson, G., Harris, R. A., Parker, B., Widlansky, M. E., Tschakovsky, M. E., & Green, D. J. (2011). Assessment of flow-mediated dilation in humans: a methodological and physiological guideline. *American Journal of Physiology - Heart and Circulatory Physiology*, *300*(1), H2–H12. <https://doi.org/10.1152/AJPHEART.00471.2010>
- Thomas, K. N., Lewis, N. C. S., Hill, B. G., & Ainslie, P. N. (2015). Technical recommendations for the use of carotid duplex ultrasound for the assessment of extracranial blood flow. *American Journal of Physiology - Regulatory Integrative and Comparative Physiology*, *309*(7), R707–R720. <https://doi.org/10.1152/ajpregu.00211.2015>
- Thrall, S. F., Tymko, M. M., Green, C. L. M., Wynnyk, K. I., Brandt, R. A., & Day, T. A. (2021). The effect of hypercapnia on regional cerebral blood flow regulation during progressive lower-body negative pressure. *European Journal of Applied Physiology*, *121*(1), 339–349. <https://doi.org/10.1007/S00421-020-04506-2>
- Tiecks, F. P., Lam, A. M., Aaslid, R., & Newell, D. W. (1995). Comparison of static and dynamic cerebral autoregulation measurements. *Stroke*, *26*(6), 1014–1019. <https://doi.org/10.1161/01.STR.26.6.1014>
- Touboul, P. J., Bousser, M. G., LaPlane, D., & Castaione, P. (1986). Duplex scanning of normal vertebral arteries. *Stroke*, *17*(5), 921–923. <https://doi.org/10.1161/01.STR.17.5.921>
- Tymko, M. M., Ainslie, P. N., & Smith, K. J. (2018). Evaluating the methods used for measuring cerebral blood flow at rest and during exercise in humans. *European Journal of Applied Physiology*, *118*(8), 1527–1538. <https://doi.org/10.1007/s00421-018-3887-y>
- Tymko, M. M., Hansen, A. B., Tremblay, J. C., Patrician, A., Hoiland, R. L., Howe, C. A., Rieger, M. G., & Ainslie, P. N. (2020). UBC-Nepal expedition: dynamic cerebral autoregulation is attenuated in lowlanders upon ascent to 5050 m. *European Journal of Applied Physiology*, *120*(3), 675–686. <https://doi.org/10.1007/S00421-020-04307-7>
- Tymko, M. M., Rickards, C. A., Skow, R. J., Ingram-Cotton, N. C., Howatt, M. K., & Day, T. A. (2016). The effects of superimposed tilt and lower body negative pressure on anterior and posterior cerebral circulations. *Physiological Reports*, *4*(17), e12957. <https://doi.org/10.14814/PHY2.12957>
- Tymko, M. M., Skow, R. J., Mackay, C. M., & Day, T. A. (2015). Steady-state tilt has no effect on cerebrovascular CO₂ reactivity in anterior and posterior cerebral circulations. *Experimental Physiology*, *100*(7), 839–851. <https://doi.org/10.1113/EP085084>
- Tzeng, Y. C., & Ainslie, P. N. (2014). Blood pressure regulation IX: cerebral autoregulation under blood pressure challenges. *European Journal of Applied Physiology*, *114*(3), 545–559. <https://doi.org/10.1007/S00421-013-2667-Y>
- Tzeng, Y. C., Ainslie, P. N., Cooke, W. H., Peebles, K. C., Willie, C. K., MacRae, B. A., Smirl, J. D., Horsman, H. M., & Rickards, C. A. (2012). Assessment of cerebral autoregulation: the quandary of quantification. *American Journal of Physiology. Heart and Circulatory Physiology*, *303*(6), H658–H671. <https://doi.org/10.1152/AJPHEART.00328.2012>
- Umbrello, M., Dyson, A., Feelisch, M., & Singer, M. (2013). The key role of nitric oxide in hypoxia: hypoxic vasodilation and energy supply-demand matching. *Antioxidants & Redox Signaling*, *19*(14), 1690–1710. <https://doi.org/10.1089/ARS.2012.4979>

- van Beek, A. H. E. A., Claassen, J. A. H. R., Rikkert, M. G. M. O., & Jansen, R. W. M. M. (2008). Cerebral autoregulation: an overview of current concepts and methodology with special focus on the elderly. *Journal of Cerebral Blood Flow and Metabolism*, 28(6), 1071–1085. <https://doi.org/10.1038/JCBFM.2008.13>
- van Campen, C. (Linda) M. C., Verheugt, F. W. A., & Visser, F. C. (2018). Cerebral blood flow changes during tilt table testing in healthy volunteers, as assessed by Doppler imaging of the carotid and vertebral arteries. *Clinical Neurophysiology Practice*, 3, 91–95. <https://doi.org/10.1016/j.cnp.2018.02.004>
- van Dorp, E., Los, M., Dirven, P., Sarton, E., Valk, P., Teppema, L., Stienstra, R., & Dahan, A. (2007). Inspired carbon dioxide during hypoxia: effects on task performance and cerebral oxygen saturation. *Aviat Space Environ Med*, 78(7), 666–672.
- van Helmond, N., Johnson, B. D., Holbein, W. W., Petersen-Jones, H. G., Harvey, R. E., Ranadive, S. M., Barnes, J. N., Curry, T. B., Convertino, V. A., & Joyner, M. J. (2018). Effect of acute hypoxemia on cerebral blood flow velocity control during lower body negative pressure. *Physiological Reports*, 6(4), e13594. <https://doi.org/10.14814/PHY2.13594>
- van Lieshout, J. J., & Secher, N. H. (2008). Point:Counterpoint: sympathetic activity does/does not influence cerebral blood flow. Point: sympathetic activity does influence cerebral blood flow. *Journal of Applied Physiology (Bethesda, Md. : 1985)*, 105(4), 1364–1366. <https://doi.org/10.1152/JAPPLPHYSIOL.90597.2008>
- van Mook, W. N. K. A., Rennenberg, R. J. M. W., Schurink, G. W., van Oostenbrugge, R. J., Mess, W. H., Hofman, P. A. M., & De Leeuw, P. W. (2005). Cerebral hyperperfusion syndrome. *The Lancet Neurology*, 4(12), 877–888. [https://doi.org/10.1016/S1474-4422\(05\)70251-9](https://doi.org/10.1016/S1474-4422(05)70251-9)
- Van Osta, A., Moraine, J. J., Mélot, C., Mairbörl, H., Maggiorini, M., & Naeije, R. (2005). Effects of high altitude exposure on cerebral hemodynamics in normal subjects. *Stroke*, 36(3), 557–560. <https://doi.org/10.1161/01.STR.0000155735.85888.13>
- Vavilala, M. S., Kincaid, M. S., Muangman, S. L., Suz, P., Rozet, I., & Lam, A. M. (2005). Gender differences in cerebral blood flow velocity and autoregulation between the anterior and posterior circulations in healthy children. *Pediatric Research*, 58(3), 574–578. <https://doi.org/10.1203/01.PDR.0000179405.30737.0F>
- Verbree, J., Bronzwaer, A. G. T., van Buchem, M. A., Daemen, M. J. A. P., van Lieshout, J. J., & van Osch, M. J. P. (2017). Middle cerebral artery diameter changes during rhythmic handgrip exercise in humans. *Journal of Cerebral Blood Flow and Metabolism*, 37(8), 2921–2927. <https://doi.org/10.1177/0271678X16679419>
- Verbree, J., Bronzwaer, A. S. G. T., Ghariq, E., Versluis, M. J., Daemen, M. J. A. P., Van Buchem, M. A., Dahan, A., van Lieshout, J. J., & van Osch, M. J. P. (2014). Assessment of middle cerebral artery diameter during hypocapnia and hypercapnia in humans using ultra-high-field MRI. *Journal of Applied Physiology (Bethesda, Md. : 1985)*, 117(10), 1084–1089. <https://doi.org/10.1152/JAPPLPHYSIOL.00651.2014>
- Vianna, L. C., Fernandes, I. A., Barbosa, T. C., Amaral, T. G., Rocha, N. G., Secher, N. H., & Nóbrega, A. C. (2018). Absent increase in vertebral artery blood flow during l-arginine infusion in hypertensive men. *American Journal of Physiology. Regulatory, Integrative and Comparative Physiology*, 315(4), R820–R824. <https://doi.org/10.1152/AJPREGU.00088.2018>
- Vickers, A. J. (2001). The use of percentage change from baseline as an outcome in a controlled trial is statistically inefficient: a simulation study. *BMC Medical Research Methodology*, 1, 1–4. <https://doi.org/10.1186/1471-2288-1-6>
- Voets, T., & Nilius, B. (2009). TRPCs, GPCRs and the Bayliss effect. *The EMBO Journal*, 28(1), 4–5. <https://doi.org/10.1038/EMBOJ.2008.261>

- Wang, J., Zheng, C., Hou, B., Huang, A., Zhang, X., & Du, B. (2019). Four collateral circulation pathways were observed after common carotid artery occlusion. *BMC Neurology*, *19*(1), 201. <https://doi.org/10.1186/s12883-019-1425-0>
- Wang, Y., Cai, A., Liu, L., & Wang, Y. (2009). Sonographic diagnosis of congenital variations of the extracranial vertebral artery and assessment of its circulation. *Journal of Ultrasound in Medicine*, *28*(11), 1481–1486. <https://doi.org/10.7863/JUM.2009.28.11.1481>
- Wang, Y. J., Chao, A. C., Chung, C. P., Huang, Y. J., & Hu, H. H. (2010). Different cerebral hemodynamic responses between sexes and various vessels in orthostatic stress tests. *Journal of Ultrasound in Medicine*, *29*(9), 1299–1304. <https://doi.org/10.7863/JUM.2010.29.9.1299>
- Warnert, E. A. H., Hart, E. C., Hall, J. E., Murphy, K., & Wise, R. G. (2016). The major cerebral arteries proximal to the circle of Willis contribute to cerebrovascular resistance in humans. *Journal of Cerebral Blood Flow and Metabolism*, *36*(8), 1384–1395. <https://doi.org/10.1177/0271678X15617952>
- Warnert, E. A. H., Rodrigues, J. C. L., Burchell, A. E., Neumann, S., Ratcliffe, L. E. K., Manghat, N. E., Harris, A. D., Adams, Z., Nightingale, A. K., Wise, R. G., Paton, J. F. R., & Hart, E. C. (2016). Is high blood pressure self-protection for the brain? *Circulation Research*, *119*(12), e140–e151. <https://doi.org/10.1161/CIRCRESAHA.116.309493>
- Washio, T., Vranish, J. R., Kaur, J., Young, B. E., Katayama, K., Fadel, P. J., & Ogoh, S. (2018). Acute reduction in posterior cerebral blood flow following isometric handgrip exercise is augmented by lower body negative pressure. *Physiological Reports*, *6*(20), e13886. <https://doi.org/10.14814/PHY2.13886>
- Washio, T., Watanabe, H., & Ogoh, S. (2020). Dynamic cerebral autoregulation in anterior and posterior cerebral circulation during cold pressor test. *The Journal of Physiological Sciences : JPS*, *70*(1), 1. <https://doi.org/10.1186/S12576-020-00732-7>
- Washio, T., Watanabe, H., Suzuki, K., Saito, S., & Ogoh, S. (2022). Site-specific different dynamic cerebral autoregulation and cerebrovascular response to carbon dioxide in posterior cerebral circulation during isometric exercise in healthy young men. *Autonomic Neuroscience : Basic & Clinical*, *238*. <https://doi.org/10.1016/J.AUTNEU.2022.102943>
- Weijis, R. W. J., Shkredova, D. A., Brekelmans, A. C. M., Thijssen, D. H. J., & Claassen, J. A. H. R. (2023). Longitudinal changes in cerebral blood flow and their relation with cognitive decline in patients with dementia: current knowledge and future directions. *Alzheimer's & Dementia : The Journal of the Alzheimer's Association*, *19*(2), 532–548. <https://doi.org/10.1002/ALZ.12666>
- West, J. B. (1982). Respiratory and circulatory control at high altitudes. *The Journal of Experimental Biology*, *100*, 147–157. <https://doi.org/10.1242/JEB.100.1.147>
- White, R. P., Vallance, P., & Markus, H. S. (2000). Effect of inhibition of nitric oxide synthase on dynamic cerebral autoregulation in humans. *Clin Sci (Lond)*, *99*(6), 555–560.
- Willie, C. K., Colino, F. L., Bailey, D. M., Tzeng, Y. C., Binsted, G., Jones, L. W., Haykowsky, M. J., Bellapart, J., Ogoh, S., Smith, K. J., Smirl, J. D., Day, T. A., Lucas, S. J., Eller, L. K., & Ainslie, P. N. (2011). Utility of transcranial Doppler ultrasound for the integrative assessment of cerebrovascular function. *Journal of Neuroscience Methods*, *196*(2), 221–237. <https://doi.org/10.1016/J.JNEUMETH.2011.01.011>
- Willie, C. K., Macleod, D. B., Shaw, A. D., Smith, K. J., Tzeng, Y. C., Eves, N. D., Ikeda, K., Graham, J., Lewis, N. C., Day, T. A., & Ainslie, P. N. (2012). Regional brain blood flow in man during acute changes in arterial blood gases. *Journal of Physiology*, *590*(14), 3261–3275. <https://doi.org/10.1113/jphysiol.2012.228551>
- Willie, C. K., Smith, K. J., Day, T. A., Ray, L. A., Lewis, N. C. S., Bakker, A., MacLeod, D. B., &

- Ainslie, P. N. (2014). Regional cerebral blood flow in humans at high altitude: gradual ascent and 2 wk at 5,050 m. *Journal of Applied Physiology*, *116*(7), 905–910. <https://doi.org/10.1152/jappphysiol.00594.2013>
- Willie, C. K., Tzeng, Y. C., Fisher, J. A., & Ainslie, P. N. (2014). Integrative regulation of human brain blood flow. *Journal of Physiology*, *592*(5), 841–859. <https://doi.org/10.1113/jphysiol.2013.268953>
- Woodman, R. J., Playford, D. A., Watts, G. F., Cheetham, C., Reed, C., Taylor, R. R., Puddey, I. B., Beilin, L. J., Burke, V., Mori, T. A., & Green, D. (2001). Improved analysis of brachial artery ultrasound using a novel edge-detection software system. *Journal of Applied Physiology (Bethesda, Md. : 1985)*, *91*(2), 929–937. <https://doi.org/10.1152/JAPPL.2001.91.2.929>
- Xu, W. H. (2014). Large artery: an important target for cerebral small vessel diseases. *Annals of Translational Medicine*, *2*(8), 78. <https://doi.org/10.3978/J.ISSN.2305-5839.2014.08.10>
- Zarrinkoob, L., Ambarki, K., Wåhlin, A., Birgander, R., Eklund, A., & Malm, J. (2015). Blood flow distribution in cerebral arteries. *Journal of Cerebral Blood Flow & Metabolism*, *35*(4), 648–654. <https://doi.org/10.1038/JCBFM.2014.241>
- Zhang, H., Wang, Y., Lyu, D., Li, Y., Li, W., Wang, Q., Qin, Q., Wang, X., Gong, M., Jiao, H., Liu, W., & Jia, J. (2021). Cerebral blood flow in mild cognitive impairment and Alzheimer’s disease: A systematic review and meta-analysis. *Ageing Research Reviews*, *71*, 101450. <https://doi.org/10.1016/J.ARR.2021.101450>
- Zhang, R., Zuckerman, J. H., Giller, C. A., & Levine, B. D. (1998). Transfer function analysis of dynamic cerebral autoregulation in humans. *The American Journal of Physiology*, *274*(1 Pt 2), H233–H241. <https://doi.org/10.1152/AJPHEART.1998.274.1.H233>
- Zhou, H., Sun, J., Ji, X., Lin, J., Tang, S., Zeng, J., & Fan, Y. H. (2016). Correlation between the integrity of the circle of Willis and the severity of initial noncardiac cerebral infarction and clinical prognosis. *Medicine*, *95*(10), e2892. <https://doi.org/10.1097/MD.0000000000002892>
- Zhu, D., Montagne, A., & Zhao, Z. (2021). Alzheimer’s pathogenic mechanisms and underlying sex difference. *Cellular and Molecular Life Sciences*, *78*(11), 4907–4920. <https://doi.org/10.1007/S00018-021-03830-W>

Appendix 1: Ethical Approval for Chapter 3

Prifysgol Bangor University
YSGOL GWYDDORAU CHWARAEON, IECHYD AC YMARFER
SCHOOL OF SPORT, HEALTH AND EXERCISE SCIENCES

FORM 1 - ETHICS REVIEW AND APPROVAL FORM

Please complete **all** parts of this form.
Please attach consent and information/debriefing sheets to **all** applications

Type of project requiring approval (tick one box only)

- Staff project PhD project
 MSc project Undergraduate project
 Class demonstration

1	Title of project	Test-retest reliability of blood flow measurements from the neck arteries using Duplex ultrasound and flow mediated dilation (FMD) in the brachial artery
2	Name and e-mail address(es) of all researcher(s)	Alex Friend alexander.friend@bangor.ac.uk Liam Colley liam.colley@bangor.ac.uk Harry Nicholson peu8d0@bangor.ac.uk Liam Joyce peu71e@bangor.ac.uk
3	Name and e-mail address of supervisor (for student research)	Dr Samuel Oliver s.j.oliver@bangor.ac.uk Dr Jamie Macdonald j.h.macdonald@bangor.ac.uk Dr Aamer Sandoo a.sandoo@bangor.ac.uk Gabriella Rossetti g.rossetti@bangor.ac.uk
4	Proposed starting date	12 th November 2018
5	Proposed duration	12 months
6	What is your research question?	What is the between day test-retest reliability of extra-cranial artery blood flow and flow mediated dilation (FMD) of the brachial artery.

FORM 1 - ETHICS REVIEW AND APPROVAL FORM

ETHICS APPROVAL ACTION

Take into account the responses to this form with particular reference to the activities listed in Q14

- This project already has approval under SSHES Ethics No. _____
(Contact Mark Chitty if you are unsure of the Ethics Register number; submit completed form to the General Office)

Signature – supervising staff member Print Name Date

- This project does NOT require referral to the Ethics Committee
(Submit completed form to the General Office)

Signature – supervising staff member S.J. OLIVER 14.12.18
Print Name Date

Signature of second staff member Anthony Blanchfield 14/12/18
(Anthony Blanchfield – ethics chair at time of submission) Print Name Date

- This project requires referral to the Ethics Committee

Submit this form, the information sheet, the customised consent form (Form 2 or 3 as appropriate) and the protocol to the SSHES Ethics Committee for consideration and approval.

If approved, Ethics Committee Chair to sign below in addition to the supervising staff member.

Signature – supervising staff member Print Name Date

Signature granting approval by Print Name Date
Chair of Ethics Committee
(Dr Anthony Blanchfield)

This completed and signed form must be submitted to the General Office for registration on the SSHES Ethics Register before data collection may commence.

Appendix 2: Ethical Approval for Chapter 4

Ethical approval granted for 2019-16489 Understanding the neurovascular, neurometabolic and neuroactivational changes in the brain in response to a low oxygen environment using multimodal magnetic resonance imaging and ultrasonography.

ethics@bangor.ac.uk <ethics@bangor.ac.uk>
Mon 11/03/2019 11:41
To: Alexander Friend <alexander.friend@bangor.ac.uk>

Dear Alexander,

2019-16489 Understanding the neurovascular, neurometabolic and neuroactivational changes in the brain in response to a low oxygen environment using multimodal magnetic resonance imaging and ultrasonography.

Your research proposal number 2019-16489 has been reviewed by the School of Psychology Ethics and Research Committee and the committee are now able to confirm ethical and governance approval for the above research on the basis described in the application form, protocol and supporting documentation. This approval lasts for a maximum of three years from this date.

Ethical approval is granted for the study as it was explicitly described in the application

If you wish to make any non-trivial modifications to the research project, please submit an amendment form to the committee, and copies of any of the original documents reviewed which have been altered as a result of the amendment. Please also inform the committee immediately if participants experience any unanticipated harm as a result of taking part in your research, or if any adverse reactions are reported in subsequent literature using the same technique elsewhere.

Appendix 3: Ethical Approval for Chapters 3, 5, and 6

COLEG GWYDDORAU DYNOL
COLLEGE OF HUMAN SCIENCES

YSGOL GWYDDORAU CHWARAEON, IECHYD AC YMARFER
SCHOOL OF SPORT, HEALTH AND EXERCISE SCIENCES

Mr Alex Friend
Bangor University
LL57 2PZ



Dear Alex,

Study Title: **Cerebrovascular function during peripheral surface cooling and acute hypoxia**

REC Reference P05-20/21

Your application for ethical approval of the above project was considered by The School of Sport Health and Exercise Sciences in accordance with Bangor University's Research Ethics Policy. I am pleased to inform you that this was approved by chair's action.

Approved documents

The documents reviewed and approved are:

Document	Version	Date
Friend 2020 - FORM1 - Ethics Review & Approval P052021	2.0	3 rd February 2021
Friend 2020 – Participant Information Sheet	2.0	3 rd February 2021

Please submit signed forms and finalized versions of all other documents to shesethics@bangor.ac.uk.

After ethical review

Any additional amendments, such as a change to the approved protocol, need to be referred to the Committee for consideration quoting the REC Reference. This includes adding new sites, investigators and extension of end dates for data collection. Breaches to the approved protocol, or other serious incidents, must be reported to the REC. Failure to comply may nullify this approval.

This approval expires on 28th February 2023. It is your responsibility to reapply/request an extension if necessary.

With best wishes,

Dr Jonathan Moore
Chair, SSHES Academic Research Ethics Committee

PRIFYSGOL BANGOR
ADEILADY Y GEORGE,
SAFLE'R NORMAL,
BANGOR, GWYNEDD,
LL57 2PZ
FFÔN: (01248) 388256
EBOST: sbes@bangor.ac.uk

BANGOR UNIVERSITY
GEORGE BUILDING,
NORMAL SITE,
BANGOR, GWYNEDD,
LL57 2PZ
TEL: (01248) 388256
EMAIL: sbes@bangor.ac.uk

DR JAMIE MACDONALD
PENNAETH YR YSGOL / HEAD OF SCHOOL

Rhif Elusen Gofrestredig/ Registered Charity Number: 141565

www.bangor.ac.uk

www.bangor.ac.uk/sport

Appendix 4: Example Medical Questionnaire and Consent Form

Date: ___/___/___

Baseline Medical and Demographics Questionnaire

ID		Name		Age	
----	--	------	--	-----	--

Are you in good health? YES NO

If no, please explain

How would you describe your present level of activity?

Tick intensity level and indicate approximate duration.

Vigorous		Moderate		Low intensity	
----------	--	----------	--	---------------	--

Duration (minutes).....

How often?

< Once per month		2-3 times per week	
Once per month		4-5 times per week	
Once per week		> 5 times per week	

Have you suffered from a serious illness or accident? YES NO

If yes, please give particulars:

Do you suffer from allergies? YES NO

If yes, please give particulars:

Do you suffer, or have you ever suffered from:

	YES	NO		YES	NO
Anaemia			Epilepsy		
Diabetes			High blood pressure		

Are you currently taking medication? I.e. Anti-inflammatories or cardiovascular medication (beta-blockers, ACE-inhibitors, nitrates)

YES NO

If yes, please give particulars:

Are you currently attending your GP for any condition or have you consulted your doctor in the last three months?

YES NO

If yes, please give particulars:

Have you, or are you presently taking part in any other laboratory experiment?

YES NO

Section A: Risk Factors and Exclusions		
A1. Are you a smoker?	<input type="checkbox"/> Yes	<input type="checkbox"/> No
A2. Do you have any of the following conditions?		
a) Diabetes	<input type="checkbox"/> Yes	<input type="checkbox"/> No
b) Cardiovascular disease	<input type="checkbox"/> Yes	<input type="checkbox"/> No
c) Haematological disease	<input type="checkbox"/> Yes	<input type="checkbox"/> No
d) Chronic infectious disease	<input type="checkbox"/> Yes	<input type="checkbox"/> No
e) Neurological disorder (e.g. Alzheimer's)	<input type="checkbox"/> Yes	<input type="checkbox"/> No
f) Neuromuscular disorder (e.g. Multiple sclerosis)	<input type="checkbox"/> Yes	<input type="checkbox"/> No
g) Musculoskeletal disorders or injury that are exacerbated by exercise	<input type="checkbox"/> Yes	<input type="checkbox"/> No
h) Claustrophobia	<input type="checkbox"/> Yes	<input type="checkbox"/> No
i) Metal implants	<input type="checkbox"/> Yes	<input type="checkbox"/> No
j) Cardiac pace maker	<input type="checkbox"/> Yes	<input type="checkbox"/> No
k) Respiratory problems (e.g. asthma, bronchitis)	<input type="checkbox"/> Yes	<input type="checkbox"/> No
l) Currently pregnant	<input type="checkbox"/> Yes	<input type="checkbox"/> No
A3. Have you ever been injured by a metallic object? (e.g. shrapnel)	<input type="checkbox"/> Yes	<input type="checkbox"/> No

Section B: Headache and Migraine

B1. How often do you suffer from headaches (excluding migraine)?

- Less than monthly Monthly Weekly Daily

B2. Do you, or have you ever, suffer(ed) from migraine?

- Yes No

If **Yes**, go to
B3

If **No**, go to C1

B3. How often do you suffer from migraine?

- Less than monthly Monthly Weekly Daily

Section C: Altitude Experience

C1. What is the approximate altitude where you live for most of the year?

Meters / Feet (delete as appropriate)

C2. Have you been to altitude before (≥ 1500 m / 5000 ft)?

Yes

If **Yes**, continue answering questions below.

No

If **No**, you have completed the questionnaire. Please pass your questionnaire to the researcher.

C3. How many days in the last year have you spent above 1500m?

Days

C4. Please give the date when you were last above 1500 m

C5. Have you been to **high** altitude (≥ 2500 m / 8000 ft) before?

Yes

If **yes**, continue answering questions below.

No

If **No**, you have completed the questionnaire. Please pass your questionnaire to the researcher.

C6. Please give the date when you were last at **high** altitude (≥ 2500 m)

Section D: High Altitude Illnesses

D1. On trips to or above 2,500 m have you suffered any of the following acute mountain sickness symptoms? Please tick the maximum severity you have previously suffered.

- | | | | | |
|-------------------------------|--|-------------------------------|-----------------------------------|--|
| a) Headache | <input type="checkbox"/> Not experienced | <input type="checkbox"/> Mild | <input type="checkbox"/> Moderate | <input type="checkbox"/> Severe/
incapacitating |
| b) Gastro-intestinal distress | <input type="checkbox"/> Not experienced | <input type="checkbox"/> Mild | <input type="checkbox"/> Moderate | <input type="checkbox"/> Severe/
incapacitating |
| c) Fatigue and/or weakness | <input type="checkbox"/> Not experienced | <input type="checkbox"/> Mild | <input type="checkbox"/> Moderate | <input type="checkbox"/> Severe/
incapacitating |
| d) Dizziness/light-headedness | <input type="checkbox"/> Not experienced | <input type="checkbox"/> Mild | <input type="checkbox"/> Moderate | <input type="checkbox"/> Severe/
incapacitating |
| e) Difficulty sleeping | <input type="checkbox"/> Not experienced | <input type="checkbox"/> Mild | <input type="checkbox"/> Moderate | <input type="checkbox"/> Severe/
incapacitating |

D2. Have you suffered previously from severe high altitude illness?

- | | | |
|---|------------------------------|-----------------------------|
| a) High altitude cerebral oedema | <input type="checkbox"/> Yes | <input type="checkbox"/> No |
| If yes , was the illness confirmed by a clinician? | <input type="checkbox"/> Yes | <input type="checkbox"/> No |
| b) High altitude pulmonary oedema | <input type="checkbox"/> Yes | <input type="checkbox"/> No |
| If yes , was the illness confirmed by a clinician? | <input type="checkbox"/> Yes | <input type="checkbox"/> No |

Those who menstruate only: Participants who menstruate are asked to provide details of their menstrual cycle. It is crucial that we test female participants in a similar phase of their menstrual cycle to minimise the effects of fluctuating sex hormones on brain blood vessel function. Participants may be asked to complete the experimental protocol(s) in the early follicular phase (i.e., during their period or during their 'off-week' of their contraceptive).

The following questions will ask you to provide detail about your menstrual cycle.

Please tick that you wish to opt in or opt out from answering these questions.

- I opt in
- I opt out
- This question is not applicable to me

Q1. At present which statement best describes your menstrual cycle? Please tick one.

1. I do have periods/withdrawal bleeds: These are regular
2. I do have periods/withdrawal bleeds: These are irregular
3. I do not have periods/withdrawal bleeds. My periods/withdrawal bleeds have stopped due to menopause, surgery, or reasons

Q2. Are you using the oral contraceptive pill/contraceptive patch/injection/implant/intra-uterine system?

Yes No

Please specify which and give details (e.g. brand name)

If yes, has your contraception changed within the last 6 months?

Yes No

Q3. How often have you had periods/withdrawal bleeds in the last year?

- > 23 days
- 24-25 days
- 26-27 days
- 28-29 days
- 30-31 days
- < 32 days
- Every 3-4 months
- Very irregular, sometimes monthly, sometimes skips several months

Q4. When was the start of your last periods/withdrawal bleeds? (DD/MM/YYYY)

PLEASE COMPLETE AND SIGN THE DECLARATION BELOW

DECLARATION

I agree that I have none of the above conditions and I hereby volunteer to be a participant in experiments/investigations during the period of (Date, Month, Year)

My replies to the above questions are correct to the best of my belief and I understand that they will be treated with the strictest confidence. The experimenter has explained to my satisfaction the purpose of the experiment and possible risks involved.

I understand that I may withdraw from the experiment at any time and that I am under no obligation to give reasons for withdrawal or to attend again for experimentation.

Furthermore, if I am a student, I am aware that taking part or not taking part in this experiment, will neither be detrimental to, or further, my position as a student.

I undertake to obey the laboratory/study regulations and the instructions of the experimenter regarding safety, subject only to my right to withdraw declared above.

Signature (*participant*) Date

Print name

Email address

Signature (*experimenter*) Date

Print name

Thank you for completing this questionnaire.

Please return the completed questionnaire to a member of the research team.

Appendix 5.1: Lake Louise Questionnaire Acute Mountain Sickness Scale

Lake Louise Questionnaire (LLQ)

A diagnosis of acute mountain sickness (AMS) is based on the following conditions;

- Exposure to altitude within the last 4 days
- Presence of a headache

AND

- Presence of at least one other symptom
- A total of 3 or more

SELF-REPORT QUESTIONNAIRE

Add together the individual scores for each symptom to get the total score.

Headache	No headache	0
	Mild headache	1
	Moderate headache	2
	Severe headache	3
Gastrointestinal symptoms	None	0
	Poor appetite or nausea	1
	Moderate nausea or vomiting	2
	Severe nausea or vomiting	3
Fatigue and weakness	Not tired or weak	0
	Mild fatigue/weakness	1
	Moderate fatigue/weakness	2
	Severe fatigue/weakness	3
Dizziness/light-headedness	Not dizzy	0
	Mild dizziness	1
	Moderate dizziness	2
	Severe dizziness, incapacitating	3

A total LLQ score of 5 or more, with the presence of headache, and at least one other symptom, the participant must be removed for the chamber/Douglas bag

If you are ever unsure about whether it is safe to leave a participant in the chamber, just remove them

Chapter 4										Condition	Time	Interaction
	00:00		00:30		01:00		01:30					
Normoxia	0.23	± 0.62	0.17	± 0.44	0.20	± 0.51	0.18	± 0.50				
Hypoxia	0.22	± 0.57	0.80	± 0.93 [†]	0.71	± 0.87 ^{*†}	1.03	± 1.14 ^{*†}	< 0.001	< 0.001	< 0.001	

Chapters 5 & 6												Condition	Time	Interaction	
	00:00		00:20		00:40		01:00		01:20		01:40				
Normoxia	0.00	± 0.00	0.05	± 0.23	0.21	± 0.54	0.11	± 0.32	0.13	± 0.34	0.15	± 0.38			
Hypoxia	0.00	± 0.00	0.15	± 0.49	0.50	± 0.71	0.67	± 0.97	0.41	± 0.87	0.47	± 0.83	< 0.001	< 0.001	0.146

Appendix 5.2. Total Lake Louise Questionnaire Acute Mountain Sickness Score in normoxia (FiO₂ = 20.9%) and in acute poikilocapnic hypoxia for Chapter 4 (FiO₂ = 12.0%) and Chapters 5 & 6 (FiO₂ = 12.5%). Data were analysed by a linear mixed model analysis. The primary outcome of interest was the effect of interaction of condition and time. * $P < 0.05$ compared to normoxia within timepoint. † $P < 0.05$ compared to 00:00 within condition. Values are raw data means (standard deviation).